Vol. 57 OCTOBER, 1953 No. 7

THE JOURNAL OF PHYSICAL CHEMISTRY

(Registered in U. S. Patent Office)

Founded by Wilder D. Bancroft

27TH NATIONAL COLLOID SYMPOSIUM, AMES, IOWA, JUNE 25–27, 1953

(Continued inside)

Founded by Wilder D. Bancroft

THE JOURNAL OF PHYSICAL CHEMISTRY

(Registered in U. S. Patent Office)

Published monthly (except July, August and September) by the American Chemical Society at 20th and Northampton Sts., Easton, Pa.

Entered as second-class matter at the Post Office at Easton, Pennsylvania.

The *Journal of Physical Chemistry* is devoted to the publication of selected symposia in the broad field of physical chemistry and to other contributed papers.

Manuscripts originating in the British Isles, Europe and Africa should be sent to F. C. Tompkins, The Faraday Society, 6 Gray's Inn Square, London W. C. 1, England.

Manuscripts originating elsewhere should be sent to W. Albert Noyes, Jr., Department of Chemistry, University of Rochester, Rochester 3, N. Y.

Correspondence regarding accepted copy, proofs and reprints should be directed to Assistant Editor, Allen D. Bliss, Department of Chemistry, Simmons College, 300 The Fenway, Boston 15, Mass.

Business Office: American Chemical Society, 1155 Sixteenth St., N. W., Washington 6, D. C.

Advertising Office: American Chemical Society, 332 West 42nd St., New York 36, N. Y.

Articles must be submitted in duplicate, typed and double spaced. They should have at the beginning a brief Abstract, in no case exceeding 300 words. Original drawings should accompany the manuscript. Lettering at the sides of graphs (black on white or blue) may be pencilled in, and will be typeset. Figures and tables should be held to a minimum consistent with adequate presentation of information. Photographs will not be printed on glossy paper except by special arrangement. All footnotes and references to the literature should be numbered consecutively and placed on the manuscript at the proper places. Initials of authors referred to in citations should be given. Nomenclature should conform to that used in *Chemical Abstracts*, mathematical characters marked for italic, Greek letters carefully made or annotated, and subscripts and superscripts clearly shown. Articles should be written as briefly as possible consistent with clarity and should avoid historical background unnecessary for specialists.

Symposium papers should be sent in all cases to Secretaries of Divisions sponsoring the symposium, who will be responsible for their transmittal to the Editor. The Secretary of the Division by agreement with the Editor will specify a time after which symposium papers cannot be accepted. The Editor reserves the right to refuse to publish symposium articles, for valid scientific reasons. Each symposium paper may not exceed four printed pages (about sixteen double spaced typewritten pages) in length except by prior arrangement with the Editor.

Remittances and orders for subscriptions and for single copies, notices of changes of address and new professional connections, and claims for missing numbers should be sent to the American Chemical Society, 1155 Sixteenth St., N. W., Washington 6, D. C. Changes of address for the *Journal of Physical Chemistry* must be received on or before the 30th of the preceding month.

Claims for missing numbers will not be allowed (1) if received more than sixty days from date of issue (because of delivery hazards, no claims can be honored from subscribers in Central Europe, Asia, or Pacific Islands other than Hawaii), (2) if loss was due to failure of notice of change of address to be received before the date specified in the preceding paragraph, or (3) if the reason for the claim is "missing from files."

Subscription Rates: to members of the American Chemical Society, $8.00 for 1 year, $15.00 for 2 years, $22.00 for 3 years; to nonmembers, $10.00 for 1 year, $18.00 for 2 years, $26.00 for 3 years. Postage free to countries in the Pan American Union; Canada, $0.40; all other countries, $1.20. Single copies, $1.25; foreign postage, $0.15; Canadian postage, $0.05.

The American Chemical Society and the Editors of the *Journal of Physical Chemistry* assume no responsibility for the statements and opinions advanced by contributors to THIS JOURNAL.

The American Chemical Society also publishes *Journal of the American Chemical Society, Chemical Abstracts, Industrial and Engineering Chemistry, Chemical and Engineering News, Analytical Chemistry,* and *Journal of Agricultural and Food Chemistry.* Rates on request.

THE JOURNAL OF PHYSICAL CHEMISTRY

(Registered in U. S. Patent Office) (Copyright, 1953, by the American Chemical Society)

Founded by Wilder D. Bancroft

VOLUME 57 OCTOBER 28, 1953 NUMBER 7

RAT LIVER LACTIC DEHYDROGENASE. II. PHYSICO-CHEMICAL STUDIES ON THE CRYSTALLINE ENZYME[1,2]

BY EDWIN O. DAVISSON,[3] DAVID M. GIBSON,[4] B. ROGER RAY AND CARL S. VESTLING

Contribution from the Department of Chemistry, University of Illinois, Urbana, Ill.

Received March 2, 1953

A study was made of crystalline rat liver lactic dehydrogenase. The sedimentation and diffusion constants were 7.39×10^{-13} sec. and 5.8×10^{-7} cm.^{2}/sec., respectively, reduced to standard conditions and at infinite dilution. An ultra-fast membrane diffusion cell was developed. The partial specific volume at 0° was 0.745 ml./g. This value agreed well with one calculated from the amino acid composition. The molecular weight was 126,000 and the molar frictional ratio was 1.13. The molecular shape was also estimated from viscosity data. The isoelectric point was found to be 6.3. Near 0° and in appropriate buffers the enzyme was shown by several tests to be a single homogeneous substance. The results of this study showed that rat liver lactic dehydrogenase differed in several respects from enzymes of identical function from other sources.

The physical and chemical properties of an enzyme not only are necessary adjuncts to the problems of isolation and identification, but also are required for a thorough understanding of the metabolic processes catalyzed by the protein. This is seen in the recent advances in enzyme chemistry that have been accompanied by the isolation and characterization of individual enzymes. Of considerable interest have been the complex systems of liver enzymes. There have been isolated crystalline catalase and glutamic acid dehydrogenase from bovine liver and alcohol dehydrogenase from equine liver.

The purpose of the present study was to isolate and study the properties of the enzyme, lactic acid dehydrogenase (LDH), from rat liver. The first contribution from this study[5] reported the successful method of isolation, presented data on chemical constitution, and gave a preliminary treatment of the kinetics of the conversion of lactate to pyruvate by the enzyme. The present contribution deals with the characterization of the crystalline enzyme and with tests to establish homogeneity. Some of the methods were based upon assay for activity and were applied to LDH in the presence of impurities. Experimental conditions were chosen so as to avoid denaturation.

(1) In part from a thesis by Edwin O. Davisson submitted to the Graduate College of the University of Illinois in partial fulfillment of the requirements for the Ph.D. degree, 1953.

(2) This investigation was aided by research grants from the du Pont Company to the Department of Chemistry, from the Research Board of the Graduate College of the University of Illinois, and from the American Cancer Society.

(3) Special du Pont Research Fellow, 1949-51.

(4) Fellow of the American Cancer Society, 1951-52.

(5) D. M. Gibson, E. O. Davisson, B. K. Bachhawat, B. R. Ray and C. S. Vestling, *J. Biol. Chem.*, **203**, 397 (1953).

Experimental Details

The sedimentation measurements, carried out at temperatures near 0°, were made with a Spinco Model (E) ultracentrifuge equipped with the Philpot-Svensson optical system with a diagonal bar. The average speed was determined by the counter reading. The temperature rise during an experiment averaged 1° per hour, based upon the initial and final rotor temperatures. The sedimentation constant was calculated by the integration method[6] and was reduced to water and 20° by the standard equation. The term $(1 - \bar{V}_{20}\rho_{20,w})$ was 0.2464 with $\bar{V}_{20} = 0.755$ and the term $(1 - \bar{V}_t\rho_t)$ was calculated for each run utilizing experimental data. Viscosity corrections were determined by experiment.

Diffusion measurements were made by the porous-disc and free diffusion methods. For the first method a small volume, ultra-fast cell was necessary because of the small volumes available and the danger of loss of enzyme activity over extended times. A satisfactory cell was constructed with a membrane thickness of 0.6 mm., a membrane diameter of 30 mm., and a "buffer side" volume of 3 ml. The membrane was made by grinding down a standard Pyrex medium-grade frit on a lapping wheel. The fragile wafer was sealed within a flat copper ring with low-temperature glass-to-metal solder. The two end sections of the cell were machined of Lucite. The copper ring was clamped between

(6) T. Svedberg and K. O. Pedersen, "The Ultracentrifuge," Oxford University Press, New York, N. Y., 1940.

these end sections—each wet with solvent—until firmly sealed. The cell was of the rotating, double-ended design and was used in the usual manner[7] in an ice-bath at 0°. Calibration was with 0.1 *N* KCl following the recommendations of Stokes.[8] This cell was about ten times as fast as the ordinary glass-membrane cells and runs on the enzyme required only a few hours. Assays of enzyme activity provided the data for calculations.

Free diffusion measurements were carried out at 0.8° in a Pearson electrophoresis apparatus utilizing the Philpot–Svensson optical arrangement with a diagonal slit. Boundaries were formed in a Tiselius-type microcell by shearing, or better, by use of a very fine capillary through which the protein solution was slowly layered beneath the buffer. Measurements on the diffusion curves were made from five-fold enlargements on Kodak Resisto Rapid N-4 paper.[9]

The diffusion coefficient by the height–area method was calculated from the mean curves constructed from the two edges of the gradient curves. The several values of $1/H_m^2$, where H_m is the maximum ordinate, were plotted against time, t. The slope of the straight line so obtained was substituted into the equation

$$D_A = \frac{A^2}{4\pi G^2} \times \frac{1}{H_m^2 t}$$

where A was the average area and G was the magnification factor. For the weight-average (second moment) diffusion coefficient a curve was divided into approximately 100 intervals and the upper and lower ordinates recorded for each.[10] Summation of these data yielded the standard deviation σ. Values of σ^2 were plotted against time and the slope of the line substituted into

$$D_m = \frac{1}{2G^2} \times \frac{\sigma^2}{t}$$

The two arms of the cell were in good agreement in all cases. No skewness was detected in any of the curves.

Densities of solutions were determined with Pyrex pycnometers. To avoid thermal degradation and its possible effect upon specific volume, all measurements, including weighings, were carried out in a cold room at 1–2°. The water thermostat was held at 0.2°. The partial specific volume $\bar{v}$ was calculated from

$$\bar{v} = \frac{1}{\rho} - \frac{(1 - w)}{\rho^2} \times \frac{d\rho}{dw}$$

where ρ and w are the solution density and weight per cent. protein, respectively.

Electrophoretic measurements were made at 0.8° in the Pearson apparatus utilizing Tiselius-type cells and shear boundaries. The scanning technique of Longsworth was used. The *p*H values were measured at 25° and not extrapolated to 0.8°. Conductances were those of the equilibrated buffers at 0°.

The solutions of crystalline native enzyme used in the physicochemical studies, unless otherwise specified, had been exhaustively dialyzed at 2° against phosphate buffer (0.0323 mole of K_2HPO_4 and 0.00323 mole of KH_2PO_4 per liter, *p*H 7.8, ionic strength 0.1). The equilibrated buffers were used along with these solutions. Protein concentrations were estimated by assay of enzyme activity and spectrophotometrically by the absorption at 280 mμ, both referred to the carefully established dry weight of the protein. Details are given in the earlier paper.[6]

Results

Sedimentation.—Enzyme preparations of low purity showed three apparent components in sedimentation with reduced Svedberg constants of 6.8, 5.0 and 2.8. Proof that the enzyme activity was associated with the 6.8 component was furnished by carefully sampling the cell after a run and comparing the specific enzyme activities (units of enzyme activity per unit total protein) of the original solution, supernatant solution, and gelatinous sediment. The Svedberg analytical separation cell[6] was applied to a number of preparations, particularly in the early stages of the isolation work. The results, based upon enzyme assays of the portions above and below the barrier, correlated fairly well with the later optical observations.

The sedimentation behavior of the crystalline enzyme was uniform and relatively simple throughout the concentration range investigated. All the sedimentation patterns were single peaks, very symmetrical and showing no evidence of more than the one component. Although optical observation of sedimentation on solutions more dilute than 0.4% was not made, there was evidence that the protein remained stable at low concentrations. Runs in the separation cell in which the protein was very dilute (as well as mixed with impurities) gave approximately the same sedimentation constant. The lack of skewness in the sedimentation curves indicated that the dilute solution forming the trailing edge was apparently sedimenting at the normal rate. The glutamic dehydrogenase from beef liver isolated by Olson and Anfinsen[11] makes an interesting contrast since in this case a pronounced skewness was observed because of dissociation (or change in shape) in dilute solution.

The sedimentation constant was concentration dependent, increasing with dilution. For the concentration range studied, 0.4 to 1.5%, the relationship was entirely linear and extrapolated to an $s_{20,w}$ of 7.39×10^{-13} sec. at infinite dilution.[12] The equation for the line was $s_{20,w} \times 10^{13} = 7.39 - 0.38c$ where c was in g./100 ml.

A sensitive test for homogeneity, as well as for the detection of boundary disturbances, is to compare the boundary spreading obtained in a sedimentation experiment with the theoretical spreading expected for an ideal homogeneous substance with a known diffusion coefficient. Calculations were carried out[6] for a typical run, and in Fig. 1 four experimental curves are compared with the theoretical curves to be expected for an ideal homogeneous substance. The very good agreement gave assurance that crystalline LDH under the given conditions was homogeneous with respect to size and shape.

Diffusion.—The porous-disc method was alone applicable for diffusion measurements on impure enzyme preparations. Early in the isolation work, using very dilute solutions, it supplied data which permitted a good estimate to be made of the molecular weight of the enzyme. It was valuable in giving information upon possible interaction effects with impurities (none was observed) and in proving that the enzymatic activity was associated with a single diffusing species. The average value of the reduced diffusion coefficient $D_{20,w}$ from runs made at several ionic strengths and enzyme concentrations and in different buffers was $5.3 \pm 0.5 \times 10^{-7}$ cm.²/sec. This value agrees well with the free diffusion data for the crystalline enzyme and substantiates the fact that the enzyme activity is the unique property of the protein isolated.

Free diffusion measurements on the crystalline enzyme gave the values presented in Table I. The increase of rate with dilution was consistent with that observed in sedimentation and suggested molecular interaction due to size and shape factors, typical of many proteins.

The diffusion curve of a homogeneous, ideal diffusing substance has the form of the normal probability curve, and for such a substance D_A and D_M should be the same. Curves of mixtures are more pointed than the normal curve; and, due to the fact that D_A is sensitive to the height of the curve, the ratio D_M/D_A can be used as a measure of polydispersity. For LDH this ratio was 1.03 at a concentration of 1.2% and is believed to indicate the essentially homogeneous character of the protein. The use of this ratio has been recently emphasized by Charlwood[13] who obtained

(7) L. Friedman and B. R. Ray, THIS JOURNAL, **46**, 1140 (1942).

(8) R. H. Stokes, *J. Am. Chem. Soc.*, **72**, 763 (1950).

(9) This photographic paper can be highly recommended for making enlargements of sedimentation and diffusion patterns. It has a specially treated, water-resistant base which permits a very short drying time (10 minutes) and which allows extremely small dimensional changes. Enlargements on Resisto paper were compared with those on ordinary paper and with enlarged tracings made directly from the negatives. The first were the most reproducible and convenient.

(10) The authors gratefully acknowledge the assistance of Mr. Wallace R. Deason in making these calculations.

(11) J. A. Olson and C. B. Anfinsen, *J. Biol. Chem.*, **197**, 79 (1952).

(12) In order to compare accurately the sedimentation constants obtained in different laboratories, Taylor [*Arch. Biochem. Biophys.*, **36**, 35 (1952)] has made the suggestion that, for the present, the data be accompanied by the sedimentation constant obtained for a standard protein in the same apparatus. We obtain 4.21 ± 0.03 *S* for $s_{20,w}$ for Armour crystallized bovine serum albumin. Control lot 284-8, at 0.9% concentration. This value differs by 2.6% from that of Taylor.

(13) P. A. Charlwood, THIS JOURNAL, **57**, 125 (1953).

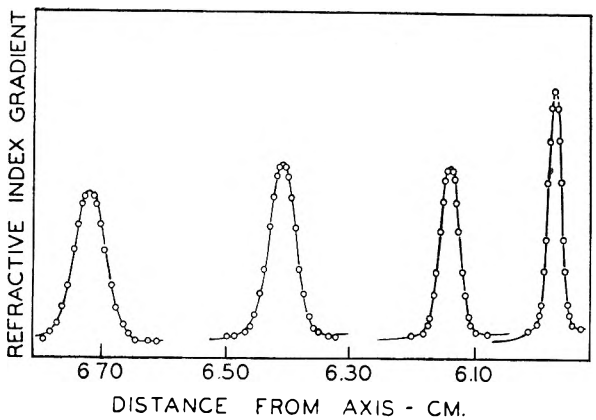

Fig. 1.—Comparison of actual and theoretical boundary spreading of LDH in sedimentation. The solid curves, right to left, were traced from enlargements of the photographs taken at the following times and bar angles: 20 min. (60°), 44 min. (60°), 84 min. (50°) and 122 min. (45°). In making the tracings the upper edges of the transparent bands on the photographic negatives were utilized. The open circles are points on the theoretical boundary curves for an ideal homogeneous substance calculated from the experimentally determined values of s and D (4.56×10^{-13} sec. and 3.32×10^{-7} cm.²/sec.). The diffusion coefficient was corrected in each theoretical curve for the influence of the centrifugal field.

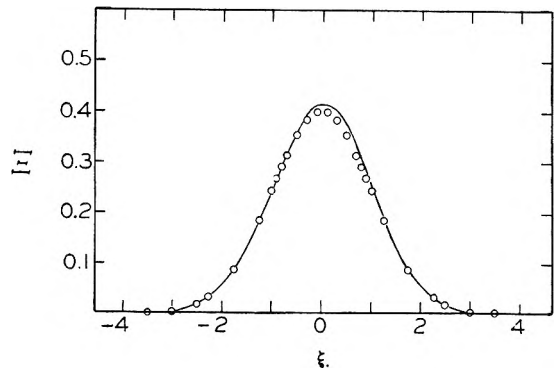

Fig. 2.—Comparison of the experimental free diffusion curve of LDH with the normal probability curve. The solid line is the normalized experimental curve. The open circles are calculated points on the normal probability curve.

a ratio of 1.04 for crystalline serum albumin. A more sensitive and detailed test of the diffusion behavior, however, is to normalize the experimental curve and compare it with the normal probability curve. This is shown for a representative case in Fig. 2. Although quite symmetrical, the experimental curve does show some anomaly at the peak. This may be due to the concentration dependence in diffusion, a slight inhomogeneity, or both.

Partial Specific Volume.—The densities of the solutions are given in Table II. A plot of density *vs.* weight per cent. gave a straight line with a slope $d\rho/dw$ of 0.002526. (There appeared to be a barely perceptible tendency for this slope to decrease with increasing concentration. More extensive density measurements would be necessary to confirm this.) Substituting the data into the equation given earlier yielded the partial specific volumes listed in Table II. By applying the customary temperature coefficient of 0.0005 per degree[6,14] $\bar{V}_{20,w}$ was calculated to be 0.755 ml./g.

The specific volumes of many simple proteins are in the range of 0.72 to 0.74 although values of 0.68 and 0.76 have been found for gelatin[15] and a human gonadotropin,[16] respectively. The specific volume should theoretically be equal to the sum of the volumes of the component groups and atoms, with allowance for interaction effects. Cohn and Edsall[17] have shown how the volume fractions of the amino acid residues in a protein may be summed to yield a calculated specific volume. Recently McMeekin and Marshall,[18] having assembled the most recent data on 19 proteins, compared the specific volumes as calculated by the above method with experimental values. The agreement in nearly every case was excellent. Apparently interaction effects are quite negligible.

The nearly complete (93.5%) amino acid composition of crystalline LDH has been given.[5] When the volume contribution of each amino acid residue was calculated and the sum of these divided by 0.935, a specific volume of 0.755 was obtained. The agreement with the experimentally derived value of 0.755 is a further substantiation of the method of Cohn and Edsall. The unusually high specific volume of LDH is due to the large proportions of leucine, isoleucine, valine and lysine and the relatively small proportions of glycine and cystine.

Viscosity Measurements.—Measurements were made at 0° using an Ostwald microviscometer constructed for the purpose. Repeated determinations were constant, there being no evidence of surface denaturation or adsorption onto the walls of the capillary. The absolute viscosities of a solution of crystalline LDH, containing 0.34 g. per 100 ml., and its equilibrated phosphate buffer were 0.018439 and 0.018199 poise, respectively. The specific viscosity increment, *i.e.*, the specific viscosity of a 1.0% solution, was 0.039. This last value permits a comparison of the "thickening effect" of different proteins on a weight basis. For instance, ovalbumin and serum albumin have values of 0.047 to 0.05 as calculated from the data of Polson.[19] The low increment for LDH may reflect the relatively low dissymmetry factor calculated for this molecule in the next section.

Molecular Weight and Shape.—From the determined values of the sedimentation constant, diffusion coefficient, and partial specific volume, the molecular weight of LDH, calculated by the Svedberg equation, was 126,000. This was, of course, representative of the undenatured enzyme in phosphate buffer at a temperature near 0°.

The molar frictional ratio f/f_0 was found to be 1.13 This is a lower value than found for most proteins,[6,14] especially in this and higher ranges of molecular weights, and indicates a low degree of asymmetry and/or hydration. Following the procedure of Oncley,[20] f/f_0 can be represented as the product of two factors f/f_e and f_e/f_0, the first representing the influence of hydration and the second the influence of asymmetry. Kramer has shown[6] that the hydration factor is related to the grams of water per gram of protein, r, by

$$f/f_e = \left[1 + \frac{r}{\bar{V}\rho_0}\right]^{1/3}$$

in which ρ_0 is the density of water. The maximum possible degree of hydration for LDH would make f/f_e equal to 1.13 and would lead to a value of 0.34 for r. On the other hand, if the entire molar frictional ratio is laid to asymmetry, $f_e/f_0 = 1.13$. In the equations of Perrin[6] this value would represent axial ratios (a/b) of 3.3 and 3.5 for prolate and oblate ellipsoids of revolution, respectively. Thus, it appears from sedimentation and diffusion data that the molecular shape of this protein can be represented as something between a sphere hydrated to the extent of 34% and an ellipsoid with an axial ratio of 3.4. The ellipsoid would have a diameter of 60 Å. and a length of 200 Å.

An empirical equation has been proposed by Polson[6] relating the specific viscosity of a protein solution and the axial ratio of the molecules. It has the form

$$\eta_{sp} = 4G + 0.098G(a/b)^2$$

where G is the anhydrous volume of protein per ml. of solution, *i.e.*, the concentration multiplied by the specific volume. This equation has given very good agreement for

(14) D. M. Greenberg, "Amino Acids and Proteins," Chapter VI, C. C Thomas, Springfield, Illinois, 1951.

(15) K. Krishnamurti and T. Svedberg, *J. Am. Chem. Soc.*, **52**, 2897 (1930).

(16) H. P. Lundgren, S. Gurin, C. Bachman and D. W. Wilson, *J. Biol. Chem.*, **142**, 367 (1942).

(17) E. J. Cohn and J. T. Edsall, "Proteins, Amino Acids, and Peptides," Reinhold Publ. Corp., Inc., New York, N. Y., 1943.

(18) T. L. McMeekin and K. Marshall, *Science*, **116**, 142 (1952).

(19) A. Polson, *Kolloid Z.*, **88**, 51 (1939).

(20) J. L. Oncley, *Ann. N. Y. Acad. Sci.*, **41**, 121 (1941).

many proteins which were not too asymmetric in shape. When the experimental data for LDH were substituted, the ratio a/b was found to be 3.4. This result serves as a further substantiation of the Polson relationship.

More recently Simha[21] has developed a theoretical relationship between the "viscosity increment" (which for our purpose may be defined as being approximately equal to η_{sp}/G with a value of 5.16) and the axial ratio of unoriented ellipsoids. Graphical solutions of the equation[20] can be utilized and for LDH the ratio a/b was found to be 4.5 for the unhydrated ellipsoid, or, alternatively, for the sphere the degree of hydration was 75%. The shape factors of LDH determined from viscosity and density data can be said to agree fairly well with those determined from sedimentation and diffusion. The agreement is about that found by Mehl, Oncley and Simha[22] for several proteins in the same f/f_0 range. In particular, the shape and degree of hydration of LDH appear to be similar to those found for egg albumin.

Electrophoresis.—Solutions of the crystalline enzyme migrated as single, symmetrical peaks in the electrophoresis apparatus at 0.8° over a *p*H range from 5.8 to 7.8 in potassium phosphate buffers of 0.1 ionic strength. Two runs are reproduced in Fig. 3. The variation of mobility with *p*H is plotted in Fig. 4. The isoelectric point was found to be 6.3.

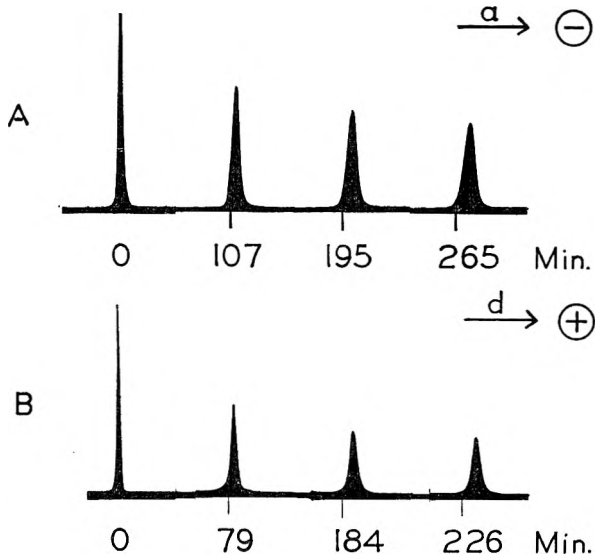

Fig. 3.—Electrophoretic mobilities of crystalline LDH. The number below each peak is the elapsed time of migration in minutes: A, mobility toward the cathode at *p*H 5.8 ($u = +0.49 \times 10^{-5}$ cm.²/v./sec.); B, mobility toward the anode at *p*H 7.8 ($u = -0.53 \times 10^{-5}$ cm.²/v./sec.).

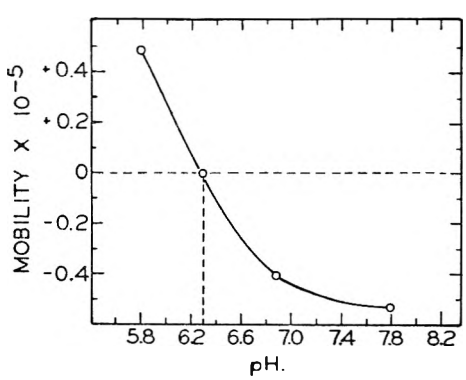

Fig. 4.—Electrophoretic mobility (cm.²/v./sec. $\times 10^{-5}$) as a function of *p*H.

(21) R. Simha, THIS JOURNAL, **44**, 25 (1940).

(22) J. W. Mehl, J. L. Oncley and R. Simha, *Science*, **92**, 132 (1940).

TABLE I

DIFFUSION COEFFICIENTS OF CRYSTALLINE LDH

Values Reduced to 20° and Water

Protein concn., g./100 ml.	Diffusion coefficient, cm.²/sec. × 10⁷ D_A	D_M
1.23	5.42	5.60
0.33	5.72	
0.00	5.82 (extrapolated)	

TABLE II

DENSITIES AND PARTIAL SPECIFIC VOLUMES OF CRYSTALLINE LDH

In Phosphate Buffer at 0.2°

Wt. % protein	Density, g./ml.	Partial specific vol., ml./g.
0	1.00541	
0.164	1.00588	0.745
.323	1.00629	.745
.780	1.00737	.746

Discussion

Crystalline rat liver LDH appeared to be a single homogeneous protein as tested by electrophoretic, sedimentation and diffusion procedures under conditions designed to minimize denaturation. A partial solubility test[5] also supported this conclusion. The physico-chemical behavior was typical of a simple globular protein. A future report will deal with the results of electrical heterogeneity tests and a more thorough investigation of the kinetics.

From sources other than liver three crystalline lactic acid dehydrogenases have been obtained and in the case of one, the Straub preparation from beef heart,[23] several physical properties have been reported. It showed two electrophoretic components, both of which migrated toward the anode over the *p*H range 5 to 7.[24-26] Isoelectric points determined by extrapolation were 4.5 and 4.8.[26] These findings are in contrast with rat liver LDH which migrated as a single component toward the cathode at *p*H 5.8 and which was isoelectric at *p*H 6.3.

The sedimentation and diffusion characteristics of the enzyme from beef cardiac muscle and that from rat liver can be compared. Meister[24] reported $s_{20,w}$ values of 6.48 and 6.36 *S* for two preparations from heart and estimated a molecular weight of 100,000 to 150,000. He gave the concentration of his first preparation as 0.9% protein. The value of $s_{20,w}$ of rat liver LDH is found to be 7.05 *S* at 0.9%. The difference in the sedimentation constants exceeds any probable experimental errors. Neilands[26] found s_{20} to be 7.0 *S* and D_{20} to be 5.3×10^{-7} cm.²/sec. for a preparation from beef heart. In neither case did he specify the medium or the protein concentration. Assuming, however, that these values were corrected to water and that the protein concentration was 1% then they agree closely with our values of 7.0 *S* and 5.5×10^{-7}

(23) F. B. Straub, *Biochem. J.*, **34**, 483 (1940).

(24) A. A. Meister, *J. Biol. Chem.*, **184**, 117 (1950).

(25) J. B. Neilands, *Science*, **115**, 143 (1952).

(26) J. B. Neilands, *J. Biol. Chem.*, **199**, 373 (1952).

cm.^{2}/sec. Neilands calculated from his data a molecular weight of 135,000.[27]

The data at hand indicate that rat liver LDH may differ with respect to several physical properties from enzymes of apparently identical function in other species and tissues. A similar situation was demonstrated in the different electrophoretic behavior of crystalline aldolase isolated from the skeletal muscle of the rat and rabbit.[28] The methods for isolation of an enzyme may alter the nature of the final products. The method for preparation of liver LDH employed ethanol at temperatures at or below 0° while the isolation procedure from beef heart incorporated acetone with several instances of exposure to temperatures in excess of 10°.[23]

(27) We do not obtain a value of 135,000 from the data presented unless an improbably high density of the medium is assumed. If the calculation is made assuming the density to be 1.000, the molecular weight becomes 124,000.

(28) J. F. Taylor, A. A. Green and G. T. Cori, *J. Biol. Chem.*, **173**, 591 (1948).

STREAMING ORIENTATION STUDIES ON DENATURED PROTEINS. IV. DENATURATION OF OVALBUMIN WITH SURFACE ACTIVE IONS[1]

BY G. FREDERICK HANNA AND JOSEPH F. FOSTER

Contribution from the Department of Chemistry, Iowa State College, Ames, Iowa

Received March 2, 1953

The denaturation of ovalbumin by surface active ions is investigated by streaming birefringence and by light scattering. Several cationic agents are shown to denature the protein rapidly at room temperature yielding solutions which show intense streaming orientation. The denatured protein aggregates, but the rotary diffusion constant decreases only slowly with increasing degree of aggregation. The results are in accord with the picture previously developed for the denaturation of ovalbumin under other conditions, namely an unfolding to yield rods of length about 600 Å. followed by an essentially lateral aggregation. Alternatively it is suggested that swelling might occur, the swollen molecules then aggregating and undergoing the unfolding step as a consequence of aggregation. With surface active anions there is no development of streaming birefringence unless the solutions are heated to a temperature sufficient to cause heat denaturation.

In previous communications in this series[2] it has been demonstrated that ovalbumin denatured by heat or by urea yields streaming birefringence and these results have been interpreted on the basis of an unfolding of the native protein molecule to yield essentially rods of molecular length about 600 A. In those studies aggregation of the denatured molecules was shown to be a complicating factor in the interpretation of the results. Under only a few selected conditions did aggregation appear to be negligible, notably at *p*H 2–3 in the absence of buffer ions.

It is well known that surface active ions are bound tenaciously by, and exert a denaturing action on, proteins.[3] The binding of anions on the alkaline side of the isoelectric point or of cations on the acid side should enhance the coulomb charge repulsion between denatured protein molecules and thereby repress aggregation. In preliminary experiments this did indeed appear to be so.[4] However, in those experiments the denaturation may properly be considered as heat denaturation, perhaps modified to some extent by the surface active ions. Fredericq[5] has demonstrated streaming birefringence in ovalbumin denatured by anionic detergents but the large magnitude of the calculated lengths together with the obvious heterogeneity of the systems makes it clear that aggregation was a predominant factor in those studies. In this investigation attempts have been made to minimize aggregation by denaturing at room temperature in the presence of detergent and an independent measure of aggregation has been obtained through the use of light scattering measurements.

Experimental

Ovalbumin.—The ovalbumin was prepared from fresh eggs by ammonium sulfate crystallization using the well known procedure of Sørensen and Høyrup. All preparations were recrystallized at least twice.

Streaming Orientation Measurements.—The instrument used in this study consists of concentric stainless steel cylinders with a gap width of 0.05 cm. and has been used in the experimental work reported in previous papers of this series.[2] Readings of the four minima in each sense of rotation were made at each gradient chosen in the range 1180–5880 sec.$^{-1}$ (180–900 r.p.m.), and average values used in calculating the extinction angles (χ). The magnitude of birefringence (Δ) was measured over the same gradient range in the usual fashion.

Lengths of the solute particles were calculated using the data of Scheraga, Edsall and Gadd[6] and the modified Perrin equation[7] relating length and molecular weight to the rotary diffusion constant function, $\eta\theta/T$.

Light Scattering Measurements.—The instrument used consists of a modified Zeiss Pulfrich photometer described by Rhees and Foster.[8] The green mercury line (λ = 5461 Å.) was used. The value of $\partial\eta/\partial c$ for ovalbumin was found to be 0.185, hence $H(= 32\ \pi^3\ n^2(\partial\eta/\partial c)^2/3N\lambda^4)$ was assigned the value 3.76×10^{-6}.

Several readings were taken at each of three angles, 45, 90 and 135°, averaged and corrected for solvent scattering. Turbidity data calculated from the 90° readings were plotted in the usual HC/τ *versus* C plot and extrapolated to zero concentration.

Preparation of Solutions.—The major portion of the work reported here involves denaturation of ovalbumin in slightly acid solution. Since the denaturing agent contains nitrogen, the application of Kjeldahl nitrogen analysis must be made prior to the addition of the detergent to obtain a measure of the protein concentration. An attempt to remove the detergent by continuous flow dialysis was unsuccessful. Clarification was found to be most satisfactory where the protein solution was subjected to filtration through fine sintered glass followed by centrifugation (20,000 *g*) for 1–2 hours. Preliminary experiments indicated that filtration of the detergent–protein solution alone was not sufficient to yield reliable results.

Weighed amounts of crystalline ovalbumin were dissolved in redistilled dust-free water and calculated amounts of clarified 0.1 *N* hydrochloric acid added. The resultant solutions were freed of traces of insoluble protein by filtration through a Corning fine sintered glass disc under pressure. The concentration of soluble protein was determined using the Pregl micro Kjeldahl analysis for nitrogen (15.75% N in ovalbumin).[9]

Sufficient Zephiran (alkyldimethylbenzylammonium chloride) was then added to give the desired detergent–protein ratio. When necessary further clarification of the denatured solution was achieved by centrifugation (20,000 *g*) for 0.5–2.0 hours.

For the light scattering measurements two methods of preparation of the dilution series were attempted and discarded as being too prone to random error. The first, that of dilution of a concentrated solution with clarified solvent,

(1) Journal paper Number J-2264 of the Iowa Agricultural Experiment Station, Ames, Iowa. Project 978. Supported in part by a grant from Swift and Company. Taken from a thesis presented by G. F. Hanna to the Graduate Faculty in partial fulfillment of the requirements for the degree Master of Science, Iowa State College, 1952.

(2) (a) J. F. Foster and E. G. Samsa, *J. Am. Chem. Soc.*, **73**, 3187 (1951); (b) E. G. Samsa and J. F. Foster, *ibid.*, **73**, 3190 (1951); (c) J. F. Foster and E. G. Samsa, *ibid.*, **73**, 5388 (1951).

(3) This subject has been reviewed by F. W. Putnam, *Adv. Protein Chem.*, **4**, 79 (1948).

(4) J. F. Foster and E. G. Samsa, *Science*, **112**, 473 (1950).

(5) E. Fredericq, *Bull. soc. chim. Belg.*, **56**, 223 (1947).

(6) H. A. Scheraga, J. T. Edsall and J. O. Gadd, Jr., *J. Chem. Phys.*, **19**, 1101 (1951).

(7) G. F. Hanna, J. F. Foster and J. T. Yang, *Arch. Biochem. Biophys.*, **44**, 15 (1953).

(8) R. C. Rhees and J. F. Foster, *Iowa State College J. Sci.*, **27**, 1 (1952).

(9) G. R. Tristam, *Adv. Protein Chem.*, **5**, 137 (1949).

was discarded since any accidental contamination appears most prominently in the most dilute sample of the series. The second method, that of addition of concentrated protein solution to clarified solvent was more satisfactory. This method also suffers, however, from the mechanical transfer of atmospheric dust during the several additions of solution.

The method of choice was the preparation, by dilution, of all the desired concentrations in 50-cc. centrifuge tubes. The diluting solvent was adjusted to ionic strength 0.02 with sodium chloride. This ionic strength was adopted on the basis of considerations previously presented.[10] The samples were then centrifuged free of foreign particles and transferred to the semi-octagonal scattering cells.

For streaming birefringence, 10 ml. of the denatured solution was diluted with 95% glycerol to yield a solution containing 80% (by weight) glycerol. These solutions were degassed by evacuation (water aspirator) for several minutes and immediately transferred to the cylinders of the flow birefringence instrument. The use of an antifoam agent (decyl alcohol) was found to be necessary only for solutions containing a high detergent concentration.

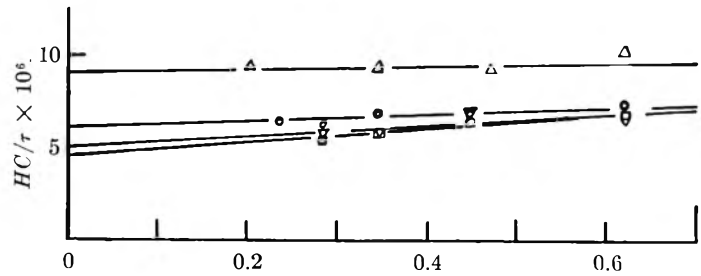

Fig. 1.—Effect of variation in the time of Zephiran denaturation on the light scattering dilution series curves; temp., 25°; *D:P* ratio, 0.30; *p*H 3.0; ionic strength, 0.02.

	△	○	▽	□
Time, hr.	15	120	260	630
Intrinsic dissymmetry, z	1.40	1.32	1.22	1.25

Results

Comparative Behavior with Cationic and Anionic Agents.—In view of the previous finding that there exists a minimum in aggregation tendencies at *p*H 2–3 it was of particular interest to carry out experiments in this range using cationic agents. For this purpose Zephiran (alkyldimethylbenzylammonium chloride where alkyl is largely dodecyl) was selected. As will be seen below this reagent is quite effective in yielding denaturation and streaming birefringence at room temperature. It was of interest, however, to make comparative studies using anionic detergents. In this case precipitation occurs on the acid side of the isoelectric point so that experiments were confined to the *p*H range 7 to 9. In a large number of such studies no development of flow birefringence has been observed unless the solutions were subjected to a sufficiently high temperature to cause heat denaturation in the absence of detergent. The results of these studies will be the subject of another communication. The contrast in the action of the cationic and anionic reagents on ovalbumin at room temperature is striking and will be considered further in the discussion.

Action of Zephiran at *p*H 3.0—A clarified 2.4% solution of ovalbumin at *p*H 3.0 was adjusted to a detergent–protein ratio of 0.30 with Zephiran and allowed to stand in a closed container at room temperature (28 ± 3°). Aliquots were removed for light scattering and flow birefringence measurements at 15, 120, 260 and 630 hours after mixing. The results demonstrate (Fig. 1) some aggregation, the particle weights essentially doubling over the period studied. The streaming orientation data shown in Fig. 2 indicate that these four samples, although slightly heterogeneous as shown by the downward trend in length with increasing gradient, gave very similar length distributions. However, the reduced birefringence suggests an increase in the proportion of orientable protein with increasing time of standing.

Extrapolation of the experimentally observed light scattering dissymmetry values to zero concentration yielded intrinsic dissymmetries (Z) which are also summarized in Fig. 1.

In the absence of detergent the experimentally determined molecular weight of ovalbumin was 45,500. An estimate of the particle weight only 20 minutes after the addition of detergent was obtained in the following manner. Calculated amounts of Zephiran were added to each cell to give a detergent to protein ratio of 0.30, mixed and turbidities read. Under such conditions a value of 95,000 was obtained, indicating an approximate doubling of particle size. However, 20 minutes was not sufficient contact time to show measurable birefringence.

To test the effect of concentration on the streaming birefringence results a stock solution was prepared, denatured as above and run first at 0.33% protein. Dilutions of 0.16 and 0.08% were prepared and run. Lengths calculated at the various gradients agreed to within 20% at the lowest gradient and 5% at the highest. The agreement in Δ/fc was similar.

Comparison of samples denatured at various Zephiran: ovalbumin (*D:P*) ratios showed no gross effects due to this variable. There appeared to be a minimum in length near 0.30 and this ratio was arbitrarily adopted for further study.

One sample was allowed to stand in the cold room (3°) at *p*H 2.5, *D:P* ratio 0.30, for five days before measurable birefringence could be obtained. At this time the particle weight was found to be 330,000, the dissymmetry only 1.10. This sample yielded good streaming birefringence but appeared to be quite heterogeneous, the lengths ranging from 1200 to 500 Å. over the gradient range 1180 to 5880 sec.$^{-1}$.

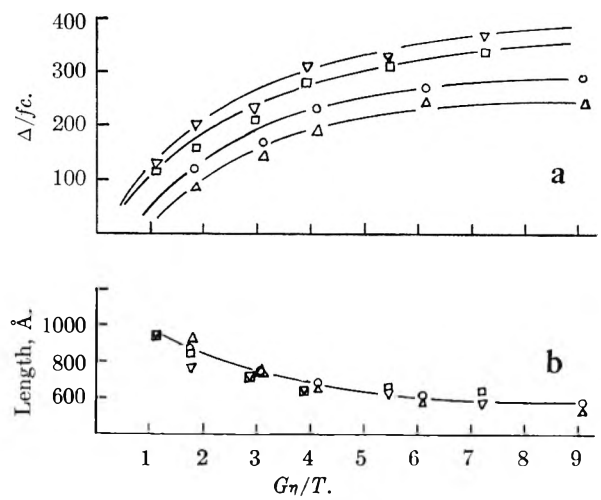

Fig. 2.—(a) Dependence of reduced birefringence on velocity gradient for ovalbumin samples denatured for varying lengths of time at room temperature. *D:P* ratio, 0.30; *p*H 3.0; in the absence of salt. Glycerol (80%) added for streaming birefringence measurements. Time in hours: △, 15; ○, 120; ▽, 260; □, 630. (b) Dependence of length, calculated on the basis of rigid prolate ellipsoidal model, on velocity gradient. Conditions as in (a). Time in hours: △, 15; ○, 120; ▽, 260; □, 330.

Effect of Heating.—The data summarized in Table I show the effect of heating a protein–Zephiran complex first denatured by standing at room temperature for 15 hours. Surprisingly only one hour heating at 37° effects a substantial reduction in aggregation with no reduction in streaming birefringence. There appears to be a significant improvement in homogeneity of the system as evidenced by a greater constancy in length at the various gradients and more important in the much greater constancy of the reduced birefringence. The sample heated for one hour at 100° underwent drastic disaggregation and probably also hydrolysis.

(10) J. F. Foster and R. C. Rhees, *Arch. Biochem. Biophys.*, **40**, 437 (1952).

TABLE I

EFFECT OF HEATING OVALBUMIN-ZEPHIRAN COMPLEX[a]

Treatment	Δ/fC	$\eta\theta/T$	Length (Å.)	M[b]
Control, 15 hr. at room temp.	120–250	1.28–2.54	730–580	167,000
15 hr. room temp., then 1 hr. at 37°	218–236	0.80–1.13	800–690	83,000
15 hr. room temp., then 1 hr. at 100°	Birefringence very weak			

[a] The streaming birefringence results are expressed as a range over the velocity gradients covered. [b] The molecular weights given in this and the following tables correspond to the values for protein alone without consideration of the bound detergent.

Behavior at *p*H 3 in the Absence of Detergent.—It was of interest to observe the effect of standing at room temperature and *p*H 3.0 on the properties of ovalbumin. Under such conditions a pronounced aggregation was observed, the particle weights being 45,500 at 12 hours, 250,000 at 96 hours and 670,000 at 240 hours. The intrinsic dissymmetries showed a marked increase, being 1.10, 1.93 and 2.12 at these same intervals. However, it is of significance that none of the samples yielded measurable streaming birefringence.

Effect of Zephiran near the Isoelectric Point.—A few experiments were performed in which Zephiran was added to isoelectric ovalbumin, yielding solutions of *p*H 4.2–4.4. Some results are summarized in Table II; in these experiments the protein concentration was 1.9%, the *D*: *P* ratio 0.30. The extent of aggregation was comparable to that obtained at *p*H 3.0 and good streaming birefringence was developed. The systems appeared to be considerably more heterogeneous than at *p*H 3, however, as judged by the greater spread in lengths and in reduced birefringence. Furthermore, the mean particle length appeared to be considerably greater in all cases than at the lower *p*H.

TABLE II

ACTION OF ZEPHIRAN ON ESSENTIALLY ISOELECTRIC OVALBUMIN AT ROOM TEMPERATURE

Time of standing	Δ/fC	$\eta\theta/T$	Length (Å.)	M	Z
Control	No measurable birefringence			85,000	1.10
2 hr., *p*H 4.2	189–263	0.36–0.61	1140–950	238,000	1.18
24 hr., *p*H 4.3	110–157	.15–.30	1550–1200	300,000	1.62
72 hr., *p*H 4.3	135–194	.12–.30	1700–1200	385,000	1.45

Effect of Buffer Ions.—It was desirable to attempt to buffer the protein–detergent systems near *p*H 3. For this purpose glycine buffer systems were selected. Table III summarizes some results in such systems at two buffer concentrations. The high ionic strength definitely promotes aggregation; however, it is of interest that the lengths obtained by streaming birefringence are not greatly different from those obtained in the absence of buffer.

TABLE III

ACTION OF ZEPHIRAN ON OVALBUMIN AT *p*H 3 IN THE PRESENCE OF GLYCINE BUFFER

Conditions	Δ/fC	$\eta\theta/T$	Length, (Å.)	M	Z
0.07 *M* glycine, 2 hr.	214–278	0.63–1.1	940–760	267,000	1.20
0.035 *M* glycine, 2 hr.	242–322	.80–1.2	850–730	340,000	1.13
0.07 *M* glycine, 24 hr.	296–415	.62–0.97	885–730	1,250,000	1.40
0.035 *M* glycine, 42 hr.	161–298	.51–0.86	960–775	1,000,000	1.43

Results with Other Cationic Agents.—Comparative experiments were carried out with several surface active agents of the cationic type. Table IV summarizes data obtained with two of these which yielded results in good qualitative agreement with those given by Zephiran. Another reagent, dodecyltrimethylammonium chloride,[11] however, yielded anomalous results. The extinction angles were near 0° and increased with increasing gradient. The sign of the birefringence was negative in contrast to the positive birefringence found in all other cases. These results suggested the presence of at least two orientable components of opposite sign of birefringence. Accordingly measurements were made on the detergent alone and as expected low extinction angles with negative birefringence were observed. It would appear that this particular detergent is less strongly bound by the protein and forms larger or more asymmetric micelles under the conditions used than the other agents. None of the other surface active agents yielded any measurable birefringence in the absence of protein.

(11) Arquad 12, Armour and Company.

TABLE IV

RESULTS WITH CATIONIC AGENTS OTHER THAN ZEPHIRAN

Time at room temp., hr.	*p*H	Δ/fC	$\eta\theta/T$	Length, (Å.)
Cetyldimethyl-β-phenylethylammonium bromide				
2	2.7	52–194	1.54–4.15	700–415
72	2.4	210–335	1.12–1.73	780–680
Dodecylammonium chloride				
48	2.2	152–333	2.42–4.57	600–490
72	2.5	128–309	1.68–3.37	680–540

Measurements on a fifth cationic agent, cetylpyridinium bromide, were inconclusive because of the relatively low solubility of the reagent.

Discussion

It is clear the Zephiran under the conditions employed does not prevent aggregation of ovalbumin on the acid side of the isoelectric point, particularly in the presence of other ions. No solutions have been found, under these or other conditions, which yield streaming birefringence in the complete absence of aggregation. The question then arises as to whether any molecular significance can be attached to the rotary diffusion constants so derived.

In Fig. 3 there are plotted lengths computed from streaming birefringence results as ranges of values obtained from 1960 to 5880 sec.$^{-1}$. The independent variable here is the weight-average particle weight as determined by light scattering. The striking result is that there is little increase in the observed length distribution as aggregation increases. Further, the observed values are very similar to those obtained in heat denaturation and urea denaturation.[2] The simplest conclusion is that denaturation yields elongated, essentially rod-shaped, molecules about 500–600 Å. in length which then aggregate laterally.

A slightly modified picture may, however, be in better accord with the failure to obtain completely unaggregated unfolded systems. According to this picture the denaturation might be imagined as a loosening or swelling of the native protein which leads to a reduction in solubility. The swollen units might then aggregate in such a manner that unfolding is forced. If this were the mechanism the lengths observed would still have an absolute significance in terms of the molecular configuration of the polypeptide chain even though the orienting units were aggregates. According to the modified mechanism it is not necessary to assume that this configuration possesses inherent stability in the absence of aggregation forces. It is perhaps worth pointing out, though not to be taken too seriously

at present, that the length approached at low degrees of aggregation corresponds to about 1.5 Å. per amino acid residue, the spacing of the Pauling α-helix.[12]

Also plotted in Fig. 3 are lengths computed from the light scattering dissymmetry values assuming rigid rods. These lengths are in general considerably greater than the corresponding values obtained by streaming birefringence. A similar discrepancy was observed by Hocking, Laskowski and Scheraga[13] in the case of bovine fibrinogen. They suggested the presence of a trace of a very large contaminant of density so near that of the solvent that it was not removed by centrifugation. Possibly a similar explanation might hold here.

The behavior at *p*H 3 in absence of Zephiran shows clearly that an entirely different pattern of aggregation is followed in the absence of detergent. The very high particle weights and dissymmetries developed in the absence of orientability in the streaming gradient suggest that very large, nearly spherical aggregates are formed. It seems probable that the light scattering observations in this case represent a relatively small proportion of the total protein and that the bulk is unmodified.

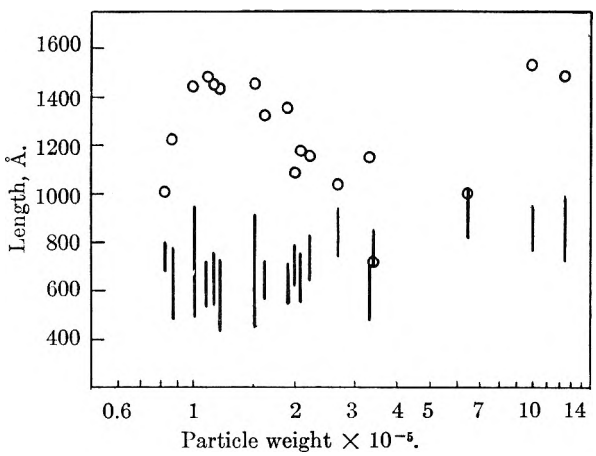

Fig. 3.—Relation between apparent particle lengths and particle weights: |, range of lengths calculated from streaming birefringence results over the gradient range 1960–5880 sec.$^{-1}$; ○, length calculated from the intrinsic dissymmetry of light scattering assuming rigid rods.

There is no apparent reason for the difference in behavior between the anionic and cationic detergents. It is well known that the anionic detergents lead to denaturation of ovalbumin at room temperature. The absence of streaming birefringence may imply that this denaturation consists essentially of swelling without unfolding and that the unfolding occurs only at elevated temperature under these conditions.

(12) L. Pauling and R. B. Corey, *Proc. Nat. Acad. Sci.*, **37**, 205 (1951).

(13) C. S. Hocking, M. Laskowski, Jr., and H. A. Scheraga, *J. Am. Chem. Soc.*, **74**, 775 (1952).

DISCUSSION

IRA KUKIN.—You mentioned that the anionic detergents did not denature the ovalbumin to give a streaming birefringence. At what values of *p*H were these studies made?

JOSEPH F. FOSTER.—The work was carried out at a *p*H value of 7 to 8. On the acid side the anionic detergent precipitates the protein.

H. B. KLEVENS.—With respect to protein–detergent interactions, it has been of interest for some time to determine whether micelles are present in these solutions and whether interaction between protein and detergent involves single ions or micelles of the latter. The results with dodecyltrimethylammonium chloride and ovalbumin at *p*H 2.2–2.5 reported above would indicate that micelles may be present in these solutions. This is interesting for previous results with anionic detergents and proteins, homogeneous as to molecular weight, indicate that, even though the binding of detergent with protein is stepwise rather than continuous, there is no evidence for the presence of micelles in these solutions. From light scattering measurements of Harrap and Schulman, *Discussions Faraday Soc.*, **13**, 197 (1953), there appears to be a continued adsorption or binding of sodium dodecyl sulfate (D) with serum albumin (A) above AD_{4n} where n is the initial number of binding sites (about 55). Recently, however, Cockbain, *Trans. Faraday Soc.*, **49**, 104 (1953), has shown by interfacial tension and by the dye titration technique that micelles are present at detergent concentrations larger than D_{4n}. For gelatin and hydrolyzed gelatin, there appears to be a definite number of D bound per protein molecule (D is a function here of the apparent molecular weight of the protein) and, at concentrations of detergent above this, the excess D forms micelles (unpublished data). Since there is this definite limit which also appears to be dependent on the molecular weight of the gelatin, this is the apparent basis for a new approach to fractionation of polyelectrolytes, which has been applied successfully to gelatin solutions by Stainsby (private communication).

JOSEPH F. FOSTER.—Binding studies, to be published elsewhere, indicate that micelles are not present in the presence of protein, under the conditions we employ, in the case of either alkylbenzene sulfonate or zephiran. Further, these detergents do not exhibit streaming birefringence, under the conditions we use, even in the micellar state. The one exception is the dodecyltrimethylammonium chloride preparation which, as mentioned in the text, does give orientation by itself and does not appear to be strongly bound by the protein.

J. L. SHERESHEFSKY.—Recent studies in my laboratory on the molecular weight of crystalline bovine albumin (Armour & Co.) by the method of monolayer formation on buffered substrates (from *p*H 4.8–7.4) showed that the supposedly denatured protein (as a result of spreading) was identical in molecular weight as when determined by the osmotic pressure method, under which conditions denaturation is not taking place. How should one characterize denaturation?

JOSEPH F. FOSTER.—There are many known cases where no change in molecular weight accompanies denaturation. Aggregation, which usually follows denaturation, might not occur in spread albumin monolayers at low surface pressures. An answer to the question is difficult indeed and quickly leads to a philosophical discussion as to what is denaturation. It is my feeling that denaturation is many different things, there being variations from protein to protein and under various conditions for a given protein. In general I think it definitely best to utilize as many different criteria as possible in attempting to characterize denaturation. Flow birefringence is particularly good for detecting gross changes in molecular shape and has been very useful in the case of ovalbumin. In other cases denaturation may not lead to such gross changes in shape. For example, I believe that serum albumin can be denatured without the appearance of flow birefringence; in that case denaturation may be essentially a swelling of the molecule.

FREE ENERGY IN CATION INTERCHANGE AS ILLUSTRATED BY PLANT ROOT–SUBSTRATE RELATIONSHIPS[1]

BY C. E. MARSHALL AND WM. J. UPCHURCH

Department of Soils, University of Missouri, Columbia, Mo.

Received March 2, 1953

Three methods for the determination of free energy changes in ionic-exchange reactions between two colloidal systems are formulated, (I) potentiometric through activity determinations, (II) by small exchange taking two cations at a time, (III) by equilibration, separation and analysis. The characteristics of a cation-exchanger Amberlite IR-120 with respect to potassium calcium and hydrogen ions are given. It is shown to be markedly multifunctional, the bonding energy for potassium showing a range from <500 to 3400 cal. per mole. In plant growth studies with soybeans, dilute suspensions of Amberlite IR-120, Wyoming bentonite and Putnam clay were compared with chlorides and bicarbonates of potassium and calcium. It is shown that the uptake of a particular cation is governed in part by the free energy change in the reaction between the acid root and the exchanger. Clear differences in uptake were found for free energy changes of 3000 cal. per mole.

The free energy changes in cation-exchange reactions are commonly considered to be small, and until recently very little attention was paid to them. Extensive work has been done on equilibrium constants, particularly by those concerned with synthetic exchangers, but the further step of proceeding from these constants to the free energy change has seldom been taken. There are good reasons for this, namely, uncertainty as to validity of the assumptions used in setting up the equations, and lack of constancy of K over a wide range of exchange conditions. These limitations, however, are not inherent in the situation. What has been needed is a sensitive means of recognizing differences between ionic sites on exchange materials, together with procedures for the formulation of exchange reactions without the usual assumptions. These objectives were first accomplished through potentiometric activity measurements; however, it can now be seen that the final result, namely, the determination of free energy changes, can be attained analytically.

Potentiometric Methods. 1.—The first potentiometric determinations which gave the free energy change for cation-exchange reactions were based on Marshall's theory of nonporous membrane electrodes.[2] This was unfortunately formulated in terms of the difference in heat of adsorption of two cations, but actually it corresponds to the free energy change in a reaction such as

$$\text{KCl} + \text{Na membrane} \rightleftarrows \text{NaCl} + \text{K membrane}$$

Later Mukherjee and Marshall applied the method to plugs of plastic clay.[3] Cells of the type

$$\text{Calomel Sat. KCl} \left| \begin{matrix}\text{KCl} \\ C_1\end{matrix} \right| \begin{matrix}\text{Membrane} \\ \text{or plug}\end{matrix} \left| \begin{matrix}\text{NaCl} \\ C_2\end{matrix} \right| \text{Sat. KCl Calomel}$$

were employed.

Values obtained for a bentonite clay were of the order of 230 cal. per equivalent for the potassium–sodium difference.

2.—Following the procedures used by Marshall and his co-workers[4-7] single cationic activities can be determined in dilute colloidal systems. If the total concentration of the given cation is known, then the ratio a/c corresponds to the ionic activity coefficient for a true solution. It is termed the fraction active (f). If a completely dissociated colloid containing the same total concentration of cation is chosen as the standard state then the cationic free energy difference between the actual system and the standard state is

$$RT \ln (c/a) = RT \ln (1/f)$$

This has been termed the cationic mean free bonding energy. It can be thought of in terms of a reaction such as Na colloid $\rightleftarrows$ $Na^+ + Colloid^- - (\Delta F)_{Na}$. Such reactions involve entropy changes as well as free energy changes and in reactions where several such dissociations are involved, both the free energies and the entropies can be treated additively. Thus an exchange such as

$$\boxed{\text{I}}^{Na} + \boxed{\text{II}}^{K} \rightleftarrows \boxed{\text{I}}^{K} + \boxed{\text{II}}^{Na}$$

can be considered as comprising four of the above dissociation reactions, the free energies being added together with due regard to sign, in order to give the mean free energy change for the whole reaction. This formulation corresponds with the concept that if each of the constituents is completely dissociated, then we have simply a mixing process with zero free energy change. It applies equally well to reactions between exchangers and salt solutions and to interchange of cations between different exchangers.

A number of studies of the dissociation of clay minerals have been published.[8-14] All indicate that a given cation can be held on a given clay with a wide range of bonding energies. Characteristic bonding energy curves are found, which vary with the clay and with the cation. The same is true of humic matter from soils and peats, and even certain synthetic resin exchangers show variations.

The examples which will be discussed below involve plant roots as exchangers. In the past few years the exchange properties of living roots have been shown to be reasonably well defined.[15-17] They interact with nutrient media by exchanging hydrogen ions for metallic cations. It is now believed that this is the predominant mechanism by which cations are taken up by plants.[18-21] We can therefore formulate the hydrogen–potassium or the hydrogen–calcium exchanges for roots as for other colloidal systems. We have for hydrogen–potassium

(1) Contribution from the department of soils, Missouri Agricultural Experiment Station, Columbia, Missouri, Journal Series No. 1352.

(2) C. E. Marshall, THIS JOURNAL, **52**, 1284 (1948).

(3) S. J. Mukherjee and C. E. Marshall, *ibid.*, **55**, 61 (1951).

(4) (a) C. E. Marshall and W. E. Bergman, *J. Am. Chem. Soc.*, **63**, 1911 (1941); (b) C. E. Marshall and C. A. Krinbill, *ibid.*, **64**, 1814 (1942).

(5) C. E. Marshall and A. D. Ayers, *ibid.*, **70**, 1297 (1948).

(6) C. E. Marshall and L. O. Eime, *ibid.*, **70**, 1302 (1948).

(7) E. O. McLean, S. A. Barber and C. E. Marshall, *Soil Sci.*, **72**, 315 (1951).

(8) C. E. Marshall and W. E. Bergman, THIS JOURNAL, **46**, 52 (1942).

(9) C. E. Marshall and W. E. Bergman, *ibid.*, **46**, 327 (1942).

(10) C. E. Marshall and C. A. Krinbill, *ibid.*, **46**, 1077 (1942).

(11) E. O. McLean and C. E. Marshall, *Soil Sci. Soc. Am. Proc.*, **13**, 179 (1949).

(12) B. Chatterjee and C. E. Marshall, THIS JOURNAL, **54**, 671 (1950).

(13) S. A. Barber and C. E. Marshall, *Soil Sci.*, **72**, 373 (1951).

(14) S. A. Barber and C. E. Marshall, *ibid.*, **73**, 403 (1952).

(15) D. E. Williams and N. T. Coleman, *Plant and Soil*, **2**, 243 (1950).

(16) M. Drake, *et al.*, *Soil Sci.*, **72**, 139 (1951).

(17) E. R. Graham and W. L. Baker, *ibid.*, **72**, 435 (1951).

(18) H. Jenny and R. Overstreet, *Proc. Natl. Acad. Sci.*, **24**, 384 (1938).

(19) H. Jenny, "Mineral Nutrition of Plants," Wisconsin University Press, Madison, Wis., Chapter 5.

(20) H. Lundegardh, *Soil Sci.*, **54**, 177 (1942).

(21) A. C. Schuffelen and R. Loosjes, *Proc. Nederland Akad. Wetenschappen*, **45**, 726 (1942).

$$(\Delta F)_{\text{Reaction}} = -RT \ln \frac{c'_K}{a'_K} + RT \ln \frac{c'_H}{a'_H} + RT \ln \frac{c''_K}{a''_K} - RT \ln \frac{c''_H}{a''_H}$$

in which c' and a' refer to the substrate and c'' and a'' to the root. This can also be written.

$$(\Delta F)_{\text{Reaction}} = RT \ln \frac{c'_H}{c'_K} \cdot \frac{a'_K}{a'_H} + RT \ln \frac{c''_K}{c''_H} \cdot \frac{a''_H}{a''_K}$$

In the case of the hydrogen–calcium interchange the free energy change per equivalent is given by

$$(\Delta F)_{\text{Reaction}} = -\frac{1}{2} RT \ln \frac{c'_{Ca}}{a'_{Ca}} + RT \ln \frac{c'_H}{a'_H} + \frac{1}{2} RT \ln \frac{c''_{Ca}}{a''_{Ca}} - RT \ln \frac{c''_H}{a''_H}$$

or

$$(\Delta F)_{\text{Reaction}} = RT \ln \frac{c'_H}{\sqrt{c'_{Ca}}} \cdot \frac{\sqrt{a'_{Ca}}}{a_H} + RT \ln \frac{\sqrt{c''_{Ca}}}{c_H} \cdot \frac{a''_H}{\sqrt{a''_{Ca}}}$$

In computing these free energy changes several alternative methods present themselves.

1. As mentioned above, in some cases it is possible to determine the respective activities and concentrations separately for each of the four systems. Titration curves extending over a considerable range are needed so that bonding energy curves can be constructed, both for hydrogen and for the metallic cation. The values to be used should be selected with due regard to the concentrations of the colloidal systems and to the position of the final equilibrium as regards composition. Recent work by McLean and Baker[22] has shown that activity measurements can be made with good reproducibility on carefully prepared plant roots.

2. A second method is based on the principle of small exchanges. For ions of the same valency, the ratios of the concentrations of two cations simultaneously released by an infinitesimally small exchange against any cation are equal to the corresponding ratios of the activities.[23] For a monovalent–divalent pair such as calcium and hydrogen the ratio $C_H/\sqrt{C_{Ca}}$ for an infinitesimally small exchange is equal to $a_H/\sqrt{a_{Ca}}$ for the original colloid. Thus by carrying out small exchanges separately on the two colloids the activity ratios are determined. The total concentrations are generally known, so that all the quantities required in the equations are available from analytical results. The separate activity ratios should be determined for various compositions so that the correct values for the final equilibrium can be selected.

3. The third method is even simpler. It is based on the fact that when two colloidal systems are in equilibrium with the same intermicellar liquid they are in equilibrium with each other. From the Donnan relationships we then have

$$a_H/a'_K = a''_H/a''_K$$

for the monovalent–monovalent case and

$$a'_H/\sqrt{a'_{Ca}} = a''_H/\sqrt{a''_{Ca}}$$

for divalent–monovalent cations. When these relationships are substituted in the appropriate equations for the free energy change all the activities cancel out and we are left with

$$(\Delta F)_{\text{Reaction}} = RT \ln \frac{c'_H}{c'_K} + RT \ln \frac{c''_K}{c''_H}$$

and

$$(\Delta F)_{\text{Reaction}} = RT \ln \frac{c'_H}{\sqrt{c'_{Ca}}} + RT \ln \frac{\sqrt{c''_{Ca}}}{c''_H}$$

respectively, for the two cases discussed. Hence, it is only necessary to separate the two colloidal systems and determine the cationic concentrations by analysis. This value of $(\Delta F)_{\text{Reaction}}$ then gives the free energy change for the particular proportions of cations found at equilibrium.

Characterization of Colloidal Media.—If it is true that the first reaction in the passage of cations from substrate to plant is an exchange against hydrogen at the root surface, then in comparing different substrates one with another, three factors should be controlled: (a) the activities in the substrates of the cation under consideration, (b) the corresponding activities of the hydrogen ion, (c) the free energy change for the exchange reaction. If two substrates are carefully matched with regard to equality of these factors then irrespective of their chemical nature or as to whether the plants grow in true solution or in a colloidal medium, the uptake by the root should be the same. The characterization of colloidal media thus involves free energy differences such as

$$(\Delta F)_H - (\Delta F)_K, \text{ or } (\Delta F)_H - (\Delta F)_{Ca/2}$$

which can be determined from the respective titration curves by measuring both the *p*H and the metallic cation activity at each point. For plants growing in dilute solutions of soluble salts the corresponding free energy difference would depend on the strength of the acid produced in the reaction. Thus with chlorides, sulfates or nitrates it would be practically zero, but with acetates or bicarbonates it would have a positive value lying somewhere between zero and the value derived from the dissociation constant of the acid. The actual figure would be calculated from the hydrogen ion activity and the total concentration of acid in the substrate at equilibrium.

The free energy change for the exchange reaction includes also the difference $(\Delta F)_{\text{Cation}} - (\Delta F)_H$ for the root itself. This quantity will, with a single cation, be taken as constant in our comparisons, although it is quite conceivable that some variation with the degree of saturation of the root surface may be present.

Amberlite IR-120.—The titration curves of dilute suspensions of Amberlite IR-120 with potassium hydroxide are given in Fig. 1, which comprises three sets of data. The top graph gives the conventional *p*H curve, the middle graph gives the curve connecting potassium ion activity with amount of base added and the bottom graph shows the cationic free bonding energies of potassium and hydrogen. The Amberlite suspension used was 0.2%. The suspension contained only particles $< 1\ \mu$, prepared by grinding Amberlite in a ball mill and removing coarser material by settling under gravity. The suspension was then electrodialyzed to remove all cations except H^+.

The curves indicate that potassium is considerably more firmly held than hydrogen up to the equivalence point. The curves probably cross close to this point.

The great influence which the accompanying or complementary ion can exert upon the bonding energy of a given cation is shown by Fig. 2. Here potassium–hydrogen and potassium–calcium Amberlites are compared using methods similar to those previously employed for clays.[11,13,14] The mean free bonding energies of potassium are plotted for the two systems as a function of the total potassium present. In presence of hydrogen as the complementary ion, potassium is held much more firmly than where calcium is the complementary ion. This effect is qualitatively similar to the

(22) E. O. McLean and F. E. Baker, *Soil Sci. Soc. Am. Proc.*, **17**, (1953).

(23) C. E. Marshall, *ibid.*, **8**, 175 (1944).

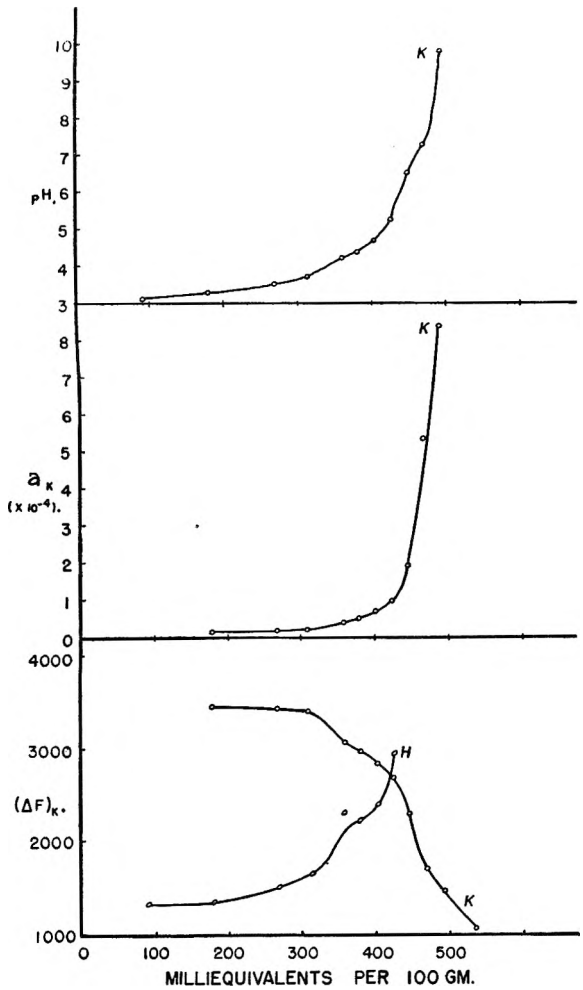

Fig. 1.—*p*H (top), potassium ion activity (middle), and cationic bonding energies of potassium and hydrogen (lower) plotted against the potassium added (in milliequivalents per 100 g.; Amberlite IR-120, particle size $<1\mu$, concentration 0.2%).

situation in the clay minerals, but the spread between the two curves is even wider in the case of the Amberlite. This is due to the low bonding energy of the hydrogen ion on Amberlite and simultaneously, the high bonding energy for calcium. Hence the difference in the two cations which complement the potassium is unusually large. We have here a very good illustration of the Jarusov effect[24] for a multifunctional surface, namely, that the cation with the greater bonding energy preempts those positions on the surface corresponding to the greater energy release, leaving for the cation of lesser bonding energy, those positions affording least energy release. The range of potassium ion bonding energies is very great—from about 500 cal. per mole, where there is a small proportion of potassium and the rest calcium, to 3400 cal. per mole for potassium–hydrogen systems with up to 70% potassium. It is evident that Amberlite IR 120 is markedly multifunctional in its dissociation—not monofunctional as has sometimes been assumed.

The characterization of calcium–hydrogen Amberlites by titration curves is rendered uncertain

(24) S. S. Jarusov, *Soil Sci.*, **43**, 285 (1937).

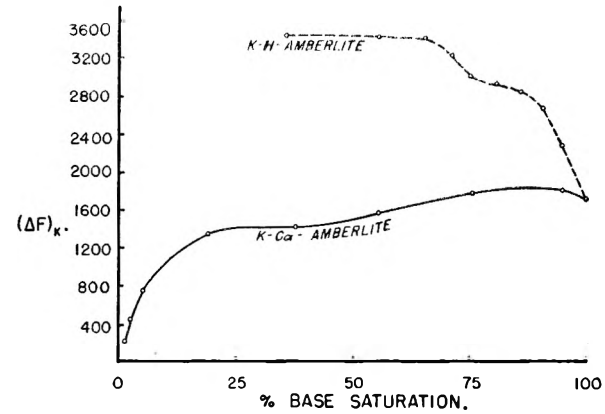

Fig. 2.—Bonding energies of the potassium ion in potassium hydrogen and potassium calcium Amberlites IR 120, as a function of the percentage saturation with potassium (particle size $<1\mu$, concentration 0.2%).

over a large part of the acid range by the extremely high bonding energy of calcium. Using 0.2% Amberlite suspensions the calcium activity was much below the correction for hydrogen ions up to *p*H 5, and the first reliable figure actually obtained was at *p*H 6.3, very close to the point of equivalence. The molar mean free bonding energy of calcium was about 3350 cal., which is higher than for any calcium clay mineral we have examined. Below equivalence the value is certainly higher than this, and probably it will approximate to twice the bonding energy for potassium, or from 5000–7000 cal. per mole.

Clay Systems.—The two clay systems, namely, Putnam clay and Wyoming bentonite which were included in the series, have already been characterized in studies reported from this Laboratory.[8–12] The cation activities were, of course, determined afresh on the systems employed for growing soybeans, and bonding energies were calculated.

True Solutions.—Chlorides and bicarbonates of potassium and calcium were used. In the case of the bicarbonates the hydrogen ion bonding energy was calculated by the same procedure as that employed for the colloidal systems.

Plant Roots.—Soybeans were grown in the respective nutrient media with continuous aeration and intermittent renewal. The frequency of change was accommodated to the rate of growth. When the plants had acquired several leaves then it became necessary to renew the solutions daily. Even this was inadequate in certain cases, hence the cation activities were determined also in the depleted solutions.

The roots were removed from the nutrient media, washed quickly in distilled water and then caused to react with $M/400$ barium chloride solution. The quantity was arranged to correspond to a 10% exchange, but in actual fact more cations passed into solution than corresponded to the chloride added. The exchange could therefore no longer be considered strictly "small." Hence the ratio of the amounts of two cations in solution would not be an exact measure of the ratio of the activities, but the general trends should still show themselves. A second exchange with a larger quantity of barium chloride was designed to give

practically complete replacement of the root cations by barium. Finally, the roots and tops were dried and analyzed separately. The systems, individually comprising two plants, were set up in triplicate. The yields were obtained separately for each and analyses were performed on the whole sample of six plants.

Experimental Results

1. **Comparisons of Chlorides and Bicarbonates as Nutrient Media.**—Considerable differences were found when chlorides and bicarbonates of potassium and calcium were employed singly as nutrient media. In each case the bicarbonate solution gave the higher uptake: by "small" release, by total exchangeable quantity and by total quantity in roots and tops. The actual yields of dry matter were closely alike in these comparisons. The *p*H values were lower in the chloride systems than in the bicarbonates by about one unit, so that it is not possible to use the calculated free bonding energy of the hydrogen in carbonic acid as the only variable in the situation. However its magnitude is such that it overshadows the *p*H variation. The calculated values range around 2500–3300 cal. per equivalent, the variability being due to particularly rapid depletion of the calcium bicarbonate systems. The fact that the *p*H values were lower in the chloride systems than the bicarbonate systems would add the equivalent of about 1360 cal. more from $(pH_1 - pH_2)RT$.

2. **Comparison of Potassium Chloride and Other Potassium Systems as Nutrient Media.**—In order to use well defined bonding energies both for hydrogen and potassium on Amberlite a point was chosen on the acid side of equivalence. This also necessitated a relatively high Amberlite concentration so as to bring the potassium activity up to the value for the true solutions. From the measured potassium activity and *p*H of the 0.5% Amberlite suspension used, the respective bonding energies of K^+ and H^+ were calculated to be $(\Delta F)_K = 2790$ cal. and $(\Delta F)_K = 2690$ cal. The difference is thus very small and the situation as regards plant roots should be essentially the same as in an acidic chloride solution at the same *p*H and the same potassium ion activity.

Tables I and II indicate that the over-all resemblance between these two treatments, although they differ in some details, is very great.

The more dilute potassium Amberlite at about the same potassium ion activity but higher *p*H can also be drawn into the comparison. The free energy change is here somewhat uncertain since we are very close to the equivalence point, but would appear to be −1100 cal. to which should be added around +3600 cal. corresponding to the *p*H difference. These roots took up considerably more potassium than did those in the acidic Amberlite, but the total growth was about the same. This last fact strongly suggests a limiting factor in the situation, namely, loss of calcium from the seedling to the Amberlite, which has a very high bonding energy for calcium.

Three systems which are closely comparable as regards *p*H and initial potassium activity are the dilute potassium Amberlite mentioned above, potassium bentonite and potassium Putnam clay. The bonding energy differences are difficult to establish with certainty, but would seem to be in the range +2000 − +3000 cal. The three systems show some differences but the order is not consistent. The over-all picture, however, is about what would be expected from a free energy change of this magnitude.

Comparison of Calcium Chloride and Other Calcium Systems.—A very clear cut comparison can be made between the calcium chloride and the calcium bentonite systems, which were closely similar as regards calcium ion activity and *p*H. The bonding energy difference per equivalent favored the bentonite system by about +2500–3000 cal. The colloidal system gave consistently the higher calcium uptake, whether measured in terms of a small exchange, or total exchangeable calcium, or total calcium content of roots and tops, or total yield of dry matter.

The calcium Amberlite system also gave similar results, but the bonding energy situation is uncertain at the *p*H employed.

TABLE I

CHARACTERISTICS OF NUTRIENT MEDIA

	System	$(\Delta F)_H - (\Delta F)_{cation}$ (cal. per equiv.)	*p*H	C_K, moles/l.	C_{Ca}, moles/l.
1	KCl	0	5.90	1.11×10^{-4}	.....
2	KCl (acidic)	0	4.55	1.67	.....
3	$KHCO_3$	+3300	7.17	1.12	.....
4	$CaCl_2$	0	5.92	..	5.6×10^{-5}
5	$Ca(HCO_3)_2$	+2500	7.10	..	5.5
6	K Amberlite 0.5%	−100	4.45	1.75	.....
7	K Amberlite 0.024%	(Uncertain)	7.20	1.60	.....
8	Ca Amberlite 0.23%	(Uncertain)	7.60	..	8.8
9	K Bentonite 0.10%	(Uncertain)	7.06	1.42	.....
10	Ca Bentonite 1.8%	+3000	5.62	..	5.6
11	K Putnam 0.17%	(Uncertain)	7.01	1.18	.....

TABLE II

COMPOSITION OF 19-DAY OLD SOYBEANS GROWN ON NUTRIENT MEDIA

	System	Cation content, meq. per 100 g. Tops K	Tops Ca	Roots K	Roots Ca	Dry matter (6 plants) Tops	Roots
1	KCl	83	10	74	17	1.27	0.32
2	KCl (acidic)	44	11	19	9	0.90	.26
3	$KHCO_3$	120	12	118	24	1.29	.43
4	$CaCl_2$	25	55	33	15	1.61	.62
5	$Ca(HCO_3)_2$	29	140	43	26	1.41	.70
6	K Amberlite (ac.)	32	7	12	5	0.93	.16
7	K Amberlite	46	12	42	8	0.92	.21
8	Ca Amberlite	33	108	34	11	2.43	1.24
9	K Bentonite	65	11	60	6	0.92	0.22
10	Ca Bentonite	22	62	24	11	2.23	0.95
11	K Putnam	47	8	68	5	1.08	0.24
12	Seed	50	12			0.90	

Discussion

These preliminary results on growing plants are naturally subject to greater variations than would be tolerated on purely inanimate exchangers. They indicate, however, that the free energy changes in cation exchange reactions are of great importance in the uptake of cations by plant roots. The precision of such experiments is likely to be considerably improved now that a start has been made. Ultimately it may be possible to record consistent differences in growth and uptake for free energy differences of only a few hundred calories per equivalent. Finally this approach helps to explain many puzzling results in the literature, in which comparisons have been made between colloidal media and true solutions or between different colloidal media. The competition between the plant root and its environment for the available cations can now receive quantitative expression.

DISCUSSION

J. TH. G. OVERBEEK.—If the plant grows slowly enough and the root can be considered to be in equilibrium with the nutrient system, growth and ion exchange should only depend upon the activities in the solution. If the amount of buffering of the solutions with respect to its ion content by the presence of ion exchange material proves to be important, this means that the *rate* of exchange is more important than the equilibrium situation.

WETTING OF FLUORINATED SOLIDS BY HYDROGEN-BONDING LIQUIDS

BY A. H. ELLISON, H. W. FOX AND W. A. ZISMAN

Naval Research Laboratory, Washington, D. C.

Received March 2, 1953

(1) A study has been made of the wettability of adsorbed monolayers of ω-monohydroperfluoroundecanoic acid. The results obtained on this surface (comprising CF_2H groups) are compared with previous results on adsorbed monolayers of perfluorodecanoic acid (comprising CF_3 groups) and solid polytetrafluoroethylene (comprising CF_2 groups). (2) It is shown that for "normal" liquids (*i.e.*, those for which only van der Waals forces of adhesion are operative) the contact angles on CF_2H surfaces are larger than on CF_2 surfaces and nearly as large as on CF_3 surfaces. (3) Alcohols, acids and amines are found to give abnormally low contact angles on CF_2H and CF_3 surfaces, but only amines give low angles on polytetrafluoroethylene. This can be accounted for by the ability of these polar liquids to form hydrogen bonds with the fluorine-containing surfaces. Esters, lacking a suitable hydrogen atom, are shown to bond only to the CF_2H surface (which can supply the necessary hydrogen atom); alcohols and acids bond to CF_2H and CF_3 surfaces; primary amines bond to all three fluorinated surfaces because of their ability to form "double" hydrogen bonds. These phenomena are believed to be new examples of the "unsymmetrical hydrogen bond" described by Pauling.

I. Introduction

Previous studies on the spreading of liquids on various low-energy surfaces[1–5] have shown that the wettability depends on the atomic composition of the surface. Hence the equilibrium contact angle θ for each liquid increases in the order $\theta_{CH_2} < \theta_{CH_3} < \theta_{CF_2} < \theta_{CF_3}$. It was of interest to compare the wettability of a surface comprising CF_2H groups with those previously studied. Such surfaces can be obtained by adsorbing on a solid surface monolayers of acids of the composition $HF_2C(CF_2)_n$-COOH. The preparation of these acids has been described by Berry.[6]

The contact angle of a liquid on a given low-energy surface usually increases with its surface tension. Exceptions to this generalization occurred[3–5] when the liquid had a marked tendency to dissolve the surface molecules of the wetted solid. In this circumstance, there was observed a lower contact angle than could be expected from the behavior of many other liquids on the given solid. In the case of the surface comprising CF_3 groups, however, two apparent anomalies appear in the data[5] which cannot be accounted for on the basis of solubility. These concern the wettability by methyl alcohol (γ_{LV} = 22.6 dynes/cm., θ = 15°) and by *n*-heptylic acid (γ_{LV} = 28.3 dynes/cm., θ = 44°). Here the contact angles are to be compared with those of *n*-octane (γ_{LV} = 21.8 dynes/cm., θ = 56°) and sec-butylbenzene (γ_{LV} = 28.7 dynes/cm., θ = 65°), respectively. However, methyl alcohol and *n*-heptylic acid exhibited "normal" contact angles on surfaces made up of CF_2, CH_3 or CH_2 groups.[1,3,4] The fact that the two liquids which showed greater than normal wetting ability both contained a polar hydrogen atom suggested that the additional adhesional energy was due to hydrogen bonding. This led us to investigate the wetting behavior of homologous series of *n*-alkanoic acids, *n*-alkanols and *n*-alkyl amines on surfaces comprising oriented CF_3, CF_2, and CF_2H groups.

(1) H. W. Fox and W. A. Zisman, *J. Colloid Sci.*, **5**, 514 (1950).
(2) H. W. Fox and W. A. Zisman, *ibid.*, **7**, 109 (1952).
(3) H. W. Fox and W. A. Zisman, *ibid.*, **7**, 428 (1952).
(4) E. Shafrin and W. A. Zisman, *ibid.*, **7**, 166 (1952).
(5) F. Schulman and W. A. Zisman, *ibid.*, **7**, 465 (1952).
(6) Kenneth L. Berry, U. S. Patent 2,559,629 (July 10, 1951).

II. Experimental Methods

Surfaces comprising CF_2H groups were formed by adsorbing from *n*-decane solution on polished platinum foil monolayers of $HF_2C(CF_2)_9COOH$ (or ω-monohydroperfluoroundecanoic acid). For the sake of brevity, this acid will be designated as ψ-undecanoic acid. Surfaces comprising CF_3 groups were formed as before[5] from *n*-decane solution of $CF_3(CF_2)_8COOH$ (designated as φ-decanoic acid). Surfaces of CF_2 groups were obtained as before[1] as smoothed solid polytetrafluoroethylene. Contact angles were determined with the contact angle goniometer described earlier.[1] Reproducibility of the platinum foils was assured by checking within ±2° the contact angle reported previously[5] for *n*-hexadecane on a close-packed monolayer of φ-decanoic acid.

Since the ψ-undecanoic acid was supplied as the pure ammonium salt, the latter was decomposed in aqueous solution and the free acid extracted with toluene. Recrystallization from toluene produced a white, flaky solid with a melting point of 96–97°. Each of the organic liquids used in this study was carefully purified as previously described[1] and was stored in the dark under refrigeration when not in use. The surface tension ($\gamma_{LV}°$) of each of these liquids was obtained from the references indicated in Table I.

III. Results

Table I lists the measured equilibrium contact angles of various liquids on the three fluorinated surfaces of interest. Previously reported contact angle data for some of these liquids on polytetrafluoroethylene[1] and on the φ-decanoic acid monolayer[5] are included for comparison. Liquids are grouped by chemical type and for each type are given in the order of decreasing surface tension. It is to be noted that as before[1–5] and with few exceptions, the lower the surface tension in a homologous series of liquids, the lower the contact angle. This rule does not hold when comparing non-homologous liquids. It is apparent that the contact angles on the CF_2H surface are from around 5 to 30° lower than those on the CF_3 surface with the exception of *n*-octylamine and *n*-heptylamine; the latter differ by an amount which is equal to or less than the experimental uncertainty. Although the CF_2H surface is less well wetted by the *n*-alkanes than the CF_2 surface, it is more wetted by liquid carboxylic acids, amines and esters. Of the miscellaneous liquids, the polar substances have a greater tendency to wet the CF_3 and CF_2H surfaces than the CF_2 surface.

In Table I will also be found the value of the work of adhesion (W_A) calculated from the approximate relation $W_A = \gamma_{LV}°(1 + \cos\theta_E)$ for each solid/liquid system. The error in W_A due to the neglect of the term $f_{SV}°$ (the free energy of immersion of the solid in the saturated vapor of the liquid) has been shown to be small for CF_3 and CF_2 surfaces.[1,5] The difference in W_A between the CF_3 and CF_2H surfaces is given in the last column of Table I for each liquid; it is about 1–3 ergs/cm.^{2} for the *n*-alkanes, the same for the *n*-alkanoic acids, 4–7 ergs/cm.^{2} for the *n*-alkanols, zero for the *n*-alkyl primary amines, and 11–15 ergs/cm.^{2} for the esters. The variation in this difference for any homologous series of liquids is small, but the differences between series is significantly larger showing the effect of the polar group.

TABLE I

WETTING OF ADSORBED FLUORINATED ACID MONOLAYERS AND SOLID POLYTETRAFLUOROETHYLENE BY VARIOUS LIQUIDS AT 20°

Liquid	Surface tension $\gamma_{LV}°$, dynes/cm.	Ref.	Equilibrium contact angle, θ, deg., upon surfaces made of: CF_3[a]	CF_2H[b]	CF_2[c]	Approximate work of adhesion, ergs/cm.^{2}, $W_A = \gamma_{LV}(1 + \cos\theta)$, for surfaces made of: CF_3	CF_2H	CF_2	ΔW_A (CF_2H – CF_3)
n-Alkanes									
Hexadecane	27.6	5	72[d]	67	46[e]	36.1	38.5	46.8	2.4
Tetradecane	26.7	5	69[d]	65	44[e]	36.3	38.0	45.9	1.7
Dodecane	25.4	5	67[d]	59	42[e]	35.3	38.4	44.3	3.1
Decane	23.9	5	62[d]	53	35[e]	35.1	38.3	43.5	3.2
Octane	21.8	5	56[d]	50	26[e]	34.0	35.8	41.4	1.8
Hexane	18.4	5	41[d]	35	12[e]	32.3	33.5	36.4	1.2
								Mean	2.7
Esters									
Tricresyl phosphate	40.9	5	82[d]	65	75[e]	46.6	58.2	51.5	11.6
Tetra (mixed phenyl cresyl) silicate	39.8	5	93[d]	71		37.6	52.8		15.2
Benzylphenylundecanoate	37.7	5	85[d]	62	67[e]	41.0	55.4	52.6	14.4
Di-(2-ethylhexyl) phthalate	31.2	5	71[d]	40	63[e]	41.4	55.1	45.4	13.7
1,6-Hexamethylene glycol di-2-ethyl hexanoate	30.2	5	66[d]	39	63[e]	42.5	53.7	43.9	11.2
								Mean	13.2
Acids									
Pelargonic	29.5	7	55	50	55	46.4	48.5	46.4	2.1
Caprylic	29.2	7	55	43	52	46.0	50.6	47.2	4.6
Heptylic	28.7	7	53	44	55	45.9	49.3	45.2	3.4
Valeric	27.4	7	23	16	48	52.6	53.8	45.7	1.2
Butyric	26.8	7	25	11	42	51.1	53.1	46.7	2.0
								Mean	2.6
Alcohols (Primary)									
n-Decyl	28.8	9	69	56	46	39.1	44.9	48.8	5.8
n-Octyl	27.6	9	66	49	48	38.8	45.7	46.1	6.9
n-Heptyl	27.2	9	63	44	48	39.5	46.7	45.4	7.2
n-Hexyl	26.2	9	60	39	50	39.3	46.5	43.1	7.2
n-Amyl	25.8	9	52	28	34	41.7	48.6	47.2	6.9
								Mean	6.8
Amines (Primary)									
n-Octyl	27.7	9	17	18	32	54.9	54.6	51.2	−0.3
n-Heptyl	27.0	9	11	13	23	53.7	53.5	51.8	−0.2
n-Amyl	25.2	8	9	5	20	50.1	50.3	48.9	0.2
n-Butyl	24.0	8	Spr.	Spr.	18	..	..	46.8	
								Mean	−0.1
Miscellaneous									
Water	72.8	5	102[d,f]	97[f]	108[e]	57.5	63.9	50.3	
Glycerol	63.4	5	101[f]	89[f]	100[e]	51.3	64.6	52.4	
Aroclor 1248	44.2	5	92[d]	83	78[e]	42.7	49.6	53.4	
Hexachlorobutadiene	36.0	5	77[d]	69	60[e]	44.1	48.9	54.0	
t-Butylnaphthalene	33.7	5	71[d]	68	65[e]	44.7	46.4	48.0	

[a] Monolayer of perfluorodecanoic acid adsorbed on platinum foil. [b] Monolayer of ω-hydroperfluoroundecanoic acid adsorbed on platinum foil. [c] Solid polytetrafluoroethylene. [d] Reference 5. [e] Reference 1. [f] Cu substrate.

Figure 1 is a graph of cosine θ_E against the surface tension $\gamma_{LV}°$ of the *n*-alkanes on the several low-energy surfaces. It is seen that the relative order of the contact angles of these non-polar liquids on the different surfaces is $\theta_{CF_2} > \theta_{CF_2H} > \theta_{CF_2} > \theta_{CH_3}$. A straight line represents the relation between $\gamma_{LV}°$ and cos θ_E for a CF_2H surface; this is consistent with the results found for other low-energy surfaces.[1-5] The parallelism of the graphs for CF_3 and CF_2H surfaces is striking.

Figures 2A, B and C are plots of cos θ against $\gamma_{LV}°$ for the *n*-alkanes (represented by the dashed line), *n*-alkanols, alkanoic acids, primary amines, and a miscellaneous group of esters on surfaces comprising close-packed CF_2H, CF_3, and CF_2 groups, respectively. It is seen that since the alcohols, acids and amines tend to wet CF_3 and CF_2H surfaces more than do the alkanes of the same surface tension, the lines in Figs. 2A and 2B of each of these families of polar liquids lie above the line for the alkanes. Only the amines show this increase in wettability on the CF_2 surface (Fig. 2C), the points for the other polar liquids clustering about the line for the alkanes. Esters wet CF_2H and CF_3 surfaces more than do the alkanes but behave "normally" on the CF_2 surface; furthermore, esters wet the CF_2H surface more than the CF_3 surface. From the slope of the straight lines of Figs. 2A, B and C it is evident that the ability of the alcohols and acids to wet surfaces comprising CF_2H and CF_2 groups is more strongly affected by increasing the chain length of the molecules than is the case with the amines.

(7) D. C. Jones and L. Saunders, *J. Chem. Soc.*, 2944 (1951).
(8) A. I. Vogel, *ibid.*, 1825 (1948).
(9) This research.

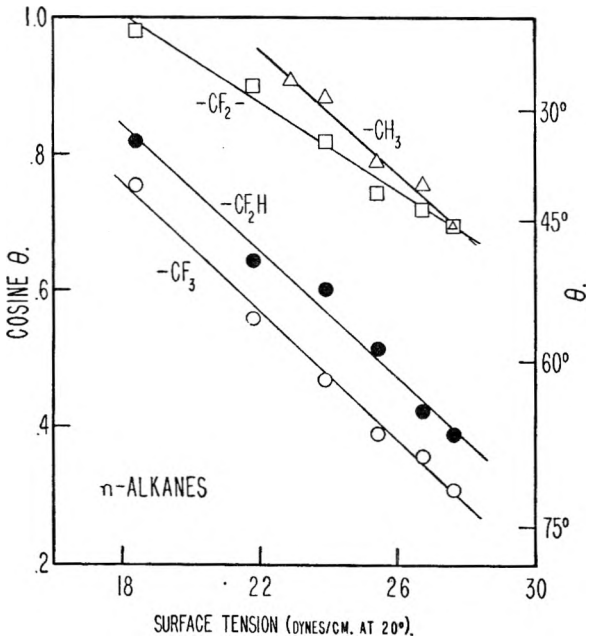

Fig. 1.—Cosine of the contact angle *versus* surface tension for *n*-alkanes on surfaces composed of $-CF_3$, $-CF_2H$, $-CF_2-$ and CH_3 groups.

were compared with those recently found for films of ϕ-dodecanoic acid.[11] This comparison reveals that the former are slightly more wettable than the latter. By interpolation the contact angles of the alkanes on a film of ϕ-undecanoic acid were estimated to be 75, 73, 70, 66 and 61° for the C_{16}, C_{14}, C_{12}, C_{10} and C_8 *n*-alkanes, respectively. Hence it can be concluded that the differences in wettability of the ψ-undecanoic and ϕ-decanoic acids are not due to differences in chain length, but are caused by differences in the wettability of a surface of close-packed and oriented CF_3 and CF_2H groups.

Discussion

Because of the homology in atomic composition of surfaces comprising CF_2H groups with thoss comprising CF_3 and CH_3 groups, it was expected that the wettability of the CF_2H surfaces would be intermediate between the other two. It is clear from the data that the wettability of CF_2H surfaces is only slightly greater than that of CF_3 surfaces and is substantially less than that of solid polytetrafluoroethylene with respect to "normal" liquids, *i.e.*, those for which only van der Waals' forces of adhesion are operative. Evidently, the CF_2H surface has the smallest free surface energy, next to the CF_3 surface,[5] of any yet investigated. Adsorbed monolayers of compounds of the general formula $HF_2C(CF_2)_nCOOH$ are therefore practically as satisfactory for producing

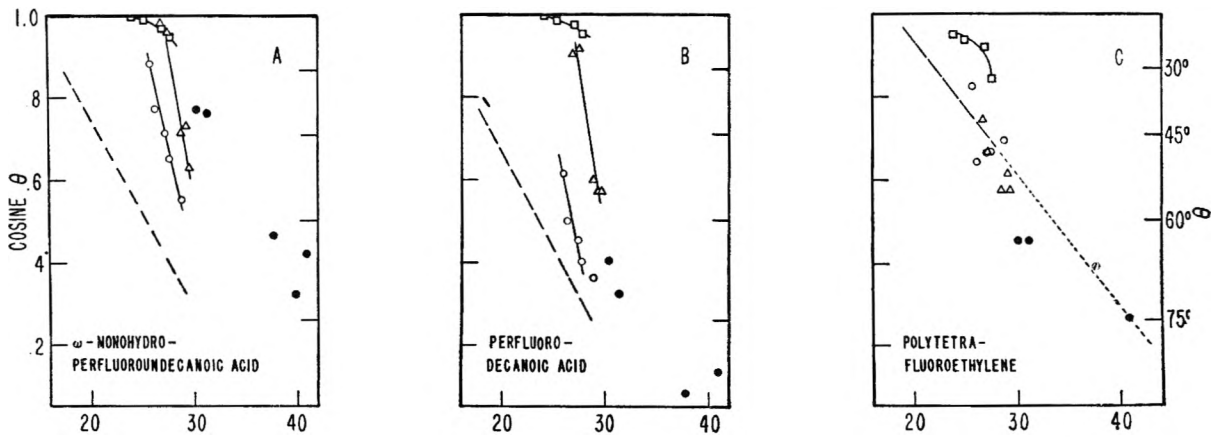

Fig. 2.—Cosine of the contact angle *versus* surface tension for *n*-alkanols, ○; *n*-alkanoic acids, Δ; *n*-primary amines, □; and esters, ●; on surfaces composed of CF_2H, CF_3 and CF_2 groups.

Bigelow, Glass and Zisman[10] have reported that the liquid *n*-alkyl acids, alcohols, and amines exhibit appreciable contact angles on platinum due to their inability to spread on their own adsorbed monolayer. The contact angles reported here for these same polar substances on monolayers of either ψ-undecanoic acid or ϕ-decanoic acid are in every case different from those found on clean platinum. It is significant that the *n*-alkyl amines have lower contact angles on an oriented monolayer of fluorinated acid than on clean platinum. This means, of course, that the amines adhere more strongly to oriented CF_2H or CF_3 groups than to CH_3 groups. But the alcohols, acids, esters and alkanes adhere less strongly to CF_2H and CF_3 surfaces than to CH_3 surfaces.

It was not feasible to compare the wettability of monolayers of the ψ-acids and ϕ-acids having the same number of carbon atoms per molecule since the ϕ-acids available to us contained an even number of carbon atoms per molecule and the process of synthesizing the ψ-acids results only in an odd member of the series.

To rule out the possibility that the observed differences in wettability between ϕ-decanoic acid and ψ-undecanoic were caused by differences in molecular chain length, the contact angles of the *n*-alkanes given here for films of ϕ-decanoic acid

organophobic surfaces (or "low-energy" surfaces) as are the perfluoroacids. This makes inviting their application as mold-release and dispersing agents or wherever surfaces with low adhesion are desirable.

The observed differences in wetting behavior of esters and primary amines on surfaces composed of oriented CF_3 and CF_2H groups cannot be accounted for except by inferring that forces exist between the molecules of liquid and the terminal fluorinated groups of the adsorbed monolayer which are stronger than van der Waals' forces of adhesion. The differences in work of adhesion found for these surfaces with the various polar liquids and the structural considerations given below constitute good evidence for concluding that hydrogen bonding contributes significantly to the observed abnormal wetting by these liquids. Through the

(10) W. C. Bigelow, E. Glass and W. A. Zisman, *J. Colloid Sci.*, **2**, 563 (1947).

(11) E. Hare, E. Shafrin and W. A. Zisman, "Properties of Films of Adsorbed Fluorinated Acids," to be published.

added effect of hydrogen bonding, the free surface energy of the solid/liquid interface (γ_{SL}) would be decreased, thus increasing cos θ for given values of the free surface energies of the liquid ($\gamma_{LV}°$) and the coated solid surface ($\gamma_{S}°$), according to the Young equation

$$\cos\theta = (\gamma_{S}° - \gamma_{SL})/\gamma_{LV}°$$

Esters.—Other evidence exists for believing that hydrogen bonding occurs between esters and a CF_2H surface. Esters exhibit much lower contact angles on this surface than do other liquids of about the same surface tension. Obviously, esters cannot form hydrogen bonds with CF_3 or CF_2 surfaces because of the lack of the necessary hydrogen atom; but such an atom can be supplied by the CF_2H surface. Pauling[12] has described an unsymmetrical type of hydrogen bond A—H...B, of which he says, "...that in general the strength...is increased by increasing the resultant positive charge of A and the negative charge of B." Because of the electronegativity of fluorine, one would expect the terminal carbon atom of the ψ-compound to be more electropositive than the adjacent carbon atoms. The negative character of the carbonyl oxygen ("B" above) of esters is well known. Hence it is plausible that there should be a weak hydrogen bond of this type.

An approximate calculation can be made of the adhesional energy due to hydrogen bonding if the area occupied by a mole of suitably oriented ester molecules is known. Measurements on a Fisher–Hirschfelder atom model of bis-(2-ethylhexyl) phthalate, for example, give an area per molecule between 80 and 166 Å.^{2} depending on the orientation. Thus there is one adsorbable carbonyl group per 40–83 Å.^{2} of the wetted surface. But the fluorinated solid surface consists of one CF_2H group per 23 A.^{2},[5] so that the adhesional energy per mole of liquid ester is the significant quantity rather than the energy per mole of adsorbed monolayer. Based on the minimum area per molecule of suitably oriented phthalate molecules, a simple calculation shows that 4.8×10^9 cm.^{2} of surface will be occupied by one mole of ester. According to the last column in Table I, the observed difference in W_A for the CF_3 and CF_2H surface for esters is 13.7 ergs/cm.^{2}, equivalent to (4.8×10^9) (13.7) = 6.6×10^{10} ergs/mole, or 1.6 kcal./mole. A similar calculation using the maximum area of the phthalate molecule gives 3.3 kcal./mole. Part of this energy is the difference in free surface energy of the CF_3 and CF_2H surfaces with respect to non-hydrogen-bonding liquids as shown by ΔW_A for the *n*-alkanes. Table I shows the average value of ΔW_A to be 2.7 ergs/cm.^{2}. Hence, the value of 13.7 ergs/cm.^{2} obtained in the above calculation must be reduced to 13.7 − 2.7 or 11.0 ergs/cm.^{2}. This correction causes the estimated extreme values of the energy attributable to hydrogen bonding to become 1.3 and 2.8 kcal./mole, respectively. These values are to be compared with hydrogen bond energies reported,[12] which vary from 1.3 kcal./mole in the N—H···N bond of ammonia to 8.2 kcal./mole in the O—H···O bond of anhydrous acetic acid.

(12) L. Pauling, "The Nature of the Chemical Bond," Cornell University Press, Ithaca, N. Y., 1945.

This attraction of esters to the CF_2H surface due to hydrogen bonding does not result in rapid solution of the film. A sessile drop of ester may be removed from the monolayer-coated solid and another put in its place to give the same equilibrium contact angle. It can be concluded that esters of carboxylic acids are normal liquids with respect to CF_3 surfaces but are abnormal as regards CF_2H surfaces.

Amines.—The abnormal ability of primary amines to wet all three types of fluorinated surfaces suggests that a "double" hydrogen bond exists in each instance presumably as

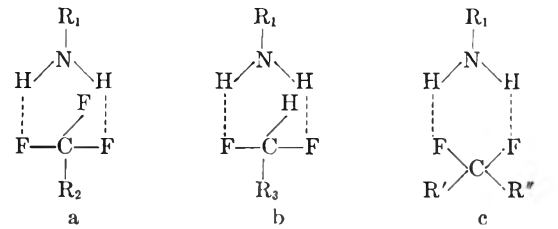

Such bonding is sterically possible in all three cases as shown by Fisher–Hirschfelder atom models. With "normal" liquids, the CF_3 surface is the least wettable and the CF_2 surface the most wettable of the three fluorinated surfaces considered here, but with the amines the reverse is true. As might be expected from configurations (a) and (b), the wettability of CF_3 and CF_2H surfaces by the amines is the same within experimental error. The lesser wettability of CF_2 surfaces by amines (Table I) is probably a consequence of the smaller electronegativity of the fluorine atoms in the CF_2 group as compared with CF_3 and CF_2H. Perfluorotertiary amines, which have low surface tensions (*ca.* 13 dynes/cm.), have been shown[5] to wet CF_3 surfaces normally. This is understandable because of the lack of the necessary hydrogen atom in tertiary amines.

Alcohols.—In the case of alcohols, one configuration is possible for the bond with each type of fluorinated surface

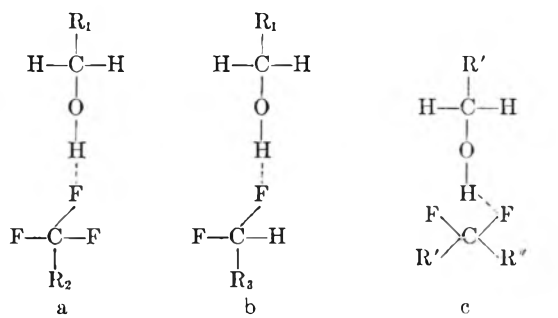

Table I reveals significantly larger values of ΔW_A for the alcohols than for the alkanes, indicating the presence of hydrogen bonding which is stronger on the CF_2H than on the CF_3 surface; but alcohols behave normally on CF_2 surfaces. Presumably these differences are a consequence of the greater electronegativity of the fluorine atoms in CF_2H groups as compared with those of the CF_3 group and the similar electronegativity of CF_2 groups as compared with the others.

The question arose as to whether the increased

adhesion of the alcohols was due to partial solution of the adsorbed monolayer in the liquid drop resting on it thus reducing the compactness of the adsorbed monolayer. Experiments showed that amyl alcohol containing, dissolved in it, sufficient ψ-undecanoic acid to deposit a monolayer of the latter on platinum (*ca.* 4% by weight) gave the same contact angle on a monolayer adsorbed from decane as the pure alcohol. Furthermore, cetane gave the same angle (67°) on the monolayer adsorbed from the amyl alcohol solution as on the monolayer adsorbed from decane. The fact that the contact angles did not change under these conditions is conclusive evidence that solubility of the monolayer in the sessile drop is not a factor in determining the equilibrium contact angle as far as the alcohols are concerned.

Acids.—The contact angles of the *n*-alkanoic acids on CF_2H and CF_3 surfaces are also significantly smaller than would be expected from the wettability of the surfaces by "normal" liquids of the same surface tension. They are smaller, too, than the *n*-alkanols of equal surface tension. Possible configurations of the bonds between the carboxyl group and CF_2H and CF_3 groups are indicated below.

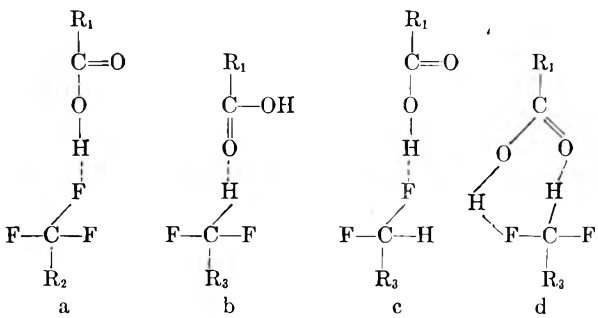

The rather small difference in W_A for the CF_3 and CF_2H surfaces (from Table I, the value of ΔW_A is 2.6 ergs/cm.^{2}), indicates that the differences in contact angle are due to the difference in free surface energy of the fluorinated surfaces rather than to any differences in hydrogen bond strength. This is to say that since configuration (a) is the only way for hydrogen bonding to occur between a carboxyl group and a CF_3 surface, that its analog, configuration (c), represents the hydrogen bond between the carboxyl group and the CF_2H surface. The discrepancy between the values of ΔW_A for the acids and alcohols is attributable to the apparently greater solubility of the fluorinated-acid monolayers in the acids. Evidence for this view was obtained as follows.

When 4% by weight of ψ-undecanoic acid and ϕ-decanoic acid, respectively, were dissolved in each of the liquid acids, the resulting solutions gave significantly larger angles on the monolayers than did the pure acids. The results are given in Table II: these are to be compared with the comparable data in Table I. The inference is that part of the abnormal behavior of the liquid *n*-alkanoic acids on the fluorinated-acid monolayers is due to the solubility of the monolayers in these liquids. If ΔW_A is calculated from the results in Table II, its value is found to be about 6.7 ergs/cm.^{2}, a value close to that found for the alcohols.

Table II

Wetting of Adsorbed Monolayers of ψ-Undecanoic Acid and ϕ-Decanoic Acid by Solutions of These Substances, Respectively, in *n*-Alkanoic Acids (4% by Weight)

Liquid containing 4% of monolayer acid	Contact angle, deg., on monolayer of ψ-Undecanoic acid	Contact angle, deg., on monolayer of ϕ-Decanoic acid
Pelargonic acid	57	72
Caprylic acid	48	66
Heptylic acid	49	68
Valeric acid	34	48
Butyric acid	30	52

This supports the view that the hydrogen bond between a carboxyl radical and the fluorinated-acid monolayer surfaces is similar in configuration to that of a hydroxyl radical and the same surfaces (*cf.* configurations (a) and (c) for the acids with configurations (a) and (b) for the alcohols). At present there seems to be no satisfactory way of evaluating the separate effects of solubility and hydrogen bonding for the acids by contact angle methods. Other methods, for example examination of infrared absorption bands characteristic of hydrogen bonding, should be able to resolve this point.

Other Polar Liquids.—Water and glycerol, which are associated liquids, would also be expected to hydrogen bond with CF_2H and CF_3 surfaces. Comparison with "normal" liquids for these is not possible since no "normal" liquids exist which have comparably high surface tensions. But water and glycerol do display higher contact angles on hydrocarbon surfaces[3] than on CF_3 and CF_2H surfaces; this is so in spite of the fact that the latter have lower free surface energies as shown by the behavior of non-hydrogen-bonding substances such as the alkanes. We are led, therefore, to infer that the lower contact angles of water and glycerol are caused by a decrease in γ_{SL} resulting from hydrogen bonding. Water and glycerol show no abnormalities on hydrocarbon surfaces.[3]

Where marked deviations from linearity of plots of cos θ_E *versus* γ_{LV}° have occurred,[1,2] the points delineating the curved portion of the plots have been those given by the very liquids which we now see are capable of hydrogen bonding to appropriate atoms of the solid surface. Therefore, it is apparent that for non-hydrogen-bonding liquids the cos θ_E *versus* γ_{LV}° relationship is linear over the entire range of values of γ_{LV}°. Deviations from linearity should lead one to suspect the action of stronger adhesive forces than van der Waals' forces at the solid/liquid interface. Hydrogen bonding represents presumably only one type of such forces.

Acknowledgment.—Thanks are due to the Organic Chemicals Department of the du Pont Company for donating to us the ω-monohydroperfluoro acid used in this study.

DISCUSSION

J. L. SHERESHEFSKY.—How were the contact angles measured and how reproducible were they?

H. W. FOX.—The methods we used in measuring the contact angles have been described in detail in some of our earlier papers. The contact angle goniometer, for example, is described in *J. Colloid Sci.*, **1**, 513 (1946). The method of forming the drops by adding small increments to the primary drop to insure that we were reading the advancing angle in mechanical equilibrium is described in *J. Colloid Sci.*, **7**, 109 (1952). Reproducibility over all was about $\pm 2°$. Most of the values were reproducible to $\pm 1°$ for different specimens of the same solid.

H. B. KLEVENS.—From extensive studies in solutions of perfluoro acids in mixed water–polar compound (alcohols ethers, acids and amines) solvents, definite evidence is accumulating which indicates that there is complex formation of a non-specified nature between perfluorocarbon chains and polar additives (Klevens, Raison and Vergnolle, unpublished data). This complexing results in marked increases in solubility and does not involve interaction with the carboxyl group. One possibility would involve a helical type arrangement of polar additives about the perfluorocarbon chain since we observe a change in various properties up to approximately a 1:1 ratio of polar compound to $—CF_2—$ in the chain. This is similar to the urea–hydrocarbon complex which occurs only in the solid state, whereas, with the perfluoroacids, this possible complexing is noted in solutions as well.

It is difficult to reconcile or interpret these results on complexing which occur in solution with the weak, so-called "hydrogen" bonding observed at liquid-solid interfaces, as proposed by Ellison, Fox and Zisman. We have observed evidence of penetration by alcohols into the perfluorocarbon region by X-ray studies but as yet no electron diffraction results have been obtained to show corresponding penetration of polar molecules into perfluoroacid monolayers. Possibly, these results, when obtained, coupled with temperature studies, may tend to clarify the mode of action between perfluorocarbon chains and polar additives.

H. W. FOX.—The reactions of fluorinated acids mentioned by Dr. Klevens have of course already been described for ethers and acetone as well as for the more polar hydrocarbon derivatives (Hauptschein and Grosse, *J. Am. Chem. Soc.*, **73**, 5139 (1951)). The latter authors mention the possibility of hydrogen-bonding as contributing to the effects they found. But it is difficult to see why the work described by Dr. Klevens on the behavior of fluorinated acids in polar hydrocarbon solvents needs to be reconciled with our work on fluorinated acid monolayers. The work of Klevens, *et al.*, which presumably shows a kind of interaction of the urea–hydrocarbon type concerns an entirely different sort of system. It should be remembered that with surfaces comprising adsorbed, close-packed monolayers, the main chain of the adsorbed molecules is not exposed; only the terminal atomic groups are available for contact with the liquid molecules. This fact rules out immediately the possibility of the urea–adduct type of complexing mentioned by Dr. Klevens for the systems we have described in our paper.

B. ROGER RAY.—Can you relate the changes in the van der Waals forces in the solid/liquid interface to the Young equation? How do you account for the linearity of cosine θ *versus* γ_L?

H. W. FOX.—I believe that this cannot be done at the present time. The Young equation contains two quantities, γ_S and γ_{SL}, which are as yet experimentally inaccessible. The linearity of cosine θ *versus* γ_L must represent the way the solid/liquid interfacial tension changes for a given surface, with changes in the liquid surface tension but until the solid surface tension can be measured, we can only infer qualitatively how the solid/liquid interfacial tension behaves.

J. C. ARNELL.—Figure 1 of your paper shows that the *n*-alkanes give different slopes on different surfaces when cosine θ is plotted against surface tension. In the absence of any polarity in the alkane molecules, has it been possible to make any quantitative deductions from the different amount of increase of the wettability caused by increasing chain length of the alkanes on different surfaces?

H. W. FOX.—We have not yet found a ready explanation for the differences in slope. Quantitative deductions will be possible when there is way of determining either the solid "surface tension" or the solid/liquid interfacial tension.

J. TH. G. OVERBEEK.—What is the evidence that the surface tension, solid/vapor, γ_{SV}, is not affected by the adsorption of the vapor of the liquid?

H. W. FOX.—To take polytetrafluoroethylene as an example, we showed (*J. Colloid Sci.*, **5**, 514 (1950)) that the contact angles of liquids as volatile as heptane are the same on this solid in air as in air saturated with the liquid vapor. For less volatile non-spreading liquids it should all the more be true.

J. TH. G. OVERBEEK.—Does the term equilibrium contact angle imply that the advancing and receding angles are the same?

H. W. FOX.—We have used the term equilibrium contact angle to mean the advancing angle in mechanical and thermal equilibrium; this is the value we think is significant in applying the Young equation to low-energy surfaces. Actually, for many of these surfaces we have found that the two angles are the same; for example, see *J. Colloid Sci.*, **7**, 465 (1952). This is the case where the surface is smooth and the liquid molecules do not permeate or attack the surface. Even on relatively rough surfaces, if the liquid is very mobile, the advancing and receding angles are frequently the same. On polytetrafluoroethylene, which is actually a sintered solid, the receding angle for relatively viscous liquids is generally smaller than the advancing angle. But if a drop of benzene is placed on this surface and liquid is carefully removed from the drop, the angle will fall momentarily and then the drop will snap into a new position with the same contact angle as it had originally.

TODD DOSCHER.—Since in the case of the monohydroperfluoro-acid films, hydrogen and fluorine atoms are exposed at the interface, both of which can according to the hypothesis presented, coordinate with the water molecule, would it not seem reasonable to expect that water would spread on such films? The contact angle is actually still very high.

H. W. FOX.—The surface of such a film is very inert. The contact angle of water on the surface is presumably substantially smaller than it would be if water were a "normal" liquid. From what we know of hydrogen-bond strengths, the contribution of hydrogen-bonding to the work of adhesion would have to be unreasonably large to make water spread on this surface. To predict how much such a contribution would be we should have to know a great deal more than is known about the detailed structure of water.

DETERMINATION OF CRITICAL MICELLE CONCENTRATION BY EQUILIBRIUM DIALYSIS[1]

BY JEN TSI YANG AND JOSEPH F. FOSTER

Contribution from the Department of Chemistry, Iowa State College, Ames, Iowa

Received March 2, 1953

In connection with studies, by equilibrium dialysis, of the binding of detergent ions by proteins it has been observed that such ions do not distribute themselves uniformly across a cellophane membrane except at concentrations below the CMC. It is demonstrated that micelles do not form in the dialyzate of detergent solutions and an explanation is given, the situation being analogous to separate phase formation. It is thus possible to measure the concentration of free ions in equilibrium with micelles (the CMC) and results are given for two sodium alkylbenzenesulfonate preparations and two alkylbenzyldimethylammonium chloride samples. In addition to the determination of CMC the method provides a measure of the inhomogeneity of the detergents studied. The anionic detergent preparations appear to contain an appreciable amount of lower homologs which do not take part in micelle formation in the concentration range investigated. The cationic detergent samples show a more complicated behavior and possible explanations are suggested.

It is well recognized that surface active ions tend to form aggregates, known as micelles, above a characteristic concentration range, with resultant anomalies in the physical-chemical properties of their solutions. Conventionally, the so-called critical micelle concentration (CMC) can be determined from the deviation of the colligative or electrical properties from those of the normal solutions, although these methods are usually not sensitive when salt is present. More recently there have been developed many other methods among which are a spectrophotometric dye method,[2] a method based on dye solubilization,[3] and methods based on spectral properties,[4] light scattering,[5,6] polarography,[7] and bubble pressure.[8] In this paper will be presented another method based on equilibrium dialysis. In the course of study of the binding of detergents by proteins we have found that detergents are never uniformly distributed across a cellophane membrane except at very low concentrations below a definite range. These results can be explained satisfactorily on the basis of micelle formation and the CMC can be determined by extrapolation from the equilibrium curves. One of the advantages of this method is that both the single ions and micelles in equilibrium can be determined in a given experiment. In the case of a homogeneous detergent, it also permits the estimation of the number of ions aggregated in the micelle and the corresponding equilibrium association constant. For mixtures of homologs it provides an estimation of the proportion of lower homologs which do not form micelles under the conditions studied and a partial fractionation can be achieved through dialysis.

Experimental

Materials.—Santomerse No. 3, principally sodium dodecylbenzenesulfonate (SDBS), was supplied by the Monsanto Chemical Company. It was freed of inorganic salts by dispersion in 95% ethanol and kept in an air-tight bottle after lyophilization. Its apparent number-average molecular weight was 354, as determined by Parr bomb sulfur analysis.

Technical alkyldimethylbenzylammonium chloride (50%) was furnished by Onyx Oil and Chemical Company. The principal constituent was *n*-dodecyldimethylbenzylammonium chloride (DDBAC). The molar concentration of a stock solution was determined by micro-Kjeldahl analysis, on the basis of one equivalent nitrogen per mole detergent.

Samples of SDBS and DDBAC (labeled 95% C_{12} isomer) were also purchased from Wipaway Products.

All buffers were made with reagent grade chemicals: (1) Phosphate–NaCl buffer—0.0321 *M* K_2HPO_4, 0.0036 *M* KH_2PO_4 and 0.100 *M* NaCl, *p*H 7.7 and ionic strength 0.20; (2) glycine–NaCl buffer—0.090 *M* glycine, 0.010 *M* HCl and 0.090 *M* NaCl, *p*H 3.3 and ionic strength 0.10.

Equilibrium Dialysis.—Visking cellophane casings, $^{20}/_{32}$ inches in diameter, were previously boiled in water three times for half an hour, followed by thorough rinsing each time. Twenty-ml. portions of detergent solution were placed in the air-tight bags and then equilibrated against equal volumes of the solvent in test tubes. In the case of SDBS it was necessary to prevent contact of the solution with rubber by covering the stoppers with aluminum foil. Controls containing solvent only were prepared in the same manner. The tubes were shaken gently for two days. Both the dialyzed solutions and the dialyzates were then diluted, if necessary, and analyzed spectrophotometrically. In case that a second equilibrium dialysis was desired, both solutions were re-equilibrated against fresh solvent separately.

Spectrophotometric Analyses.—Measurements of the ultraviolet absorption of detergent solutions were made on a Beckman model DU spectrophotometer. The optical densities of SDBS and DDBAC were determined at the wave lengths of 223 and 263 mμ, respectively (see below).

Results

Ultraviolet Absorption by Detergent Solutions.—In order to study the mass relation between the micelles and single ions of detergent, it is necessary to measure quantitatively the detergent concentrations. A spectrophotometric method was thus developed for this purpose.[9] The ultraviolet absorption spectrum of SDBS in phosphate–NaCl buffer is shown in Fig. 1, where a maximum absorption is observed at a wave length of 223 mμ. The optical densities at maximum absorption of a series of dilute SDBS solutions were found to follow Beer's law within the ranges studied (optical densities below 2). The apparent molar extinction coefficient, ϵ, was 11,100. The assumption was made that the various homologs of varying alkyl group possessed the same ϵ (see Discussion).

Random errors were frequently observed in the second decimal of the optical readings. The most serious source of error came from the dialysis bags. Even with pretreatment (boiling), a blank reading of about 0.05 or higher in optical density was usually present. This was not too serious for high SDBS concentrations, but would introduce appreciably large errors at very low SDBS concentrations.

(1) Journal paper No. J-2268 of the Iowa Agricultural Experiment Station, Ames, Iowa. Project 1223. This research has been supported by the Office of Naval Research under Contract Nonr-803(00).

(2) M. L. Corrin, H. B. Klevens and W. D. Harkins, *J. Chem. Phys.*, **14**, 480 (1946).

(3) I. M. Kolthoff and W. Stricks, THIS JOURNAL, **52**, 915 (1948).

(4) W. D. Harkins, H. Krizek and M. L. Corrin, *J. Colloid Sci.*, **6**, 576 (1951).

(5) P. Debye, THIS JOURNAL, **53**, 1 (1949).

(6) P. Debye, *Ann. N. Y. Acad. Sci.*, **51**, 575 (1949).

(7) E. L. Colichman, *J. Am. Chem. Soc.*, **72**, 4036 (1950).

(8) A. S. Brown, R. U. Robinson, E. H. Sirois, H. G. Thibault, W. McNeill and A. Tofias, THIS JOURNAL, **56**, 701 (1952).

(9) The ultraviolet method is applicable only to detergents containing aromatic groups.

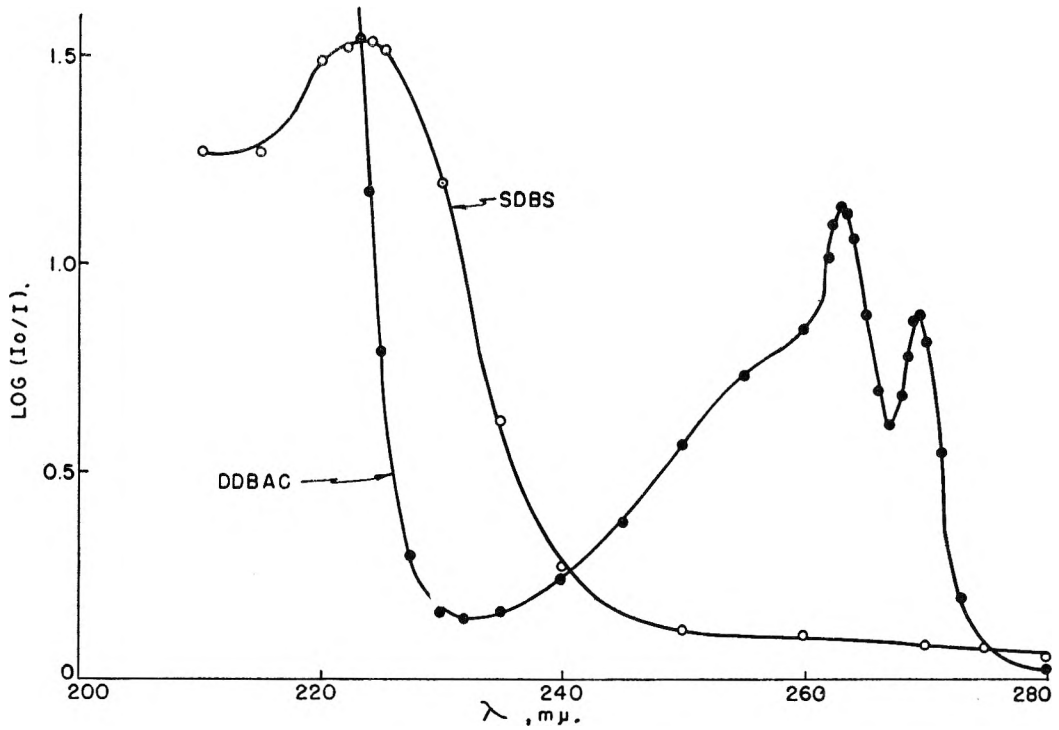

Fig. 1.—Ultraviolet absorption spectra of detergent solutions: ○, SDBS, 1.38 × 10^{-4} *M*., in phosphate–NaCl buffer (*p*H 7.7, Γ/2 = 0.20); ●, DDBAC, 2.86 × 10^{-3} *M*, in glycine–NaCl buffer (*p*H 3.3, Γ/2 = 0.10).

Thus control runs were frequently made to minimize this trouble.

Also shown in Fig. 1 is the absorption spectrum of DDBAC in glycine–NaCl buffer, where two maximum peaks are observed at the wave lengths 263 and 269 mμ. The former had a slightly higher molar extinction coefficient, ε, of 400 and thus was taken for routine analyses. Again Beer's law was obeyed within the concentration range used. Actually there existed another much higher maximum absorption around 210 mμ, which, however, was not used because of the limitation of the instrument.

Equilibrium Dialysis Curves on SDBS.—In Fig. 2 are shown the results on SDBS by equilibrium dialysis at different salt concentrations. In very dilute solutions the SDBS concentrations were virtually equivalent on both sides of the membrane. As the concentrations increased the curves deviated from the ideality of simple electrolytes with resultant curves of much smaller slopes, indicating the formation of micelles. In this stage the concentration in the dialyzate represented the single ions (D_s) which were equivalent to those in equilibrium with the micelles inside the membrane after due correction for Donnan equilibrium. The concentrations in the dialyzed solutions represented the sum of both the single ions and the micelles in monomeric units (D_m). Since these solutions were diluted to concentrations below CMC it was not necessary to consider possible difference in absorption properties between micelles and free ions. The results on unbuffered solutions are shown as curve I, where the D_s concentrations inside the membrane were calculated from those outside after due correction for the Donnan effect. Curves II and III were carried out in phosphate–NaCl buffers at ionic strengths of 0.10 and 0.20, respectively.

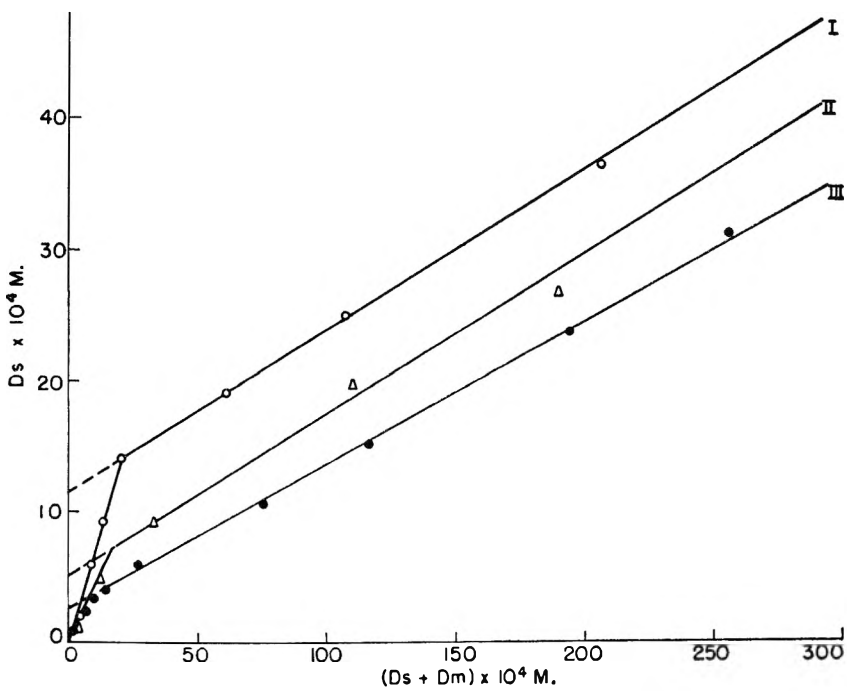

Fig. 2.—Equilibrium dialysis curves of SDBS solutions at 25 ± 3°. Solvents: I, water; II, phosphate–NaCl buffer (*p*H 7.7, Γ/2 = 0.10) and III phosphate–NaCl buffer (*p*H 7.7, Γ/2 = 0.20).

Second equilibrium dialyses of both the dialyzed solution and the dialyzate of curve III are illustrated in Fig. 3 (curves IIIa and IIIb). Also shown in Fig. 3 are experiments on partially fractionated SDBS solutions. Curves IV and V were the results of fractionation by dialysis. A 100-ml. volume of 5% solution in phosphate–NaCl buffer was dialyzed twice against one liter of fresh buffer for one day each, and the equilibrium curve was made on the dialyzed solution (curve IV). Another 200-ml. volume of 5% solution was dialyzed continuously against 16 liters of buffer which

flowed at the rate of about 5 ml. per minute (curve V). In curve VI the fractionation of SDBS solution was achieved by a precipitation method. This was done in the following way: a 1% SDBS solution (buffered) was stored overnight at 1–3°. After centrifugation the precipitate was redispersed in fresh solvent and equilibrium dialysis runs carried out.

Equilibrium Dialysis Curves on DDBAC.—Analogous to Figs. 2 and 3, a series of equilibrium dialysis curves for DDBAC are plotted in Fig. 4. Curve I represents the results on unbuffered solutions, curve II the results in glycine–NaCl buffer, and curve III the results of the second equilibrium dialysis of the dialyzates of solutions from curve II. In addition results are shown for the second dialysis of the dialyzed solution from II and for a sample partially purified by dialysis of a 5% solution against two changes (1 l.) of buffer. These results are seen to fit curve II within the limits of accuracy.

Values of CMC.—In Table I are listed the values of CMC for SDBS and DDBAC as determined by the equilibrium dialysis method. These values were determined by extrapolation of the second linear portion of the plots of D_s *versus* $(D_s + D_m)$ to zero on the ordinate for reasons which will be discussed.

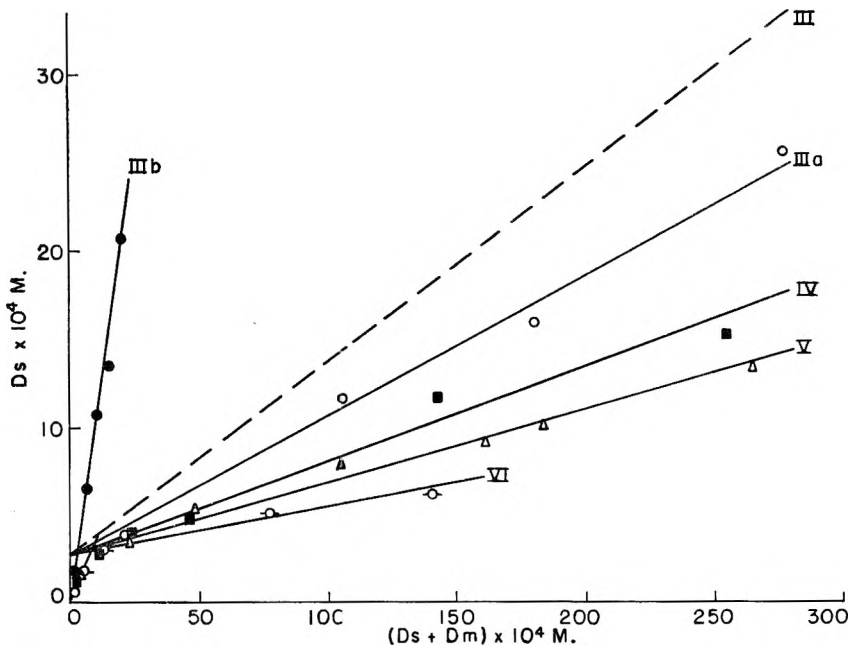

Fig. 3.—Equilibrium dialysis curves of SDBS solutions in phosphate–NaCl buffer (*p*H 7.7, Γ/2 = 0.20) at 25 ± 3°: III, unfractionated, same as III in Fig. 2; IIIa and IIIb, second equilibration of the dialyzed solution and the dialyzates of curve III, respectively; IV, fractionated, by batch dialysis; V, fractionated, by continuous dialysis; and VI, fractionated, by precipitation at low temperature. For methods of fractionation, see text.

TABLE I

CMC OF DETERGENTS

Detergent	Solvent	Temp., °C.	CMC × 10⁴ *M*
Santomerse No. 3	Water	25	12
		2	1.8
	Phosphate–NaCl Buffer (*p*H 7.7)		
	(a) Γ/2 0.10	25	5.2
	(b) Γ/2 0.20	25	2.8
SDBS (Wipaway Products)	Same as (b)	25	2.0
DDBAC (Onyx Oil and Chemical Co.)	Water	25	24
		2	21
	Glycine–NaCl *p*H 3.3, Γ/2 0.10	25	8.5
DDBAC (Wipaway Products)	Same	2	3.9

Discussion

Basis for the Determination of CMC.—Since the micelles are in equilibrium with single ions, it might be expected that a distribution of micellar sizes exists. Experimentally, the critical concentration is, however, limited to a narrow range, and the large micelles are favored in the distribution. As a first approximation, assuming a single species of micelle to exist, the aggregation of ions to form micelles can be conveniently expressed by the equilibrium

$$nD \rightleftarrows D_n \qquad (1a)$$

where n is the number of single ions aggregated in a micelle. Let K be the apparent equilibrium association constant, since the activity coefficients are not determined. Then

$$K = \frac{D_n}{(D)^n} = \frac{D_m/n}{(D_s)^n} \qquad (1b)$$

where D_m and D_s are the respective concentrations of micellar and single ions in monomeric units. During equilibrium dialysis the single ions can diffuse freely through the cellophane membrane, whereas the micelles remain non-diffusible because of their large sizes. It was first assumed, on the basis of the reversibility implicit in (1), that at equilibrium micelles would exist on both sides in equal concentrations. As soon as some of the single ions pass through the membrane, more micelles would dissociate and the equilibrium shift to the left. This, however, turned out to be not true, as is well illustrated in the equilibrium dialysis curves, where the detergent concentration in the dialyzate is much smaller than that in the dialyzed solution except in extremely dilute solutions. The possibility of the existence of non-diffusible impurities was ruled out because of the fact that the deviation was not a linear function of the total amount of detergent used. The effect of insufficient dialysis was also eliminated. In a preliminary study equilibrium was usually reached after several hours shaking at room temperature. Thus two-day dialysis proved more than enough for equilibration. In fact prolonged dialysis of a period of over one month virtually did not affect the results obtained.

The only logical explanation seems to be that the diffused single ions in the dialyzates did not associate to form micelles. In order to prove this a second equilibrium dialysis was thus carried out for both the dialyzate and the dialyzed solution of the first equilibration, separately, against fresh solvent. As is clearly illustrated in Fig. 3 (curves

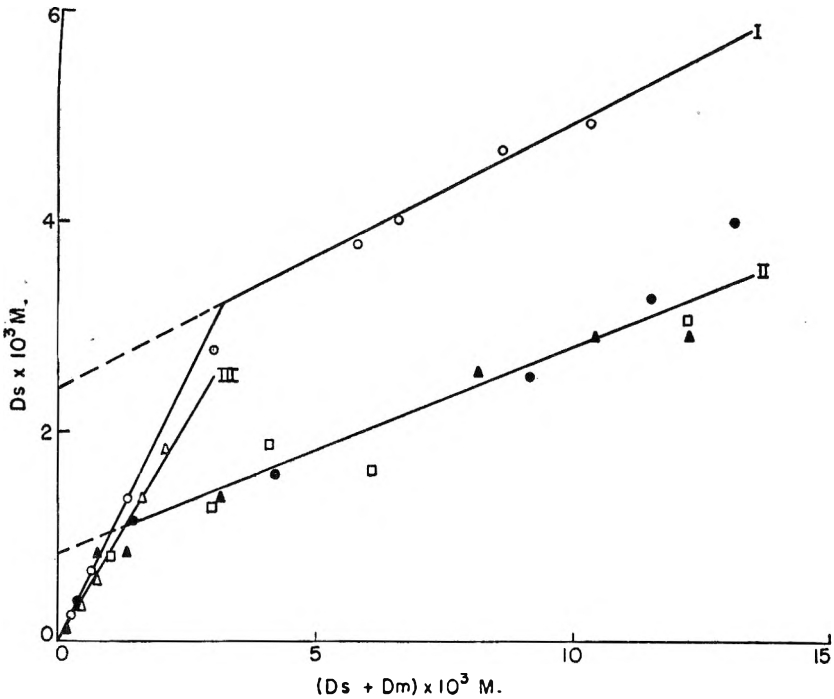

Fig. 4.—Equilibrium dialysis curves of DDBAC at 25 ± 3°. Solvents: I, water; II and III, glycine–NaCl buffer (*p*H 3.3, Γ/2 = 0.10). Curve II, ●, first equilibration; ▲, second equilibration; and □, fractionated, by batch dialysis. Curve III, Δ, second equilibration of the dialyzates of ● in curve II.

III and IIIa and b), after re-equilibration of the first dialyzate the detergent concentrations on both sides of the membrane are indeed equivalent to each other (curve IIIb), a fact indicative of the absence of micelles. On the other hand the opposite is true for curve IIIa, where again the micelles play a determinant role. The fact that curves III and IIIa do not coincide can be easily explained on the basis of heterogeneity of the detergent (see below).

It is thus clear that micelles will not form in the dialyzate and it is desirable to seek a theoretical basis for this fact. Such an explanation is not difficult, indeed is quite obvious in view of the known properties of detergent micelles. Thus, if the value of n in equation (1) is large, of the order twenty or over as generally appears to be the case, the concentration of free detergent in equilibrium with micelles is essentially a constant (it will depend only on the nth root of the micelle concentration). This, in fact, is the significance of the CMC. Thus the free concentration in the dialyzate can never exceed this concentration by an appreciable amount. If it is further assumed that the rate of formation of micelles is typical of nucleation processes in general, that is depends directly on the excess concentration over and above the critical concentration, it is clear that micelle formation will not proceed at a finite rate.[10]

This does not imply that all micelles must be of uniform size. It does seem to require, however, that no micelles exist having n values of less than perhaps 5 or so.

(10) The situation is thus analogous to the rate of phase formation in two-phase systems, for example, in the equilibration of liquid with vapor in which case it is found that the liquid phase does not form in the "receiver" so long as uniform temperature is maintained. We are indebted to Dr. R. S. Hansen for a helpful discussion of this point.

At very low concentrations the dialyzates in general were found to contain somewhat less SDBS than the dialyzed solution. This is interpreted as meaning that higher molecular-weight homologs are present which form micelles at concentrations below the range studied.

Heterogeneity of Detergents.—It has been known that increase by one CH_2-group in the alkyl chain of detergent homologs roughly decreases the CMC by about 70%. For a commercial detergent like Santomerse No. 3, the lower homologs of the alkylbenzenesulfonates would be expected to form micelles at much higher concentrations than the higher ones. It is further concluded that a certain fraction of the detergent did not form micelles at all under the conditions studied. This conclusion was reached on the basis of the following facts. First, the D_s values in the dialyzate increased appreciably with the increase in $D_s + D_m$ in the dialyzed solution, contrary to the fact that above CMC the free ions should increase only slightly with increase in total concentration. Neglecting the Donnan correction in the presence of salt, the concentrations of the single ions on both sides of the membrane minus 2 × CMC were equal to about 20% of the initial SDBS solution used, indicating that a definite portion of the detergent remained in a molecularly dispersed state even at considerably higher concentrations. Secondly, the D_s values could be well over the solubility of SDBS as a whole (at 1–3° in phosphate–NaCl buffer observable turbidity appeared at about 0.01%). Thirdly, in Fig. 3, curves III and IIIa did not coincide, contrary to the presumed thermodynamical reversibility of equation (1). In fact above CMC the slope of curve IIIa was much smaller than that of curve III, presumably because of the removal of half of the lower homologs which did not form micelles in the first equilibration. It is because of the presence of these impurities that it is desirable to carry out the extrapolation in order to determine the CMC. As can be seen in Fig. 3, the intercepts of curves III and IIIa on the ordinate are almost identical. This seems to justify the method of extrapolation.

The situation in the case of the cationic detergent samples is similar. The slope of the first linear region is very nearly 1.0 suggesting that in this case no homologs are present which form micelles at lower concentration than the indicated CMC. The results are more complicated, however, in that the slope of the second linear region is not appreciably altered by dialysis. Thus this second region cannot be explained on the basis of contamination by homologs which do not take

part in micelle formation. No really adequate explanation can be given at this time but two possibilities suggest themselves (1) lower homologs are present which will not themselves form micelles in this concentration range but which will participate in micelles formed essentially of higher homologs, and (2) the micelles formed possess a relatively broad range in size distribution so that the all-or-none reaction in equation (1) is a poor approximation. At concentrations above those shown in Fig. 4 a few experimental points have been obtained which suggest that the curve eventually levels off. It should be pointed out that the results with this class of detergents appear to be much less reliable and more scattered than with the other, partially due to the much lower extinction coefficient and perhaps partially due to the fact that much less time has been spent in this case so that the techniques used are not so well developed.

It is of interest that substantially the same results were obtained with the SDBS samples from the two sources, as well as with the two DDBAC samples. It would be of interest to perform similar experiments with samples of the highest possible purity.

Another point deserves consideration, that is, the effect of detergent heterogeneity on the ultraviolet absorption. In a preliminary experiment it has been found that the absorption curves of both the dialyzate and dialyzed solution are similar to that of the whole detergent and have their peaks at 223 and 263 mμ for the two cases. However, it is quite conceivable that the molar extinction coefficients, ϵ, of different homologs might be somewhat different from one another. Since the actual distribution of homologs was not known, it is almost impossible to make any correction in the determination of the detergent concentrations. It was therefore assumed that all the homologs had the same ϵ values, which probably is not too far from the fact. In the extreme cases, the slopes of the equilibrium curves might be somewhat shifted.

Partial Fractionation of SDBS.—As it has been concluded that the lower homologs in the SDBS did not form micelles under the conditions studied, it is thus possible to carry out partial fractionation of the detergent. From Fig. 3 it is evident that most of the lower homologs could be removed either through dispersion in the supernatant solution at low temperature (curve VI, precipitation method) or through batch or continuous dialysis (curves IV and V, dialysis methods). Consequently the slopes of these curves were much smaller than that of unfractionated SDBS.

Calculation of n and K.—Theoretically the experimental data obtained from equilibrium dialysis would enable one to calculate the number of single ions aggregated in a micelle, n, and the equilibrium association constant, K, provided the distribution of micelle sizes (n) is narrow. From equation (1b), we obtain

$$\log D_m - \log n = n \log D_s + \log K \qquad (2)$$

After equilibration the concentrations of SDBS inside the membrane (D_i) and outside (D_o) are

$$D_i = D_s + D_m \text{ and } D_o = D_s \qquad (3)$$

Substituting (3) into (2) and rearranging the equation, we have

$$\log D_o = (1/n) \log (D_i - D_o) + (1/n) \log (1/nK) \qquad (4)$$

Since D_i and D_o are experimentally determinable, a plot of D_o *versus* $(D_i - D_o)$ on a logarithmic scale should give a straight line with a slope equal to $1/n$. The value K can also be determined from the intercept together with the value of n.

Owing to the presence of lower homologs which do not form micelles under the conditions studied, it is necessary to modify equation (4). Let D_t be the initial total concentration of SDBS used and α the mole per cent. of lower homologs. Then, after equilibration equation (3) becomes

$$D_i = D_s + D_m + \alpha D_t/2 \qquad (4a)$$

and

$$D_o = D_s + \alpha D_t/2 \qquad (4b)$$

Consequently, equation (4) becomes

$$\log (D_o - \alpha D_t/2) = (1/n) \log (D_i - D_o) + (1/n) \log (1/nK) \qquad (5)$$

The term $(D_i - D_o)$ will still be the same, but the apparent D_s $(= D_o)$ in equation (4) will be much greater than it should be. Thus, the graphic value of n according to equation (4) will be too small to be of any meaning. Since the value of α could not be accurately determined, no further speculation on the values of n and K are given here.

Influence of Salt Concentration and Temperature on CMC.—From Fig. 2 it is clear that our results are at least qualitatively in agreement with the known fact that addition of salt decreases the CMC. A plot of CMC values for SDSB *versus* the gegenion concentrations on a logarithmic scale gave a straight line with a slope of -0.3. According to Hobbs' theory[11] the slope should be around -0.5. No great significance can be attached to this result since only three experimental points were available. However, it seems indirectly to prove that the "abnormal" equilibrium dialysis curves were really the results of micelle formation.

Owing to the low solubility of SDBS in buffered solution at 1–3°, the CMC at this temperature could not be determined. For aqueous solution without salt, it is surprising to find that the CMC was much lower than that at room temperature as indicated in Table I. In the literature no general conclusion has been reached with regard to the temperature effect on CMC and this question still awaits further investigation.

For aqueous solutions without salt, the Donnan correction became an important factor. Our experimental calculations on the single ions in equilibrium with the micelles were based on the assumption that there were no gegenions aggregated to the micelles. This would tend to give a slope of the equilibrium curve somewhat smaller than it should be and consequently some errors might be introduced in the extrapolated CMC value.

Huff, McBain and Brady[12] reported a CMC value for Santomerse No. 3 of 0.005 M at 30° and 0.0065

(11) M. E. Hobbs, THIS JOURNAL, **55**, 675 (1951).

(12) H. Huff, J. W McBain and A. P. Brady, *ibid.*, **55**, 311 (1951).

at 50° whereas Paquette, Lingafelter and Tartar[13] obtained a value of 0.0012 *M* at 60°. Our results are of the same order of magnitude, although the temperature was different. Huff, *et al.*,[12] observed a distinct positive slope in their plots of *g vs. m* (*g* = osmotic coefficient) above the CMC. It now seems probable, in view of our results, that this was largely due to the low molecular-weight impurities. More recently, Brown and co-workers[8] have observed four CMC values for Santomerse No. 3, the highest of which (0.002 *M*) was close to what we have found. It was not possible to determine the lower CMC values in the present study because of the limit of sensitivity of the ultraviolet absorption technique. However, as has been mentioned earlier, our equilibrium curves did indicate the presence of micelles below the CMC reported.

In conclusion, it is felt that the observation that distinction can be made between micelles and free ions through equilibrium dialysis should prove to be of considerable value. By use of techniques other than ultraviolet absorption it should be possible to extend the method to other detergents, and perhaps to lower concentration ranges. As a means for obtaining information on the degree of homogeneity of a detergent specimen it should be of some importance. Finally, it seems probable that there may be other, entirely different, implications which should be considered, for example the distribution of lipids across living membranes.

DISCUSSION

KAROL J. MYSELS (Communicated by J. Th. G. Overbeek).—The paper by Jen Tsi Yang and J. F. Foster presents ideas which could be of far-reaching significance in the theory of association colloids. These are all based on the statement that the only logical explanation of their results is that the single ions in the outer solution do not associate to micelles. I would like to point out, however, that there is no direct evidence whatsoever in their paper that micelles are absent in the dialyzate, such as light scattering, solubilization, or conductivity effects. The only fact is that the optical density of the outside solution is above the CMC and below the optical density of the inside solution.

The authors used technical products which presumably contain considerable amount of non-detergent water-insoluble oils with the same aromatic nuclei and hence similar optical density.

There seems, therefore, to be an alternative explanation which is much simpler and not so revolutionary. The cellophane membrane is not permeable to the oils, which remain solubilized in the inside solution above the CMC and deposit on the walls during equilibration below it. Thus, below the CMC the optical densities are approximately equal on both sides. Above the CMC the solubilized oils have two effects: (1) They contribute to the optical density of the inside solution, and (2) they lower the activity of the micelles and thus cause a higher concentration of detergents in the inside solution.

Obviously on repeated dialysis the effects observed by the authors would be expected.

If the hypothesis of the authors of the paper is correct, the same effect should be obtainable without difficulty in pure detergents. We are attempting to conduct such a test, but it may be mentioned that Dean and Vinograd (*J. Phys. Chem.*, **46**, 1091 (1942)) found that a much purer detergent (Aerosol) diffused normally toward equal concentration through cellophane between solutions which were both above the CMC.

H. B. KLEVENS.—As has been mentioned above, it is unfortunate that these preparations were not better characterized. However, ultrafiltration and the above dialysis technique repeated with sodium dodecyl sulfate have been found to yield almost identical curves and are generally consistent with the results reported here. Subsequent measurements have shown that the dialyzate of Santomerse is composed of low molecular weight non-micellar material by the dye titration technique. McBain ("Advances in Colloid Science," Vol. I, Interscience Publishers, New York, N. Y., 1942, p. 133) in reporting some results from his laboratory states that Merrill has found that solubilizers are effective in bringing insoluble substances into aqueous solution, even when separated from them by a membrane permeable only to ions; and that Vinograd found that a solubilized dye does not pass through a membrane into water but that the detergent does. However, when a detergent solution is external to the membrane, both detergent and oil pass through. These various data would tend to indicate that the solubilized oil stabilized the micelle. These results are not self-consistent nor are they completely in accord with the above discussion of Mysels and Overbeek. They indicate that the passage or non-passage of sufficient concentrations of surfactant to produce micelles may depend to a large extent on the particular experimental and environmental conditions.

JOSEPH F. FOSTER.—The suggestion of Dr. Overbeek and Dr. Mysels is a very interesting one which had not occurred to us. We must admit the possibility, indeed probability, of contaminants of the type suggested. The critical point of dispute is whether or not micelles form in the dialyzate. Qualitatively we can say that the turbidity of the dialyzates is very low, approaching that of the buffer itself. I agree that it would be very desirable to test more carefully for the presence of micelles by turbidity and dye-solubilization studies.

JOSEPH F. FOSTER (Communicated).—Following the question raised by Drs. Overbeek and Mysels we performed the following experiment: twenty ml. of a 5% Santomerse solution in phosphate buffer (*p*H 7.7, Γ/2 0.20) dialyzed for 24 hours against the same buffer at room temperature (with shaking). The concentration in the dialyzate was determined to be 0.011 *M* by ultraviolet absorption assuming all species to have the molar extinction coefficient used in our paper. The dialyzed solution and the original undialyzed solution were diluted to approximately the same concentration with buffer (actual concentrations determined by ultraviolet absorption were 0.013 and 0.015, respectively). Turbidities, determined at 90° without correction for dissymmetry but corrected for solvent scattering, were 0.16×10^{-4} for the dialyzate, 72×10^{-4} for the dialyzed solution, and 100×10^{-4} for the undialyzed solution at the concentrations indicated. The turbidity of the dialyzate was only about 10% greater than that of the buffer alone. In addition solutions were dye tested for the presence of micelles by the pinacyanol chloride method of Corrin, Klevens and Harkins, *J. Chem. Phys.*, **14**, 480 (1946).

Both the dialyzed and undialyzed solutions showed solubilization of the dye, the solution being clear and deep blue. The dialyzate, on the other hand, yielded only a weak pink color, the bulk of the dye settling out, definitely indicating the absence of detergent micelles in spite of the fact that the total concentration was of the order of 100 times the CMC for the detergent sample as a whole.

These results appear to confirm rather conclusively our contention that the results we observed are due to the failure of nucleation and micelle formation in the dialyzate.

We would like to point out also that unless it can be shown that Aerosol OT is a completely homogeneous preparation, the results of Dean and Vinograd, *J. Phys. Chem.*, **46**, 1091 (1942), cited by Drs. Overbeek and Mysels as in conflict with our contentions, cannot be taken as evidence for or against our mechanism.

(13) R. G. Paquette, E. C. Lingafelter and H. V. Tartar, *J. Am. Chem. Soc.*, **65**, 686 (1943).

A GENERALIZATION OF THE POLANYI THEORY OF ADSORPTION FROM SOLUTION

BY ROBERT S. HANSEN AND WALTER V. FACKLER, JR.

Contribution No. 230 from the Institute for Atomic Research and the Department of Chemistry, Iowa State College, Ames, Iowa[1]

Received March 2, 1953

The Polanyi theory of the adsorption from solution of solutes of limited solubility is corrected and generalized to non-ideal solutions of complete miscibility. Necessary assumptions and their limitations are discussed. Isotherms for the adsorption of water, propanol-1 and butanol-1 from the vapor phase at 25° have been measured and the results used to calculate isotherms for the adsorption of propanol-1 and butanol-1 from aqueous solutions. The calculated isotherm is in qualitative and rough quantitative agreement, in the case of propanol-1–water, with that observed experimentally. Deviations in the butanol-1–water system are more pronounced. Reasons for these deviations and appropriate corrections are suggested.

I. Introduction

So far as the authors are aware the only attempts at general theories of adsorption from solution are due to Polanyi,[2] Ostwald and de la Izaguirre[3] and Kipling and Tester.[4] Problems incident to the formulation of such theories have been extensively reviewed by Kipling.[5]

Of these treatments, that of Ostwald and de la Izaguirre is strongly empirical, and its limitations are excellently presented by Kipling and Tester.[4] The treatment of Kipling and Tester is limited to umimolecular adsorption, and will be discussed in a later paper. The treatment of Polanyi, with corrections and modifications, appears suited for the discussion of multimolecular adsorption from solution. It is the purpose of this paper to correct and generalize the theory of Polanyi and to test the generalization experimentally.

The Polanyi theory of adsorption from solution developed from the Polanyi theory of adsorption of single component gases[2a] and was limited to solutions of slightly soluble solutes.[2b] The Polanyi theory of gas adsorption (for condensable gases which we shall consider in this paper) may be summarized as follows: at any point in the neighborhood of an adsorbent surface there exists an adsorption potential ϵ; points with the same value of ϵ form a surface approximately parallel to the adsorbent surface and enclosing with the surface a volume ϕ. The function $\epsilon(\phi)$ is assumed temperature independent. Given an adsorption isotherm $\eta(P/P_0)$, the function $\epsilon(\phi)$ can be calculated by use of the equations

$$\epsilon = RT \ln P_0/P \qquad (1)$$

$$\phi = n\bar{v}_1 \qquad (2)$$

in which P is the pressure at which n moles of gas are adsorbed, P_0 is the saturated vapor pressure and $\bar{v}_1$ is the liquid molar volume at the temperature of the adsorption isotherm. The function $\epsilon(\phi)$ being established from one isotherm, isotherms at any other temperature can be calculated from these same two equations. The status of this theory to 1942 has been reviewed by Brunauer.[6] More recently, theoretical developments due to Halsey[7] and Hill[8] can be considered as furnishing analytical forms to the function $\epsilon(\phi)$ of the type $\epsilon = k/\phi^n$ or $\epsilon = k/\phi^3$.

Polanyi's theory as applied to adsorption from solution[2] cannot be general, for it is not symmetric with respect to solute and solvent. This may be seen most readily from his equation 9A which, in modern notation, can be expressed in the form

$$\bar{V}_2\epsilon_1 - \bar{V}_1\epsilon_2 = -\bar{V}_2 RT \ln a_1 \qquad (3)$$

in which a_1 is the activity of component 1 referred to a standard state of pure component 1. By exactly parallel arguments it follows that

$$\bar{V}_1\epsilon_2 - \bar{V}_2\epsilon_1 = -\bar{V}_1 RT \ln a_2 \qquad (4)$$

and therefore

$$\bar{V}_1 \ln a_2 = -\bar{V}_2 \ln a_1 \qquad (5)$$

But this is impossible, since both a_2 and a_1 have unity as upper bounds, and $\bar{V}_1$ and $\bar{V}_2$ are both usually positive.

II. Theoretical

Consider a solid adsorbent in equilibrium with a binary liquid solution of components 1 and 2. Let $\Delta\phi$ be an infinitesimal volume increment enclosed between two equipotential surfaces ϕ and $\phi + \Delta\phi$. Considering $\Delta\phi$ invariant the condition for equilibrium between material in $\Delta\phi$ and bulk solution follows from the invariance of total free energy under constrained infinitesimal mass transfer. Thus

$$\delta F = 0 = (\mu_{1\phi} - \mu_{1B})\delta\eta_{1\phi} + (\mu_{2\phi} - \mu_{2B})\delta\eta_{2\phi} \qquad (6)$$

subject to

$$\delta\Delta\phi = 0 = \bar{\bar{V}}_{1\phi}\,\delta\eta_{1\phi} + \bar{\bar{V}}_{2\phi}\,\delta\eta_{2\phi} \qquad (7)$$

whence

$$\frac{\mu_{1\phi} - \mu_{1B}}{\bar{\bar{V}}_{1\phi}} = \frac{\mu_{2\phi} - \mu_{2B}}{\bar{\bar{V}}_{2\phi}} \qquad (8)$$

in which $\mu_{i\phi}$ and $\bar{\bar{V}}_{i\phi}$ are the chemical potential and partial molar volume of component i at the position ϕ and μ_{iB} is the chemical potential of component i in bulk. Now

$$\mu_{i\phi} - \mu_{iB} = \mu^\circ_{i\phi} - \mu^\circ_{iB} + RT \ln \frac{a_{i\phi}}{a_{iB}} \qquad (9)$$

in which the activity $a_{i\phi}$ is referred to pure liquid component i at ϕ, a_{iB} to pure liquid i in bulk. From (8) and (9) it follows that

$$\frac{a_{1\phi}}{a^{\alpha}_{2\phi}} = \frac{a_{1B}}{a^{\alpha}_{2B}}\, e^{-[(\mu^\circ_{i\phi} - \mu^\circ_{1B}) - \alpha(\mu^\circ_{2\phi} - \mu^\circ_{2B})]/RT} \qquad (10)$$

where

$$\alpha = \bar{\bar{V}}_{1\phi}/\bar{\bar{V}}_{2\phi}$$

Assumptions. I.—$\mu^\circ_{i\phi} - \mu^\circ_{iB} = -\epsilon_i(\phi)$, the Polanyi

(1) Work performed in the Ames Laboratory of the Atomic Energy Commission.

(2) (a) M. Polanyi, *Verh. deut. physik. Ges.*, **18**, 55 (1916); (b) M. Polanyi, *Z. Physik*, **2**, 111 (1920).

(3) Wo. Ostwald and R. de la Izaguirre, *Kolloid-Z.*, **30**, 279 (1922).

(4) J. J. Kipling and D. A. Tester, *J. Chem. Soc.*, 4123 (1952).

(5) J. J. Kipling, *Quart. Rev.*, **V**, No. 1, 61 (1951).

(6) S. Brunauer, "The Adsorption of Gases and Vapors," Oxford University Press, London, 1945, pp. 95-120.

(7) G. D. Halsey, *J. Chem. Phys.*, **16**, 931 (1948)

(8) T. L. Hill, *ibid.*, **17**, 590 (1949).

potential of pure component i at ϕ as obtained from the gas adsorption isotherm of component i.

2.—$\tilde{\bar{V}}_{i\phi}$ is the same function of $x_{i\phi}$, the mole fraction of i at ϕ, as $\tilde{\bar{V}}_{iB}$ is of x_{iB}, the mole fraction of i in bulk. In this paper we have used the molar volumes of the pure liquids rather than the partial molar volumes; this simplifies calculations considerably and with the systems used was a minor approximation; it is not in principle a necessary one.

3.—$a_{1\phi}/a^{\alpha}{}_{2\phi}$ is the same function of $x_{1\phi}$ as $a_{1B}/a^{\alpha}{}_{2B}$ is of x_{1B} the latter function being determinable experimentally by activity measurements. With these assumptions (10) becomes

$$\frac{a_{1\phi}}{a^{\alpha}{}_{2\phi}} = \frac{a_{1B}}{a^{\alpha}{}_{2B}} e^{\epsilon_i(\phi) - \alpha\epsilon_2(\phi)/RT} \qquad (11)$$

which is of the form

$$G(x_{1\phi}) = G(x_{1B})f(\phi) \qquad (12)$$

For a specified x_{1B} and ϕ, $G(x_{1\phi})$ is determined by equation (11), and hence, by assumption 3, $x_{1\phi}$ is obtained by inversion. For any value of x_{1B} the predicted adsorption is therefore

$$\frac{V\Delta c_1}{m} = \int_0^{\infty} \left(\frac{x_{1\phi}}{\bar{V}_{\phi}} - \frac{x_{1B}}{\bar{V}_B}\right) d\phi \qquad (13)$$

in which $\bar{V}_{\phi}$ and $\bar{V}_B$ are the molar volumes at ϕ and in bulk, respectively.

It should be noted that, if $\epsilon_i(\phi)$ happens to be of the form k_i/ϕ^3, as would be expected from Hills's treatment[8] then $f(\phi)$ becomes exp k/ϕ^3, where $K = \frac{1}{RT}(K_1 - \alpha K_2)$, and because of the nature of the function $G(x_{1\phi})$, $x_{1\phi}$ will be always greater or always less than x_{1B}, so that inversion of adsorption appears to be impossible in this case. Different exponents of ϕ in Halsey type potential functions may well lead to adsorption inversion. In any event, the possibility of using analytical forms for $\epsilon_i(\phi)$ is attractive.

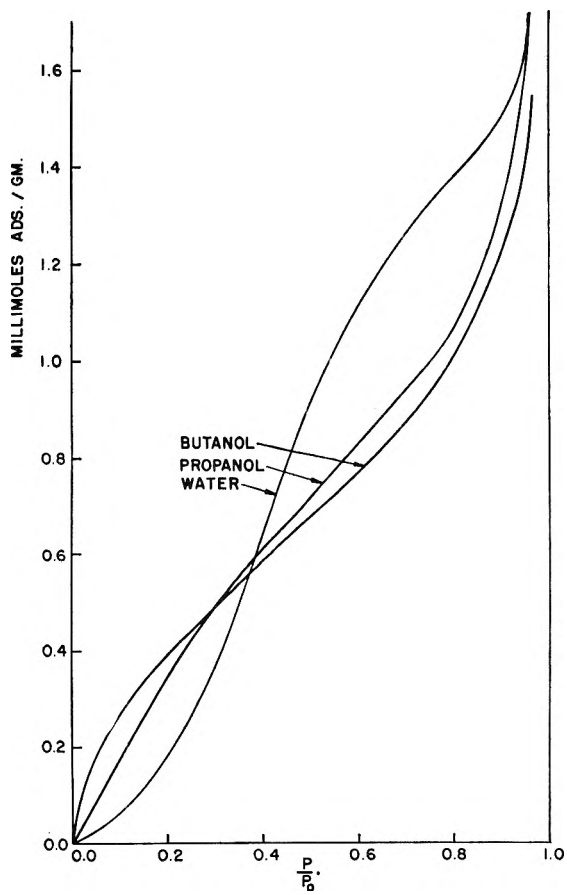

Fig. 1.—Isotherms for the adsorption of water, propanol-1 and butanol-1 by Spheron-6 at 25°.

It should further be noted that an analogous development, using a constant area rather than a constant volume increment constraint, could be made and would be suitable, subject to validity of assumptions analogous to those made herein, for the discussion of unimolecular adsorption.

Finally, certain reservations concerning the validity of the three assumptions basic to this development should be stated explicitly. These are: 1. The clearest indication of the nature of the functions $\epsilon(\phi)$ of which we are aware is contained in Hill's paper. Basically, $\epsilon(\phi)$ is attributed to the total van der Waals attraction between a molecule in the adsorption region and all of the molecules in a semi-infinite slab of adsorbent. Between each molecule in the slab and the molecule in the adsorption region there exists an interaction energy of the form β/r^6, r being the distance between interacting molecules. Integrating this over the slab leads to a total interaction energy of the form γ/x^3, where x is the distance of the adsorbed molecule from the slab, proportional to ϕ. The ϕ^{-3} dependence of $\epsilon(\phi)$ follows immediately.

The basic van der Waals interaction, if carried out through a dielectric, can be shown by trivial modification of the treatment given by Pauling and Wilson[9] to depend inversely on the square of the dielectric constant, which would lead to the same dependence on the part of $\epsilon(\phi)$. This would have no effect on the form of $\epsilon(\phi)$ in single component adsorption, but could in principle cause $\epsilon_i(\phi)$ to vary, at fixed ϕ, with composition of material enclosed between ϕ and the adsorbent surface in the case of multicomponent adsorption.

2. The partial molar volumes of materials in the neighborhood of the adsorbent surface might differ from their values in bulk solutions of the same composition because of orientation and compression due to the adsorption potential. For liquids well below critical temperatures and moderate adsorption potentials (less than 10 kcal.) deviations due to these effects should be minor.

3. Strong orientation of adsorbed molecules may alter the interaction between components of the binary solution in the neighborhood of the surface and thereby alter activity coefficients at fixed composition. Again, this effect could be expected to be more important at higher adsorption potentials.

III. Experimental

Isotherms for the adsorption of water, propanol-1, and butanol-1 on Spheron-6 at 25° were determined gravimetrically using a magnetically compensated balance of the type described by Edwards and Baldwin.[10] The balance was enclosed in a sealed glass system. Vapor was introduced into this system through a sidearm which led to a bulb containing the corresponding liquid. The pressure at which adsorption occurred was the vapor pressure of the liquid at the temperature of this bulb. Approximately 0.5 g. adsorbent was placed in a platinum bucket which was suspended from one end of the balance; the other end of the balance was counterweighted with platinum wire. The adsorbent and the reservoir bulb were thermostated independently, the adsorbent at 25.00 ± 0.02°, the bulb reservoir to temperature necessary for desired pressure to within 0.1°. Pressures were computed from measured bulb temperatures using vapor pressure data from the International Critical Tables (in the case of butanol-1 this involved extrapolation of measured data, for which the lowest temperature at which a vapor pressure was given was 20°. Isotherms for the adsorption of propanol-1 and butanol-1 from aqueous solution were available from work of Hansen and Craig.[11] Activity data were taken from work of Butler, Thomson and MacLennan.[12]

The Spheron-6 was purified by heating in high vacuum to 1000° for 24 hours, cooled, and stored in a mason jar for subsequent use; the same material was used for solution adsorption and gas adsorption measurements. Prior to gas adsorption measurements the Spheron-6 was outgassed at 25° for 12 hours. The surface area was determined by the Brunauer–Emmett–Teller method using nitrogen adsorption to be 114 square meters per gram.

(9) L. Pauling and E. B. Wilson, Jr., "Introduction to Quantum Mechanics," McGraw-Hill Book Co., Inc., New York, N. Y., 1935, pp. 384-5.

(10) F. C. Edwards and R. R. Baldwin, *Anal. Chem.*, **23**, 357 (1951).

(11) R. S. Hansen and R. P. Craig, to be published.

(12) J. A. V. Butler, D. W. Thomson and W. H. MacLennan, *J. Chem. Soc.*, 674 (1933).

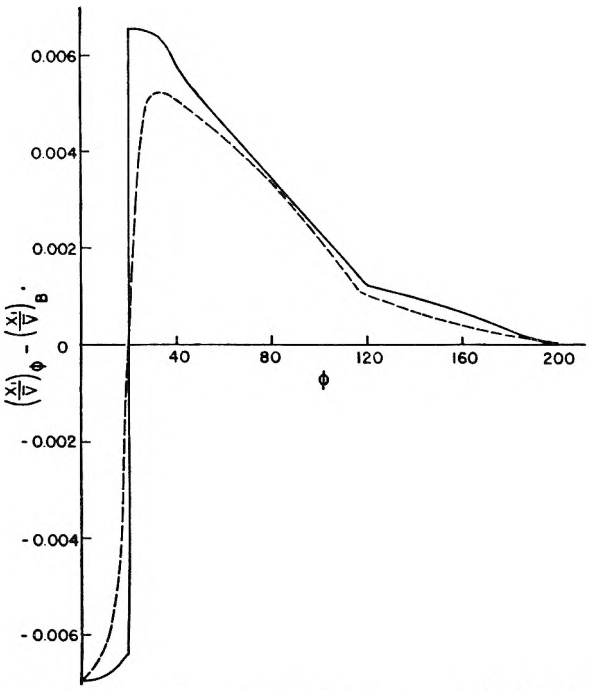

Fig. 2.—Dependence of calculated concentration of propanol-1 with distance from surface. Bulk mole fraction of propanol-1 is 0.200.

IV. Results

Isotherms for the adsorption of water, propanol-1 and butanol-1 on Spheron-6 are presented graphically in Fig. 1. Hysteresis on desorption appeared negligible in the case of propanol-1 and butanol-1, but was appreciable in the case of

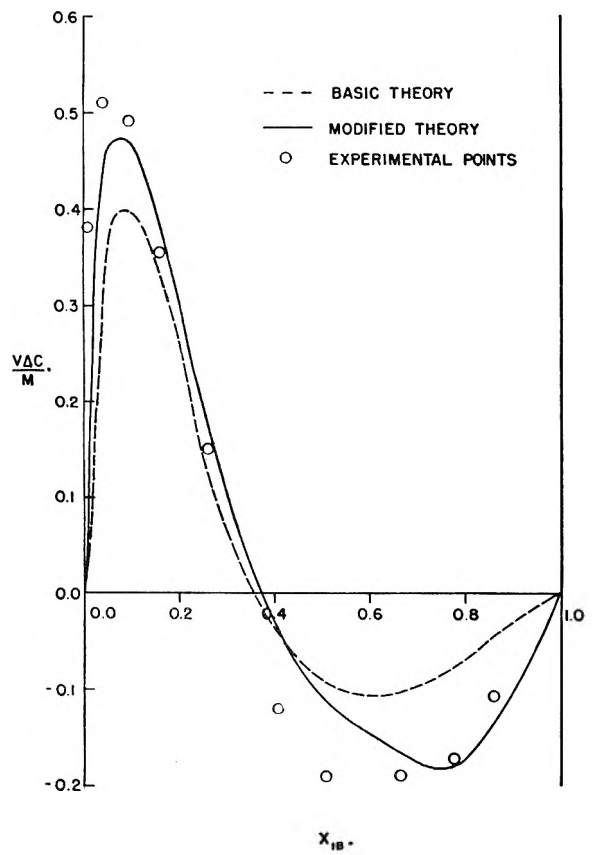

Fig. 3.—Adsorption of propanol-1 from aqueous solution by Spheron-6 at 25°.

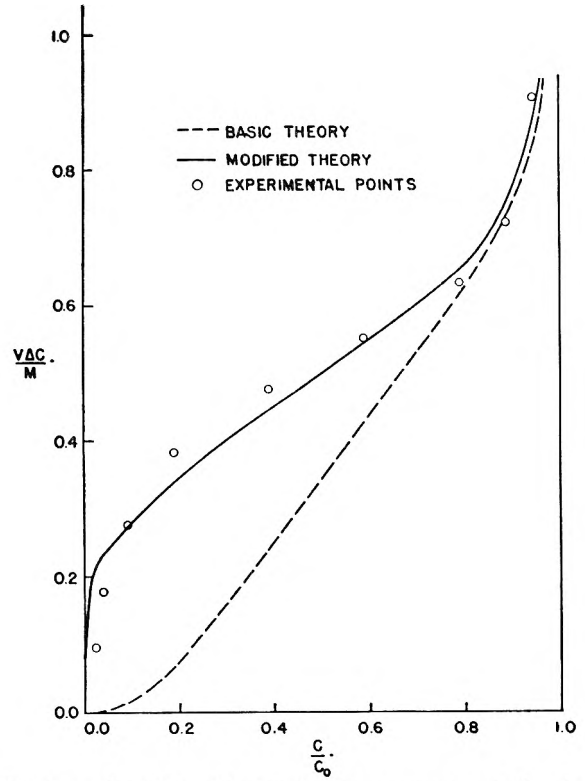

Fig. 4.—Adsorption of butanol-1 from aqueous solution by Spheron-6 at 25°.

water over the entire reduced pressure range (the desorption isotherm was higher than the adsorption isotherm by very nearly 0.2 millimole per gram over the range $0.2 < p/p_0 < 0.7$, the difference decreasing to 0.1 millimole per gram at $p/p_0 = 0.1$ and 0.9). The adsorption isotherm shown was used in calculations; it lay between isotherms reported by Anderson and Emmett[13] for Spheron-6 and Spheron-6 outgassed at 950 to 1000°.

A representative plot of $(x_{1\phi}/\bar{V}_\phi - x_{1B}/\bar{V}_B)$ as a function of ϕ as calculated using the theory developed herein is shown (broken line) in Fig. 2. Isotherms calculated for the adsorption of propanol-1 and butanol-1 from aqueous solution, obtained by graphical integration from graphs such as Fig. 2, are shown (broken lines) in Figs. 3 and 4. Points are values obtained by measuring adsorption from solution. In these figures, ordinates are $\bar{V}\,\Delta c/m$, the apparent adsorption from solution, in millimoles per gram; the abscissa is mole fraction propanol in the propanol–water case, reduced concentration (concentration divided by saturation concentration) in the butanol–water case.

Estimated experimental errors in solution and gas adsorption isotherms are not in excess of 0.02 millimole per gram. The errors in gas adsorption isotherms correspond to uncertainties in calculated solution adsorption isotherms which are also approximately 0.02 millimole per gram.

V. Discussion

The calculated isotherm for the adsorption of propanol-1 from aqueous solution by Spheron-6 is seen to be in equalitative and rough quantitative agreement with that observed experimentally. Calculated amounts adsorbed are lower in magnitude than those observed by about 20% at low mole fractions of propanol-1, 40% at high mole fractions.

The calculated isotherm for the adsorption of butanol-1 from aqueous solution is seen to agree well with that observed at high reduced concentration, but to be far too low at low reduced con-

(13) R. B. Anderson and P. H. Emmett, THIS JOURNAL, **56**, 756 (1952).

centration, so that the calculated isotherm has a monotone curvature rather than the sigmoid shape observed.

Both the propanol-1 and butanol-1 calculated isotherms correspond to deviations in the $\epsilon_{i(\phi)}$ of the same order of magnitude. Greater isotherm deviations result in the butanol-1 case because here the mole fraction is a discontinuous function of the activity; therefore at a given ϕ an increase of 100 cal. in $\epsilon_1(\phi) - (\bar{V}_1/\bar{V}_2)\epsilon_2(\phi)$ may lead to formation of a butanol-rich phase over a finite neighborhood of ϕ especially if the slope of this function, which we may call the effective adsorption potential of the alcohol, is not very great.

Graphs of the type of Fig. 2 in every case indicated that water was concentrated in the immediate vicinity of the surface, and even at moderately high alcohol concentrations the theory indicated an appreciable fraction (up to 0.75) of a complete monolayer of water to be next to the solid surface, with the alcohol beginning to concentrate past this layer. In terms of the theory, this results from the fact that, although the adsorption potential per mole is greater for the alcohol than for water over the entire range of ϕ, the adsorption potential per unit volume is greater for water than for alcohol in both cases for $\phi < 20$ mm.^{3}. While none of the adsorption potentials could be fit by single functions of the form k/ϕ^n the adsorption potential for water was a more rapidly decreasing function of ϕ than those of the alcohols. Qualitatively, this would be expected if the adsorption potential for water was due to an attracting (two dimensional) layer, as with a surface oxygen complex layer,[12] which would lead to a potential of the form k/ϕ^4, and the adsorption potentials for the alcohols were due to an attracting slab leading to potentials of the form k/ϕ^3. A surface oxygen complex layer on a carbon slab should lead to terms of both types for all adsorbates, but in the cases considered here the terms could very well dominate in the manner indicated. The calculated concentration of water in the immediate neighborhood of the surface would have been yet more pronounced had the desorption isotherm for water been used in calculation of the adsorption potential.

For values of ϕ greater than 40 mm.^{3} the adsorption potential of water is negligible and adsorptions for higher values of ϕ are controlled by the adsorption potentials of the alcohols. Especially in the range $20 < \phi < 70$ mm.^{3}, these are too low to account for the observed adsorption from solution.

It was found possible to improve agreement between calculated and observed adsorption isotherms markedly by modifications of the effective adsorption potential suggested by graphs such as Fig. 2. These modifications were as follows: 1. For values of ϕ less than 20 the adsorption potential of the alcohol was neglected. 2. For values of ϕ greater than 20 a term $k/(\phi - 10)^4$ was added to the effective adsorption potential.

The effects of these modifications are indicated as solid curves in Figs. 2, 3, and 4. The form of the term added for values of ϕ greater than 20 is suggested by the form of interaction between a layer of dipoles centered at $\phi = 10$ with dipoles and polarizable molecules on a surface ϕ; since the density of the dipole layer, dipole moments and polarizabilities are known the order of magnitude of K can be estimated theoretically; the order found was of this order of magnitude.

These modifications are believed appropriate only for the systems here studied, and result probably from the complexity of a carbon–oxygen complex surface, possibly interacting irreversibly with water. It is hoped that a more satisfactory test of the theory developed can be conducted in the near future.

DISCUSSION

TODD DOSCHER.—Doesn't the conclusion that a film of water is primarily adsorbed on the carbon violate one of the chief assumptions of the theoretical development? Certainly, the presence of the water dipoles on the surface will cause the subsequent sorption of the alcohol to be different both in kind and degree from that on the carbon surface. The modification of the theory which is introduced would have to be specifically determined for each system, and its practicability as a general theory would be lost.

ROBERT S. HANSEN.—In our opinion the absorption of water in a layer of oriented dipoles does violate one of the basic assumptions of the theoretical development, and therefore necessitates a correction of the type made. Indeed, the correction used was obtained theoretically. The interaction energy between a dipole (1) and a polarizable molecule (2) at distance r is

$$u = (\alpha_1 u_2^2 + \alpha_2 u_1^2)/r^6 \qquad (1)$$

If the polarizable molecule interacts with an infinite film of dipoles of surface density σ at distance z the interaction energy becomes

$$u = \pi(\alpha_1 u_2^2 + \alpha_2 u_1^2)/2z^4 \qquad (2)$$

Replacing z by $(\phi - 10)/1000A$, where A is the specific surface area and ϕ is in mm.^{3}, setting $\sigma = 5.85 \times 10^{14}$ dipoles/cm.^{2} (computed by dividing the number of molecules of water in 20 mm.^{3}, the value of ϕ at the indicated water layer limit, by the surface area of the absorbent) and converting to calories per mole there is obtained

$$E_{int} = 6.22 \times 10^8/(\phi - 10)^4 \text{ cal./mole for propanol-1}$$

$$E_{int} = 7.60 \times 10^8/(\phi - 10)^4 \text{ cal./mole for butanol-1}$$

It is presumed that corresponding interaction energies between water dipole layer and water are already included in the measured $E_2(\phi)$.

It is felt that the assumptions involved in the development or the theory have been clearly stated; the claim to generality is of course subject to validity of assumptions. In the experimental work herein described corrections for deviations could be made in an apparently straightforward manner, but it is hoped that experimental work can be presented in the near future where such corrections will not be needed.

PAPER CHROMATOGRAPHY OF CHLOROPLAST PIGMENTS: SORPTION AT A LIQUID-LIQUID INTERFACE

BY HAROLD H. STRAIN

Argonne National Laboratory, Lemont, Illinois

Received March 2, 1953

The interface between two immiscible liquids, such as water and petroleum ether, exhibits selective affinity for chloroplast pigments. With water or aqueous solutions fixed in porous filter paper, this sorption at the interface between the liquids serves for the chromatographic separation of mixtures of chloroplast pigments dissolved in petroleum ether. With counter flow of water droplets and petroleum ether solutions of the pigments, sorption at the liquid–liquid interface may be utilized for the continuous resolution of the mixtures into two principal fractions, the more sorbed and the less sorbed components.

Introduction

The resolution of mixtures by chromatography has usually been attributed to three principal distribution phenomena. These selective distribution processes are the sorption of solutes at the interface between a solid and a liquid or gas, the partition of solutes between a fixed, dispersed liquid and a mobile solvent, and the distribution of a solute between a chemically reactive substance as an ion exchange resin and a liquid or gas.[1]

Many of these distribution processes have also been employed in paper chromatography.[1] Paper chromatography by adsorption on the paper itself was utilized for the separation of carbon disulfide-soluble chloroplast pigments by Brown[2] in 1939. It was applied to the one-way and two-way separation of water-soluble dyes by Liesegang[3] in 1943. Paper chromatography by partition of the solutes between immiscible liquids was utilized for the separation of mixtures of amino acids by Consden, Gordon and Martin[4] in 1944. Reversal of the liquid phases in the paper was introduced by Boldingh[5] in 1948.

Mixtures of chloroplast pigments have now been resolved chromatographically by sorption on the surface of a liquid fixed in paper. The paper was either of cellulose or of glass fibers. The pigments themselves were insoluble in the fixed liquid which was modified so that it eluted the pigments from the surface of the glass or cellulose fibers. Separate experiments demonstrated that the pigments were sorbed at the liquid–liquid interface in the absence as well as in the presence of the supporting paper.

With paper as the sorbent or as the supporting medium and by suitable selection of fixed and mobile solvents, a single mixture of chloroplast pigments has now been resolved by sorption on the cellulose or glass, by sorption on a liquid and by partition between two immiscible liquids with either liquid fixed in the paper. The sequence of the pigments in the chromatograms varies with the solvent and the sorbent as already reported for analogous separations in columns.[6,7]

(1) H. H. Strain, *Anal. Chem.*, **21**, 75 (1949); **22**, 41 (1950); **23**, 25 (1951); **24**, 50 (1952).

(2) W. G. Brown, *Nature*, **143**, 377 (1939).

(3) R. E. Liesegang, *Naturwissenschaften*, **31**, 348 (1943); *Z. anal. Chem.*, **126**, 172 (1943).

(4) R. Consden, A. H. Gordon and A. J. P. Martin, *Biochem. J.*, **38**, 224 (1944).

(5) J. Boldingh, *Experientia*, **4**, 270 (1948).

(6) H. H. Strain, *Ind. Eng. Chem., Anal. Ed.*, **18**, 605 (1946).

(7) H. H. Strain, *J. Am. Chem. Soc.*, **70**, 588 (1948).

Materials.—Cellulose paper was Eaton–Dikeman Grade 301, 0.03 or 0.05 inch thick. Glass paper was obtained from the Naval Research Laboratory.[8]

For the separation of pigments by sorption on the surface of the glass or the cellulose, the paper was used without special treatment or after drying at 100°. For the separation of pigments on the surface of a fixed liquid, the paper was moistened with water and with solutions of polyhydroxy compounds such as glycerol or sorbitol. The solutions (10%) in water were poured over the paper, the excess solution was poured off, and the moist paper was pressed between dry paper for several hours. The paper was also moistened with glycerol or sorbitol in methanol and was then allowed to stand until all the methanol had evaporated. For a few separations, the paper was moistened with solutions containing mixtures such as glycerol plus glycine and urea, and glycerol plus methanol (10%). The solutions of the polyhydroxy compounds were utilized to prevent dehydration of the paper and also to prevent sorption of the pigments on the fibers of the paper because the polyalcohols and acids are known to elute traces of sorbed xanthophylls from polysaccharides and from glass.[9]

For the separation of the pigments by partition between immiscible solvents, the paper was sprayed with 70, with 80 and with 90% methanol or dipped into these solutions and blotted. In order to reverse the phases and to fix hydrocarbon material in the paper, a solution of vaseline (petrolatum) (about 5%) in petroleum ether was poured over paper which was dried in a hood.

The pigment mixtures to be examined by adsorption were prepared from plant material. For preparation of the pigments of green leaves, fresh grass (10 g.) was cut into sections 1 to 2 mm. long and suspended in 100 ml. of methanol containing about 30 ml. of petroleum ether. After about 0.5 hr., the liquid was decanted through a small piece of cotton into a separatory funnel. Aqueous salt solution (about 400 ml.) was added, and after gentle swirling of the solutions, the aqueous layer was removed. The deep green, petroleum ether solution was washed once or twice with water. Owing to the lability of the pigments, this solution was protected from bright light, and was not employed after it had stood for more than a few hours.

The xanthophylls neoxanthin and violaxanthin were prepared from the leaf extract by chromatographic adsorption.[10] The similar fucoxanthin was prepared from extracts of brown algae.[11] Carotenes were obtained from carrots.

Separations in Paper.—The mixtures were resolved in paper strips 3 × 20 cm. The solution of the mixture was placed in a spot about 7 mm. in diameter near one end of the strip which was stood in a little wash liquid contained in a covered, 2-l. beaker. Because of the rapid flow of the wash liquid into the porous paper, the separations were complete in 20 to 40 minutes.

The separation of leaf pigments by sorption on cellulose paper, by sorption on glass paper, and by sorption on these papers moistened with water or with aqueous glycerol is illustrated by Fig. 1. Similar separations were obtained with paper moistened with glycerol in methanol and dried

(8) T. D. Callinan, R. T. Lucas and R. C. Bowers, Naval Research Laboratory, May 1951, Washington, D. C.

(9) H. H. Strain, *Ind. Eng. Chem.*, **42**, 1307 (1950).

(10) H. H. Strain, W. M. Manning and G. Hardin, *Biol. Bull.*, **86**, 169 (1944).

(11) H. H. Strain and W. M. Manning, *J. Biol. Chem.*, **146**, 275 (1942).

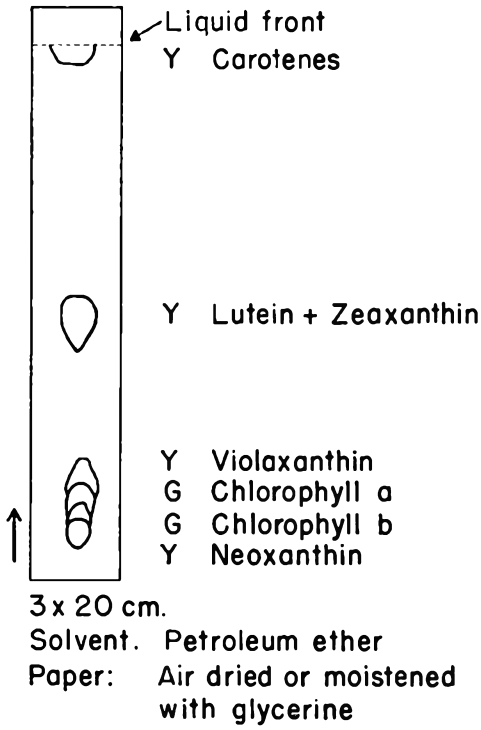

Fig. 1.—Chloroplast pigments separated by sorption on moist or dry glass or cellulose paper: solvent, petroleum ether; Y, yellow; G, green.

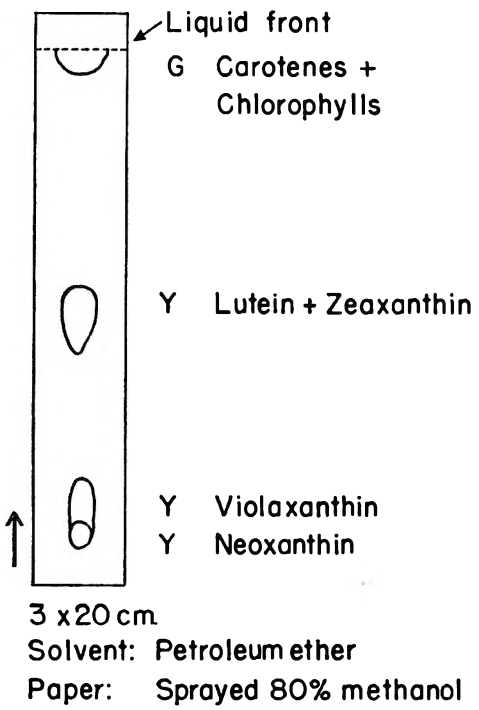

Fig. 3.—Chloroplast pigments separated by partition between methanol (80%) on the paper and petroleum ether.

in air for 24 hours. In each of these experiments, petroleum ether was employed as the wash liquid.

Figure 1 shows the color of the zones, their sequence, and the degree of separation usually obtained. The resolved pigments were identified by their color, by their spectral properties, by mixed chromatograms, and by the blue color produced by exposing the sorbed violaxanthin to the vapors of concentrated hydrochloric acid.[10]

Paper that had been moistened with solutions of tartaric acid or of lactic acid also yielded initial separations like that

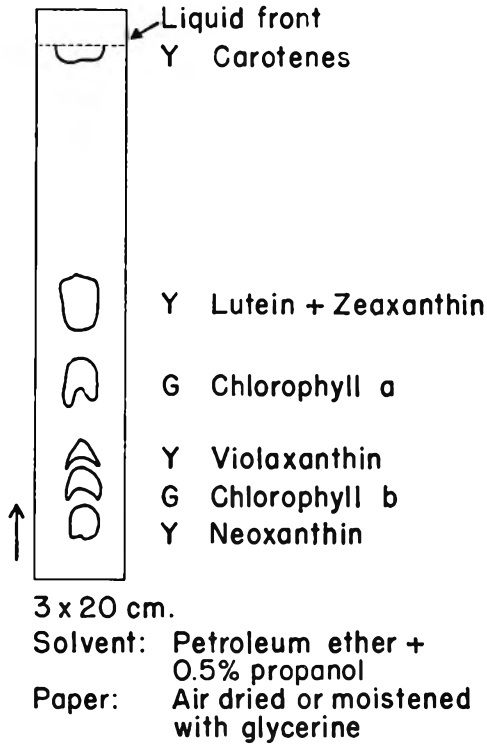

Fig. 2.—Chloroplast pigments separated by sorption on moist or dry paper: solvent, petroleum ether plus 0.5% propanol.

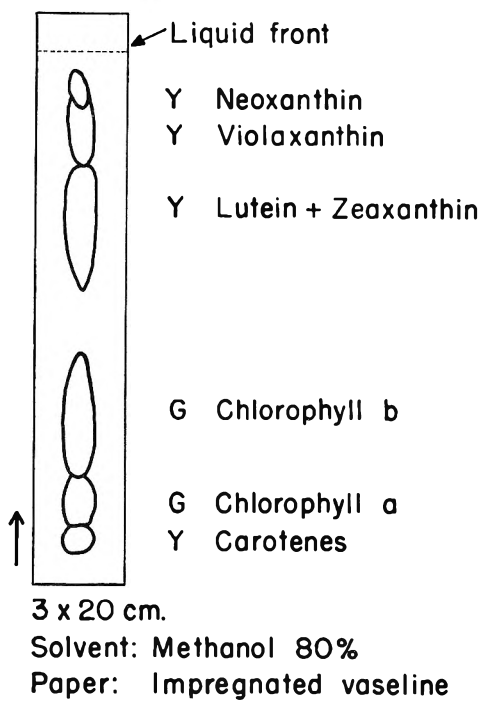

Fig. 4.—Chloroplast pigments separated by partition between petroleum ether plus vaseline on the paper and methanol (80%).

shown in Fig. 1. But these acids gradually removed the magnesium from the chlorophyll forming the corresponding pheophytins which were much less sorbed than the chlorophylls themselves.[10]

The addition of a little propanol to the petroleum ether wash liquid produced separations like that in Fig. 2. This solvent mixture decreased the sorbability of the chlorophylls relative to that of the xanthophylls.[10] The same effect was observed when the pigments were sorbed on dry paper or

on paper moistened with water or with aqueous glycerol solutions.

The separation of the chloroplast pigments with methanol (80%) fixed in glass or cellulose paper and with petroleum ether as the mobile solvent is shown in Fig. 3. With 90% methanol in the paper, all the pigments migrated more slowly than with 80% methanol. Under these circumstances there was some separation of carotenes from chlorophylls. With 70% methanol in the paper, the pigments migrated fast with poor resolution.

With vaseline fixed in the paper, and with 80% methanol as the mobile solvent, the pigments separated as shown in Fig. 4. With 90% methanol as the wash liquid, all the pigments except the carotenes migrated rapidly and separated incompletely from one another. With 70% methanol, all the pigments except neoxanthin and violaxanthin migrated very slowly and were not separated.

This reversal of the sequence of the chromatographic zones makes possible the complete separation of the less sorbed pigments from the more sorbed pigments as commonly effected in columns by variation of solvent.[10] By separation of the pigments with one solvent fixed in paper followed by readsorption of each pigment and with the other solvent fixed in the paper, absolute separations of all the pigments from one another has been achieved.[1]

Mixtures of carotenes with fucoxanthin were examined by means of the four methods illustrated by Figs. 1 to 4. With each method, the petroleum ether-soluble, nonsorbed carotenes were readily separable from the alcohol-soluble, strongly sorbed fucoxanthin.

As indicated by the sorption sequences, the sorption of the pigments at the liquid–liquid interface was similar to the sorption on glass, on cellulose and on powdered sugar.[11] There was no indication of a separation of α- and β-carotenes, or of lutein and zeaxanthin. In this respect, there is a distinct difference between sorptive magnesia and the sorptive systems represented by Figs. 1 to 4, because magnesia is especially effective for the resolution of mixtures of carotenes and for the separation of mixtures of lutein and zeaxanthin.[7]

Separations at the Petroleum Ether–Water Interface of Droplets.—Pigments such as neoxanthin and fucoxanthin, that are insoluble in water, that contain many hydrophilic hydroxyl groups, and that contain a large hydrocarbon skeleton with affinity for petroleum ether, have a marked affinity for the interface between water and petroleum ether. When a solution of these pigments in petroleum ether was shaken with water, the pigments accumulated on the surface of the water droplets and were removed from the petroleum ether. When the water droplets coalesced, the pigments were liberated to the petroleum ether.

When droplets of water from an atomizer were allowed to fall through solutions of neoxanthin or of fucoxanthin in petroleum ether contained in a narrow tube 1 to 2 m. tall, the pigments accumulated on the droplets and were carried to the bottom of the solution. There they were liberated as the droplets coalesced, and under favorable conditions, the liberated pigments were concentrated so that they separated from the solution. In this way, the xanthophyll was removed from the petroleum ether in the tube.

Carotenoid pigments without hydrophilic groups, as for example the carotenes, were not sorbed at the petroleum ether–water interface and were not removed from the petroleum ether solution with water droplets. Chlorophylls were weakly sorbed and were slowly removed from the solution.

This selective sorbability of the polyhydroxyxanthophylls on water droplets served for the continuous separation of two substances such as carotene and fucoxanthin that differed with respect to their sorbability. As an example, a solution of fucoxanthin and carotene in petroleum ether was allowed to flow upward through a long tube. Water droplets falling downward through the solution collected the fucoxanthin and liberated it as the drops coalesced. The separated fucoxanthin was then removed mechanically or by various supplemental flow methods. Both the water and the petroleum ether could be recycled to make the process continuous.

With these petroleum ether–water systems, the sorbent, which is the interface, is formed, destroyed, and regenerated over and over again. For substances that are sorbed at a liquid–liquid interface these sorption procedures may be made the basis of practical separations.

NOTE ADDED MAY 13, 1953.—A photograph of the paper chromatogram of chloroplast pigments prepared by Brown in 1939 has recently been reproduced.[12] Additional separations of chloroplast pigments by adsorption on paper with various organic solvents have also been reported.[13]

DISCUSSION

IRA KUKIN.—Concerning the separation of the neoxanthin type compounds by separation at a petroleum ether–water interface, could not one get a similar type of separation by a solvent–solvent type of extraction, as, for example, petroleum ether–methanol? Is there any advantage to your extraction method which at first glance would appear to be more cumbersome, tedious, and less efficient?

J. L. SHERESHEFSKY.—The suggested variant of chromatographic method consisting of sending a spray of immiscible liquid through a solution of several components is based on the preferential adsorption of one of the components will be separated first, may be predicted from the relative lowering of the surface tension of the solutions of each component in the given solvent.

CHARLES G. DODD.—The author has emphasized the similarity between adsorption at an extended liquid-liquid interface formed by water droplets passing through a petroleum ether solution and adsorption within cellulose or glass paper at water interfaces restrained as films surrounding cellulose or glass fibers. Apparently water is held in an essentially bulk phase enveloping each fiber if the paper were moistened previously with glycerol or glycols. I should like to ask the author if this corresponds with his concept of the intermolecular geometry of the systems such as those in Figures 1 and 2 of the paper? Is this the manner in which the extended interface is developed?

HAROLD H. STRAIN.—In the moist paper the aqueous phase is presumed to envelop each fiber so that the liquid forms a porous, rather than a continuous, bulk phase. The separations at the liquid–liquid interface (Fig. 2) were more effective and more convenient than the separations based upon the solvent–solvent extraction or partition (Figs. 3 and 4).

The experiment with falling droplets was introduced to show that the surface of the droplets is an effective sorptive medium even in the absence of the paper. Falling particles of sorptive solids and falling droplets of liquids already had been utilized for the partial resolution of mixtures of solutes. These procedures serve primarily for the segregation of the solutes into two principal fractions, the more sorbed and the less sorbed components. Where applicable, continuous extraction by the sorption of a solute on the surface of droplets is a convenient and economical separatory procedure.

(12) H. H. Strain, Technion Year Book 1952–53, American Technion Society, New York, 1953, p. 85.

(13) L. Bauer, *Naturwissenschaften*, **39**, 88 (1952).

THE SORPTION OF BENZENE BY FATTY ACIDS[1]

BY J. C. ARNELL

Contribution from the Defence Research Chemical Laboratories, Canada

Received March 2, 1953

The sorption of benzene by the even-numbered fatty acids from caprylic to stearic inclusive has been measured using a standard volumetric adsorption apparatus modified for working with benzene. The isosteric heats of sorption have been calculated by means of the Clausius–Clapeyron equation and the results obtained are explained in terms of liquid solutions (caprylic), solid solutions (stearic) and transition systems (capric). Hysteresis loops were found with palmitic and stearic acids at low sorptions and low temperatures. In each case there appeared to be a maximum temperature above which hysteresis was not found. These observations are explained in terms of normal crystal forces and partial melting points.

Introduction

During some experimental work on the sorption of benzene by aluminium soaps, anomalous behavior was observed between the isotherms of two different soap samples. This behavior was at the time believed to be due to the presence of free fatty acid in one of the samples and as a check, the sorption of benzene by stearic acid was measured. It was later found that the anomalous behavior in the soap experiment was not due to free fatty acid, but the stearic acid isotherm proved to be sufficiently interesting to merit a further investigation of the benzene sorption of the even numbered fatty acids from caprylic (C_8) to stearic (C_{18}). This paper presents the results of this investigation.

Apparatus and Technique

A standard volumetric adsorption apparatus was modified for this work. Mercury cut-offs were used instead of stopcocks where the volume change resulting from their use was not important. Where it was necessary to have stopcocks, special mercury sealed ones were used and lubricated with a benzene-resistant stopcock grease made of dehydrated glycerol thickened with commercial silica aerogel by the method of Puddington.[2] A sample of acid was sealed into a small bulb which was separated from the calibrated vapor bulbs by a mercury sealed stopcock. The pressure in the system was read on a short mercury manometer, which was constructed of "Trubore" tubing. A small bulb was incorporated into the apparatus beside the vapor bulbs and was used to condense vapor during desorption cycles and thus eliminate the multiplicity of points characteristic of desorption in a volumetric adsorption apparatus. The liquid benzene was stored in a bulb closed by a mercury sealed stopcock which was separated from the remainder of the apparatus and from the vacuum line by two mercury cut-offs. A magnetic stirrer was incorporated in the sample bulb when studying caprylic and capric acids, which were either liquid initially or formed liquid layers during the course of sorption, to provide adequate stirring.

The benzene used as the sorbate was redistilled reagent quality, which was degassed by repeated cycles of freezing in Dry Ice–acetone mixture and evacuation, followed by thawing. The fatty acids were all Eastman Kodak Co. white label samples, which were used without further preparation.

To obtain an isotherm, a weighed sample of an acid was sealed into the adsorption bulb, which was then surrounded by a water thermostat at the required temperature. The sample was then evacuated until a pressure of about 10^{-5} cm. was obtained, at which time the pumping was discontinued and the dead volume of the adsorption bulb determined by helium expansion. The helium was then pumped out until a pressure of about 10^{-5} cm. was obtained after which the adsorption bulb was closed off and the mercury cut-off to the vacuum system raised. After a desired amount of benzene vapor had been let into the apparatus, the mercury level in the second cut-off was raised to a mark on the tube. The mercury level was always adjusted to this mark before any pressure reading was made to ensure that the volume of the apparatus was known. As the mercury manometer was made of 9.52 mm. "Trubore" tubing, the change in the apparatus volume due to the mercury movement resulting from pressure changes could be calculated. The amount of benzene vapor sorbed was calculated in the usual way from the $P-V-T$ relationships of the vapor before and after admission to the adsorption bulb.

(1) Issued as DRCL Report No. 121.

(2) I. E. Puddington, *Anal. Chem.*, 21, 316 (1949).

Experimental Results

Over six hundred points were obtained during the sorption measurements with the six acids and in order to condense the presentation of these data only the pressures at which certain fixed quantities of benzene were sorbed at different temperatures are given below. The figures quoted below were all read off the isotherms drawn through each set of data.

Caprylic Acid.—This acid was liquid over the range of temperatures used and was included to provide reference data for the vapor pressure of benzene dissolved in a liquid acid for comparison with the similar data obtained on the longer chain solid acids. Only two isotherms were obtained at temperatures of 29.2° and 41.6°. Equilibrium was very slow being attained in this system, taking a minimum of several hours with vigorous stirring. In many instances the system was left overnight before taking the equilibrium reading. Difficulty was experienced in getting desorption points and as only partial results were obtained, they have been omitted. The experimental results are given in Table I.

TABLE I

SORPTION OF BENZENE BY LIQUID CAPRYLIC ACID

Vol. sorbed, cc. STP/g.	Equilibrium pressures at different temp., mm. 29.2°	41.6°
4	4.25	7.25
8	8.37	14.20
12	12.31	20.84
16	16.12	27.23
20	19.77	33.36
24	23.15	39.22
28	26.32	44.72
32	29.34	49.80
36	32.28	54.57
40	35.08	...

Capric Acid.—Isotherms were determined over a range of temperatures from 14.5 to 32.1°. This region covered sorption in both the solid and liquid phase, as the acid melted in the region 31–32°. A liquid phase was formed at all temperatures as the benzene tended to dissolve part of the acid and form a second phase. Some drift toward increasing pressures with higher sorbed volumes was observed at all temperatures and was thought to be due to small quantities of impurities which dissolved during the early stages of sorption and lowered the vapor pressure of the benzene even more than the acid. The desorption points tended to be at slightly lower pressures than the corresponding absorption points and were in some cases incomplete. Great difficulty was experienced in attaining equilibrium on desorption, due to such occurrences as the crystallization of the acid from the solution to form a skin on the surface, when an increment of vapor was withdrawn. The experimental results are given in Table II.

Lauric Acid.—Isotherms were determined at three tem-

TABLE II

SORPTION OF BENZENE BY CAPRIC ACID

Vol. sorbed, cc. STP/g.	Equilibrium pressures at different temp., mm. 14.5°	19.8°	22.8°	27.9°	28.8°	32.1°
0.5	20.7	18.0	19.0	10.5	..	0.6
1.0	27.5	23.1	22.1	12.2	10.2[a]	1.3
1.5	30.5	25.6	23.5	13.1	10.9	2.0
2.0	31.9	27.5	24.5	13.6[a]	11.3	2.7[b]
2.5	32.6	28.8	25.5	14.1	11.5	3.4
3.0	33.1	29.9	26.1	14.6	11.7[b]	4.1
4.0	33.4	31.1	27.0[a]	15.5[b]	12.0	5.4
5.0	33.6[a]	31.6	27.7	16.2	12.2	6.7
6.0	33.8	32.1	28.1	16.7	12.4	8.0
7.0	34.0	32.5	28.4	17.0	12.5	9.3
8.0	34.2	32.7	28.7	17.1	12.6	10.7
9.0	34.4	32.9	29.0[b]	17.2	12.7	12.0
10.0	34.6	33.1	29.3	17.3	..	13.2
12.0	35.0	33.3[b]	29.7	17.5	..	15.7
14.0	35.6	33.5	30.0	18.1	..	18.1
16.0	36.1	33.7	30.4	19.4	..	20.5
18.0	36.5	34.0	30.8	21.2	..	22.9
20.0	37.0[b]	34.2	31.4	22.8	..	

[a] Indicates the point at which the acid appeared moist. [b] Indicated the point at which a definite liquid phase was present.

peratures, 22.0, 24.6 and 30.0°. The acid was in the solid phase throughout these experiments, although preliminary signs of moistening were apparent near the point of maximum pick-up on the 22.0° sorption curve (21 cc. STP/g.). Only a few desorption points were obtained and they showed a slight inconsistency, due probably to non-equilibrium. The experimental results are given in Table III.

TABLE III

SORPTION OF BENZENE BY LAURIC ACID

Vol. sorbed, cc. STP/g.	Equilibrium pressures at different temp., mm. 22.0°	24.6°	30.0°
0.5	29.4	23.3	13.8
1.0	33.4	29.7	22.6
1.5	36.3	33.9	28.6
2.0	38.4	37.0	32.8
3.0	41.5	41.6	38.5
4.0	44.1	45.0	42.3
5.0	46.5	47.5	45.1
6.0	48.1	49.4	47.5
7.0	49.7	51.0	49.5
8.0	51.1	52.3	51.1
9.0	52.4	53.4	52.6
10.0	53.4	54.3	53.8
12.0	55.0	55.7	..

Myristic Acid.—Isotherms were determined over a temperature range of 0.0 to 21.3°. The acid was in the solid phase at all times and no indication of the formation of a liquid phase was observed. Desorption points were obtained at all but the highest and lowest temperatures and in all cases checked the sorption points. The experimental results are given in Table IV.

Palmitic Acid.—This acid was investigated over a temperature range of 17.6 to 23.6°. Below a temperature of 23.6°, a hysteresis loop was found at lower pressures. The loop was quite large at the lowest temperature studied and decreased in size with increasing temperature, until it disappeared around 23.6°. The loop appeared completely reproducible, as indicated by a second cycle at one temperature. Except for the region where hysteresis was found, the desorption points checked those obtained on sorption. The experimental results are given in Table V.

Stearic Acid.—Isotherms were determined over a temperature range of 20.0 to 39.7°. The hysteresis loops found with palmitic acid were also present in these isotherms, but the temperature at which they disappeared (34°) was higher. As this was the first acid to be examined

TABLE IV

SORPTION OF BENZENE BY MYRISTIC ACID

Vol. sorbed, cc. STP/g.	Equilibrium pressures at different temp., mm. 0.0°	10.2°	11.4°	17.0°	19.9°	21.3°
1.0	6.9	10.0	11.0	13.5	14.4	14.8
2.0	10.6	16.0	17.6	22.0	24.2	25.1
3.0	13.2	20.5	22.1	27.8	30.7	32.0
4.0	15.3	24.0	25.5	32.1	35.6	37.3
5.0	16.9	26.9	28.3	35.6	39.7	41.6
6.0	18.2	29.1	30.5	38.5	43.1	45.1
7.0	19.2	30.9	32.4	40.8	45.8	48.0
8.0	19.9	..	34.0	42.9	48.1	50.4
9.0	..	..	35.3	44.6	50.1	52.5
10.0	..	..	36.5	46.2	51.9	54.3
12.0	..	..	38.4	48.7	54.8	57.2
14.0	..	..	40.1	..	..	59.5

TABLE V

SORPTION OF BENZENE BY PALMITIC ACID

Vol. sorbed, cc. STP/g.	Equilibrium pressures at different temp., mm. 17.6° Ads.	Des.	21.3° Ads.	Des.	22.3° Ads.	Des.	23.6°
0.25	15.2	13.2	13.2	8.5	11.2	7.0	7.5
0.5	20.1	15.5	17.2	11.6	15.2	11.2	13.8
0.75	22.4	17.2	19.5	14.5	18.4	15.9	18.8
1.0	24.0	19.0	21.5	18.0	21.0	20.0	23.3
1.25	25.4	21.1	24.5	23.1	25.0		27.2
1.5	26.5	23.7	27.4		28.3		30.5
1.75	27.7	25.9	30.2		31.1		33.4
2.0	29.0	28.1	32.9		34.0		36.3
2.5	31.9		37.5		38.7		41.1
3.0	35.0		41.5		42.8		45.2
4.0	40.0		47.6		48.9		52.0
5.0	44.0		51.9		53.6		57.6
6.0	47.3		55.2		57.5		62.0
7.0	49.9		58.0		60.9		65.3
8.0	52.0		..		..		67.9

and the appearance of the hysteresis loop was completely unexpected, a great many measurements were made to ensure that the hysteresis loop was reproducible. Seven runs were made on one sample at 29.2° and two on a second sample at the same temperature. Of these first runs, the first four were on the sample in its original state and the last three on the first sample were obtained after the acid had been partially dissolved in condensed benzene and recrystallized, in an attempt to determine differences due to crystal size. No appreciable difference was found between the two sets of curves, although equilibrium was established very slowly after recrystallization due to the solidity of the mass. The first isotherm on a fresh sample of acid was found to give a hysteresis loop, which was slightly displaced toward higher pressures, when compared to subsequent curves at the same temperature. The remainder of these isotherms were in agreement. The experimental results are given in Table VI.

Calculation of Isosteric Heats

By making use of the Clausius–Clapeyron equation[3]

$$\left(\frac{\mathrm{d}\ln p}{\mathrm{d}(1/T)}\right)_n = -\frac{q_{\text{isosteric}}}{R}$$

it was possible to calculate the differential heats of sorption from the isosteres of the various acids given in the preceding tables. As each acid has been found to exhibit a different relationship between the calculated heat and quantity of benzene sorbed, the calculations have been treated individually below. Following common usage, the isosteric heat has been considered positive when heat is evolved.

Caprylic Acid.—When the quantity of benzene sorbed at each of the two temperatures was plotted against the relative pressure, all the points lay on a single curve which indicated

(3) S. Brunauer, "The Adsorption of Gases and Vapors," Princeton Press, Princeton, N. J., 1943, p. 223.

TABLE VI

SORPTION OF BENZENE BY STEARIC ACID

Vol. sorbed, cc. STP/g.	Equilibrium pressures at different temp., mm. 20.0° Ads.	20.0° Des.	25.3° Ads.	25.3° Des.	29.2° Ads.	29.2° Des.	31.0° Ads.	31.0° Des.	33.0° Ads.	33.0° Des.	34.7°	39.7°
0.25	22.5		20.0		18.2		14.9		8.4	7.2	4.2	6.2
0.50	30.5		28.0		24.3		20.5	18.5	15.5	10.6	8.3	11.5
0.75	34.9		33.3		29.0	26.9	24.8	20.2	19.8	13.0	12.5	16.4
1.0	37.4		36.1		32.5	28.6	27.8	21.5	22.5	16.0	16.4	20.5
1.25	39.3		38.4	37.3	34.4	29.8	29.9	22.7	24.6	18.8	20.2	24.8
1.5	41.1		40.3	38.1	35.5	30.8	31.5	24.1	26.5	21.7	23.8	28.5
1.75	42.3	41.7	41.8	38.7	36.5	31.8	32.6	25.6	28.1	25.0	27.0	32.0
2.0	43.2	42.0	42.8	39.2	37.3	32.7	33.6	27.5	30.0	28.4	30.5	36.0
2.25	44.2	42.6	43.7	39.4	38.1	33.6	34.7	29.8	32.1	31.2	33.6	39.5
2.5	45.0	43.0	44.5	40.0	38.9	34.5	35.7	32.0	34.0		36.5	43.3
2.75	45.6	43.3	45.1	40.3	39.5	35.5	36.9	34.5	36.6		39.2	46.8
3.0	46.2	43.6	45.6	40.6	40.2	36.5	38.0	36.8	39.1		41.6	49.8
3.5	47.1	44.0	46.5	41.2	41.6	38.2	41.2		44.0		46.5	55.4
4.0	47.7	44.3	47.1	41.8	42.9	40.2	45.0		48.2		51.0	60.5
4.5	48.0	44.9	47.5	42.5	44.3	43.6	48.6		52.0		55.0	65.3
5.0	48.4	45.3	47.8	43.3	46.7		51.7		55.8		58.6	69.8
6.0	49.0	46.3	49.0	45.5	52.3		57.3		62.3		65.5	78.5
7.0	49.7	47.0	50.4	49.0	56.9		62.1		68.0		71.5	..
8.0	50.4	47.4	53.1	52.6	60.9		66.5		73.0		76.8	..
9.0	50.9	47.9	56.0		64.5		70.6		..		81.4	..
10.0	51.3	48.4	58.7		67.9		74.3		..		85.3	..
11.0	51.6	48.9	61.2		70.8		77.5		..		..	..
12.0	52.0	49.4	63.5		73.5		..		..		..	..
13.0	52.3	50.7	65.5		75.7		..		..		..	..
14.0	52.9	52.3	67.2		77.7		..		..		..	..
15.0	53.9	53.7	68.9		79.5		..		..		..	..
16.0	55.0		70.4		81.1		..		..		..	..
17.0	56.3		71.9		82.7		..		..		..	..
18.0	57.5		73.2		84.1		..		..		..	..
20.0	59.8		..		..		..		..		..	..

that the differential heat of mixing was very small. This was checked by calculating the isosteric heats for sorptions ranging from 4 to 36 cc. STP benzene/g. acid. The average value obtained was 8.04 ± 0.07 kcal./mole as compared to a calculated value for the heat of vaporization of pure benzene of 8.18 kcal./mole.

Capric Acid.—The sorption of benzene by capric acid was much more complicated. With the exception of the 32.1° isotherm, all the measurements were made on the solid acid and from the results obtained, it appeared that the benzene did not form a solid solution in the acid crystals as had been expected. This was concluded from the fact that after approximately 3 cc. STP benzene/g. acid had been sorbed, the acid appeared to become moist as if the benzene was condensing on the outside of the crystals and forming a saturated solution of acid in benzene. As more benzene was sorbed the moistening was extended until a definite liquid layer was formed. Thus the isotherms obtained were, apart from the lower ends, determinations of the vapor pressures of a saturated solution of the acid in benzene at different temperatures. Although the acid used was Eastman "White Label" quality, nevertheless the slight deviation from the vertical of all the isotherms suggested that small quantities of impurities were affecting the vapor pressures.

It was impossible to calculate any heats from these data as no straight lines were obtained when the isosteric values were plotted according to the Clausius–Clapeyron equation. In order to check whether the isotherm data represented the vapor pressure of a saturated solution, a rough experiment was carried out to determine the vapor pressures over the same temperature range. Two sets of determinations were made using a different batch of Eastman acid—the first containing a larger ratio of benzene to acid than the second. There was a possibility that the first results may be slightly high owing to a minor contamination with air, as the system proved very difficult to deaerate. However, four or five freezing and thawing cycles with evacuation were carried out before any pressure measurements were made. The comparative results are plotted in Fig. 1. The rather narrow range of temperature used for the vapor pressure work was occasioned by the large change in the solubility of the acid in the benzene in this temperature range. Between

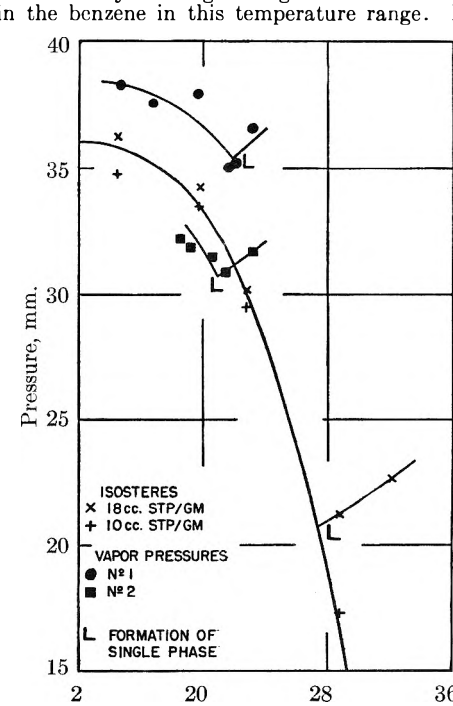

Fig. 1.

18 and 23° the system changed from a solid cake with no apparent liquid present to a crystal free solution at the fixed component ratios used.

Lauric Acid.—Lauric acid appeared to be the first acid of the series that sorbed the benzene without any apparent change. The only indication of any moistening due to the formation of a solution of the acid in benzene occurred at a sorption of 21 cc. STP benzene/g. acid at 22.0°. The heats as calculated from the Clausius–Clapeyron equation proved quite interesting as they were of the opposite sign to normal heats of sorption and are discussed later in this paper. The calculated heats are shown in Fig. 2 and ranged from

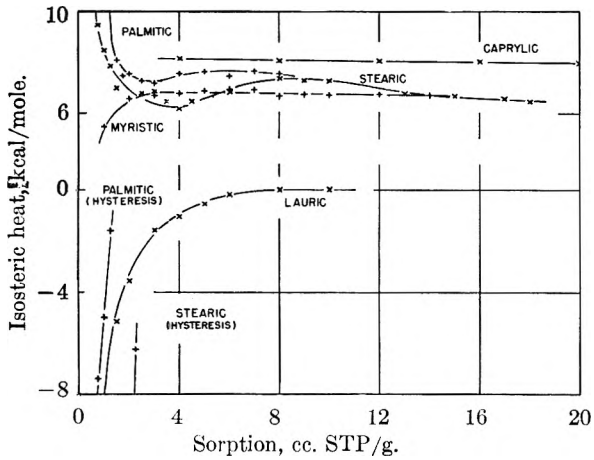

Fig. 2.

−16.7 kcal./mole benzene at a sorption of 0.5 cc. STP benzene/g. acid to approximately zero at 10 cc. STP benzene/g. acid.

Myristic Acid.—Myristic acid gave normal values for the isosteric heats after the first small amount of benzene was sorbed. Below a sorption of 3 cc. STP benzene/g. acid the calculated heats are a little below the average, being 5.49, 6.56 and 6.69 kcal./mole benzene for sorptions of 1, 2 and 3 cc. STP benzene/g. acid, respectively. The isosteric heats for higher sorptions averaged 6.78 ± 0.10 kcal./mole benzene.

Palmitic Acid.—Apart from the regions that showed hysteresis effects, palmitic acid gave heats of sorption similar to myristic acid except at low sorptions where the values were larger instead of smaller. The isosteric heats for sorptions of 2 cc. STP benzene/g. acid and higher averaged 7.45 ± 0.20 kcal./mole benzene and at lower sorptions were 11.1 and 8.08 kcal./mole benzene at 1.50 and 1.75 cc. STP benzene/g. acid, respectively. The hysteresis was considered to be caused by difficulties in the benzene molecules penetrating the crystal lattice and this was partially borne out by the isosteric heats calculated using the adsorption sides of the hysteresis loops. The resultant heats ranged from −11.3 to −1.60 kcal./mole benzene for sorptions of 0.25 and 1.25 cc. STP benzene/g. acid, respectively.

Stearic Acid.—The stearic acid results were again very complicated, as the isotherm data fell into three distinct categories. The first was the low sorption region below the hysteresis loops; the second the region of the hysteresis loops; and the third the essentially normal section of each isotherm above the hysteresis loops. The heats calculated from results in the first category were negative at the start and became positive as the sorption increased; the values calculated from the adsorption side of the hysteresis loops were all very negative, being −26.6 kcal./mole benzene at 0.50 cc. STP benzene/g. acid and increasing to −6.3 kcal./mole benzene at 2.25 cc. STP benzene/g. acid. Above the hysteresis loops the isosteric heats were high at the start (14.9 kcal./mole benzene at a sorption of 0.25 cc. STP benzene/g. acid) and levelled out at about 6.8 kcal./mole benzene at higher sorptions. There appeared to be a minimum in these last heats, which may be seen in Fig. 2 where all the calculated heats are shown. These results tend to confirm the recent work of Dean and Hayes[4] who calculated the differential heats of sorption of *n*-hexane on stearic acid monolayers. They found that on dilute stearic acid monolayers the initial heat of sorption was high but fell rapidly and after passing through a minimum of about 6 kcal./mole benzene, gradually rose to approach the heat of vaporization of benzene. On close packed monolayers the heat of sorption was very low at small sorptions and rose with increasing sorption and finally reached the value for the heat of vaporization.

Discussion

It is possible to offer qualitative explanations for the various results that have been reported above based on the relative solubilities of the different acids in benzene and their difference in melting points.

Starting with the smallest of the acid molecules studied, caprylic acid is a liquid at the temperatures of the experiments and is miscible with benzene in all proportions. Little interaction between the two compounds would be expected and the heat of sorption (solution) proved to be practically the heat of vaporization of pure benzene.

Turning to the largest of the molecules studied, at the higher temperatures and higher sorptions stearic acid appeared to absorb benzene vapor to form a solid solution with a reasonable amount of interaction, as indicated by an average heat of sorption of about 6.8 kcal./mole benzene. This figure is quite consistent with the concept that there will be a small amount of energy required for the benzene to penetrate the acid structure and for this structure in turn to swell. At lower temperatures and lower sorptions hystersis was found, accompanied by higher negative heats. This hysteresis effect only appeared at temperatures below about 34° and the hysteresis loops increased in size as the temperature was decreased. In determining the change in the density of stearic acid with temperature, Puddington[5] found that at approximately this same temperature the linear relationship between density and temperature underwent a change of slope and attributed it to a partial melting of the crystals, due to the fusion of the hydrocarbon ends of the fatty acid molecules. The hydrocarbon chain in a stearic acid molecule is sufficiently long that it might be expected to resemble the corresponding hydrocarbon octadecane, with respect to crystal bonding and thus have a melting point near that of the hydrocarbon. Octadecane melts at 28° and it is to be noticed that this temperature is quite close to that at which the hysteresis effects disappear. It is suggested therefore that stearic acid undergoes a partial melting at a temperature of about 34°. Below this temperature the crystal lattice of stearic acid will be quite rigid owing to the van der Waals forces between the hydrocarbon chains of the individual molecules of the crystal. Under these circumstances it will be difficult for a benzene molecule to penetrate the crystal to form a solid solution and appreciable energy will be required; hence the high negative heats at low sorptions. The gradual decrease in the size of the hysteresis loops with increasing temperature is assumed to be a purely physical effect. The penetration of a benzene molecule into the fatty acid crystal will cause some displacement in the relative positions of parallel acid molecules and will reduce the mutual bonding. If sufficient benzene enters the crystal

(4) R. B. Dean and K. E. Hayes, *J. Am. Chem. Soc.*, **74**, 5982 (1952).

(5) I. E. Puddington, unpublished work.

it will cause appreciable swelling and reduce the bonding to a point similar to that found above the partial melting point. Under these circumstances the isotherm will have a similar shape to those at higher temperatures. The nearer the temperature is to the partial melting point, the fewer the bonds to be ruptured before the restriction to benzene penetration disappears and hence the observed decrease in the size of the hysteresis loops with increasing temperature. The hysteresis loops are considered to be of the kind that have been found to accompany sorption when the solid undergoes appreciable swelling during the take-up of vapor. Examples of these systems are the sorption of water by wood,[6] cellophane,[7] proteins[8,9] and high polymers.[9] When the temperature is above this partial melting point, the restrictions to benzene penetration of the crystal disappear and simple solid solutions appear to form readily.

Additional proof of this premise is found in the data on palmitic acid. In this case similar hysteresis loops were found at the lower temperatures and their disappearance occurred at about 23°, which is 3° above the melting point of hexadecane, the corresponding hydrocarbon. A similar effect was also looked for with myristic acid, but no indication of hysteresis was found due possibly to the fact that it would only be expected to occur below about 10° and the only isotherm measured below this temperature was at 0°, which is also below the freezing point of benzene. Thus as indicated above, myristic acid gave heats of sorption consistent with palmitic and stearic acids and with the concept of a simple solid solution.

Capric and lauric acids present a different picture and are considered to show the transition between a liquid solution of a fatty acid in benzene and a solid solution of benzene in a fatty acid. Capric acid is quite soluble in benzene and as the chain length increases, so the solubility of fatty acids in benzene decreases, with the result that stearic acid is only slightly soluble. On the basis of the foregoing, lauric and capric acids would be expected to sorb benzene vapor readily and show a normal heat of sorption; instead, however, high negative heats are again in evidence and capric acid apparently does not form a solid solution with benzene. It is felt that in both these cases the increased solubility in benzene is responsible for the experimental results. Capric acid does not sorb benzene because it is so soluble that instead it tends to dissolve in any benzene that condenses on the crystals. The negative heats that are indicated from the vapor pressure–temperature relationship (Fig. 1) are fortuitous and are due to the fact that in the temperature range studied the increase of solubility of capric acid in benzene with temperature is so large that the vapor pressure lowering due to the increased solubility is greater than the increase in the vapor pressure of pure benzene over the same temperature interval. This results in a decrease in the vapor pressure of a saturated solution with an increase in temperature, which gives a negative heat with the Clausius–Clapeyron equation. Although lauric acid did not appear moist until a sorption of 21 cc. STP benzene/g. acid, it is considered nevertheless that the same explanation can be applied to the negative isosteric heats.

It is hoped to extend this work both from the theoretical point of view and a study of similar vapor sorptions on fatty acids.

(6) W. W. Barkas, Report No. P. 82, Forest Products Research Laboratory, England (1948).

(7) S. E. Smith, *J. Am. Chem. Soc.*, **69**. 646 (1947).

(8) G. N. S. Rao, K. S. Rao and B. S. Rao, *Proc. Indian Acad. Sci.*, **25**, 221 (1947).

(9) B. Katchman and A. D. McLaren, *J. Am. Chem. Soc.*, **73**, 2124 (1951).

PHYSICAL ADSORPTION ON UNIFORM SURFACES[1]

BY W. M. CHAMPION AND G. D. HALSEY, JR.

Contribution from the Department of Chemistry and Chemical Engineering, University of Washington

Received March 2, 1953

Stepless isotherms on a uniform surface have been calculated, using modifications of Hill's treatment of lateral interaction. However the assumptions necessary for success are so specific and unreal that the necessity of assuming surface heterogeneity for real isotherms is demonstrated.

In earlier papers[2-4] we have criticized current theories of adsorption, and introduced the assumption of a non-uniform surface to reconcile theory and experiment. It is unjustified, however, to conclude that this assumption is correct without making an extreme attempt to calculate sensible isotherms on a uniform surface. In this paper we do succeed in calculating such isotherms, but we show that the other assumptions necessary are both very specific and unreal.

Stepwise Adsorption.—We have asserted[2] that on a plane uniform surface adsorption would proceed in a stepwise fashion as pressure increases. Using the equations of Hill[5] we will show that these equations predict steps when they are modified to take account of energy transmitted from the adsorbent to the n'th layer. The equations we have solved numerically are

$$p/p_0 = [(\theta_n - \theta_{n+1})/(\theta_{n-1} - \theta_n)] \times \exp\{(-E_n/kT) + (w/kT)(-2\theta_n + 1)\}$$

$$\theta = \sum_{n=1}^{\infty} \theta_n ; \quad \theta_0 = 1$$

where $E_n = E_1/n^3$, that is, employing the cube law of force decay discussed elsewhere.[3,4,6]

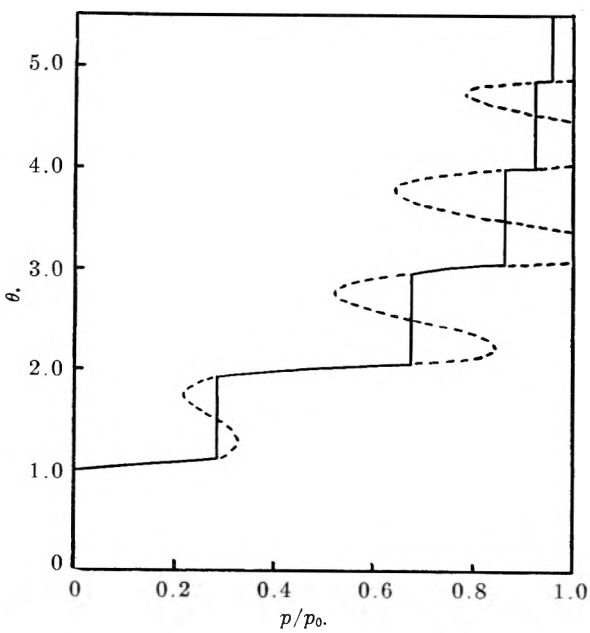

Fig. 1.—Stepwise isotherm calculated with cube law for decay of surface energy.

Setting $E_1/kT = 10$ and $w/kT = 8/3$, the isotherm in Fig. 1 was calculated by trial and error. The steps were located by using the rule of equal areas on the loops, with the isotherm plotted against log p/p_0.[7]

The choice of the lateral interaction parameter $w/kT = 8/3$ is rather unimportant, as long as it is somewhat greater than the critical value of two. Further increase of w/kT only sharpens the steps a little more by widening the amplitude of the loops. The cube law force field from the surface separates the steps, prevents them from all falling at $p/p_0 = 1$ and thereby making application of the rule of equal areas to the loops obvious.

The Removal of the Steps.—It seems reasonable to assert, that if the lattice constant of the adsorbent is not compatible with that of the adsorbate, that then the periodic structure of the surface would prevent the ad-atoms from assuming the optimum configuration for interaction. Thus w/kT would be reduced, and adsorption could proceed without steps. It appears that this is really true in the first layer, and we shall now examine the effect of extending the assumption to higher layers. One may imagine, for example, that the unfavorable lattice distance in the first layer imposes a similar distance on the second, etc.

It is necessary, however, that high layers eventually assume the structure of the bulk adsorbate, because otherwise the isotherm would fail to predict the assumed condensation pressure p_0 of the bulk phase.

We therefore modify Hill's equations again by introducing parameters g_n

$$p/p_0 = [(\theta_n - \theta_{n+1})/(\theta_{n-1} - \theta_n)] \times \exp\{(-E_n/kT) + (w/kT)(-2g_n\theta_n + 1)\}$$

$$\theta = \sum_{n=1}^{\infty} \theta_n; \ \theta_0 = 1; \ w = -E_L/2$$

where g_n varies from zero in the first layer to unity when n is large. The parameters g_n reflect the ability of each layer to interact horizontally, relative to the bulk phase. We shall not need to make any theoretical estimates of g_n simply because it emerges that the specifications of no steps restricts g_n to small values.

In addition, if upon reducing the value of g_n one retains the $1/n^3$ law for E_n, the net energy of adsorption is reduced so much that almost no adsorption takes place at all, until, very near $p/p_0 = 1$, all the layers for which g_n has been substantially reduced go on at once. Therefore, in any layer for which $g_n < 1$, E_n must be increased to compensate for the loss in horizontal interaction.

(1) Supported by Contract No. AF 19(604)-247 with Air Force Cambridge Research Laboratories.

(2) G. D. Halsey, Jr., *J. Chem. Phys.*, **16**, 931 (1948).

(3) G. D. Halsey, Jr., *J. Am. Chem. Soc.*, **73**, 2693 (1951).

(4) G. D. Halsey, Jr., *ibid.*, **74**, 1082 (1952).

(5) T. L. Hill, *J. Chem. Phys.*, **15**, 767 (1947).

(6) T. L. Hill, *ibid.*, **17**, 590 (1949).

(7) R. H. Fowler, "Statistical Mechanics," 2nd Ed., Cambridge University Press, New York, N. Y., 1936, p. 795.

For example, if all $g_n = 0$, E_n must increase to a constant value everywhere to ensure condensation at p_0, and the BET isotherm emerges. This necessary assumption of a constant force field is only a formal reminder of the unreality of the BET hypothesis of no horizontal interaction.

Two isotherms calculated using specific values of the parameters are shown in Figs. 2 and 3. The

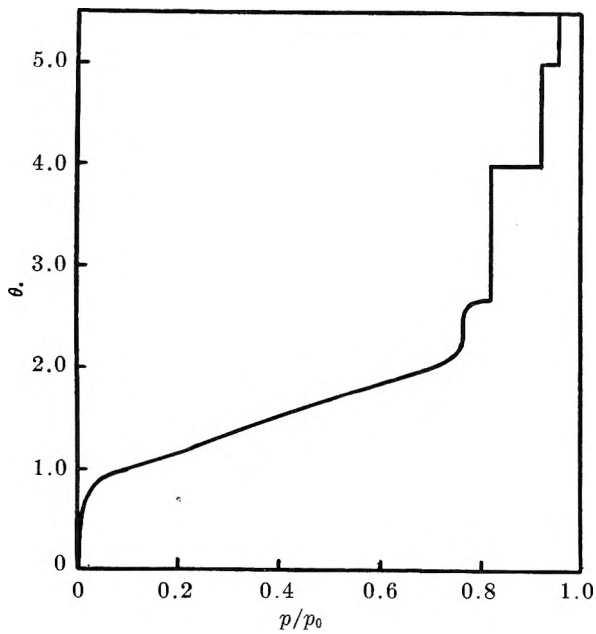

Fig. 2.—Isotherm with first step in third layer.

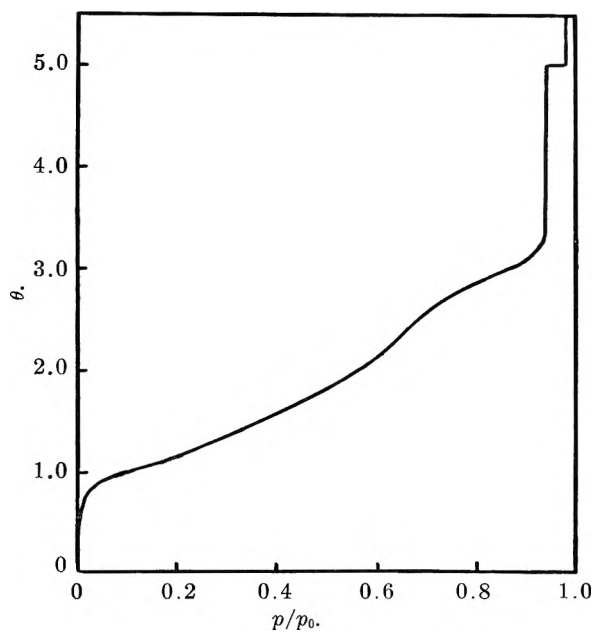

Fig. 3.—Isotherm with first step in fourth layer.

values of the parameters chosen are given in Table I. BET plots are shown in Fig. 4. In both cases E_L/kT was set equal to 10, making $w/kT = 5$ when $g = 1$. In other words, if we assumed that the heat of vaporization is given roughly by Trouton's rule, that the lateral and horizontal interactions are equal, and that the isotherm is taken below the boiling point, then these values are as small as possible. At any lower temperature, the step-forming tendency is greater, because w/kT is larger.

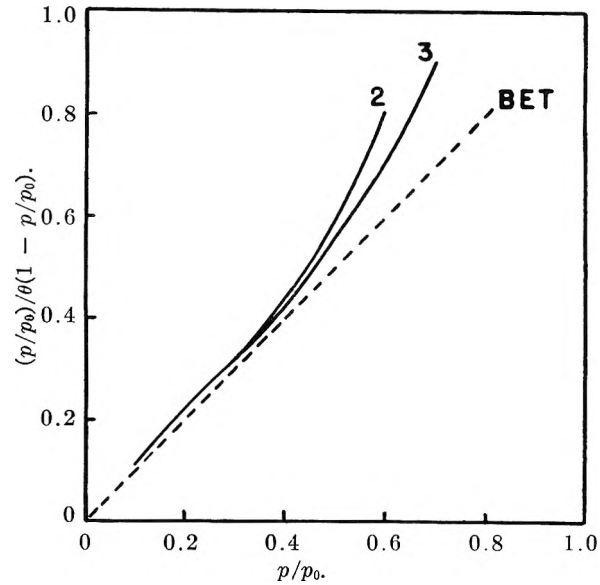

Fig. 4.—BET plots of Figs. 2 and 3.

TABLE I

	Figure 2		Figure 3	
n	g	E_n/kT	g	E_n/kT
1	0	10	0	10
2	0.2	4.8	0.2	4.625
3	0.4[a]	3.5	0.3	4.1
4	1	0.40	0.4[a]	3.25
5	1	.08	1	0.15

[a] This value of g gives the critical value of the interaction energy.

Discussion of the Isotherms.—The isotherm of Fig. 2 looks normal and gives a good BET plot below $p/p_0 = 0.4$. The steps have been suppressed only below $\theta = 3$. Above that value the treads grow relatively short. The riser of the first step is longer than one layer because the third layer is completed and the fourth layer filled in one step.

Because of this fact, although $g_4 = 1$, E_4 has to be larger than the cube law value to put this step below $p/p_0 = 1$.

In Fig. 3 one more step has been removed. The choice of g's has made the isotherm somewhat "bumpier," which shows how sensitive the isotherms are to this choice.

A glance at the values of E_n shows the unreality of the assumptions. As long as steps are eliminated E_n can hardly be allowed to decline at all, much less to follow the cube law. Such an assumption is contrary to present day theories of molecular forces. It is also apparent that both isotherms are more or less bumpy in the vicinity of integral θ's. This bumpiness is extremely sensitive to the choice of g's for a given value of E_L/kT. It is thus sensitive to temperature changes. Therefore, in order to reproduce smooth experimental isotherms over a reasonable temperature range, g_n would have to be an arbitrary function of temperature so designed to always eliminate bumps. (In passing one should remark that the occasional bumpy isotherm experimentally encountered has an easy explanation in terms of an almost uniform surface.)

Conclusion.—The equations of Hill are based on cubic packing rather than hexagonal packing. To be consistent we should have assigned (as he did) $^2/_3$ of E_L to lateral interaction rather than $^1/_2$. As Hill has pointed out, the solution assuming hexagonal packing is very difficult but, as we have pointed out, such a refinement increases the tendency to form steps, because of edge effects associated with the pyramidal piles of molecules. We have also made E_L/kT as small as possible. We therefore consider the following conclusion conservative: the unreality of the assumptions concerning both surface forces and film structure necessary to calculate smooth isotherms on a uniform surface justifies the assumption of a non-uniform surface to explain smooth isotherms.

DISCUSSION

J. L. SHERESHEFSKY.—An adsorption isotherm of nitrogen on glass spheres at liquid air temperature obtained in my laboratory (Shereshefsky and Weir, *J. Am. Chem. Soc.*, about 20 years ago) and also of oxygen on the same adsorbent (unpublished) indicate the presence of the upper branch of a loop, as shown by the dotted curve in Fig. 1 of this paper. This phenomenon, which we assumed to be due to a phase transition, occurred at very low pressures, approx. 10^{-3} mm. The surface apparently was uniform, as indicated by the Langmuir type isotherms of other adsorbates on the same glass spheres.

A THERMISTOR CALORIMETER FOR HEATS OF WETTING; ENTROPIES FROM HEATS OF WETTING AND ADSORPTION DATA

BY A. C. ZETTLEMOYER, G. J. YOUNG, J. J. CHESSICK AND F. H. HEALEY

Surface Chemistry Laboratory, Lehigh University, Bethlehem, Pennsylvania

Received March 2, 1953

A calorimeter employing a thermistor as the temperature sensing element has been constructed. Heats of immersion in water have been obtained for asbestos, rutile, graphon and silica. The thermistor showed excellent sensitivity and stability. The various factors found to influence the reproducibility of the heat measurements are discussed. Heats of immersion in water were measured for asbestos on which various fractions of a water monolayer had been adsorbed; these heats decreased linearly with surface coverage. This behavior, together with the shape of the isosteric heat curves, was taken as an indication that the surface was homogeneous. Absolute entropies of water adsorbed on asbestos were calculated by two methods: (1) from adsorption isotherm data obtained at two temperatures, and (2) from a combination of heats of immersion and single isotherm data. Although the second method gave considerably more precision, both sets of results were in good general agreement.

Introduction

In order to provide further information on the interaction between surfaces and adsorbates supplemental to that obtained from gas adsorption measurements, heats of immersion were desired. For such measurements there is a need for a convenient and relatively inexpensive calorimeter free from inherent errors. The small amount of heat liberated by immersion of a solid requires a detector of a high order of sensitivity. Hutchinson[1] has reported on the use of a thermistor in immersion calorimetry but gave no data on either the sensitivity or stability. In recent cryoscopic work in this Laboratory[2] thermistors were shown to have both high sensitivity and good stability; this work suggested a detailed investigation of their use in calorimetry. The performance of a calorimeter utilizing a thermistor as a temperature sensitive element has been tested and found entirely satisfactory for the measurement of heats of immersion.

Recently, Jura and Hill[3] have pointed out that theoretically the absolute entropies of adsorbed molecules can be obtained from a combination of heats of immersion with spreading pressures from a single isotherm with considerably more accuracy than entropy calculations dependent on the difference in spreading pressures obtained at two temperatures. It was pertinent to inquire, then, whether the calorimetric approach was experimentally capable of yielding data of sufficient precision to permit accurate evaluation of entropies from heats of immersion. An additional purpose of this investigation was to compare the results determined by this method with values obtained from isothermal data alone. Because of extensive adsorption studies on asbestos underway in this Laboratory, the asbestos–water system was chosen for this comparison.

Part I. A Thermistor Calorimeter for Heats of Wetting

The Calorimeter.—The calorimeter used to measure heats of wetting, Fig. 1, consisted of a wide-mouth, silvered Dewar flask cemented to a Plexiglas ring to which the Plexiglas top could be bolted when assembled. The apparatus was fitted with a vacuum seal stirrer, A; a small heating coil, B, of 5 ohms resistance for calibration; and the thermistor, C.[4] The sample tube was held firmly in the sample holder, D, and broken by tapping the steel rod, E, resting on top of the sample tube, F.

The apparatus was housed in a specially constructed constant temperature air-bath except for the stirrer and breaker rod which extended through the top of the bath. The walls of the bath were two inches thick and consisted of alternate layers of sheet cork and aluminum foil separated by air pockets. The temperature was controlled by a cooling coil and a 100-watt heater operated by a micro mercury-to-mercury thermoregulator and thyratron relay. Air circulation in the bath was produced by a 10-inch bucket-blade propeller turning at 1750 r.p.m. The temperature variation in the air bath was less than ±0.005°.

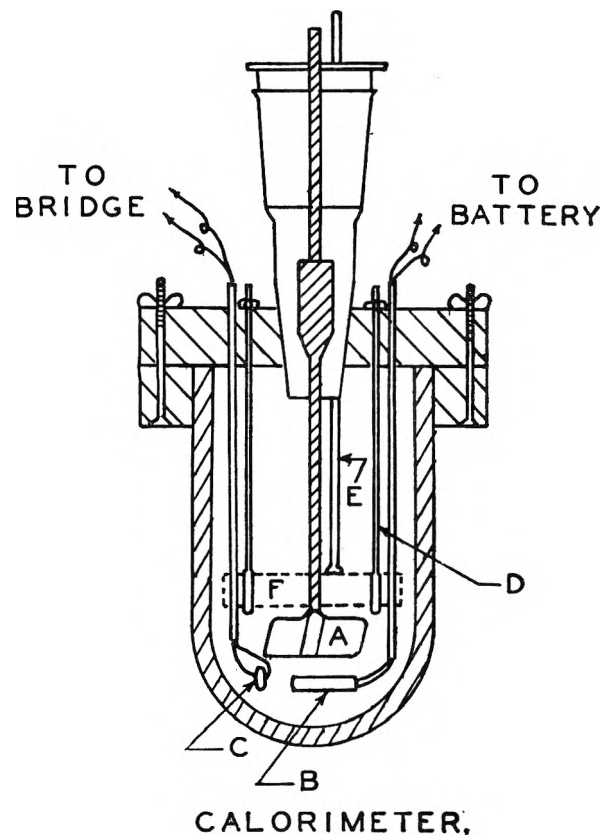

CALORIMETER.

Fig. 1.—Heat of immersion calorimeter: A, stirrer; B, heater; C, thermistor; D, sample holder; E, breaking rod; F, sample tube.

As pointed out by Boyd and Harkins,[5] the following factors were of primary importance in developing the calorime-

(1) E. Hutchinson, *Trans. Faraday Soc.*, **43**, 443 (1947).

(2) R. R. Myers, Ph.D. Thesis, Lehigh University, 1952.

(3) G. Jura and T. L. Hill, *J. Am. Chem. Soc.*, **74**, 1598 (1952).

(4) The thermistor, 15A, was supplied by the Western Electric Co., Allentown, Pennsylvania.

(5) G. E. Boyd and W. D. Harkins, *J. Am. Chem. Soc.*, **64**, 1190 (1942)

ter: type and rate of stirring; high accuracy of the measurement of temperature changes; accurate determination of the electrical energy equivalent; and rapid attainment of thermal equilibrium with the calorimeter. In addition, the attainment of a suitable rating period before breaking the sample tube and the stability of the thermistor were also found to be important considerations.

Stirring.—A desired rate of stirring was predetermined by observing the dispersion of samples of various particle size and density. A stirring rate of about 150 r.p.m. gave optimum dispersion and a minimum heating effect. To aid in the complete wetting of the powders only 3- to 8-g. samples were used in 350 ml. of water.

Temperature Measurement.—The comparatively small temperature increases accompanying the wetting of a solid amounted to about (0.01°) for most of the samples used in the calorimeter. These temperature changes were followed by measuring the change in resistance of the thermistor by means of a Mueller resistance bridge (Eppley Co., No. 301). At 25° the thermistor had a resistance of approximately 103 ohms and a temperature coefficient of approximately 5 ohms per degree. The Mueller bridge, used in conjunction with a Leeds and Northrup Type HS galvanometer, was found capable of detecting changes of resistance of 0.0001 ohm.

Rating Period.—The slopes of the temperature or resistance *versus* time plots were found to influence greatly the accuracy of the determination of temperature increases. Therefore, these slopes were made small enough so that the smallest changes of temperature detectable on the Mueller bridge could be measured easily. Thus, for example, it was possible to measure temperature changes of 0.00002° (0.0001 ohm) if this change took place over a 20 to 60 second period.

When the air-bath and calorimeter were at the same temperature, the heat evolved due to stirring gave a rating period with a slope of about 0.0070 ohm per minute. A suitable initial rating period was obtained by the simple expedient of heating the calorimeter contents until a temperature differential of about 0.4° was established between the calorimeter and the bath. The rating period thus obtained had a slope of about 0.0001 to 0.0005 ohm per minute. The curve was found to be linear during the 5 to 10 minute rating period. The heat of immersion usually raised the temperature about (0.01°), an amount which did not materially affect the final rating period.

Sample Tube Breaking.—The sample tubes were made of specially constructed, thin wall glass tubing. In initial experiments, tubes were broken by screwing down a steel rod, but it was found that some heat was evolved from the friction of the rod against the sample bulb; although small, this heat could be practically eliminated by shattering the bulb by tapping the breaker rod lightly. Blank runs indicated that the heat effect resulting from breaking in this fashion was so small that it contributed only from 0.2 to 0.4 joule to the total heat. A correction of 0.3 joule was applied to all measurements.

Calorimeter Calibration.—Calibrations were carried out by comparing the temperature change due to immersion of powders to the temperature change caused by a known amount of electrical energy introduced by the heater. A calibration was carried out after each run. In the small temperature range studied a linear relationship[6] was found between the change in resistance, ΔR, of the thermistor and the electrical energy input, ΔQ. The stability of the thermistor was entirely satisfactory; over a three-month period the $\Delta R/\Delta Q$ slope remained constant at 0.00246 ± 0.00003 ohm/joule.

Procedure.—The samples were evacuated at 400° for 4.0 hours before heats of immersion were obtained, then were sealed off under vacuum and transferred to the sample holder. Exactly 350 ml. of distilled water at a temperature below 25° was added to the Dewar flask. Stirring was begun and bath and calorimeter were allowed to reach temperature equilibrium. The temperature of the calorimeter was raised slightly above the bath temperature by means of the heating coil. A time–resistance curve was then followed until a steady change in resistance was observed for a 6-minute rating period. The slope of this initial curve was not allowed to exceed 0.0001–0.0005 ohm per minute. Then the sample was broken under the liquid and the time noted. Time–resistance readings were continued for 5–10 minutes after breaking. The heat of wetting was always evolved within one or two minutes after breaking.

Experimental Results and Reproducibility.—In Table I values of the heats of immersion for a variety of powders

TABLE I

HEAT OF IMMERSION OF SOLIDS[a] IN WATER AT 25°

Sample	Specific area,[b] m.²/g.	Heat of immersion, ergs/cm.²	Av. deviation, ergs/cm.²	Minimum heat evolved, joules	Maximum error due to heat of breaking, %
Asbestos[c]	20.0	850	±20	30.0	0.3
Graphon[d]	83.0	51	± 6	7.5	1.3
Rutile[e]	7.3	550	±18	18.0	0.6
Silica[f]	0.96	564	±16	4.0	2.5

[a] Solids evacuated at 400° for 4.0 hours. [b] All areas determined from nitrogen adsorption data except asbestos for which water adsorption data were used. [c] 7-R fiber, Canadian Johns–Manville Company. [d] Furnished by Godfrey L. Cabot Company. [e] Titanium pure R-300, du Pont Company. [f] New Jersey Silica Sand Company.

are given. The breaking errors were computed for the smallest amount of a particular sample used and, thus, are maximum values. The average deviations represent a measure of the reproducibility of the results. However, a combination of factors such as weighing, pretreatment, activation and evacuation of the samples as well as calorimetric behavior affect these values.

The immersional heat values found for silica and rutile differ by 16 and 30 ergs/cm.², respectively, from the values found for these materials by Harkins.[5] Since the purity and history of the samples undoubtedly differ, this represents good agreement. The low heat value found with graphon is not surprising since graphon is a hydrophobic solid which exhibits a large contact angle with water.

Part II. Entropies from Heats of Wetting and Adsorption Data

Water Vapor Adsorption Measurements.—The apparatus employed for water vapor adsorption measurements in this research was similar to the type described by Orr[7] except for the following changes: (1) Apiezon B was used in the manometers since this oil was found not to absorb water vapor; (2) absolute adsorption pressures were measured rather than differential pressures. A cathetometer was used for reading low pressures on the oil manometer. The limit of sensitivity was about 0.004 mm. Hg; considerable scatter in the data was found below pressures of 0.09 mm. The dead space volumes were calibrated with helium. Blank runs determined that adsorption of water by the apparatus was negligible.

The asbestos samples were evacuated at 25° for 12 hours at 10^{-5} mm. before adsorption measurements were taken. These conditions were chosen since it was desired to remove only the physically adsorbed water from the surface of asbestos. An increase of the evacuation temperature to 425° was found to be necessary before the more tightly bound water could be completely removed.[8]

Heats of Adsorption and Entropy of the Adsorbed State from Isothermal Data.—The isosteric heats of adsorption, $H_G - \bar{H}_S$, and equilibrium heats of adsorption, $H_G - H_S$, with the corresponding entropy values, $S_G - S_S$, were calculated for the adsorption of water vapor on asbestos. The isosteric heat values were calculated in the usual manner

(6) Over large temperature ranges a linear relationship exists between ln R and $1/T$.

(7) Orr, *Proc. Roy. Soc. London*, **173A**, 347 (1939).

(8) A comprehensive discussion of adsorption by asbestos is to be published later.

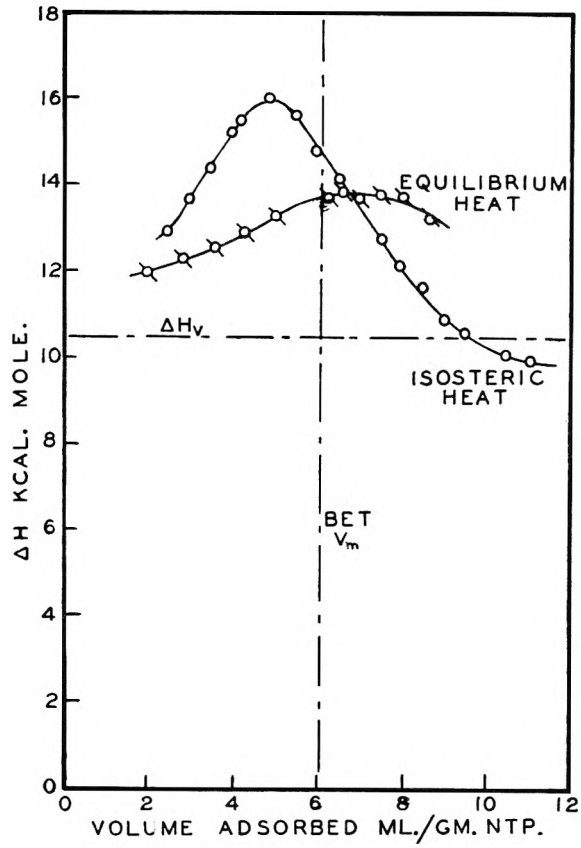

Fig. 2.—Heats of adsorption for water on asbestos, T = 20°.

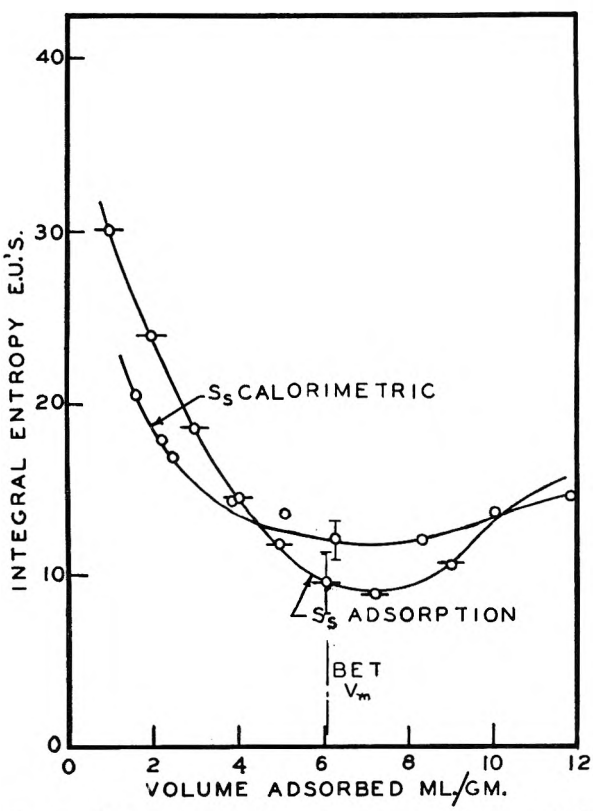

Fig. 3.—Entropy curve for water on asbestos, T = 20°.

from the Clausius–Clapeyron equation at constant volume adsorbed. The equilibrium heats of adsorption were obtained[9] from the Clausius–Clapeyron equation at constant spreading pressure, φ. Thus, it was necessary to determine the spreading pressure as a function of the equilibrium pressure at two temperatures from isothermal data either by graphical integration of the Gibbs equation

$$\varphi = kT \int_0^p \Gamma d \ln p$$

where Γ is the surface concentration, or by integration of a plot of V/p *vs.* p. Integrations of both V *vs.* ln p and V/p *vs.* p plots were carried out graphically by use of a polar planimeter. Although spreading pressures obtained by integration of either plot agreed quite closely, the plot of V *vs.* ln p could be extrapolated to zero coverage with more reliability.

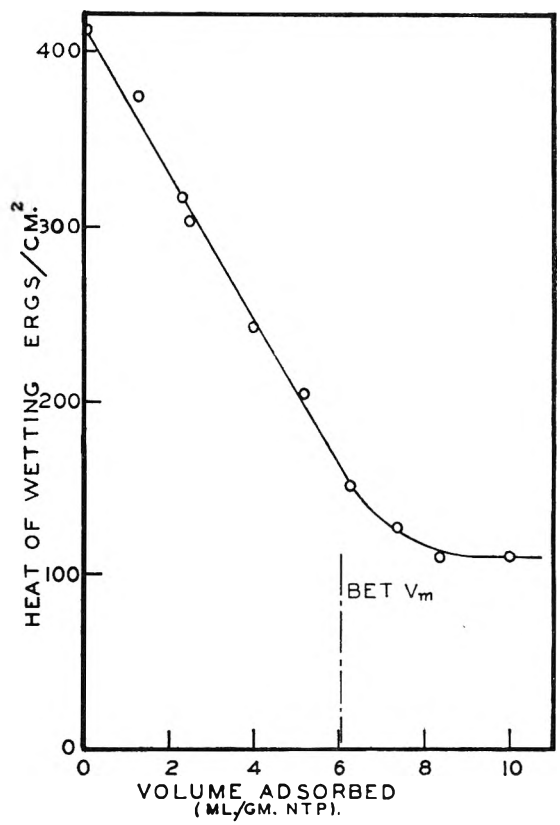

Fig. 4.—Heats of wetting of asbestos by water, T = 25°

The equilibrium and the isosteric heats of adsorption for water vapor on asbestos are presented in Fig. 2 and are indicative of adsorption on a homogeneous surface.

The entropy terms, $S_G - S_S$, were evaluated from the equilibrium heats of adsorption by the relation $S_G - S_S = H_G - H_S/T$. The entropy of water vapor, S_G, was calculated at the various equilibrium pressures and the absolute entropy of the adsorbed state, S_S, plotted in Fig. 3, was determined as a function of volume adsorbed.

Entropy of the Adsorbed State from Heats of Wetting.—The entropy of the adsorbed state was also calculated independently from the equation

$$T(S_S - S_L) = \frac{U - U_0}{N_S} + \varphi/\Gamma - kT \ln x \quad (1)$$

(9) The symbols and method of calculations correspond to those indicated by Hill, *J. Am. Chem. Soc.*, **17**, 520 (1949).

as developed by Jura and Hill.[3] In this equation S_L refers to the entropy of the liquid adsorbate (in equilibrium with vapor), $U - U_0$ is the difference in the heat of wetting between the clean solid, U_0, and the film coated solid, U, and x is the relative equilibrium pressure of the film coated solid.

The film coated asbestos samples were prepared on the adsorption apparatus and sealed off at the desired equilibrium pressure. Care was taken to ensure that the temperature of the sample was not altered during the cutting-off operation. Values for the heats of wetting for evacuated asbestos and for the film-covered asbestos at various coverages are presented in Fig. 4. The linear relation between the heat of wetting and volume adsorbed up to about monolayer coverage is notable and was taken to be indicative of surface homogeneity since the heat evolved on wetting is dependent only on the amount of bare surface present and not on the energy of particular parts of the surface; the energy of the adsorption sites is constant. The heat of wetting measurements thus support the conclusions of surface homogeneity drawn from the isosteric and equilibrium heat of adsorption curves.

The term $T(S_S - S_L)$ was calculated from equation 1 and the entropy of the adsorbed state, S_S, was evaluated. The entropy of the adsorbed state as a function of volume of water vapor adsorbed is also presented in Fig. 3 in comparison with the entropy curves as determined from the equilibrium heat values.

Comparison of Methods.—Figure 3 contains the entropy curves obtained from calculations based on both calorimetric and adsorption data. The agreement obtained is remarkably good despite the larger errors inherent in φ calculations from adsorption data. The errors in these entropy values were computed from the equation of Hill and Jura[3]

$$S'_S - S_S = \frac{1}{\Gamma}\frac{\Delta a}{\Delta T}$$

where S'_S and S_S are the apparent and true entropy values and Δa is the error in the spreading pressures. The estimated maximum error in entropy varied from over 100% at low pressures to about 20% at monolayer coverage. In computing the error in entropy values obtained from calorimetric data, errors from the following sources were considered: (1) errors in the determination of φ; (2) errors in the determination of $U - U_0/N_S$; (3) errors in determining the relative pressure. Errors in entropy values obtained from calorimetric data were found to range from *ca.* 35% at low coverage to 8% at monolayer coverage. Thus it is apparent that considerably more reliance can be placed on the entropy values obtained from the latter method.

Acknowledgment.—The authors gratefully acknowledge the financial support provided by the Office of Naval Research, Project NR 057-186, Contract N8onr-74300. We also wish to thank Miss Yung-fang Yu for assistance in obtaining some of the adsorption data.

DISCUSSION

J. TURKEVICH.—What else have you learned concerning the internal structure of asbestos from adsorption measurements?

A. C. ZETTLEMOYER.—Messrs. Healey and Young from our Laboratory have made a detailed study of asbestos (to be published later) using adsorption and heat of wetting measurements. They have found that for degassing temperatures up to 400° the nitrogen, argon and oxygen areas are about one-half those measured with water and ammonia. When degassed at 425°, polar and non-polar gases give the same results. Water vapor adsorption returned the asbestos to the original state. The postulate was made that water plugs seal the ends of the 150Å capillaries (a capillary structure is also suggested by the electron micrographs obtained by Dr. Turkevich). This suggestion seemed to be confirmed by heat of wetting measurements on completely degassed samples equilibrated with ascending water vapor pressures. Final heats of immersion were in accord with the expected result of the outer area times 118 ergs/cm.^{2} which is the heat evolved when unit area of water surface is destroyed.

ANON.—How were the sample tubes made?

A. C. ZETTLEMOYER.—They were blown carefully from selected tubing. A dozen blank runs were made to establish the breaker error.

EDWIN E. ROPER.—The difference in surface area of asbestos as measured by nitrogen and argon (9 m.^{2}/g.) contrasted to that by ammonia and water (17 m.^{2}/g.) recalls the area differences tabulated by Brunauer for a silica gel. A similar trend is shown there, so that this observation on asbestos is not unique but the unusual result here is the eventual agreement in surface areas after the 425° outgassing removed all the water. The reversible nature of this area change after addition of water to the anhydrous asbestos seems to substantiate Dr. Zettlemoyer's explanation However, retention of water at 425° implies strong chemisorption of this substance. Since the covering power of all four adsorbent gases is calculated from the assumption of hexagonal packing in the respective bulk liquid phases, is it possible that some differences might be expected in the type of packing that occurs in the adsorbed phase?

A. C. ZETTLEMOYER.—Different packing factors for the two classes of adsorbates could hardly account for the differences of almost 100%.

CHARLES G. DODD.—In discussion of this paper, Dr. Zettlemoyer pointed out that the surface areas of asbestos as measured by water and ammonia adsorption were about twice those obtained by nitrogen, argon or oxygen adsorption, if the asbestos was heat treated below 425° prior to measurement, but areas determined by adsorption were the same for all gases if the asbestos was evacuated at 425° prior to measurement. Dr. Zettlemoyer suggests that water plugs each end of the asbestos tubelets so that internal surfaces are unavailable to nitrogen argon, and oxygen in the former case.

I would like to suggest that differential thermal analysis experiments with control of the water vapor atmosphere in equilibrium with the sample might aid in confirming the presence of the water plugs.

THE ADSORPTION OF BENZENE AND WATER VAPOR BY MOLYBDENUM DISULFIDE[1]

BY E. V. BALLOU AND SYDNEY ROSS

Department of Chemistry, Rensselaer Polytechnic Institute, Troy, New York

Received March 2, 1953

Adsorption isotherms of nitrogen, benzene and water vapor on molybdenum sulfide have been determined. A hydrophilic layer of molybdenum trioxide is found on sulfide surfaces that have been heated to 110°. The oxide layer is largely removed by treatment with ammonium hydroxide at room temperature, or by this treatment followed by hydrogen sulfide gas at 125°. The oxide-free surface is found to be hydrophobic. The amount of water vapor adsorbed is proportional to the extent of surface oxidation.

Introduction

The hexagonal crystal structure of molybdenum disulfide has, like graphite, a pronounced cleavage of the (0001) planes, which is the source of the early confusion of the two substances and their common function as solid lubricants. But while our knowledge of the nature of the surface of graphite is extensive, little of a corresponding character is known of molybdenum disulfide. The present investigation was undertaken to answer the fundamental question of whether the surface of molybdenum disulfide is, like that of graphite, non-polar and hydrophobic. While several qualitative methods are available for obtaining an answer to this question, it was thought that by comparing the adsorption isotherms for water and for benzene vapor a quantitative account would be gained, and the effects of different treatments of the surface could be most precisely determined.

Materials and Methods

Molybdenum disulfide, obtained from the natural mineral *molybdenite*, is purified by the Climax Molybdenum Company, by a method described by Killeffer and Linz.[2] The purified material has an assay of 99% MoS_2 (complete analysis involves certain difficulties). This is supplied by the Climax Molybdenum Company as Grade No. 3. In this form the powder appears to have traces of an oily contaminant on the surface. It has a nitrogen BET area of about 3 sq. m./g. A sample was pulverized for the authors by the Micronizer Company, thus increasing the specific surface to about 10 sq. m./g. After comminution the powder is readily wetted by water and appears to have lost the traces of oily contamination on its surface. Nevertheless, before use in this investigation, all samples were washed with various organic solvents, as described below.

The apparatus for nitrogen adsorption was based on the design of Bugge and Kerlogue.[3] Nitrogen gas, obtained as 99.9% pure from the Matheson Company, Inc., was further purified by heating to 300° in the presence of copper turnings, and then leading it through a liquid nitrogen trap. The helium was a spectroscopically pure grade from the Air Reduction Company.

Water vapor and organic vapor adsorption were measured by use of an apparatus described by Harkins and Jura.[4] Since this apparatus has stopcocks in the adsorption system, some care had to be taken to minimize adsorption of the organic vapor by the stopcock grease. The satisfactory use of fluorocarbon oils as lubricants in contact with organic vapors has been described by Davis, Grossman and Harris.[5] A sample of *Fluorolube Grease GR-362* was supplied by the kindness of the Hooker Electrochemical Company and found, on testing, to be satisfactory for organic vapors in the relative pressure range below 0.5. At higher relative pressures a slow absorption of organic vapors by the grease could be detected.

The water used as adsorbate was distilled and boiled conductivity water. The organic solvents were each distilled and dried over sodium immediately before use.

The temperature at the sample was controlled by circulation of water around the sample holder from a constant temperature bath. The temperature at the sample was adjusted to ±0.05° by means of a thermoregulator in the main bath. The thermometer was compared to an N.B.S. calibrated thermometer.

Preliminary Treatment of Adsorbent.—Preliminary experiments were performed on adsorbent 1 as described below. When it was suspected that oxide coating covered the sample, other treatments were introduced to remove the oxide coating. All the experiments were made with the "micronized" material of *ca.* 10 sq. m./g.

Adsorbent 1.—The sample was extracted for an hour with acetone, then for an hour with water in a Soxhlet apparatus. It was then dried in air for six hours at 110°.

Adsorbent 2.—The sample was extracted for an hour with carbon tetrachloride, an hour with benzene, a half-hour with acetone and an hour with water in a Soxhlet apparatus, with vacuum drying at room temperature after each extraction. The sample was then made into a slurry with a dilute solution of ammonium hydroxide (1.44 meq. wt./g. solid). It was then washed with distilled water by stirring, centrifuging and decanting until the *p*H of the supernatant liquid was less than 7. The solid was dried in a vacuum at room temperature.

Adsorbent 3.—A portion of adsorbent 2 was placed in a glass tube inside a furnace and dry hydrogen sulfide gas passed through it for 12 hours at 125°. This treatment was based on a method reported for the preparation of MoS_2 from MoO_3.[6,7] The sample was then maintained in a vacuum for 12 hours at 175°.

Adsorbent 4.—To determine if any residual sulfur was present on adsorbent 3, a portion of it was washed with carbon disulfide, by stirring, centrifuging and decanting. It was then washed in a similar way with benzene, and dried at room temperature in a vacuum.

Adsorbent 5.—To ascertain the effect of prolonged drying at 110°, a sample was treated with dilute sodium hydroxide solution (1.44 meq. wt./g. solid), then washed with water in a Soxhlet apparatus until the extract was neutral. This solid was then dried in air at 110° for 45 days.

Samples described as "activated" were desorbed at 10^{-4} mm. or less at 200° for 3–6 hours. "Non-activated" samples were desorbed at 10^{-4} mm. or less at room temperature, after a series of sorption–desorption cycles to saturation with the vapor.

Results

The experimental results are presented in a series of figures in which the water vapor and benzene vapor adsorption isotherms are compared for each adsorbent. Figures 1 and 2 refer to adsorbent 1, activated at 300° (Fig. 1) and

(1) Part of a Thesis presented by E. V. Ballou to the Graduate School of Rensselaer Polytechnic Institute, in partial fulfillment of the requirements for the degree Doctor of Philosophy.

(2) D. H. Killeffer and A. Linz, "Molybdenum Compounds," Interscience Publishers, Inc., New York, N. Y., 1952, pp. 196–197.

(3) P. E. Bugge and R. H. Kerlogue, *J. Soc. Chem. Ind.*, **66**, 377 (1947).

(4) W. D. Harkins and G. Jura, *J. Am. Chem. Soc.*, **66**, 1356 (1944).

(5) P. T. Davis, J. H. Grossman and B. L. Harris, *Anal. Chem.*, **21**, 194 (1949).

(6) E. H. M. Badger, R. H. Griffith and W. B. S. Newling, *Proc. Roy. Soc. (London)*, **A197**, 184 (1949).

(7) Treatment of adsorbent 2 with dry hydrogen sulfide gas at 125° does not necessarily convert all of the MoO_3 to MoS_2. However the extent of the surface oxidation is thereby reduced.

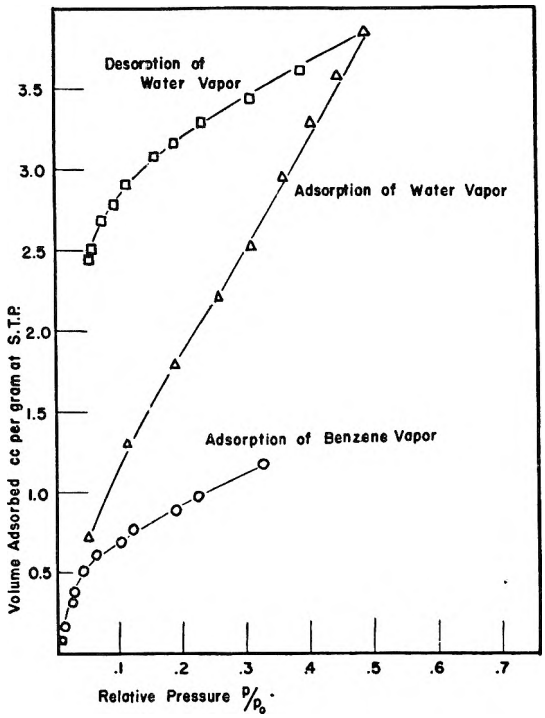

Fig. 1.—The adsorption of water at 25.0° and benzene at 26.0° on activated adsorbent 1.

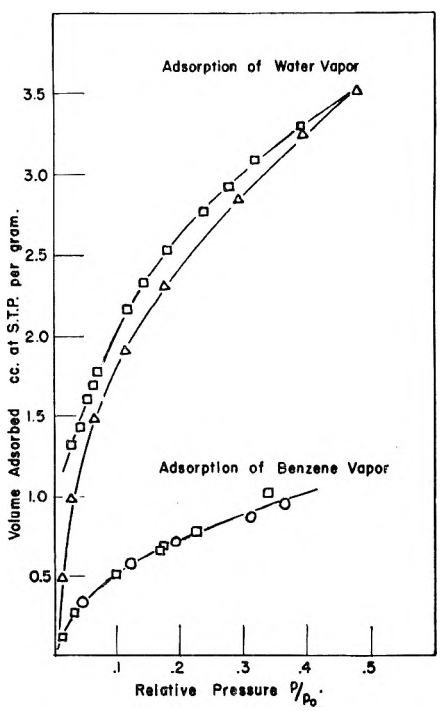

Fig. 2.—The adsorption of water at 25.0° and benzene at 26.0° on non-activated adsorbent 1.

non-activated (Fig. 2). Figure 3 shows the two isotherms for adsorbent 3, activated at 180° for benzene, and for water, non-activated, after a single sorption-desorption cycle to saturation with water vapor. Certain points on Fig. 3 refer to adsorbent 4. Figure 4 shows isotherms for benzene, toluene and *n*-heptane on adsorbent 1, activated at 300° and for toluene on adsorbent 1, non-activated after a single sorption-desorption cycle with water vapor.

Results for isosteric heats of adsorption were obtained from isotherms at two different temperatures, by application

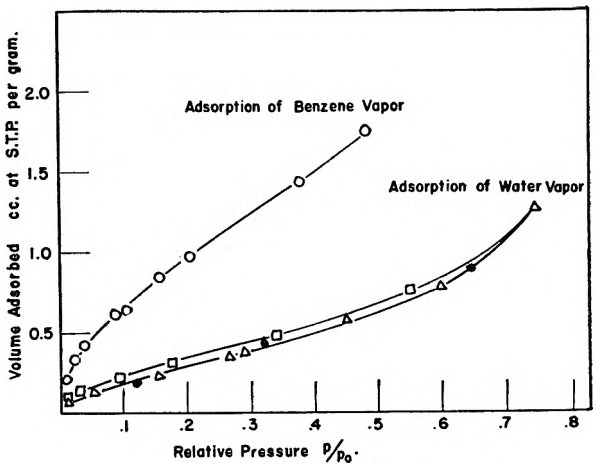

Fig. 3.—The adsorption of water on non-activated adsorbent 3 (Δ = adsorption, □ = desorption) and activated and non-activated adsorbent 4 (●), and of benzene on activated adsorbent 3 at 20.0°.

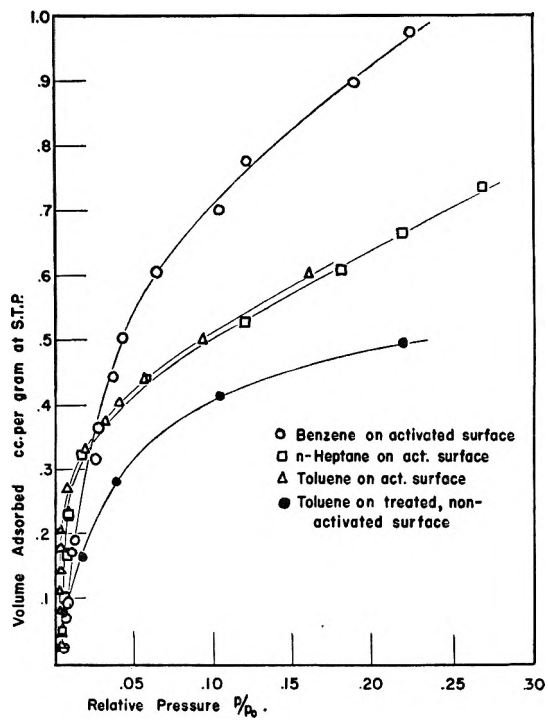

Fig. 4.—The adsorption of benzene, *n*-heptane and toluene on activated adsorbent 1 and toluene on water-treated, non-activated adsorbent 1 at 26.0°.

of the Clausius–Clapeyron equation. The temperatures were 10° apart. These results are plotted as a function of V/V_m, where V_m refers to the point of monolayer coverage as found by the BET equation, applied to each adsorbate. The isosteric heats of adsorption for benzene on adsorbents 2 and 3 are shown in Fig. 5, and are seen to coincide. The isosteric heats of adsorption for water on adsorbents 2 and 3 are shown in Fig. 6. Since the water isotherm for adsorbent 2 has a hysteresis loop, both the adsorption and desorption branches are used.

Discussion of Results

The variation of the water vapor and benzene vapor isotherms with the pretreatment of the adsorbent, particularly as the treatment was designed to remove a suspected layer of molybdenum trioxide

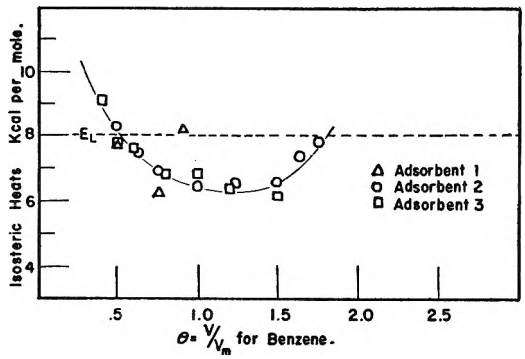

Fig. 5.—Isosteric heats of adsorption of benzene on activated adsorbent 1 from 26.0 and 36.0° adsorption isotherms, and on activated adsorbents 2 and 3 from 20.0 and 30.0° adsorption isotherms.

on the surface, confirms an interpretation of the results based on that supposition. Adsorbent 1 shows a much greater adsorption of water vapor than of benzene vapor. Although the pretreatment with water in a Soxhlet apparatus may have removed what oxide is originally on the surface, it is restored by the drying at 110° for six hours. The oxide makes the surface hydrophilic and is also responsible for the large hysteresis loop on the activated sample (Fig. 1). Both the size of the loop and the amount of benzene adsorbed is reduced in the non-activated sample (Fig. 2). In this figure, the water isotherm was obtained after 10 consecutive sorption–desorption cycles to saturation with water vapor, and then pumping off at room temperature. The benzene isotherms were obtained after saturating the same sample on which the water adsorption had been determined for 3 days with benzene vapor, followed by pumping off for a week. A second isotherm was determined on the same sample after its exposure to benzene vapor, with only ten minutes pumping off. The two isotherms coincide. This benzene isotherm shows less benzene adsorbed than the benzene isotherm of Fig. 1. In this connection an analogous effect is to be observed with toluene adsorbed on a water-treated, non-activated sample (Fig. 4), where the amount of adsorption of the organic vapor is again reduced. Presumably the non-activated surface contains bound water in the form of hydrated oxide.

There is a dramatic reversal of the situation when the original oxide on the surface is removed by treatment with ammonium hydroxide and further oxidation is kept low by drying the sample at room temperature in a vacuum (adsorbent 2). The adsorption of water vapor is now reduced and the adsorption of benzene vapor is increased. The non-hydrophilic surface of the adsorbent is materially increased. The adsorption of water vapor is still further reduced by the treatment of the sample with H_2S (Fig. 3). Since this treatment may have caused deposition of sulfur on the sample, the solid was washed with carbon disulfide and after activation for 7 hours at 195°, some points on the water vapor isotherm redetermined. They were found to lie on the same isotherm as the non-activated adsorbent 3 (Fig. 3). Adsorbent 5 was heated at 110° for 45 days, after the original surface oxide had been removed by reaction with sodium hydroxide.

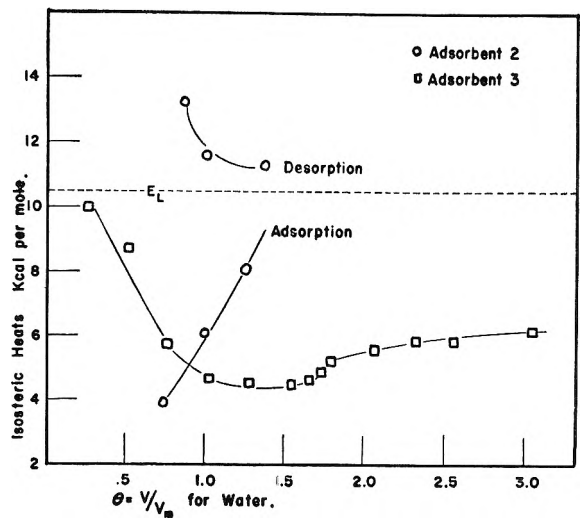

Fig. 6.—Isosteric heats of adsorption of water on activated adsorbent 2 and non-activated adsorbent 3 from 20.0 and 30.0° adsorption isotherms.

The benzene isotherm shows that a strongly hydrophilic, oxide surface is now present.

It is clear from these results that every treatment designed to remove oxide, such as reaction with ammonia or with hydrogen sulfide, results in a corresponding reduction of the hydrophilic character of the surface, as measured by the adsorption of water vapor, and concomitantly an increase in the hydrophobic character, as measured by the increase in the adsorption of benzene vapor. Similarly, every treatment designed to increase oxide on the surface, by drying for different times at 110°, results in a corresponding increase in the hydrophilic character of the surface.

The extent of the oxidation of the surface of molybdenum sulfide can be estimated roughly from the amount of standard base that is neutralized when the solid is slurried for 30 minutes with a solution of sodium hydroxide.[8] The acidity thus neutralized, in meq. wt./g. (acid number), corresponds with the amount of water vapor adsorption on the different adsorbents (Table I). This is further proof that the hydrophilic surface is caused by the presence of molybdenum trioxide.

An application of the BET theory to the different isotherms provides a means of comparing the extent of adsorption of each vapor and its variation with the treatment of the adsorbent. Table I gives the values for the specific surface in sq. m./g. as determined by the BET method.[9] The areas for nitrogen, benzene and water are those recommended by Livingstone[10] as normally providing the best agreement with the nitrogen isotherm values, usually taken as standard. This agreement is lacking in the present adsorbents, particularly for the water vapor adsorption, indicating that water and, to a

(8) The major reaction is the combination of molybdenum trioxide with sodium hydroxide. An X-ray diffraction diagram of the residue from an ammonia-neutralized slurry reveals lines of ammonium sulfate as well as ammonium molybdate. It is therefore probable that sulfuric acid contributes to the acidity of the water slurries of these finely ground samples.

(9) S. Brunauer, "The Adsorption of Gases and Vapors" Vol. 1, Princeton University Press, Princeton, N. J., 1945, p. 149, *et seq.*

(10) H. K. Livingstone, *J. Colloid Sci.*, **4**, 447 (1949).

lesser extent, benzene adsorb on a portion only of the total surface (as determined by nitrogen adsorption). The proportionality between the specific surface covered by the water and the acid numbers shows that the oxidized portions of the surface chiefly account for the adsorption of water vapor. Benzene vapor is more catholic in its choice of adsorption sites, but when the surface is heavily oxidized (adsorbents 1 and 5) covers less than the total area.

TABLE I

SPECIFIC SURFACE AREAS (SQ.M./G.) OF MOLYBDENUM DISULFIDE AS DETERMINED BY NITROGEN, BENZENE AND WATER ADSORPTION ISOTHERMS

Adsorbent	Nitrogen (σ = 15.4 Å.²)	Benzene (σ = 32.3 Å.²)	Water (σ = 10.8Å.²) Adsorption	Water (σ = 10.8Å.²) Desorption	Acid no., meq. wt./g.
1-Activated	9.9	7.5	6.3	7.4	1.3
1-Non-activated	..	6.8	7.0	7.0	
2-Activated	11.8	8.9	2.0	1.9	0.35
3-Activated	9.1	9.1	1.2	1.2	0.18
3-Non-activated	..	...	0.95	1.0	
4-Activated	..	...	1.0	...	..
4-Non-activated					
5-Activated	..	5.5	..	...	3.4

The other organic vapor isotherms shown in Fig. 4 are of interest in affording a comparison of molecular covering areas on the same surface. To correspond with the area of 7.5 sq.m./g. as found from benzene with σ = 32.3 Å.², the corresponding values would be toluene 50.2 Å.² and *n*-heptane 49.0 Å.²

The isosteric heats for the adsorption of benzene vapor on adsorbents 1, 2 and 3 are plotted on the basis of the specific surfaces given in column 3 of Table I, *i.e.*, V_m from the benzene isotherm of each adsorbent. On that basis it is found that there is a good agreement for the adsorbents 2 and 3 (Fig. 5). The isosteric heat of adsorption of benzene is not affected by the difference in treatment of the sample, which merely provides more or less hydrophobic surface on which the benzene adsorption can take place. The general trend is for a rapid drop of the isosteric heat at $V/V_m = 0.5$, where it is approximately equal to the heat of liquefaction. After $V/V_m = 1.0$ the isosteric heat becomes constant and then rises toward the heat of liquefaction. The heats on adsorbent 1 show very different behavior, but the isotherms were not carried far enough to enable us to ascribe much significance to this difference.

The isosteric heats for the adsorption of water vapor (Fig. 6) are complicated by the presence of the hysteresis loop. For adsorbent 3, where the hysteresis loop is small, the heat drops in value until $V/V_m = 1$, then levels off and rises gradually. The heat of adsorption is well below the heat of liquefaction at $V/V_m = 1$ and rises only gradually toward it as V/V_m increases. V_m from the water isotherm of this adsorbent actually represents only a fraction of the total available surface, probably the small residual hydrophilic fraction. The remainder of the surface is hydrophobic and because of that influence the isosteric heat, which is averaged over the whole surface, rises only slightly toward the heat of liquefaction even for relatively large amounts adsorbed.

It is of interest that the heats of adsorption of water on the oxide surface are similar in general behavior to those of benzene on the hydrophobic surface, and the actual magnitudes of the heat values are not far apart. It is this circumstance that accounts for the clear-cut transition of the surface from hydrophilic to hydrophobic when most of the oxide layer is removed.

Acknowledgment.—The authors gratefully acknowledge the aid given to this work by a grant from the Kennecott Copper Corporation.

DISCUSSION

TODD DOSCHER.—Do you know how much of the surface must be converted to the oxide before the material becomes hydrophilic?

SYDNEY ROSS.—No.

J. C. ARNELL.—I would like to suggest that the small residual hysteresis loop which is found after repeated cycling with water vapor is due to the swelling of the adsorbent caused by penetration of the crystal lattice by the water molecule. We have experienced a similar effect in my laboratory in the low temperature adsorption of nitrogen on an Acheson graphite and we feel this can be interpreted on the same basis. Such a penetration might also explain the decrease in isosteric heat with increasing coverage to $V/V_m = 1$.

A. C. ZETTLEMOYER.—We recently calculated the isosteric heats of adsorption of water on Graphon from the measured heats of immersion, using the Thermistor calorimeter described here earlier today. Graphon has about 0.01% of its surface available for water sorption against the 10% for Dr. Ross's Adsorbent 3. Oxygen complexes on the surface of graphite play an analogous role in water sorption to the molybdenum oxide on the surface of molybdenum sulfide. Our calorimetric heats of adsorption plotted against volume of water vapor adsorbed, as shown in the accompanying

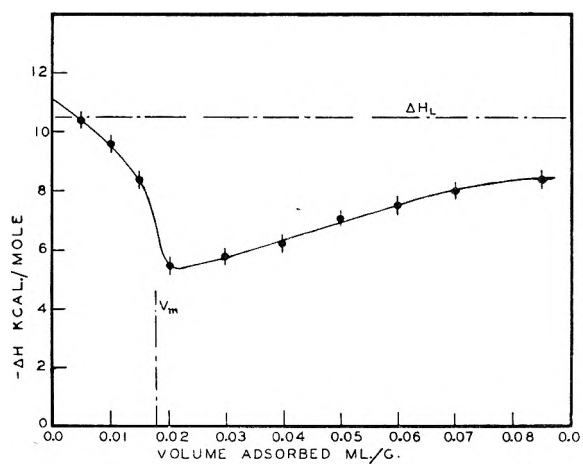

Fig. A.

graph (Fig. A.), are very strikingly similar to Fig. 6; similarities include the general shape of the curve, the large negative net heats, the minimum just beyond the V_m for water vapor, and the magnitude of the heats of adsorption. The first sites covered appear to be more energetic than the later ones, and the heat rises somewhat for the second layer, apparently because water molecules sorb more energetically on the previously adsorbed molecules. Cluster adsorption would explain the findings in both cases. Both graphite and molybdenum disulfide have strongly hydrophobic surfaces that have little tendency to sorb water vapor; in both cases the water that does sorb at low relative pressures is picked up by traces of oxidized material on the surface. This dual coincidence is responsible for the striking similarities between Fig. 6 of Dr. Ross's paper and our diagram for water sorption on Graphon.

SYDNEY ROSS.—Another similarity of graphite and molybdenum disulfide is in their application as solid lubricants. Dr. R. H. Savage of the General Electric Company has

tested graphite, boron nitride, mica and molybdenum disulfide as solid lubricants at very low pressures. He found that molybdenum disulfide differed from the other solids in continuing to act as a lubricant even in the presumed absence of an adsorbed layer of water. It is difficult, however, to obtain a specimen of molybdenum disulfide that is entirely free of oxide, and it is even more difficult to free molybdenum trioxide of its strongly bound water. I therefore suggest that molybdenum disulfide is not exceptional in its ability to lubricate in the absence of sorbed water, but exceptional in the difficulties that it poses to the removal of the last traces of water.

HEATS AND ENTROPIES OF ADSORPTION ON A HOMOGENEOUS CARBON SURFACE[1]

By John Mooi, Conway Pierce[2] and R. Nelson Smith

Contribution from the Department of Chemistry, Pomona College, Claremont, Cal.

Received March 2, 1953

Isotherms are reported for ethyl chloride adsorption on a carbon of unusually homogeneous surface. Six isotherms taken at temperatures from −78 to 75° are shown. Isosteric heats and differential and integral entropies have been calculated from the isotherms.

In a recent publication Pierce and Smith[3] have reported data for the adsorption of ethyl chloride on a new sample of Graphon which seems to have an unusually homogeneous surface. The adsorption isotherms were of unusual shape, being convex to the pressure axis in the region below V_m, and the isosteric heats calculated from them showed a maximum near V_m. It seemed worthwhile to obtain additional data for this system. Isotherms have now been obtained over a wide range of temperature, and energies and entropies have been calculated from them.

Experimental

Ethyl chloride adsorption isotherms were determined at −78, −25, 0, 25.2, 50.5 and 75.2°. Adsorption was determined by a gravimetric method. The apparatus and procedure were identical with those described previously.[3,4] The Graphon sample used was the same 13 g. as in earlier measurements.[3]

Before starting the measurements the sample was pumped to a McLeod vacuum and baked out at about 400° with pumping for at least two hours. This was increased to six hours if the sample had been exposed to air.

Temperatures above 0° were obtained by use of a water thermostat and mercury regulator. Zero degrees was maintained by an ice-bath. To obtain −25° melting carbon tetrachloride was used. Solid CCl_4 was obtained when required by the addition of small amounts of Dry Ice to the liquid. Temperature was controlled by this method to ±0.5°. This fluctuation made necessary a measurement of p_0 for each adsorption measurement. An ethyl chloride vapor pressure thermometer was constructed for this purpose. Although very little temperature fluctuation was observed during the measurement of a single point of the isotherm, the vapor pressure was found to fluctuate from 141.5 to 148.5 mm. between the various measurements. The temperature of −78° was obtained by surrounding the sample with powdered Dry Ice. Either by the use of a stream of CO_2 gas through the bath or by the use of a 0.5-watt heater at the bottom of the container it was possible to control the temperature to ±0.05°.

For the temperatures from 25 to 75°, for which the ethyl chloride has a vapor pressure above 1 atmosphere, no attempt was made to measure p_0 directly. The values of p_0 used were obtained by interpolation from the data given by Stull.[5] At 0 and −78° measurements of p_0 were made giving values of 472 and 3.37 mm., respectively, in excellent agreement with the Stull data. Measurement of p_0 at −25° is mentioned above.

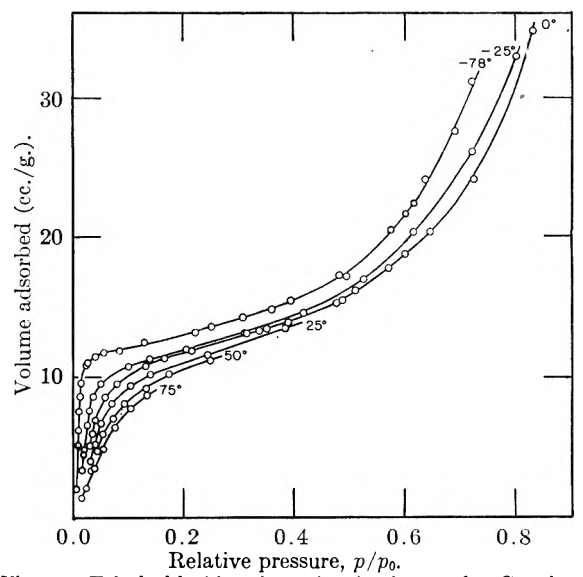

Fig. 1.—Ethyl chloride adsorption isotherms for Graphon

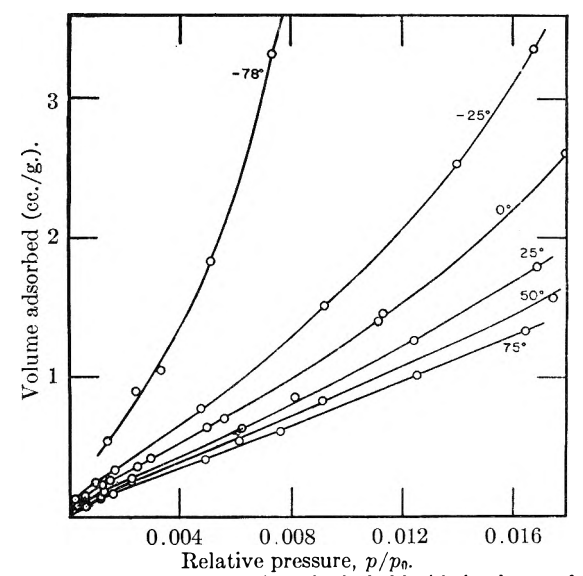

Fig. 2.—Low pressure portion of ethyl chloride isotherms for Graphon.

Results and Discussion

The adsorption isotherms obtained are shown in Figs. 1 and 2. Figure 1 shows the isotherms com-

(1) This is a report of work conducted under Contract N8onr54700 with the Office of Naval Research.

(2) University of California, Riverside, Calif.

(3) W. C. Pierce and R. N. Smith, *J. Am. Chem. Soc.*, **75**, 846 (1953).

(4) R. N. Smith, *ibid.*, **74**, 3477 (1952).

(5) D. R. Stull, *Ind. Eng. Chem.* **39**, 517 (1947).

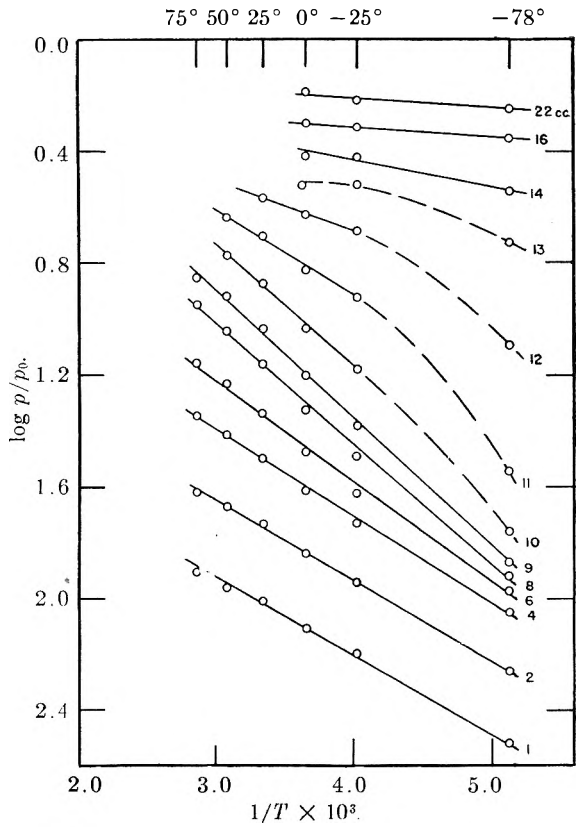

Fig. 3.—Clausius-Clapeyron plots of ethyl chloride adsorption data.

plete while Fig. 2 shows the low pressure portion only on an enlarged scale. The same general features of the isotherm show up at every temperature: an initial concave (to the p/p_0 axis) portion, probably due to adsorption on the heterogeneous parts of the surface; a convex region, where the adsorption builds up on the homogeneous surface; a point B at the completion of the monolayer; a nearly level portion followed by a sharp increase in V where multilayer adsorption occurs. Although these features are found in all the isotherms they are seen to become less distinct as the temperature increases. Since the pressure that could be used in the adsorption was limited to 1 atmosphere by the apparatus used, isotherms of 25, 50 and 75° are not run far past point B. Isotherms for the lower temperatures have, however, been obtained at pressures high enough so that adsorption corresponding to about three times that required for the completion of the monolayer has been observed. It is interesting that even at −78° no hump at $2V_m$ is found with these isotherms as has been found by Joyner and Emmett[6] for the adsorption of nitrogen on Graphon.[7] The second hump seems to be due to the completion of the second layer before the higher layers form to any considerable extent. That this does not occur with ethyl chloride adsorption may be due to the higher temperature used or may be due to differences in packing of the larger molecule which would make the formation of a second layer less distinct.

Isosteric heats have been calculated from the isotherms by use of the Clausius–Clapeyron equation. Data for various amounts of adsorption were taken from the smoothed isotherms and plotted (Fig. 3) as log p/p_0 *versus* $1/T$. In general the points for any constant amount of adsorption fall near a straight line, indicating that the heat of adsorption does not change greatly with temperature. In the region near V_m (11–13 cc.) the lines curve in such a way as to indicate a much higher heat of adsorption at −78° than at 0° or above. A possible explanation for this is that near V_m a given volume of adsorbate may be held differently at two different temperatures. Consider, for example, 100 molecules which may at −78° form a completed first layer over a certain area of the surface. The heat of adsorption of the hundredth molecule would be quite high since a large contribution to the heat is made through its contact with the carbon surface and an additional contribution is made by the cooperative effect from the array of previously adsorbed molecules into which it fits. At −25°, however, due to the expansion of the adsorbate, this same area would probably be completely filled with only 95 molecules. The heat of adsorption of the hundredth molecule, which in this case must be adsorbed in the second layer, is considerably lower than at −78°, since both contact with the carbon and the cooperative effect have been lost. This would bring about the sort of deviations found in the region of point B. Eleven cubic centimeters of ethyl chloride appears to be almost completely adsorbed in the first layer at −78°, but at −25° a considerable amount seems to have been forced into the higher layers. The log p *versus* $1/T$ plot, then, is found to be curved so as to be much steeper at the lower temperature.

This situation raises questions regarding the applicability of the Clapeyron equation to heats of adsorption. The differential form of the equation is certainly rigorous.[8] For practical application, however, it is necessary to use the Clapeyron equation in integral form with data from two or more isotherms. If the range of temperature is large, as it usually must be if the calculated heats are to be reasonably accurate, the situation near V_m is likely to be that discussed above. If the adsorbed molecules do not all occupy the same surface sites at the two temperatures the interpretation of the measured heat becomes somewhat ambiguous.

The calculated isosteric heats are shown in Fig. 4 as a function of the amount of adsorption. These data were calculated from the log p/p_0 *versus* $1/T$ plots. In the region from 10 to 12 cc. only the linear portion at the higher temperature was considered. In general shape this curve resembles those obtained for nitrogen adsorption on Graphon by Beebe, Biscoe, Smith and Wendell[9] by a calorimetric method and by Joyner and Emmett[6] from their isotherms. The new curve, however, shows a much deeper minimum after the initial drop, and a higher

(6) L. G. Joyner and P. H. Emmett, *J. Am. Chem. Soc.*, **70**, 2353 (1948).

(7) Personal communications from R. A. Beebe and W. R. Smith indicate that the $2V_m$ hump is more pronounced on the new Graphon than on the sample used by Joyner and Emmett.

(8) T. L. Hill, "Advances in Catalysis," Vol. IV, Academic Press, Inc., New York, N. Y., 1952, p. 244.

(9) R. A. Beebe, J. Biscoe, W. T. Smith and C. B. Wendell, *J. Am. Chem. Soc.*, **69**, 95 (1947).

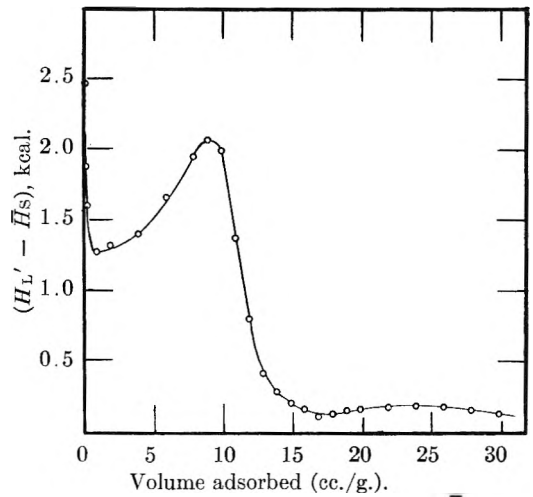

Fig. 4.—Isosteric heats of adsorption ($H_L' - \bar{H}s$) of ethyl chloride on Graphon.

sharper maximum in the region of V_m. This can probably be interpreted to mean that the new Graphon sample has a much more homogeneous surface than the sample used for the nitrogen adsorptions. It does not seem wise, however, to read too much into the differences between the curves since different adsorbent gases were used.

The heat curve reported by Pierce and Smith[3] for this sample is somewhat in error as might be expected for calculations from two isotherms taken only 10° apart. The new data show quite clearly that even for this sample the heats are high for very low adsorption as deduced by Pierce and Smith from the shape of the isotherms. A minimum is found at $V = 0.8$ cc. Isosteric heats cannot be found very accurately in the region of very little adsorption, however. Too much significance should not be attached to the actual values for the heat where the adsorption is less than about 1 cc. The curve has now been extended also to much greater adsorption, and a second maximum is found in the region of $V = 23$ cc. This is at roughly $2V_m$ and the increased heat may very well be due to the influence of the coöperative effect in the second layer. It is interesting that this maximum is found even though there is no hump in the isotherm corresponding to it.

Figure 5 is a plot of the differential and integral entropies as calculated by the method of Hill, Emmett and Joyner[10] from the isotherms at 0 and −25°. Data from these isotherms are shown rather than those at higher temperatures since these isotherms were run out to higher values of V. However, since the heats show generally no change with temperature, the entropies also show no change, and curves calculated between isotherms taken at the higher temperatures quite closely resemble those shown over the values of V for which data have been obtained. Use of the −78° isotherm gives entropies different from the rest, but since the heat values at −78° show abnormalities it is to be expected that the entropies calculated from this isotherm will also.

(10) T. L. Hill, P. H. Emmett and L. G. Joyner, *J. Am. Chem. Soc.*, **73**, 5102 (1951).

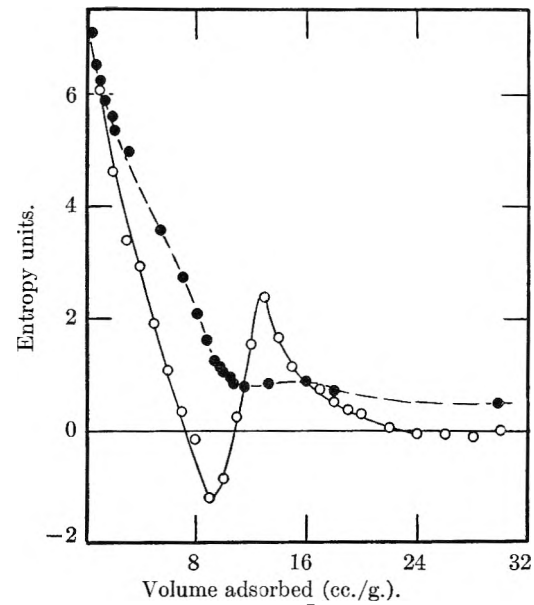

Fig. 5.—Differential entropy ($\bar{S}s - S'_L$) and integral entropy ($Ss - S_L$, shown as the broken line) determined from isotherms at 0 and −25°.

In the differential entropy curve can be seen a further demonstration of the similarity between the ethyl chloride–Graphon system and the nitrogen–Graphon system of Emmett and Joyner. The explanation of the curve presented by them seems quite reasonable. On a uniform surface the initial adsorption should be expected to be quite random and the entropy of the adsorbed material to be much higher than that of the liquid. As the monolayer is completed and additional adsorbed molecules force the layer into a more ordered array, the change becomes negative. Adsorption into the higher layers again increases randomness and the entropy goes through a maximum before approaching the entropy of the liquid asymptotically. The ethyl chloride data show no second dip of the entropy into the negative region. This must be added to the other evidence indicating an absence of distinct second layer formation for ethyl chloride. A comparison of the two systems makes it seem quite likely that the second minimum observed by Joyner and Emmett is due to the completion of the second layer in a fairly ordered array before much higher layer adsorption takes place.

The integral entropy of the ethyl chloride adsorbed layer remains greater than that of the liquid over the full extent of the adsorption. A very slight maximum and minimum are found where this curve crosses the differential entropy curve. Hill, Emmett and Joyner[10] have shown how the minimum in the integral entropy curve may be used as a thermodynamic measure of the volume adsorbed in the monolayer. This method seems equally applicable here. V_m determined this way is 11 cc., in good agreement with V_m determined less precisely from point B. There can be no check of this value against V_m determined from the Brunauer–Emmett–Teller equation since the equation is not applicable to isotherms of this shape, and the usual BET plot shows no linear portion.

THE ADSORPTION OF ETHYL ALCOHOL VAPOR ON GLASS SPHERES IN SYSTEMS OF DIFFERENT POROSITIES

BY J. L. SHERESHEFSKY AND E. R. RUSSELL

Chemistry Department, Howard University, Washington, D. C.

Received March 2, 1953

Adsorption of ethyl alcohol vapor on glass spheres approximately 3 mm. in diameter was studied. Four isotherms at 0° were obtained, each involving the same spheres and the same number of them, but carried out at a different porosity. The porosities of the systems corresponded to 10.25, 10.80, 11.1 and 11.35 contacts per sphere. From zero pressure to relative pressure 0.25 the isotherms are practically identical, but from this point to saturation the isotherms diverge in a direction of increasing adsorption with increasing number of contacts per sphere. It is shown that the estimated volume per contact agrees with the observed, and the mechanism of the adsorption process is interpreted in terms of the capillary condensation theory.

Introduction

Capillary condensation has been frequently used in the interpretation of adsorption of vapors in porous bodies. These interpretations have been mainly extended to high relative pressures close to saturation.[1] The objection to the application of this theory to lower relative pressure is primarily based on the fact that the Kelvin equation gives improbably low values for the pore sizes.[2] In recent years a considerable amount of evidence[3-8] has become available in the literature as to the abnormal behavior of liquids held in microscopic pores or crevices. Of particular interest in this connection is the abnormal vapor pressure lowering in artificial capillary systems[9-12] devised with the purpose of testing the Kelvin equation. It seemed to us, in view of this evidence, that the objection referred to may not be valid, and we were encouraged to undertake this study of adsorption in a system of constant total surface and variable pore content. We were guided by the following considerations.

It is known that a system consisting of a large number of uniform spheres in random packing may be considered as a mixture of the hexagonal and cubical arrays, where the average number of contacts per sphere is approximately a linear function of the porosity.[13] In an adsorption system consisting of a number of spheres each contact made by two adjacent spheres may be considered as a region of capillary action, where under appropriate conditions capillary condensation will take place. With a large and fixed number of spheres, the number of contacts may be varied within certain limits, while the total surface available to adsorption remains practically constant. This will be true for perfectly smooth surfaces and for imperfect surfaces possessing, crevices, cavities or protrusions. When such a system is packed under a high vacuum, it is probable that a certain fraction of the contacts will be so close as to preclude adsorption from taking place on the areas involved. If the areas of contact are appreciable and the number of such contacts is large, the available surface will be larger in a system of high porosity than in one of low porosity. If the adsorption process is purely a surface phenomenon of a mono- or polymolecular type, the adsorption capacity at a given pressure will be greater in a system of high porosity than in one of low porosity, and *vice versa*.

One arrives at the same conclusion when considering contacts in which the spheres do not meet perfectly, and are separated by small distances. In a low porosity system the spheres are more closely packed, and the distances of approach are on an average smaller than in a system of high porosity. If the adsorption process is of a polymolecular layer type, thinner adsorption layers would be favored in a system of low porosity.

If capillary condensation is a part of the adsorption process, the adsorption capacity will be greater in a system of lower porosity, since the capillary capacity of the system is higher. Each contact, whether perfect or imperfect, will serve as a seat of capillary action. The imperfect contact is generally due to surface imperfections, such as point protrusions, and is in a sense a multiple point contact.

Experimental

Apparatus.—The apparatus for measuring adsorption was of the conventional volumetric type, except that mercury cut-offs were included instead of stopcocks. The vessel containing the adsorbate was provided with a graduated neck, and was connected to the apparatus by means of a mercury sealed ground glass joint. This arrangement allowed rotation of the vessel into a horizontal position. In this position, it was possible to change the system of spheres from low to high porosity without exposing it to the atmosphere, and also to loosen the spheres during activation to prevent cracking of the vessel. In activating the spheres, the system was heated to a high temperature causing considerable expansion. The graduated neck allowed for the determination of the volumes occupied by the spheres at different packing, and hence the porosities.

The two main parts of the apparatus, the pre-expansion and the adsorption volumes were 175 and 240 cc., respectively. The latter volume included the free space in the vessel containing the spheres. These volumes were calibrated with helium, using Boyle's law. The spheres and part of the adsorption volume, namely, 33 cc., were kept at 0°; the pre-expansion volume and 207 cc. of the adsorption volume were kept at room temperature. The pressures were measured with a cathetometer accurate to 0.02 mm.

Materials.—Soft glass spheres made in Czechoslovakia

(1) J. W. McBain, "The Sorption of Gases and Vapors by Solids," G. Rutledge & Sons, Ltd., London, 1932, p. 443.

(2) Reference 1, p. 438.

(3) F. W. Parker, *J. Am. Chem. Soc.*, **43**, 1011 (1921).

(4) A. S. Coolidge, *ibid.*, **46**, 680 (1924).

(5) J. J. Trillat, *Compt. rend.*, **180**, 1839 (1935).

(6) Jean Perrin, *Kolloid-Z.*, **51**, 2 (1930).

(7) A. Maurice Taylor and A. King, *J. Optical Soc. Am.*, **23**, 308 (1933).

(8) B. Deryagin, *Z. Physik*, **84**, 657 (1933).

(9) J. L. Shereshefsky, *J. Am. Chem. Soc.*, **50**, 2966 (1928).

(10) J. L. Shereshefsky and Clarence P. Carter, *ibid.*, **72**, 3682 (1950).

(11) K. V. Chmutoff, *J. Phys. Chem.* (*U.S.S.R.*), **9**, 345 (1937).

(12) K. V. Chmutoff, *Colloid J.* (*U.S.S.R.*), **11**, 44 (1948).

(13) W. O. Smith, Paul D. Foote and P. F. Busang, *Phys. Rev.*, **34**, 1271 (1929).

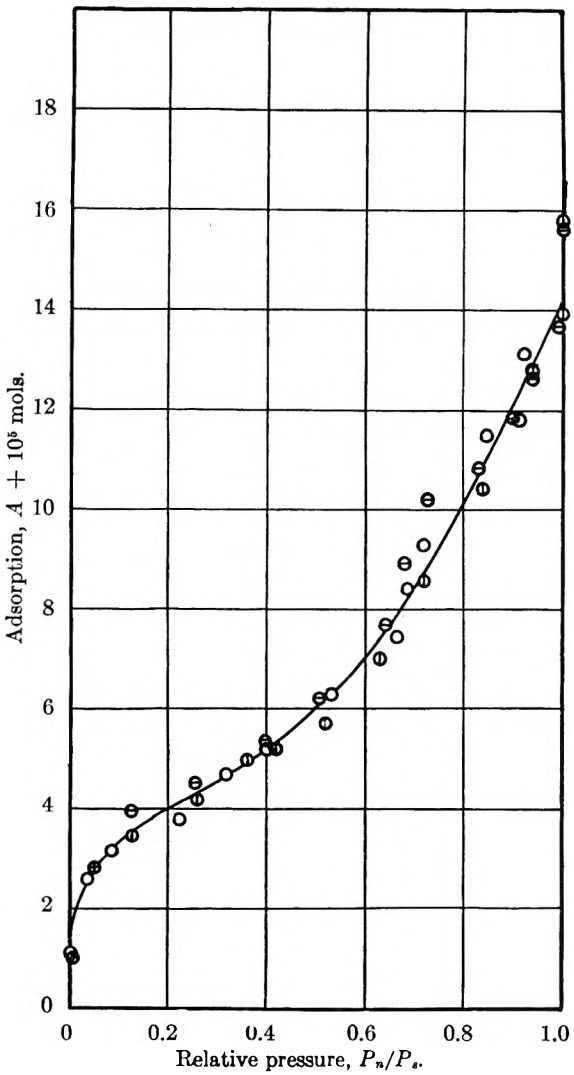

Fig. 1.—Adsorption of ethyl alcohol on glass spheres: temp., 0°; porosity, 0.340; contacts, 10.25 per sphere. ○, run 2; ⊖, run 3; ⓘ, run 4.

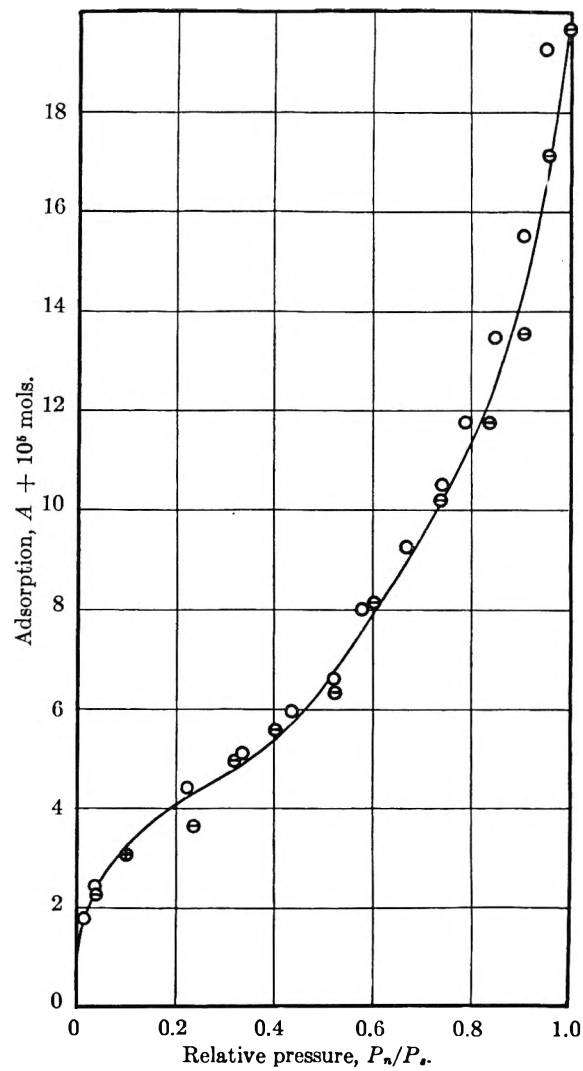

Fig. 2.—Adsorption of ethyl alcohol on glass spheres: temp., 0°; porosity, 0.317; contacts, 10.80 per sphere. ○, run 2; ⊖, run 3.

and distributed by American Supply houses were used for the adsorbent. The spheres were sifted and those approximating 3.0 mm. in diameter were retained. They were cleaned with concentrated nitric acid for a few minutes, with dilute nitric acid for several hours, and were washed with running distilled water for 18 hours. During the washing, which was done in a Büchner funnel, the spheres were always under water; washing was followed by drying in an oven at 200° for two hours and cooling in a desiccator. When cooled they were weighed and transferred to the adsorption vessel. The number of spheres taken was determined by weight, the average weight per sphere having been established beforehand.

Ethyl alcohol was used as adsorbate. It was purified and dried in accordance with the method of Weissberger and Proskauer.[14] The drying was repeated several times. The dissolved air was removed from a few cc. of the alcohol placed in the storage vessel consisting of two bulbs connected to the apparatus by repeated distillation from one bulb to the other and frequent pumping. Absence of absorbed gases was established with the McLeod gage, using sticking of condensed vapor in the tip of the capillary as indicator.

Procedure.—The activation of the spheres which have been exposed to the atmosphere consisted of alternating evacuation at a high temperature with saturation with the vapor of the adsorbate at the temperature of the experiment. To obtain reproducible surface conditions this treatment was repeated two or three times. The vessel and spheres were rotated into a horizontal position and heated in an electric furnace to 300°, while maintaining a vacuum of 10^{-5} mm. of mercury. At the end of two hours of continuous heating and pumping the vessel was returned to its vertical position and allowed to cool. When sufficiently cool to allow further cooling in an ice-bath, the spheres were now saturated with alcohol vapor and allowed to stand in contact with it for several hours. The activation between runs consisted of heating at 300° and pumping to maintain a high vacuum for two hours. Since the spheres were not exposed to the atmosphere, it was found unnecessary to repeat the process in order to obtain reproducible measurements.

Packing of the spheres to the desired porosity was attained by uniform tapping of the vessel held in vertical position. At the completion of the activation the spheres were usually loosely packed, but if not sufficiently so they were loosened by rotating the vessel. It was found that spheres packed to porosities corresponding to eight contacts per sphere or less gave systems of insufficient stability. At these porosities accidental jarring of the vessel, or the vibrations caused by the oil pump, caused changes in the porosity of the system. Packings corresponding to higher numbers of contacts per sphere were not affected during the course of the experiment, and were found to be easily reproducible. The porosities were obtained from the calculated volume of the spheres and from the volume which they occupied in the vessel.

The adsorption measurements were carried out by first introducing vapor into the pre-expansion volume, V_1, and

(14) Arnold Weissberger and Erich Proskauer, "Organic Solvents," The Clarendon Press, New York, N. Y., 1935, p. 118.

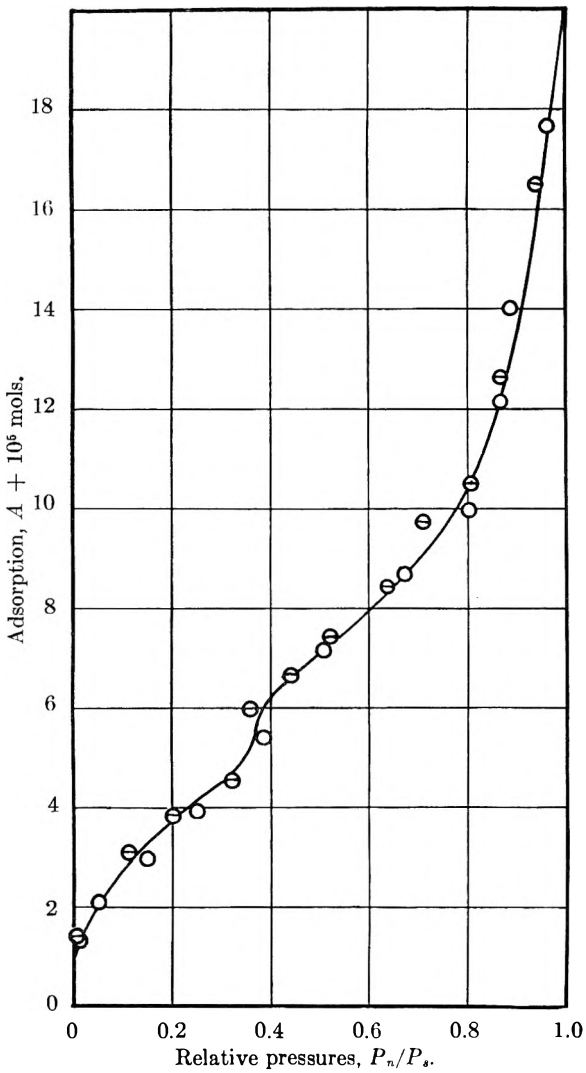

Fig. 3.—Adsorption of ethyl alcohol on glass spheres: temp., 0°; porosity, 0.304; contacts, 11.1 per sphere. ○, run 1; ⊖, run 2.

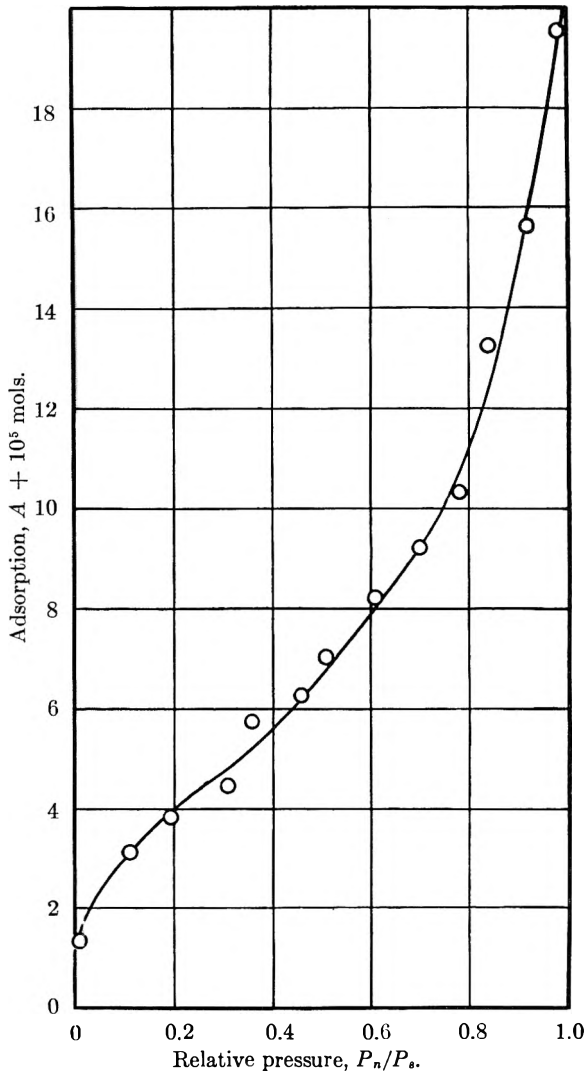

Fig. 4.—Adsorption of ethyl alcohol on glass spheres: temp., 0°; porosity, 0.295; contacts, 11.35 per sphere.

observing its pressure in the manometer. The vapor was then allowed to expand into the adsorption volume. Readings of the resulting pressure were made frequently until constancy was obtained. The time for obtaining equilibrium varied from two to thirty minutes, depending on the pressure, more time being required at the lower pressures. To introduce an additional quantity of vapor the adsorption and pre-expansion volumes were again separated, and the same manipulation followed as in introducing the first quantity. A complete isotherm took from 12 to 20 additions of vapor.

In preparing the apparatus for a new series of measurements, the spheres were first activated in the manner described above, and then adjusted to occupy the desired volume in the manner described, without having to disconnect the adsorption vessel and exposing the spheres to the atmosphere.

The adsorption was calculated by means of the equation

$$A = (P_n^\circ - P_n)\frac{V_1}{RT} - P_n\frac{V_2}{RT} - P_n\frac{V_2'}{RT_0} \qquad (1)$$

where A is the adsorption in moles, P_n° is the pressure in the pre-expansion volume for point n on the isotherm, P_n is the equilibrium pressure for point n, V_1, V_2 and V_2' are the volumes referred to above, T is the room temperature and T_0 is the temperature of the ice-bath. The number of contacts per sphere was calculated from the two equations

$$f = 0.2595\,x + 0.4764(1 - x) \qquad (2)$$

$$c = 6\,\frac{1 + 1.828x}{1 + 0.414x} \qquad (3)$$

where f is the observed porosity, x is the fraction of the total volume of spheres packed hexagonally, and c is the number of contacts per sphere.

Results and Discussion

The isotherms given below refer to ethyl alcohol at 0° as the adsorbate and to 5505 glass spheres as the adsorbent. In Fig. 1 are given the results of the measurements with the spheres packed to give the average number of 10.25 contacts per sphere. Figure 2 shows the isotherm obtained for a system with an average number of 10.80 contacts per sphere, Fig. 3 for 11.1 contacts per sphere and Fig. 4 for 11.35 contacts per sphere.

The adsorption measurements at the four different porosities were not made in the order in which they are presented. First were made the runs at 10.25 contacts per sphere; then the first run at 11.1 contacts, followed by the single run at 11.35 contacts; then the second run at 11.1 contacts; and finally the runs at 10.80 contacts per sphere. This procedure was adopted because in the literature are reported instances in which adsorption increased or

TABLE I

MOLES OF ETHYL ALCOHOL VAPOR ADSORBED AT DIFFERENT POROSITIES

Porosity	P_a/P_s 0.1	0.2	0.25	0.3	0.4	0.5	0.6	0.7	0.8	0.9	0.95
0.340	3.2	4.0	4.3	4.5	5.2	5.9	6.9	8.5	10.2	12.3	13.2
.317	3.0	3.9	4.3	4.8	5.6	6.5	7.8	9.5	11.5	14.2	16.7
.304	2.9	3.8	4.3	4.8	5.8	7.0	8.0	9.3	10.8	14.1	17.0
.295	3.0	3.9	4.3	4.9	5.8	7.0	8.0	9.3	11.4	14.9	17.3

decreased with successive and repeating measurements. It was thought that should this behavior manifest itself in the present measurements it could not with this procedure be misconstrued. The absence of a consistent change in the isotherms in the order in which they were obtained was assumed as an indication of the absence of the phenomenon referred to. This together with the reproducibility of the isotherms for each packing seems therefore to establish that the differences observed were caused by the variation in the number of contacts per sphere.

Although the spheres appeared to have fire-polished surfaces, the cleaning process to which they were subjected undoubtedly caused considerable corrosion. The total surface of the spheres was many times larger than the apparent surface. Adsorption measurements with methylene blue, on the basis that 1 mg. is equivalent to ten thousand sq. cm., showed that the surface of the 5505 spheres was 52,848 sq. cm. Assuming a monomolecular layer of alcohol molecules oriented with the hydrocarbon part toward the vapor phase and occupying 20 sq. A. units per molecule, the total surface is equivalent to 4.36×10^{-5} mole of alcohol. With the nature of the two molecules being so different, it is rather striking that this value corresponds on all isotherms to the inflection at the relative pressure of approximately 0.25. Other investigators,[15,16] on the strength of entirely different evidence, have also interpreted similar inflection points to mark the completion of a unimolecular layer.

Since the total surface in the several systems was approximately the same, it is consistent that in the range from zero to 0.25 relative pressure, the isotherms for all porosities are practically identical. The small differences showing decreasing adsorption with increasing number of contacts per sphere are perhaps due to decreasing surface resulting from the increasing number of perfect contacts. This portion of the curves follows the Langmuir isotherm.

From the relative pressure of 0.25 to saturation the isotherms diverge in directions of increased adsorption with decreasing porosity. Table I shows that this divergence begins at a relative pressure of about 0.3 and increases continuously to saturation. An exception to this regularity in behavior is the point at the relative pressure 0.8 on the isotherm of porosity 0.304, which shows an appreciably lower adsorption than the corresponding point on isotherm of porosity 0.317. However, disregarding this point on isotherm of porosity 0.317, as it is perhaps due to an experimental error, the adsorption at this relative pressure increases as we proceed from porosity 0.340 to porosities 0.304 and 0.295.

The isotherm of porosity 0.295 does not differ much from the 0.304 isotherm. These two porosities are close to the limiting hexagonal array, and do not perhaps differ as much in the number of contacts per sphere as the calculations indicate. Another possibility is that the distance of separation in a contact is reduced, thus counteracting the effect of increased number of contacts.

It seems to us, before considering the applicability of capillary condensation, that these results speak against polymolecular layer adsorption. In the first place, as shown by the monomolecular regions of the isotherms, the total surface of the system seemed to have decreased with decreasing porosity. Although this decrease was not large, it was appreciable enough to be measured. Had polylayers been formed at higher relative pressures, greater differences in adsorption in the same direction would have shown up.

Secondly, we should expect, on the basis of polylayer formation, decreasing adsorption with decreasing porosity also in the case of imperfect contacts, *i.e.*, when two adjacent spheres make a contact extending over a microscopic area and include a narrow gap. Contacts of this type most likely were much more numerous than the perfect ones, because of the approximate spherical shape of the spheres and the imperfections on their surfaces. These contacts while not preventing adsorption from taking place would restrict the number of monolayers that could condense in more porous systems.

The contrary was true. As we have seen, the amount of adsorption increased with decreased porosity, or, which is the same, with increased contacts per sphere. This fact, it appears to us, can be explained on the basis of the capillary condensation theory, and the quantity adsorbed at a contact can be shown to be of the right order of magnitude.

If we assume that the condensed vapor at the contact of two perfect spheres is in the form of a ring of liquid with radii of curvature R_1 and r, as shown in Fig. 5, geometrical considerations show that

$$1/r \cong 1/x \qquad (4)$$

and

$$1/R_1 \cong 1/2R_2x \qquad (5)$$

where x is a half of the widest separation of the spheres at the line of contact with the condensed vapor, and R_2, R_1 and r are the radii of curvature of the spheres, the ring and the concave surface of the liquid ring. It is to be noted that the curvature of the ring is positive and that of the surface is negative. The values of x and R_1 may be obtained with the aid of the Kelvin equation

(15) W. C. Bray and H. D. Draper, *Proc. Natl. Acad. Sci.*, **12**, 297 (1926).

(16) P. H. Emmett and S. Brunauer, *Trans. Electrochem. Soc.*, **71**, 13 (1937).

$$\frac{2.3\,aRT}{\sigma M}\log\frac{P_n}{P_s} = -\left(\frac{1}{x} - \frac{1}{2R_2x}\right) \qquad (6)$$

where P_n/P_s is the relative pressure, σ, d and M are the surface tension, density and molecular weight of the liquid adsorbate, and R and T are the gas constant and the temperature, respectively.

The application of this equation at a relative pressure of 0.5, at which point the difference in adsorption between the 0.295 and the 0.340 porosity isotherms is 110 millimoles of alcohol, shows that x is 8.85 Å. and that R_1 is 1.63 microns. However, it has been shown in direct tests of the Kelvin equation that the radii thus calculated are much smaller than the observed. Thus Shereshefsky and Carter[10] found that at a relative pressure of 0.975 the calculated radius is one eighty-second as large as the directly measured radius of the capillary, and K. V. Chmutoff[11,12] found at a relative pressure of 0.82 that the Kelvin value was about a hundredth as large as the directly measured crevice formed by two optical lenses in contact with each other.

It is therefore reasonable to suppose that the actual value of x at a relative pressure of 0.5 is about two hundred times larger than the calculated one, namely, about 1700 Å., and the value of R_1 correspondingly greater, *i.e.*, about 22.6 microns.

The approximate volume of a liquid ring around a contact may be taken as half of the volume of the cylinder ABCD shown in Fig. 5, and is given by the expression $2\pi R_1^2 x$. Substituting the estimated values in this expression, we obtain that the volume of the liquid ring is approximately 2.7×10^{-10} cc. Now, the volume of a liquid ring around a contact of real spheres, as those used in this experiment, may be considerably larger than the one in this ideal contact between perfectly spherical and perfectly smooth spheres.

In a random packing of spheres which are only approximately spherical, the contacts are most stable when made at the relatively flatter contours of the sphere's surface. This produces contacts of more extended areas than would prevail between ideal spheres. Furthermore, due to the irregularities of the surface each contact may actually contain a number of points of contact between the protruding particles of each surface of the adjacent spheres. Thus, each contact formed is in reality a multiple of pores in which condensation may take place. The total volume of this contact is considerably greater than that of an ideal contact.

In ascribing the increase in adsorption at the relative pressure under consideration to the increase in the number of contacts in the system, we see that 110 millimoles, or 62.5×10^{-5} cc. of liquid alcohol were adsorbed at 6050 contacts, or that the volume of a contact is approximately 1×10^{-7} cc. This value is about three hundred and fifty times greater than the estimated volume of an ideal contact. We do not know the factor relating the volume of the real contact with that of the ideal, but it is reasonable to assume that it is approximately equal to the roughness factor of the sphere's surface, which is 35. We see thus that there is fair agreement between the observed and estimated values of the volume of a contact.

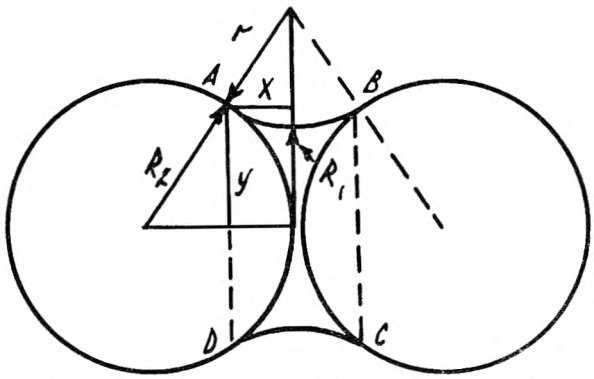

Fig. 5.—Relation between radii of curvature of ring of adsorbate round a contact of two spheres. R_2 and R_1 are the radii of the spheres and the ring, respectively; r is the radius of curvature of the concave surface of ring.

The adsorption process, as it appears from these experiments, seems to consist, first, in the formation of a unimolecular layer on the surface of the adsorbent. The formation of this layer which follows the Langmuir equation is completed at relatively low pressures. Capillary condensation seems to begin to manifest itself also at low pressures, as the formation of the monolayer is completed. The condensation of water vapor in a crevice formed by the contact of two optical lenses was directly observed[11,12] to take place at low relative pressures. It is also evident from the steep rise at relative pressure 0.35 in isotherms of Figs. 3 and 4.

DISCUSSION

J. C. ARNELL.—I would like to call the authors' attention to work by Carman and Raal which appeared in the *Proc. Roy. Soc.* (*London*), 209A, 59–69, 69–81 (1951) in which a comparison was made of the physical adsorption of CF_2Cl_2 on loose powders and porous plugs of silica and Carbolac-1. In general they found that at low pressures the plugs and powders gave identical results, while at higher pressures the adsorption became increasingly greater for the plugs until their pore space is filled and the adsorption limit is reached. Above this point the adsorption becomes greater for the powders. The plugs also showed marked hysteresis at higher pressures which indicated capillary condensation and no similar effect was found for the powders. In addition, the authors examined a series of plugs at different porosities and showed the limitation imposed on the maximum pick-up with decreasing pore space. The experimental data are used to calculate pore size distribution and strong evidence is presented to show that tightly packed aggregates of particles occur and that the pore size becomes increasingly uniform as the porosity is decreased.

J. TH. G. OVERBEEK.—In Table I a definite increase in adsorption is shown when the porosity decreases from 0.340–0.317 (increase in number of contacts per sphere 0.55). A further decrease of the porosity from 0.317–0.295 (corresponding to a second increase of the number of contacts by 0.55) shows hardly any change in adsorption. This does not seem to fit into the explanation given, where the increased adsorption should be proportional to the number of contacts.

CHARLES G. DODD.—The data presented by Dr. Shereshefsky do not appear to constitute proof that multimolecular adsorption played no role in his experiments. The authors state that "...as shown by the monomolecular regions of the isotherms, the total surface of the system seemed to have decreased with decreasing porosity." Actually, the authors had pointed out previously that the "point B" of each isotherm occurred at the same area regardless of porosity. At relative pressures below about 0.25 the isotherm data points are almost superimposable. I do not understand why they thought the total surface decreased with decreasing porosity.

Secondly, the authors state, "...we should expect, on the basis of polylayer for mation, decreasing adsorption with decreasing porosity also in the case of imperfect contacts,..." I do not agree that this should be expected. The real contacts of 3-mm. diameter spheres would not appreciably affect the building up of a few adsorbed layers because these few layers would require only a few angstrom units of depth. The authors' results may be interpreted in terms of capillary condensation, but they do not rule out the possibility of multilayer formation.

THE CHARACTERIZATION OF PHYSICAL ADSORPTION SYSTEMS. I. THE EQUILIBRIUM FUNCTION AND STANDARD FREE ENERGY OF ADSORPTION

By Donald Graham

Contribution No. 146 from Jackson Laboratory, E. I. du Pont de Nemours and Co., Wilmington, Delaware

Received July, 13, 1953

A simple function representing adsorption equilibrium provides the basis for a clean cut classification of physical adsorption systems, in terms of surface uniformity and adsorbate interaction. In the ideal case involving localized, non-interacting adsorption on a uniform surface, this function becomes the equilibrium constant. The effects of factors contributing to non-ideality usually appear singly during deposition of the first half of the first monolayer. The accompanying departure from constancy of the equilibrium function is related in kind to the nature of the particular factor responsible. For an ideal system, the standard free energy of adsorption is calculated from the equilibrium constant. Non-interacting adsorption on two kinds of sites is resolved to yield the fraction of the total surface and the standard free energy of adsorption associated with each kind of site.

Introduction

Although a fair variety of applicable data is now available, no method for an unambiguous characterization of adsorption systems has appeared. This failure has been due to at least three factors. (1) The shape of any multilayer isotherm yields very little information regarding the nature of deviations from ideality in the first monolayer. (2) Empirical expressions for multilayer isotherms lack valid quantitative relationship to adsorption energies. (3) The heat of adsorption is limited in significance by appreciable experimental error at low coverage and by complicating factors at higher levels.

The above difficulties are overcome by application of a function which represents adsorption equilibrium, and is constant under ideal conditions, to the lower part of the isotherm.

For the adsorption process: free adsorptive molecules + vacant sites $\rightleftarrows$ occupied sites; if all sites are identical and if occupancy of one site exerts no influence upon those adjacent (no adsorbate interaction), the equation for the equilibrium constant is written

$$\frac{\text{(Activity of occupied sites)}}{\text{(Activity of vacant sites)(Activity of free adsorptive molecules)}} = K$$

If it is assumed that the activity coefficients of the occupied and unoccupied sites are the same, the equation becomes

$$K = \frac{(\theta)}{(1 - \theta)C}$$

in which θ equals the fraction of the surface covered, and C the activity of the free adsorptive molecules in units of either concentration or pressure. In most cases of low coverage, the concentration or pressure in the mobile phase is sufficiently low to permit the assumption of an activity coefficient of unity.

It is interesting to note that the equation for the equilibrium constant can be rewritten

$$\theta = \frac{KC}{1 + KC}$$

which is the familiar Langmuir[1] isotherm in which the usual kinetic terms have been replaced by constants readily determined from equilibrium data.

The standard free energy of adsorption may be calculated for an ideal system (or for a system which behaves as a combination of two ideal systems) from the equilibrium constant

$$-\Delta F^\circ = RT \ln K$$

This quantity represents the decrease in free energy of the system in the transfer of one mole of adsorptive molecules from the standard state in the mobile phase to the adsorbed layer at $\theta = 0.5$, and constitutes a measure of the strength of the adsorption bond.

Equilibrium constants are obtained only from systems approaching the ideality embodied in the assumptions outlined above. However, the equilibrium function

$$\theta/(1 - \theta)C$$

in its departure from constancy often indicates the nature of the factor responsible for non-ideality as follows.

The adsorption bond may be augmented by lateral interaction between adsorbate molecules on adjacent sites. Adsorbate interaction is favored by a weak bond to the adsorbent or by polar groups in the molecules being adsorbed. It usually becomes important only after occupation of a measurable portion of the surface, varying inversely with the strength of the interaction. This effect is indicated by a tendency for the equilibrium function to increase with adsorption, reflecting an increased opportunity for adsorption on sites with nearest neighbors occupied.

Non-ideality due to adsorbate interaction cannot be resolved in terms of any fixed distribution of

(1) I. Langmuir, *J. Am. Chem. Soc.*, 40, 1361 (1918).

different kinds of sites because the character of the sites changes with adsorption.

It is apparent from the form of the equilibrium function that when sites of different kinds are present, the strongest are most completely filled at any level of over-all coverage. Surface non-uniformity is therefore recognizable in an immediate tendency for the value of the equilibrium function to decrease with adsorption.

The simplest case of surface non-uniformity is that involving only two kinds of sites. The Langmuir[1] isotherm was extended to include systems of two (or more) kinds of sites but practical application has been limited by the nature of the constants used.

Two, more recent, attempts to treat interfaces with two kinds of sites[2,3] have been based on the use of two values for the constant C of the B.E.T. (Brunauer, Emmett, Teller) equation. This approach is unsound due to lack of a valid relation between the heat of adsorption and the B.E.T. constant C. In an application to experimental data[4] the nitrogen–magnesia interface was chosen to exemplify a "dual" surface. Treatment of the same data[5] by the methods outlined herein yields an equilibrium function essentially constant up to $\theta \sim 0.5$, showing a high degree of ideality—a more acceptable characterization for adsorption of non-polar molecules on the surfaces of cubic crystals.

A more satisfactory method for resolving a system with two kinds of sites comprises treatment as two separate surfaces in equilibrium with the same mobile phase. Each surface is assigned a characteristic equilibrium constant and the two combined to give

$$\theta = \frac{\alpha K_1 C}{1 + K_1 C} + \frac{(1 - \alpha) K_2 C}{1 + K_2 C}$$

in which

K_1 = equilibrium constant for stronger sites
K_2 = equilibrium constant for weaker sites
α = fraction of total surface occupied by stronger sites
C = concn. (or pressure) of adsorptive molecules in the mobile phase

This has the form of the Langmuir[1] isotherm for systems of two kinds of sites; but, as in the ideal case, the constants are more readily determined from the isotherm.

Direct solution of this expression for K_1, K_2 and α is very involved. Solutions by trial and error, however, may be considerably simplified by the use of certain approximations. If the data embrace a wide range of coverage and K_1 and K_2 are sufficiently different, it may be assumed, for a first approximation, that only the stronger sites are occupied at the lower end of the isotherm. Equating the equilibrium functions for two points in this region to K_1 provides approximate values for K_1 and α. It may also be assumed that, at high coverage, only weaker sites are vacant; but, this assumption is limited in value by complications. In any case, the best final values are obtained by trial, fitting the constants to the experimental data.

Interacting adsorption on a non-uniform surface usually shows the effects of both factors. Unless the interaction completely dominates the system, increasing coverage brings an initial drop in the equilibrium function followed by a rise as interaction becomes appreciable. It will be shown later that a balance between the two effects may be mistaken for ideality.

The foregoing relations are illustrated in Fig. 1 and are exemplified in the pages which follow, by application to adsorption data from the literature.

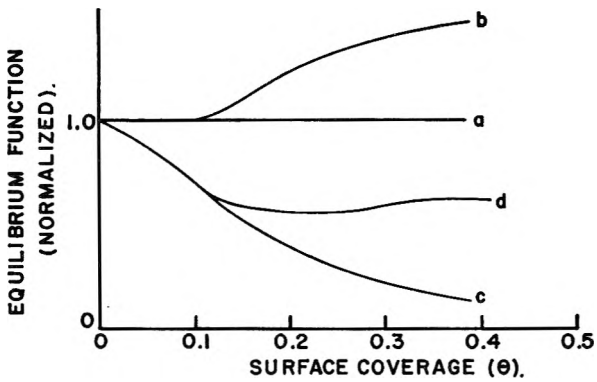

Fig. 1—Types of adsorption systems: a, ideal; b, uniform—interacting; c, non-uniform—non-interacting; d, non-uniform—interacting.

Detailed consideration of non-ideality due to multilayer adsorption or capillary condensation is omitted from this paper. It may be shown by consideration of the second layer equilibrium function (from data at $\theta = 1.5$) that at a coverage below $\theta = 0.5$, second layer effects are usually negligible (0.1–0.2%). Capillary condensation has been treated exhaustively in other papers and is easily recognizable through hysteresis.

Application to Experimental Isotherms

A. Ideal Systems. (a) Adsorption of Non-polar Molecules on Single Crystal Faces.—The adsorption of nitrogen and argon on single crystal faces of copper and zinc offer the most definitive examples of ideality.[6,7] The data from these systems yield satisfactory equilibrium constants (within the limit of precision of the data) up to a coverage of $\theta \sim 0.4$ as shown in Table I.

There is no indication of surface non-uniformity and the evidence for very slight interaction at the lower levels may be due to experimental error. Interaction becomes very important at coverage above $\theta \sim 0.4$.

Similar results are obtained from the data representing other crystal faces, with the 110 face the strongest adsorber, as shown

Crystal face	100	110	111
$\Delta F°$ (cal./mole) at 78.1°K.	590	640	580

This supports Rhodin's conclusion that although the atoms are less closely spaced in the 110 face, its geometry is the most favorable to the adsorption of nitrogen.

(2) W. G. McMillan, *J. Chem. Phys.*, **15**, 390 (1947).
(3) W. C. Walker and A. C. Zettlemoyer, THIS JOURNAL, **52**, 47 (1948).
(4) A. C. Zettlemoyer and W. C. Walker, *ibid.*, **52**, 58 (1948).
(5) A. C. Zettlemoyer and W. C. Walker, *Ind. Eng. Chem.*, **39**, 69 (1947).
(6) T. N. Rhodin, *J. Am. Chem. Soc.*, **72**, 5691 (1950).
(7) T. N. Rhodin, THIS JOURNAL, **57**, 143 (1953).

TABLE I

THE ADSORPTION OF NITROGEN ON THE 110 FACE OF COPPER AT 78.1°K.

(From a smooth curve through the points representing sample 1, Fig. 2, ref. 6.)

(P_0 = vapor pressure of N_2 at 78.1°K. = 83.2 cm.). For the process $N_{2(sat.\ vapor)} \rightarrow N_{2(adsorbed)}$, $K = 60$, and $-\Delta F^\circ = 640$ cal./mole.

Nitrogen adsorbed (10^{-6} g./g.)	Fraction of surface covered θ	Equilibrium pressure P, cm.	Relative pressure $P/P_0 \times 10^2$	Equilibrium function $\theta/(1-\theta)(P/P_0)$
0.050	0.093	0.14	0.17	60
.100	.185	.31	.37	61
.150	.28	.52	.63	62
.200	.37	.77	.93	63
.250	.46	.95	1.14	75
.300	.56	1.10	1.32	96
.350	.65	1.30	1.56	119

Polycrystalline copper[8] (within the precision with which the data can be read from the published plot of the isotherm) adsorbs nitrogen like a single crystal face but with a slightly lower standard free energy change. However, the degree of non-uniformity due to the presence of different crystal faces might not be resolved from the available data.

The isotherms for the adsorption of nitrogen or argon on the 1011 crystal face of zinc are comparable in ideality with those for nitrogen on copper.

It must not be concluded from the above that the adsorption of gases (even non-polar gases) on metal surfaces is always homogeneous. The adsorption of nitrogen on platinum[9] shows increasing evidence of non-uniformity with lowering temperature. Whether this is due to surface structure, contamination, or inherent properties of platinum is not apparent.

(b) Adsorption of Nitrogen on Graphon.—Graphon (prepared by heat-graphitization of Spheron 6, a Cabot Channel Black) adsorbs nitrogen with a high degree of ideality as indicated by the stepped character of the multilayer isotherm.[10]

Low coverage adsorption data[11] confirm this characterization by yielding an equilibrium function of high constancy up to $\theta \sim 0.7$ (see Table II).

This standard free energy of adsorption is about double that observed on copper or zinc surfaces. The lower lateral interaction, evidenced by the relatively smaller increase in the value of the equilibrium function with coverage, may be directly due to this higher bonding energy. The fall-off at coverage above $\theta = 0.7$ suggests the necessity for some shifting of adsorbate molecules to permit occupancy of the last portion of the adsorbent surface.

(c) Adsorption of Heptane on Graphite.—Adsorption isotherms for *n*-heptane on graphite of low ash content (<0.004% ash) have been reported for both low[12] and high[13] coverage. Values of the equilibrium function at varying coverage are given in Table III.

TABLE II

THE ADSORPTION OF NITROGEN ON GRAPHON AT 78.4°K.

(From data of Joyner and Emmett, run 5 smoothed by plotting.)

Nitrogen adsorbed, cc./g. S.T.P.	Fraction of surface covered θ	Relative pressure $P/P_0 \times 10^3$	Equilibrium function, E.F.	Standard free energy change $-\Delta F^\circ$, cal./mole
2.76	0.15	0.07	2520	1230
4.0	.22	.11	2560	1230
6.0	.33	.19	2590	1230
8.0	.44	.30	2620	1230
10.0	.55	.45	2720	1240
12.0	.66	.72	2700	...
14.0	.77	1.6	2090	...
16.0	.88	6.0	1220	...

TABLE III

THE ADSORPTION OF HEPTANE ON LOW ASH GRAPHITE AT 25°

(From data of Harkins, Jura and Loeser, refs. 12, 13.)

First layer		Second layer	
θ_1	E.F.	θ_2	E.F.
0.32	1090	0.13	1.47
.40[a]	910	.19	1.53
.50	1050	.23	1.50
.60	1040	.28	1.56
.67	940	.41	2.32
$K = 1050$		$K = 1.50$	
$-\Delta F^\circ = 4140$ cal./mole		$-\Delta F^\circ = 240$ cal./mole	

[a] This discontinuity is attributed by the authors to phase transition.

Discontinuities in the lower isotherm, ascribed by the authors to phase transitions (a conclusion which should be checked on Graphon) occurring up to a coverage of $\theta \sim 0.4$, limit the significance of the characterization of the first layer. However, a high degree of uniformity with very little interaction is indicated.

The high value of $-\Delta F^\circ$ combined with the area occupied by one molecule (64 sq. Å.) indicates that the molecule lies flat with each $-CH_2-$ group contributing additively to the total. This is consistent with reported measurements of heats of adsorption.[14]

The point of greatest interest in regard to this system is the uniformity of the first heptane layer as an adsorbing surface. The second layer is treated in the same way as the first except that the content of the first layer is subtracted from the total quantity of heptane adsorbed in calculating the values of θ.

The more important interaction observed in the second layer is consistent with the hypothesis that a strong adsorption bond (such as was observed for the first layer) tends to weaken interaction.

(8) T. N. Rhodin, *J. Am. Chem. Soc.*, **72**, 4343 (1950).

(9) F. J. Wilkins, *Proc. Roy. Soc.* (*London*), **A164**, 510 (1938).

(10) M. H. Polley, W. D. Schaeffer and W. R. Smith, THIS JOURNAL, **57**, 469 (1953).

(11) L. G. Joyner and P. H. Emmett, *J. Am. Chem. Soc.*, **70**, 2353 (1948). Original Data: Document 2530, American Documentation Institute, 1719 N St., N.W., Washington 7, D. C.

(12) G. Jura, W. D. Harkins, and E. H. Loeser, *J. Chem. Phys.*, **14**, 344 (1946).

(13) W. D. Harkins, G. Jura, and E. H. Loeser, *J. Am. Chem. Soc.*, **68**, 554 (1946).

(14) M. H. Polley, W. D. Schaeffer, and W. R. Smith, *ibid.*, **73**, 2161 (1951).

For the second layer adsorption of heptane on graphite, of higher ash content (0.46%), the same degree of ideality was observed but the value of $-\Delta F^\circ$ was increased to 400 cal./mole. Ideality in adsorption of non-polar molecules therefore may be more a matter of surface structure than of chemical purity, although the strength of the adsorption bond appears to be quite sensitive to impurities.

B. Non-ideal Systems. I. A Strongly Interacting Adsorbate on a Homogeneous Surface.—In the earlier examples, it was shown that nitrogen is adsorbed almost ideally on uniform surfaces up to a coverage of $\theta \sim 0.4$. Above this point, appreciable interaction is indicated by an increasing equilibrium function. The *n*-heptane isotherm showed much weaker interaction.

It would be expected that more polar compounds would interact more strongly and at lower coverage.

(a) Ethyl Chloride on Graphon.—Reported isotherms for the adsorption of ethyl chloride on Graphon[15] show ideality up to $\theta \sim 0.1$; and, above that point, a rapid rise in the equilibrium function, indicating strong interaction of the adsorbate molecules. Typical results are shown in Table IV.

TABLE IV

THE ADSORPTION OF ETHYL CHLORIDE ON GRAPHON. AN EXAMPLE OF INTERACTING ADSORPTION ON A UNIFORM SURFACE

(From measurements of Mooi, Pierce and Smith.)

Temp. = −78°		Temp. = 0°		Temp. = 75°	
θ	E.F.	θ	E.F.	θ	E.F.
0.030	31	0.042	11	0.027	7.2
.058	31	.079	11	.056	7.4
.11	32	.13	12	.083	7.5
.20	41	.18	14	.11	7.6
.33	61	.33	20	.19	9.4
		.65	37	.38	12.0
		.83	49	.64	18.0

(b) Methanol on Graphon.—The isotherm for the adsorption of methanol on Graphon[16] at 0° shows very much stronger interaction, with no detected zone of ideality at low coverage, see Table V.

TABLE V

THE ADSORPTION OF METHANOL ON GRAPHON AT 0°. AN EXAMPLE OF STRONGLY INTERACTING ADSORPTION ON A UNIFORM SURFACE

θ	0.04	0.09	0.20	0.33	0.61	0.86
E. F.	0.40	0.67	1.25	2.0	5.2	17.7

A more detailed, quantitative study of adsorbate interaction is in progress and will be reported later.

II. Non-interacting Adsorption on Non-uniform Surfaces. (a) Surfaces with Only Two Kinds of Sites.—Non-interacting adsorption of a polar compound in two different orientations on a non-porous surface would be expected to involve two kinds of sites. Polar molecules tend to interact strongly but this tendency can be minimized by use of a polar solvent. In such cases, it must be recognized that the standard free energy of adsorption obtained is an over-all value, including all solvent effects involved.

An example is found in the adsorption of butyric acid from aqueous solution by graphite.[17]

The data used are those for graphite A (0.035% ash) as given in Table II of ref. 17, specifically the uncorrected values of the molality and the quantity of butyric acid adsorbed (x/m). Applicable solution activity data are not available but it may be assumed that the activity coefficient is relatively constant over the range of significance (the first four points). The true values of K_1 and K_2 would vary inversely with the activity coefficient but its difference from unity is probably small, and the resolution would not be otherwise affected. This system was readily resolved to give the following

$K_1 = 125$ $\quad -\Delta F_1^\circ = 2850$ cal./mole
$K_2 = 2.5$ $\quad -\Delta F_2^\circ = 540$ cal./mole
$\alpha = 0.20$

The extent to which the model reproduces the experimental results is shown in Table VI.

TABLE VI

THE ADSORPTION OF BUTYRIC ACID FROM AQUEOUS SOLUTION BY GRAPHITE. AN EXAMPLE OF ADSORPTION ON TWO KINDS OF SITES

(From data of Fu, Hansen and Bartell)

θ_1 = fraction of strong sites occupied; θ_2 = fraction of weak sites occupied; x_1/m = millimoles butyric acid/g. carbon on strong sites; x_2/m = millimoles butyric acid/g. carbon on weak sites.

No.	Equilibrium molality	x/m, mmoles per g.	$\alpha = 0.20$, $K_1 = 125$		$1 - \alpha = 0.80$, $K_2 = 2.5$		Calcd. $x/m = (x_1/m + x_2/m)$	Diff. exp. − calcd. x/m
			θ_1	x_1/m	θ_2	x_2/m		
1	0.0072	0.078	0.475	0.069	0.0177	0.010	0.079	−0.001
2	.0159	.119	.666	.097	.0380	.022	.119	.000
3	.0436	.183	.845	.123	.0983	.058	.181	+ .002
4	.097	.248	.924	.135	.195	.114	.249	− .001
5	.194	.321	.960	.140	.327	.191	.331	− .010
6	.284	.357	.973	.142	.415	.243	.385	− .028
7	.496	.439	.984	.144	.550	.322	.466	− .027
8	.730	.507	.990	.145	.645	.377	.522	− .015
9	1.04	.593	.993	.145	.714	.417	.562	+ .031

The following observations are believed important: (1) The excellent agreement with the "dual" model and the fact that the butyric acid adsorbed never exceeds the requirement for a complete monolayer indicate very little, if any, multilayer adsorption. (2) Interaction appears to be small, particularly on the stronger sites. Experimental results are duplicated by the model, within about 1% up to $\theta_1 = 0.92$ and $\theta_2 = 0.20$. (3) The fact that K_1 represents only one fifth of the total adsorbing surface suggests a chemical difference between sites on the solid surface. This difference may affect only those adsorption processes offering a possibility for dipole interaction or hydrogen bonding. Thus K_1 ($-\Delta F^\circ = 2.8$ kcal.) may represent a hydrogen bond, and K_2 ($-\Delta F^\circ = 0.5$ kcal.) a van der Waals bond.

(15) J. Mooi, C. Pierce and H. N. Smith, Presented at National Colloid Symposium, Ames, Iowa, June, 1953, THIS JOURNAL, 57, 657 (1953).

(16) C. Pierce and P. N. Smith, *ibid.*, 54, 354 (1950)

(17) Y. Fu, R. S. Hansen and F. E. Bartell, *ibid.*, 52, 374 (1948)

(b) **Non-interacting Adsorption on Sites of More Than Two Energy Levels.**—The higher levels of non-uniformity in non-interacting physical adsorption usually involve porous adsorbents, with non-polar adsorbates at low coverage, or polar adsorbates from solution in polar solvents. The adsorption of nitrogen on Spheron 6[11] offers a good example. Attempts to resolve this system in terms of sites of only two kinds left systematic differences between calculation and experiment of 4 to 10% at coverages which, for the butyric acid/water/graphite system, gave differences of about 1%.

Frequency distributions for the adsorption energies of systems of this class have been approximated by methods reported in the literature.[18-21]

Such treatments must be used with care and they fail when interaction is important.

III. Strongly Interacting Adsorption on a Non-uniform Surface.—The most complex adsorption system limited to a single adsorbate involves strong cooperative adsorbate interaction on a non-uniform surface. Such cases are frequently found in the adsorption of a polar compound on a porous surface. An important feature of this class is that the effects of the two factors are opposite. They may balance one another (after the interaction becomes important) to the extent that (if the initial portion of the isotherm is disregarded) the system appears ideal. An example of such a pseudo-ideal system is found in the adsorption of ammonia on charcoal.[22,23] This system has unfortunately been cited as an example of ideality in at least two important references.[24,25]

The variation of the equilibrium function with coverage as summarized in Table VII illustrates the attainment of this balance after completion of about 20% of the first monolayer.

(18) G. Halsey and H. S. Taylor, *J. Chem. Phys.*, **15**, 624 (1947).

(19) R. Sips, *ibid.*, **16**, 490 (1948); **18**, 1024 (1950).

(20) J. M. Honig and L. H. Reyerson, THIS JOURNAL, **56**, 140 (1952).

(21) J. M. Honig, *ibid.*, **57**, 349 (1953).

(22) A. Titoff, *Z. physik. Chem.*, **74**, 641 (1910).

(23) C. B. Richardson, *J. Am. Chem. Soc.*, **39**, 1828 (1917).

(24) S. Brunauer, "The Adsorption of Gases and Vapors, Vol. I, Physical Adsorption," Princeton University Press, Princeton, N. J., 1943.

(25) D. H. Everett, *Trans. Faraday Soc.*, **46**, 957 (1950).

TABLE VII

THE ADSORPTION OF AMMONIA ON NUTSHELL CHARCOAL. AN EXAMPLE OF SURFACE NON-UNIFORMITY WITH STRONG INTERACTION

(From Richardson's data)

θ	0.076	0.162	0.288	0.425	0.560	0.695
E. F.	55	36	20	21	22	20

Summary.—Using the ideal localized monolayer for reference, the behavior of the equilibrium function with increasing coverage provides a simple but effective basis for characterizing adsorption systems.

Ideal systems give valid equilibrium constants, which in turn yield the related standard free energy of adsorption. This value constitutes a measure of the strength of the adsorption bond and varies widely with the adsorbate and with the molecular character, purity, and physical structure of the adsorbent. Nitrogen and argon are adsorbed on non-porous surfaces with a high degree of ideality up to $\theta \sim 0.4$. Normal heptane is adsorbed almost ideally on non-porous carbon with a high $-\Delta F^\circ$ due to interaction of each $-CH_2-$ group with the carbon surface.

Adsorbate interaction causes a rise in the equilibrium function which usually becomes important only after measurable coverage has been attained. This occurs at $\theta \sim 0.4$ with some non-polar adsorbates but earlier and more strongly if the adsorbate contains polar groups. Interaction appears to be impaired by strengthening the bond to the adsorbent or by using a polar solvent.

Surface non-uniformity is indicated by an immediate fall in the equilibrium function, apparent at the lowest coverage. The special case of non-interacting adsorption on two kinds of sites is resolved to yield the standard free energy of adsorption and the fraction of total surface associated with each kind of site.

Strongly interacting adsorption on a non-uniform surface usually shows the initial drop in the equilibrium function associated with surface non-uniformity, followed by an upward trend due to interaction. The two effects are occasionally so balanced that, except at the lowest coverage, constancy of the equilibrium function gives a false suggestion of ideality.

THE FORMATION OF COLLOIDAL GOLD

BY JOHN TURKEVICH, PETER C. STEVENSON AND J. HILLIER

Chemistry Department, Princeton University, and R.C.A. Laboratories, Princeton, New Jersey

Received March 2, 1953

An electron microscope study has been made of the process of reduction of gold chloride to colloidal gold. A method was found of producing gold of uniform size in the diameter range of 200–1500 Å. It was found that the particle size distribution curve of colloidal gold preparations is not an error curve but is determined by the kinetics of the process: the nucleation stage and the growth stage. A theory of nucleation is proposed based on the formation of auric ion–organic reducing agent complex which on attaining proper size decomposes to form a gold nucleus. This theory is shown to be in agreement with experiment. The exponential law of growth of the colloidal gold was also established.

The classical studies on the formation of colloidal gold have established that the process consisted of three stages, nucleation, growth and possible coagulation.[1–3] A thorough study of these stages was difficult since colloidal particles could not be seen and had to be characterized by indirect methods of observation. The development of the electron microscope with its resolution of 15 Å., has permitted a direct and detailed examination of colloidal gold preparations.[4] A survey of a number of gold sol preparations with the electron microscope showed the colloidal particles varied in size, shape and size distribution. A thorough study[5] in two gold sol systems (produced by gold chloride–sodium citrate and by gold chloride–hydroxylamine hydrochloride) showed that nucleation and growth stages do succeed each other, can be separated in time and therefore studied individually. Such a study has revealed that in a colloidal gold preparation, the average particle size, the per cent. deviation of the particle size from the average, and the very character of the distribution curve were determined by the kinetics of the two processes. The distribution curve was found to be not a Gaussian probability curve but of individuality and character determined by the nucleation process. The growth process merely modified the distribution curve by determining its position on the size coördinate and its spread in size.

Sodium Citrate Gold Sol.—The production of colloidal gold by reduction of gold chloride with sodium citrate was found to be particularly suited for the study of the nucleation process.

Ninety-five ml. of chloroauric acid solution (containing 5 mg. of Au) was heated to the boiling point and 5 ml. of 1% sodium citrate solution was added to the boiling solution with good stirring. After about a minute a very faint greyish pink or greyish blue tone appeared and in a period of five minutes it darkened to deep wine and red color. This method of production of colloidal gold sol is an adaptation of the one proposed by Hauser and Lynn.[6]

The particles were spherical in shape and had an average size of 200 Å. with a 12% deviation from the mean. The particle size distribution curve was skew in shape with the number of particles increasing gradually with size reaching a maximum at 200 Å. and then dropping rapidly. It was found that the time for completion of the reaction increased by a factor of two as the reaction temperature was lowered ten degrees. The uniformity of the preparation indicated that the nucleation process was virtually complete when the growth of the nuclei had become significant. The fact that one obtains a sharper distribution curve at lower temperatures and a smaller particle size could be interpreted to mean that the growth process has a higher temperature coefficient than the nucleation stage.

Growth Medium.—In order to study the nucleation process one must not only have an experimental criterion for the existence of nuclei but also means for determining their number as a function of time. The second system studied (hydroxylamine hydrochloride–gold chloride) was well suited to this purpose.

If equal volumes of gold chloride (0.01% Au) and 0.0275% hydroxylamine hydrochloride are mixed in a scrupulously clean apparatus, no production of metallic gold takes place for some hours. If gold nuclei are introduced an instantaneous reduction takes place.

The hydroxylamine hydrochloride–gold chloride solution is a pure growth medium. It can therefore be used as a criterion of the presence of nuclei. Any solution which produces colloidal gold instantaneously if added to this growth medium, must contain nuclei. Furthermore, it was shown that the particle size obtained by this growth process was given by the formula

$$D = D_0 \sqrt[3]{(W_{Au} + W_{Cl})/W_{Au}}$$

where

D = the diameter of the final gold particle
D_0 = diameter of the nuclei
W_{Au} = wt. of gold present as nuclei
W_{Cl} = wt. of gold present as gold chloride

The validity of this formula establishes the fact that the formation of nuclei is slight during the growth or development process. It also permits one to grow a given colloidal solution to any desired size in the colloidal range. A further observation was made that the per cent. deviation from the mean of the developed sol obtained by growth from another size, was the same as that of the original sol used as the nucleating material. This was taken to indicate that the law of growth was

(1) R. Zsigmondy and P. A. Thiessen, "Das Kolloid Gold," Akademische Verlag, Leipzig, 1925.

(2) H. Rinde, "The Distribution of Sizes of Colloidal Gold Sols Prepared According to the Nuclear Method," Uppsala, 1928.

(3) H. B. Weiser, "Inorganic Colloid Chemistry," Vol. 1, John Wiley and Sons, Inc., New York, N. Y., 1933.

(4) J. Turkevich and J. Hillier, *Anal. Chem.*, **21**, 475 (1949).

(5) J. Turkevich, P. C. Stevenson and J. Hillier, "Discussion of the Faraday Society on Size and Shape of Colloidal Particles," Leamington Spa, England, July, 1951.

(6) Hauser and Lynn, "Experiments in Colloid Chemistry," McGraw-Hill Book Co., New York, N. Y., 1940, p. 18.

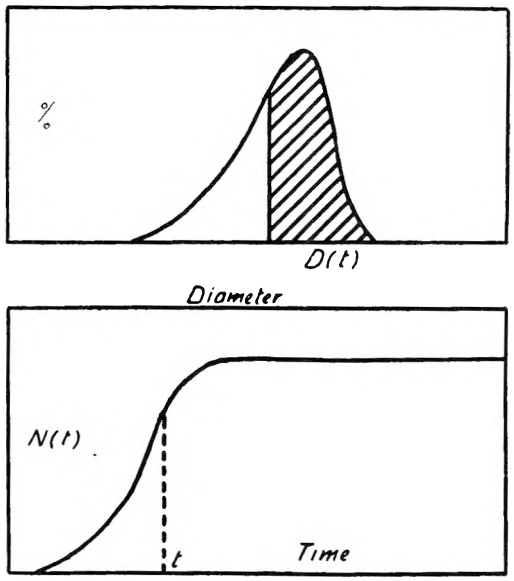

Fig. 1.—Relation between particle size distribution curve and the nucleation curve.

$$dD/dt = CD \qquad (1)$$

This method of development was an integral part of the technique of studying the nucleation process for, by it, nuclei difficult to observe directly could be brought into the range of observation of either the slit-ultramicroscope, the electron microscope or a nephelometer.

To check further the validity of the growth law, a sample of the 200 A. citrate gold sol was divided in half and one half was grown to form particles of 300 Å. The two halves were then mixed together and the particle size, determined with an electron microscope, indicated peaks at 200 and 300 Å. This specimen was again grown to double the size. Examination of this developed specimen showed that the two peaks have shifted at 400 to 600 Å., indicating that the ratio of the radii stays constant during growth. This was taken as further evidence for the exponential law of growth (1).

Chemical analyses indicated that the growth reaction involved the reaction of one mole of hydroxylamine with one of gold chloride suggesting the following equation for the reaction.

$$HAuCl_4 + NH_2OH \longrightarrow Au + 4HCl + NO$$

The reaction is first order with respect to auric ion, hydroxylamine and the hydroxyl ion.

The growth process was also studied in the sodium citrate–gold chloride system. It was found both by optical and electron microscopic methods that the rate of growth is again exponential, that the size of the nucleus is about 50 ± 5 Å. and that the process is zero order in the reagents.

Nucleation Process.—It is difficult to observe directly the nucleation stage in the formation of the gold sols. Preliminary evidence indicated that the nuclei are very small, of the order of 50 Å. or less in diameter, and that they had but a transitory existence in the early stages of the reaction. Two methods were used to determine the nucleation rate in the gold chloride–citrate system. In one method, samples were taken at different times from a nucleating solution and used to inoculate a definite amount of gold chloride–hydroxylamine solution. The size of the particles so developed was determined either by the slit-ultramicroscope, nephelometer, or electron microscope. The diameter of the developed particles is inversely proportional to the cube of the number of nuclei originally present. The details of this process have been reported elsewhere.[5]

In the second method, the kinetics of nucleation was determined from the particle size distribution curve of the *completed* preparation of the gold sol. This method is based on the assumption that the principal cause of the *spread in particle* size of a gold colloid is the *spread in time* in the nuclei formation. Particles formed early in the nucleation process begin to grow immediately so that in the final sol the particles that first formed and hence had the longest time to grow, attained the largest size. Nuclei which formed later attained smaller and smaller sizes corresponding to shorter and shorter growing times. The particle size distribution curve of a sol can be considered as a regularly distorted mirror image of the nucleation curve. A typical size distribution curve (upper curve) and a nucleation curve (lower curve) of a typical colloid are shown schematically in Fig. 1. The marked diameter D in the size distribution curve was chosen to be the diameter finally attained by those particles which had formed during nucleation at the time t, marked on the nucleation curve. The ordinate of the nucleation curve at t represents the total number of particles present in the unit volume of the solution at time t and consequently formed in time interval t. On the other hand, this is equal to the total number of particles with diameter greater than D, or

$$N(t) = \int_{D(t)}^{\infty} n(D)\, dD \qquad (2)$$

This definite integral is the shaded area under the distribution curve and is a function of t, the lower integration limit. The latter is given by the integrated form of the law of growth (1)

$$\log D\,(t) = \log D_0 + ct \qquad (3)$$

where

D is the diameter of the particle at time t
D_0 is the diameter of the nucleus
c is a constant

If one obtains from independent observations the values of D_0 and c one can derive from the particle size distribution curve the rate curve for nucleation.

Several implicit assumptions were made in this treatment. In the first place all nuclei were assumed to form with the same diameter; secondly the law of growth was assumed to hold for nuclei as for the larger particles and finally it is assumed that the addition of hydroxylamine hydrochloride in the development process stopped the nucleation instantaneously.

Kinetics of Nucleation.—An examination of the nucleation curves obtained under different conditions (Fig. 2) shows that they have four regions: an induction period region, an autoaccelerating portion, a "linear portion" and finally a decay portion.

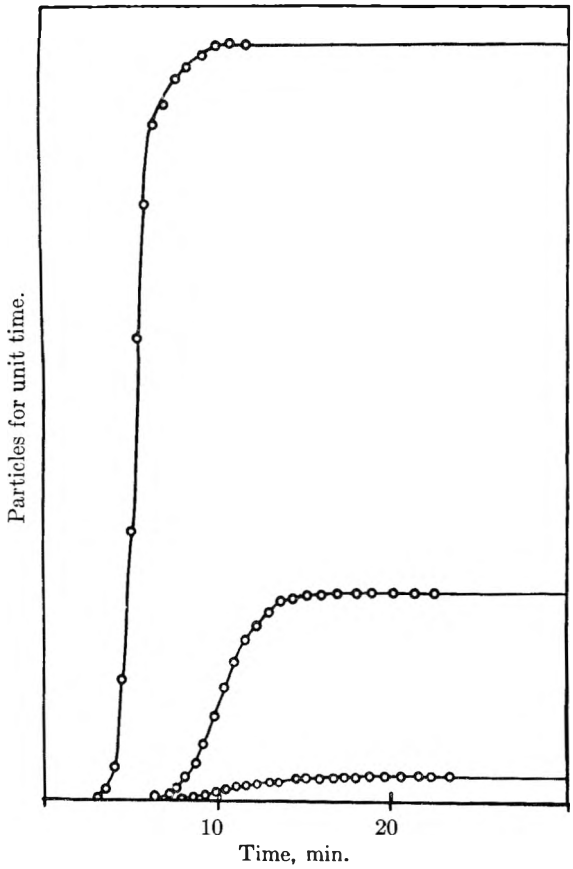

Fig. 2a.—Nucleation curves at various over-all concentrations of the gold chloride–sodium citrate system: upper curve, double standard concentration; middle curve, standard concentration; bottom curve, half standard concentration.

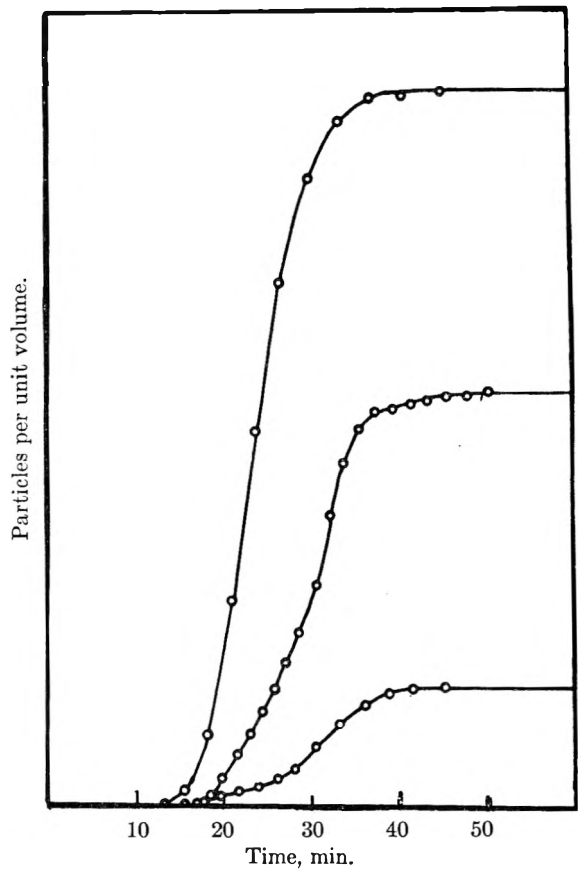

Fig. 2b.—Nucleation curves at various ratios of sodium citrate to gold chloride: upper curve, one-half the citrate concentration; middle curve, one-fifth citrate concentration; bottom curve, one-tenth of citrate concentration.

The induction period can best be studied by nephelometric examination of the developed samples. Its duration decreases with increase in temperature, the approximate induction time being 26 minutes at 15°, 5 minutes at 30°, 3 minutes at 39° and 2 minutes at 49°, giving an approximate activation energy of 10 kcal./mole. The process responsible for the induction period seems to be chemical in nature and may be interpreted as a removal of an inhibitor for the nucleation process. However, a study of the chemistry of the reduction of gold chloride with sodium citrate indicates that the cause of the induction is to be found in the oxidation of the citrate ion to acetonedicarboxylate ion. For when the latter is prepared by dehydrating citric acid with sulfuric acid, purified by crystallization and then used for the preparation of a gold sol, the induction period is less than one minute. This is taken to indicate that the induction period was associated with the production of a sufficient number of acetonedicarboxylate ions for the nucleating process.

The autoaccelerating portion of the curve can be interpreted to show that in this portion the rate of production of acetonedicarboxylate is faster than its utilization in the nucleation process.

The "linear portion" of the nucleation curve in the gold chloride–citrate system can best be understood in terms of the behavior of the gold chloride–acetonedecarboxylate system. The gold sol formed by the latter reagents has a particle size distribution curve different from that obtained with the citrate as a reducing agent. This can be used to construct a nucleation curve (Fig. 3) whose appearance is very similar to the latter portions of the nucleation curve of the gold chloride–citrate system. Furthermore if one replots the nucleation curve as log $(N_\infty - N_t)$ *vs.* time where N_∞ is the total number of nuclei formed at infinite time and N_t is the number of nuclei formed at time t, one gets a straight line, indicating that the nuclei are formed by a unimolecular decomposition of a precursor. To isolate the percursor of these nuclei the gold chloride–citrate system at its pale-grey stage was passed through the anion-exchange resin Amberlite 1R-4. The emergent solution had not changed in color but had lost its power to liberate iodine from iodide solutions, indicating that the auric ion had been removed. It did, however, produce a colloid when introduced into the growth medium. Electron microscopic examination of the precursor solution showed that it contained 200 Å. diffuse particles of irregular shape. These seemed to break up under bombardment of the electron beam in the microscope to form smaller denser particles suggesting the break-up of an organic–metallic polymer.

The slope of the last portion of the nucleation curve decreases rapidly with time suggesting that

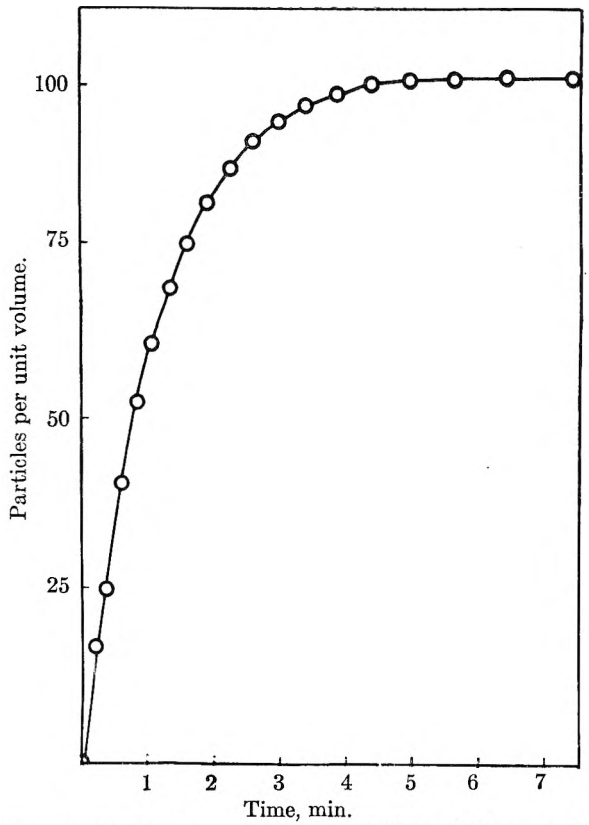

Fig. 3.—Nucleation curves for colloidal gold from gold chloride and sodium acetonedicarboxylate.

one of the reagents is exhausted. Chemical analysis on the other hand shows that at the end of the nucleation less than 5% of both the citrate and the gold have been used up. The explanation of cessation of nucleation at this point is just as important as its origin. Again it may be found in the acetonedicarboxylate ion. To form a nucleus many acetonedicarboxylate ions must condense with many auric ions to produce a polymer of such a size that when the polymer decomposes it will produce a stable gold particle. Since the nucleus is about 40 Å. in diameter, about 1000 gold chloride molecules and a similar number of acetonedicarboxylate ions are involved in the nucleus formation. On the other hand, the growth process undoubtedly involves a small number of the same reagents adsorbed on the surface of the existing nuclei. Thus the deceleration of the nucleation process and its final disappearance is not due to the exhaustion of the original reagents but to the competitive effect of the growth process.

Mechanism of Nucleation in Gold Sols.—On the basis of the above experiments, we wish to advance the following "organizer" mechanism for the formation of a nucleus. The fundamental difficulty in building up a nucleus is the accumulation of a sufficiently large local concentration of atoms to produce a particle whose size is greater than just demanded by the stability of the particle. Its size must be sufficiently great also to permit growth. The fluctuation theory describes the production of such large local concentrations as being a rare but significant event and due to the statistical nature of physical events. The same result may be attained by postulating that the nucleating agents gradually build up a *chemical* complex between themselves and gold ions, organizing the latter into a macromolecule (precursor of the nucleus). When the size of the macromolecular inorganic–organic polymer is sufficiently great, it will undergo a molecular rearrangement to produce the metal nucleus and oxidation products of the organizer.

THE REACTION OF HYDROGEN AND OXYGEN ON SUBMERGED PLATINUM ELECTRODE CATALYSTS. I. EFFECT OF STIRRING, TEMPERATURE AND ELECTRIC POLARIZATION[1]

BY M. J. JONCICH[2] AND NORMAN HACKERMAN

Defense Research Laboratory and Department of Chemistry, The University of Texas, Austin, Texas

Received March 2, 1953

Hydrogen and oxygen, dissolved in a stirred solution of dilute sulfuric acid, combine to form water on the surface of a submerged platinum catalyst. The rate of this reaction was studied as a function of the stirring rate, temperature and electric potential applied to the catalyst. Cathodic polarization of the catalyst was ineffective in changing the reaction rate. Anodic polarization, using a platinized platinum anode and a smooth platinum wire cathode, caused a periodic change in the reaction rate as a function of time. The rate was increased by a.c. polarization at frequencies < 10 c.p.s.; the highest rate being observed at the lowest frequency used (0.01 c.p.s.) and at a current of approximately 1 milliampere. Periodic behavior was observed for platinum and palladium; but not for rhodium and iridium. A mechanism, consistent with the experimental data was postulated in which the periodic change in the rate on anodic polarization was ascribed to periodic buildup and decomposition of oxide on the catalyst surface.

Introduction

Paal and Hartmann[3] found that hydrogen and oxygen, dissolved in aqueous solution would combine on the surface of colloidal platinum or palladium. Hofmann and co-workers[4] showed that all the platinum group metals were effective catalysts for the reaction. The greatest portion of the work was carried out on the metals; platinum, palladium and iridium, and the results were interpreted in terms of an electrochemical mechanism.

It was felt that the catalytic aspects of this reaction should be studied further, particularly under conditions wherein either an anodic, cathodic, or alternating potential was impressed on the catalyst. It was also desirable to study it over long periods of time, both under polarizing conditions and without polarization. The catalyst used for most of the experiments was platinized platinum whose surface area (at the beginning of the experiments) was known from gas adsorption measurements. Platinum was also used in the form of smooth wire, as were palladium, rhodium and iridium.

Experimental

A catalytic reaction system was designed and built which has several advantages over more conventional systems. This system has been described in detail elsewhere[5] but a brief discussion of its characteristics is desirable here. Hydrogen and oxygen, generated in one portion of the system by electrolysis, were recombined on a submerged catalyst in another portion of the system at a rate equal to the rate of their generation. The rates were equalized by keeping the pressure of the system constant, using a metal bellows with an electronic current regulator. The electrolysis current, which is directly porportional to the rate of the reaction, was recorded automatically. This system makes possible the study of very slow reaction rates over long periods of time using completely automatic methods.

The solution about the catalyst (always 0.01 *N* H_2SO_4) was stirred vigorously by a magnetic device. This also assured saturation of the solution with hydrogen and oxygen. The system was sensitive to pressure changes of 0.3 mm. H_2O so it was necessary to use an air-bath whose temperature was kept constant to ±0.01°. The total pressure of the system in all cases was 740 mm. Hg and consisted of the partial pressures of the stoichiometric mixture of hydrogen and oxygen plus the saturation water vapor pressure.

Preparation of Catalysts.—The platinized platinum catalysts were prepared by electrodeposition from a solution containing 2.42% H_2PtCl_6 and 0.001% $Pb(OAc)_2$. Solutions of H_2PtCl_6 purified by prolonged electrolysis yielded deposits which were light in color and non-adherent. Addition of trace amounts of lead produced deposits which were black and adherent. These observations are in agreement with those of MacNevin and Levitsky.[6]

The cathode during electrodeposition was a 5-cm. length of platinum wire (0.091 cm. diam.) having a total apparent area of 1.44 cm.^{2}. The anode was a cylinder of platinum gauze 5 cm. in diameter and 5 cm. in length. This arrangement, rather than 2 parallel plates, was used to minimize edge effects. The electrodeposits were prepared at 20.9 amp./dm.^{2} (apparent) for 120–130 minutes.

The surface areas of the platinized electrode catalysts were measured with krypton at −195.8°. This was needed to determine the reproducibility of the method of preparation and to allow calculation of true current density in the polarization experiments. After plating 30 minutes specific surface values of 0.89 and 1.47 m.^{2}/g. were obtained in two runs, while after plating 120 minutes values of 0.39 and 0.68 m.^{2}/g. were obtained. During these experiments, extreme precautions were taken to keep the conditions constant. Although the reproducibility was not good, it can be seen that the shorter the plating time, the higher the specific surface of the deposit.

Stirring Rate and Temperature Effects.—The catalyst used was a platinized platinum electrode whose total area as determined by krypton adsorption was 322 cm.^{2}. The total weight of platinum black was 0.0363 g. A piece of bright platinum wire was placed parallel and 0.5 cm. away from the platinized piece. The two electrodes were introduced into the catalytic reaction system through a ground-glass joint and the system brought to pressure and temperature equilibrium. The electrolysis cell current was recorded by an Esterline-Angus Recorder as a function of time while the stirring rate and temperature were varied independently. Precise measurements of the rate could be obtained by cutting the recording paper along the ink line and weighing it. Each gram of paper corresponded to 8.14 ± 0.08 coulombs.

The catalytic activity was determined at stirring rates of 0, 100, 200, 300, 400, 500 and 600 r.p.m. An optimum obtained at 400 r.p.m. and further increase of the stirring rate produced no measurable increase in the speed of the reaction. A synchronous motor rotating at 520 r.p.m. was used for the remainder of the experiments.

The reaction was allowed to proceed for 10 to 48 hours at 29.45, 34.37, 39.65 and 48.20°, respectively. The rate remained constant to within 5% in each case. Corrections were made for changes in gas solubility and in water vapor pressure, and the energy of activation calculated to be 11,000 cal./mole.

(1) Resulting from research done under Bureau of Ordnance Research and Development Contract NOrd-10639.

(2) Department of Chemistry, University of Tennessee, Knoxville, Tenn. This paper is based on a dissertation presented in partial fulfillment of the degree of Doctor of Philosophy.

(3) C. Paal and W. Hartmann, *J. prakt. Chem.*, **80**, 337 (1909); **93**, 106 (1916).

(4) K. A. Hofmann, *et al.*, *Ber.*, **49**, 2369 (1916); **53B**, 298 (1920); **55B**, 573, 1265 (1922); **56B**, 1165 (1923); **57B**, 1969 (1924).

(5) K. W. Hannah, M. J. Joncich, and N. Hackerman, *Rev. Sci. Instruments*, in press.

(6) W. M. MacNevin and M. Levitsky, *Anal. Chem.*, **24**, 973 (1952).

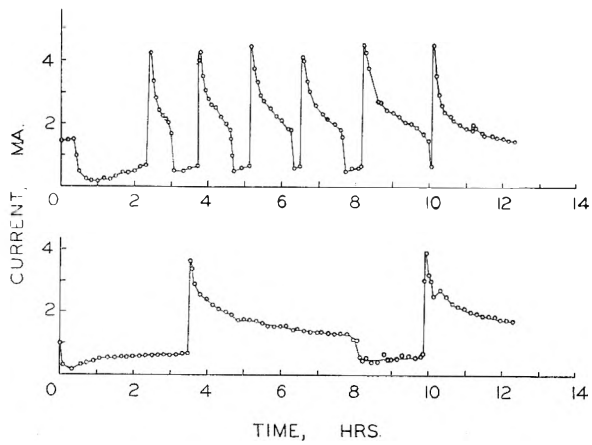

Fig. 1.—Length of induction period as a function of intensity of anodic polarization: upper, 1.0 ma.; lower, 0.5 ma.

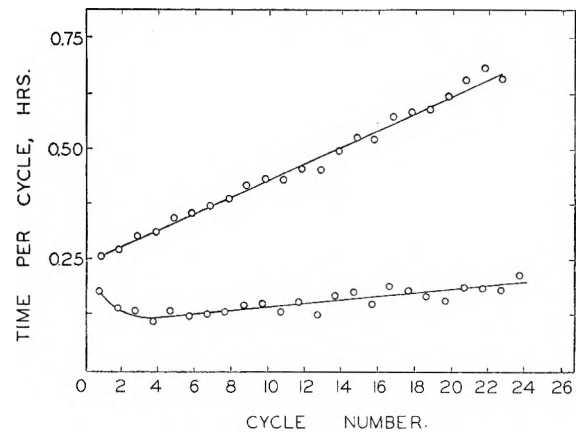

Fig. 2.—Upper curve, length of activation periods as a function of cycle number; lower curve, time between activation periods as a function of cycle number.

Anodic Polarization Effect.—Polarization was brought about by passing current between the platinized electrode (anode) and the bright platinum electrode (cathode). The shiny electrode is considered to be catalytically inert since its area is negligible in comparison with the platinized electrode. The polarizing current came from a series arrangement of four 45-volt batteries. Variable resistors in series with the batteries provided for current adjustment as measured by a milliameter. This arrangement provided a constant current source since a large voltage supply and a large resistance was used.

A series of determinations on the effect of anodic polarization were carried out. Anodic polarization of 0.5 ma. was applied initially. After 30 minutes the polarizing current was increased to 1.0 ma. and maintained constant until it was cut off after 6 hours. After a total polarization time of 2 hours, a sudden increase in the electrolysis cell current was observed. The activity then decreased and a periodic change in activity occurred until the polarization was discontinued. Although the electrolysis current changed periodically between 3 and 1 ma., the polarization current was not changed. After the fifth period of increased activity, the anodic polarization was discontinued. The activity of the catalyst rose immediately to a value almost as high as the previous maximum points of activity, and then gradually decayed to its original prepolarization value.

The effect produced by a short-lived and vigorous anodic polarization, 15 minutes at 5 ma., of the catalyst was determined. Hydrogen and oxygen were liberated at the electrodes. Polarization was then discontinued and the catalyst activity measured for the next 20 hours. The activity rapidly went through a maximum at 4.2 ma., then gradually decayed to 1.5 ma.

A second low polarization was carried out but now the 0.5 ma. stage was eliminated and 1.0 ma. was applied initially. Immediately upon polarization the activity decreased rapidly to zero. Stopping the polarization at this point caused the activity to increase rapidly. Upon further polarization, the time required for the activity to decrease to zero increased, until after three such cycles of alternate polarization and non-polarization, the reaction proceeded without interruption of the polarization. The typical periodic change in activity was then observed. These and other experiments indicate that the catalyst must become gradually conditioned to a polarization treatment if the polarizing current is of the order of 1.0 ma. or larger.

Although the electrolysis cell current decreased to zero for high initial polarization, this does not necessarily mean that the catalytic activity was zero in these instances, since current through the electrodes in the reaction cell may be used for production of hydrogen and oxygen. If this is true, the curves should be displaced upward on polarization by the amount of the polarizing current.[7]

A period of induction, dependent upon the magnitude of the polarizing current, was always observed before onset of periodicity. This effect, as well as the periodic phenomenon, is illustrated in Fig. 1; the upper curve shows the results obtained with 1.0 ma. polarization and the lower with 0.5 ma. The induction periods were 2 hours and 3.5 hours, respectively. In this case a polarizing current of 1.0 ma. did not decrease the electrolysis cell current to zero as before, indicating that an electrode which had been polarized previously retained some effect of this polarization treatment.

Another point illustrated by Fig. 1 is that the periods of increased activity become longer as the polarizing current is decreased. In the upper curve the last period of activation was of 2 hours duration, while in the lower curve it was 4.6 hours for the first period of activation. From these and other data, the inverse proportionality of the length of the periods and the magnitude of the polarizing current was firmly established. In Fig. 1 the catalytic activity is given in terms of the electrolysis cell current required to keep the pressure constant. A current value of 1 ma., for example, corresponds to a recombination rate of 1.74×10^{-4} cc./sec. of the stoichiometric mixture of hydrogen and oxygen at standard conditions.

Whenever periodic behavior was manifest, the periods of increased activity, for a given polarizing current, increased in length with time. Further, upon prolonged polarization the curves became erratic in that fluctuations within a period of activation were observed, *i.e.*, a secondary periodicity.

Figure 2 shows the change in periods of activation as the reaction proceeds. Each complete period is designated as a cycle, which is resolved into two parts (a) the portion corresponding to the time of increased activity (Fig. 2, upper) and (b) the time between the periods of increased activity (Fig. 2, lower). The anodic polarization in this case was 2.0 ma.; but similar curves were obtained using higher and lower polarization values. Upon increasing the polarization, both curves are displaced downward, the slopes tending to smaller values. On decreasing polarization both curves are displaced upward, with an evident increase in the slope of both lines. The effect on these factors of increasing the temperature from 38.0 to 43.1° was determined qualitatively only since they vary with time and cycle number. The data indicate that the time between activation periods is independent of temperature and that the time of activation is reduced as the temperature is increased.

The potential between the platinized electrode and the inert platinum electrode was recorded in some of these experiments. Although a constant current source was used to provide the polarizing current, there was a periodic change in potential between the two electrodes, which, on the time scale, corresponded exactly to the observed periodic changes in the catalyst activity.

Cathodic Polarization Effect.—The effect of cathodic polarization of the platinized electrode was less significant than that of anodic polarization, and in many cases was barely perceptible. With cathodic polarization of 1.0 to 3.0 ma. the catalytic activity usually decreased slightly and became irregular. No regular periodicity such as observed with anodic polarization was detected in this current range. If the catalyst was anodically polarized shortly before application of the cathodic polarization, a slight activation lasting

(7) Further, it should be pointed out that the curves originally obtained on the recorder were continuous and that points shown on the curve serve merely as an aid in transcription of the original curve.

several minutes was observed. The activity then rapidly decayed to its original unpolarized value.

At 0.3 ma. cathodic polarization, a periodic fluctuation of the voltage between 0.43 and 0.08 v. was observed. The electrolysis cell current did not undergo these fluctuations, but increased by 0.2 ma. from the constant, unpolarized value, and remained constant at this value during the entire course of the cathodic polarization. Upon discontinuing the cathodic polarization, the electrolysis cell current decreased to its original value. Although many different cathodic polarization currents were used, this is the only case in which any periodicity was detected.

A.C. Polarization Effect.—A Hewlett-Packard, low frequency, rectangular wave generator was used as the current source. The effect of a.c. polarization of the platinized and inert electrodes at frequencies ranging from 100 to 0.01 c.p.s. and currents of 0.50 to 5.0 ma. was studied. Starting with a catalyst whose initial unpolarized activity corresponded to an electrolysis current of 0.9 ma., it was found that a.c. polarization in the above range caused either an increase in activity or had no effect, depending upon the frequency and current values. The greatest effect was observed at a current of 1.0 ma. and a frequency of 0.01 c.p.s. In this case the electrolysis cell current was increased from 0.9 to 2.0 ma., corresponding to more than a 100% increase in catalytic activity. At either lower or higher current values, the activity decreased. Increasing the frequency from this value also caused a decrease in the activity. It is possible that lower frequency values would be even more effective; but 0.01 c.p.s. was the lower limit of the instrument used.

Potential-Current Relationships.—The potential between the inert platinum electrode and the catalyst was determined as a function of the current passing through these two electrodes. The conditions were maintained the same as during the catalyzed reaction rate determinations. The electrolysis cell current was discontinued during the short time required to carry out each experiment. These measurements were repeated many times and in each case a hysteresis effect was observed. Although the curves were not completely reproducible, the deviations were small and consisted principally in differences in the size of the hysteresis loops. This was dependent upon the time spent on each current value. Figure 3 shows this effect on anodic treatment. The time spent on each point was 4 minutes. The curves were obtained by starting at the lowest current value, increasing the current stepwise to 8.0 ma. and then decreasing the current in the same manner to its lowest value again. Cathodic treatment also gave hysteresis effects.

Smooth Catalysts.—A series of experiments was carried out in which both electrodes in the reaction system were smooth platinum wires, all other conditions being the same as before. Without polarization, the activity was roughly a third of that previously observed for the platinized electrode. At a polarizing current of 0.10 ma., periodicity was observed in the potential between the two electrodes. The periods were much shorter than those observed previously, the average being 1.0 minute. The potential values fluctuated between 0.5 and 0.8 v. Although there was a tendency toward periodicity in the electrolysis cell current, it was not clear-cut. This was undoubtedly because of the slow response time of the current control system in comparison to the high frequency of the periodicity. The highest electrolysis cell current value obtained was 1.1 ma.

Experiments were also carried out using smooth wires of rhodium, iridium and palladium. Periodicity similar to that with platinum was observed with palladium. There was no periodicity either in the electrolysis cell current or in the potential value with rhodium and iridium.

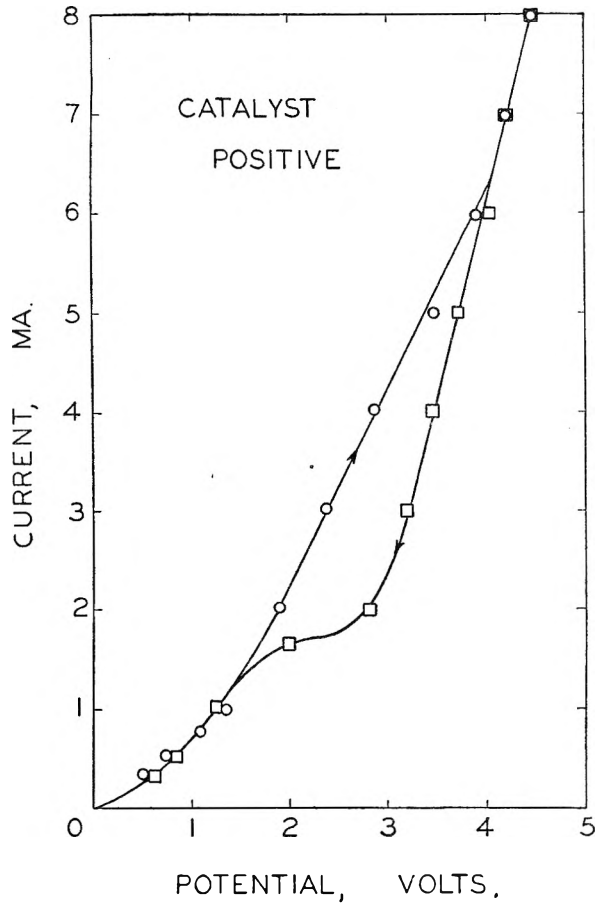

Fig. 3.—Polarizing current as a function of polarizing voltage.

Discussion

The non-dependence of reaction rate on stirring rate in the range used and the calculated energy of activation indicates that the oxidation was not diffusion controlled.

The most interesting results were the marked increases in catalytic activity obtained on electrolytic polarization. The unexpected change in reaction rate on anodic polarization is real and not a phenomenon peculiar to the apparatus. Depolarization by oxygen at the cathode and by hydrogen at the anode was considered, and it was concluded from calculations similar to those made by Hickling and Salt[8] and from these experimental results that this factor was of importance only at the lowest current density values. The inability of an electrochemical mechanism to explain the results led to postulation of a catalytic mechanism.

Periodic change in reaction rates are not rare[9] and in systems containing metals it is usually associated with a metastable form of the surface. The evidence obtained on anodic polarization of the catalyst indicates that periodicity is caused by build-up and breakdown of a surface film. The nature of this film is implied from the work carried out on the polarization of platinum electrodes. El Wakkad and Emara[10] state that a platinum electrode brought from the potential of hydrogen evolution to that of oxygen evolution first forms PtO on its surface, then PtO_2, and finally evolves oxygen. The PtO_2 is unstable, decomposing to PtO.

With this as a basis, it is assumed that a critical mixture of PtO and PtO_2 obtains which is more active as a catalyst for this reaction than either of the two oxides alone. The work of Selwood and his

(8) A. Hickling and P. W. Salt, *Trans. Faraday Soc.*, **37**, 319 (1941).

(9) E. S. Hedges and J. E. Myers, "The Problem of Physico-Chemical Periodicity," E. Arnold and Co., London, 1926.

(10) S. E. S. El Wakkad and S. H. Emara, *J. Chem. Soc.*, 461 (1952)

co-workers[11,12] shows that the activity of a supported oxide catalyst may be critically dependent upon the percentage of metal. It is postulated that when the catalyst is anodically polarized, its activity is not altered appreciably until a critical composition of PtO and PtO_2 is obtained on the surface. When this stage is reached, the activity increases suddenly. Continued anodic polarization causes the oxides to pass this optimum composition, *i.e.*, to one of greater PtO_2 content. The rate then decreases proportionally to the rate of formation of additional PtO_2, and therefore to the magnitude of the polarizing current. The sharp decrease in activity, terminating the activated period, then corresponds to the decomposition of the PtO_2. The time between activation periods corresponds to that required to reach the optimum composition again, and the whole cycle is then repeated periodically.

These ideas are consistent with the experimental data. With increased anodic polarization the duration of the periods of activation decreased, indicating that the surface passed through the optimum catalytic condition at rates which were directly proportional to the magnitude of the polarizing current. The time between periods of activation was much shorter than the induction period, suggesting that some oxide was always present during those intervals. The induction period should be the time required for the platinum surface to become oxidized to the critical composition of PtO and PtO_2 and should be inversely proportional to the magnitude of the polarizing current, as was observed.

The increase in length of activation periods as a function of time may be explained by roughening of the catalyst surface as reaction proceeded. Since the polarizing current remained constant, a longer time was required to complete the cycle. Roughening of the surface has been observed for the gaseous reaction of hydrogen and oxygen on platinum[13] and on copper.[14] This idea is substantiated by the fact that low surface area platinum wires exhibited periodic behavior with much shorter activation periods than those observed for the platinized electrodes.

The cause of the secondary periodicity on prolonged anodic polarization is not obvious. Probably some of the oxide film sloughed off because of the vigorous stirring and the secondary periodicity arose while this part of the surface was "repaired" and brought to the same condition as the rest. The longer the polarization, the greater the surface roughening and the greater the number of sites which needed repairing.

The result obtained upon drastic, short-lived anodic polarization is consistent with these postulates. It would be expected that such treatment would produce a surface with more than the optimum amount of PtO_2. Upon discontinuation of the polarization, decomposition of the PtO_2 took place, the oxide composition passing through the optimum state during this process. The maximum in activity observed in the initial part of the experiment followed by a decrease in activity substantiates this hypothesis.

The effect of temperature change on periodicity indicates (a) that the time required to reach the optimum condition of the catalyst is dependent only on the magnitude of the polarizing current, and (b) that PtO_2 decomposition is accelerated by temperature increase, making the activated periods of shorter duration.

The fact that true periodic behavior was observed in the case of platinum and palladium, but not for rhodium and iridium may be related to some of Hofmann's work.[4] He found that pretreatment of iridium with hydrogen or oxygen did not change its catalytic activity, while platinum and palladium when treated with oxygen showed increased activity. The latter exhibit periodicity, which in this investigation has been attributed to an oxide film on the surface. Thus it is suggested that iridium and rhodium oxides are not better catalysts than their metals for this reaction.

There does not seem to be any change in the catalytic activity that can be attributed to cathodic polarization. However, upon cathodic polarization of the platinized electrode, the inert electrode is made anodic and slight fluctuations in activity and slight increase in total activity may be caused by this.

The potential *vs.* current hysteresis (Fig. 3) is not unique to this research. Bockris and Azzam[15] recently reported a very similar curve. The Tafel equation relating overpotential and current is different for an oxide-covered platinum electrode and for a "clean" platinum electrode.[16] Thus, the curve obtained on increasing the current represents the variation of potential and current for a platinum surface initially free of oxide, while the descending curve shows these factors for an oxide coated platinum electrode. On increasing the current again, the results coincided with those previously obtained on going down the curve. The positions of the loops correspond approximately to the current values at which periodicity was observed.

Since on a.c. polarization, a frequency of 10 c.p.s. or greater did not affect the activity, it is concluded that activation takes longer than 0.1 second. The significance of the maximum activity observed at approximately 1.0 ma. a.c. polarization is not yet apparent.

There is an increasing tendency, in the current literature, to attribute the cause of many of the phenomena occurring in electrochemical systems to impurities. In this work the solutions were pre-electrolyzed between auxiliary electrodes at least 24 hours, as a precaution against impurities. The introduction of a fresh catalyst into a system containing solutions pre-electrolyzed for several weeks gave the same results as had been observed previously. Thus, either impurities were not present or, if present, they were without appreciable effect.

One other possibility was explored, namely, that

(11) P. W. Selwood, "Advances in Catalysis," Vol. 3, Academic Press, Inc., New York, N. Y., 1951, p. 27-106.

(12) J. Mooi and P. W. Selwood, *J. Am. Chem. Soc.*, **74**, 1750 (1952).

(13) I. Langmuir, *ibid.*, **40**, 1361 (1918).

(14) H. Leidheiser and A. T. Gwathmey, *ibid.*, **70**, 1200 (1948).

(15) J. O'M. Bockris and A. H. Azzam, *Trans. Faraday Soc.*, **48**, 145 (1952).

(16) F. Tödt, *Z. Elektrochem.*, **54**, 485 (1950).

chemisorbed oxygen, rather than a stoichiometric oxide, was the cause of the phenomena described. However, to date this approach has not lent itself to formulation of a satisfactory explanation.

STUDIES ON SILICIC ACID GELS. XVII. DIALYSIS OF THE GEL MIXTURE AND OF THE GELS

BY CHARLES B. HURD, MARVIN D. SMITH, FRANK WITZEL AND ARTHUR C. GLAMM, JR.

Contribution from the Butterfield Chemical Laboratory, Union College, Schenectady, N. Y.

Received March 2, 1935

Dialysis of hydrosols, made by mixing solutions of sodium silicate and acetic acid, shows that simpler silicic acids predominate at first. As the sol ages, more complex materials form. The simpler molecules are able to diffuse through collodion membranes. Withdrawal of simpler silicic acids by dialysis apparently disturbs the equilibrium, resulting in the formation of more of the simpler molecules by hydrolysis of the complex polysilicic acid. This is the reverse of the reaction which results in gel formation. Even in a gel or an old hydrosol, the existence of simpler molecules in a type of equilibrium appears to have been demonstrated. A discussion of the theory of condensation of silicic acids and of the reverse process is given.

Introduction

Dialysis has been used to purify hydrosols of silicic acid or hydrous silica since the pioneer work of Graham.[1] Where hydrosols have been made by mixing solutions of sodium silicate and acid, dialysis has removed excess acid and sodium salts. Rate of dialysis and amount of silica in the dialyzate were studied by Zsigmondy[2,3] and by others.

It has been concluded that sizable amounts of silica can dialyze from freshly prepared sols, but that this decreases with age of the hydrosol and that no silica can dialyze out as the sol approaches the setting time. This has been explained by particle size.

Remembering that precipitates of hydrous silica and silicic acid gel are soluble in sodium hydroxide and that, furthermore, most chemical reactions are reversible, Hurd and Merz[4] have studied the dialyzate with particular attention to low concentrations of silica. They found that the concentration of silica in the dialyzate, resulting from dialysis, for a fixed time, of samples drawn successively from a given hydrosol, decreased with age of the hydrosol. It never became zero but approached a constant value as hydrosols neared the setting point. The same was true if the sol set to a gel and the gel was broken up and placed in the dialysis sack.

In their work, they used sols of sufficiently short setting time so that the time used for dialysis permitted actual changes in the sol. We report here experiments with sols of such long setting time that changes in the sol samples during dialysis can be neglected. We also report dialysis experiments here involving such long periods that an equilibrium must be established inside and outside the dialysis sack.

Experimental

Hydrosols were prepared by pouring sodium silicate solutions into acid solutions and mixing thoroughly by pouring back and forth.

Silicate solutions were prepared by dilution of E brand silicate (Philadelphia Quartz Company), analyzed by titration with standard H_2SO_4 and methyl orange. The SiO_2 content was obtained from the NaOH equivalent and Na_2O: SiO_2 ratio, also gravimetrically and colorimetrically. The solutions used were approximately equivalent to 1.0 *N* NaOH.

Silica in the dialyzate was determined gravimetrically and, especially for low concentrations, colorimetrically. Essentially, Winkler's[5] method was used, forming the yellow silicomolybdate color, with K_2CrO_4 solutions as standards. We found it reliable. In the early part of the work (Smith), only gravimetric methods were used, but in the later parts (Witzel and Glamm) both methods were used.

Dialysis sacks were made of collodion. Six-inch test-tubes were filled with U.S.P. Collodion, Code No. 1611, General Chemical Company, drained and allowed to dry for 15 minutes. The tube was filled with distilled water for 10 minutes, the sacks removed and kept under distilled water. Only for Table IV was the drying time for the sacks varied.

The silicate and acid solutions were measured out, enough for all of the samples to be withdrawn. They were thermostated to give correct temperature. The time of mixing was taken, called 0 time for age of the sol. Sols were kept covered in the thermostat. Long setting mixtures, 100 hours or more, were used.

Measurements of *p*H were by the quinhydrone method as previously described.[6]

Samples of 10 ml. were withdrawn at definite time intervals after mixing, placed in collodion sacks just removed from distilled water. The sacks were tied and suspended in an 8-inch test-tube for 10 minutes in 50 ml. of the dialyzing solution. This had the same concentration of sodium acetate and acetic acid as the sol inside the sack. The only difference lay in the silica or silicic acid.

Results

It was necessary to know whether use of a collodion sack rendered it less permeable, in other words, did the pores become clogged as dialysis proceeded. Tests showed no tendency for clogging, as follows, with one example.

Three samples of 10 ml. each, of a mixture with setting time 168 hours, were placed in identical collodion sacks at 21 hours. The sacks were hung in stoppered containers with 50 ml. of dialyzing solution. At 50 hours, 5 ml. of the first sample was withdrawn, placed in a fresh sack, in 50 ml. of fresh dialyzing solution. The original sack still containing 5 ml. and already used 29 hours, was placed in 50 ml. of fresh dialyzing solution. Both were run 43 hours more. The dialyzate for each was analyzed. This is sample 1 in Table I. Sample 2 ran for 308 hours, was divided and the two parts were dialyzed 76 hours more before analysis. Sample 3 ran 838 hours, was divided and ran 68 hours more before the two parts were analyzed.

These are typical data. They show that the pores of the collodion sacks do not become clogged during dialysis of the silicic acid sol.

Solutions kept in glass containers dissolve very small amounts of silica or silicates. Since we have used very

(1) T. Graham, *Ann. Physik*, **190**, 187 (1861); *Ann. Chem. Pharm.*, **121**, 1 (1862).

(2) R. Zsigmondy, *Kolloid-Z.*, **8**, 55 (1911).

(3) R. Zsigmondy and R. Heyer, *Z. anorg. Chem.*, **68**, 169 (1910).

(4) C. B. Hurd and P. L. Merz, *J. Am. Chem. Soc.*, **68**, 61 (1946).

(5) L. W. Winkler, *Z. anorg. Chem.*, **27**, 511 (1914).

(6) C. B. Hurd and R. L. Griffeth, THIS JOURNAL, **39**, 1155 (1935).

TABLE I

TESTS SHOWING THAT COLLODION SACKS DO NOT CLOG

Sample	Amount SiO_2 through original sack	Amount SiO_2 through new sack
1	0.0050	0.0052
2	.0029	.0028
3	.0029	.0025

sensitive methods, this appeared important. Table II shows the result of leaving the sodium acetate–acetic acid solution in contact with glassware for various lengths of time.

TABLE II

SILICA PRESENT IN SOLUTIONS WHICH HAVE NOT BEEN IN CONTACT WITH GEL MIXTURES

Time of exposure	SiO_2 in p.p.m.
10 min.	154
1 hr.	154
70 hr.	152
170 hr.	157

This shows an average of 155 p.p.m. SiO_2 in the solutions which have been in contact with glassware. It may have been in the sodium acetate, acetic acid or water. Since it was essentially constant, as shown by Table II, it was subtracted from all results for SiO_2, giving figures which follow in this paper.

Numerous runs were made to study dialysis of the silicic acid hydrosols, in terms of the age of the sol. A typical run gave the graph of Fig. 1. The mixture set in 288 hours. Temperature was 20°. Samples of 10 ml. were withdrawn from the mixture at definite time intervals since the sol was produced. Time of dialysis through collodion sacks into 50 ml. of dialysis solution, containing the same concentration of sodium acetate and acetic acid as were present in the gel mixture, was 10 minutes. The abscissa is the age of the sol before the sample was withdrawn.

As the graph shows, the amount of SiO_2 in whatever form, dialyzing through the collodion membrane in 10 minutes, decreased rapidly as the gel mixture aged before the sample was withdrawn for dialysis. This was expected. The curve reached a value of about 505 p.p.m. SiO_2 at the time the mixture set, 288 hours from the time it was mixed. Up to this time, 10 samples, each of 10 ml., had been withdrawn from the original mixture for dialysis, each in a fresh sack.

All dialyses following were from sample 10 in the same sack since the gel had set. It was kept, between dialyses, in fresh samples of 50 ml. dialyzing solution. Intervals between the 10-minute dialyzing runs, in fresh 50 ml. of dialyzing solutions, were 20 hours or more. Analyses of the 50-ml. solutions for 10-minute dialyses showed the SiO_2 dropping as low as 325 p.p.m. at 500 hours, but rising until a value of 875 p.p.m. was reached at 2800 hours, where the run was stopped. This is more than 100 days.

The 50-ml. solutions in which the sack was kept between the 10-minute runs after the 428th hour were analyzed. The long duration of exposure should have made these reach equilibrium with the SiO_2 inside the sack. The final value appears to be 0.00426 g. of SiO_2 per ml. or 4260 p.p.m. Obviously this is the summation of all SiO_2 present.

An interesting fact, noted in each run, was that the concentration of the SiO_2 in the dialyzate both for the 10-minute and the 20-hour or more dialysis, decreased to a minimum after the gel had set and then rose to a steady value. We know of no explanation as yet.

Continuous dialysis, where the liquid outside the collodion membrane was drawn away slowly, being replaced steadily by fresh solution, was studied. During this time the contents of the collodion tube were not disturbed. If dialysis started soon after the mixture of acid and silicate was prepared, that is, within a few minutes, between 95 and 100% of the SiO_2 in the tube (0.190 g. SiO_2) could be removed, but the total time of dialysis was 2000 hours. During the first hour of dialysis, 0.0717 g. of SiO_2 passed through the membrane. The mixture inside the tube did not set at all, too much SiO_2 having been removed. If an hour elapsed after the mixture was prepared, before dialysis started, only

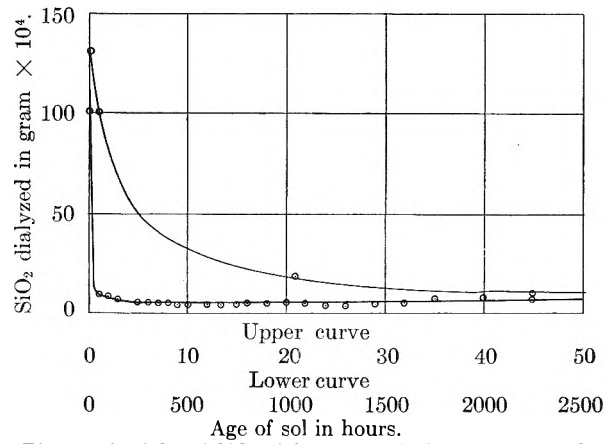

Fig. 1.—Weight of SiO_2 dialyzed in relation to age of sol.

0.0549 g. of SiO_2 dialyzed out in the total time. Table III shows the complete group of results.

The collodion membranes used so far have all been made in the same way, with a drying time of 15 minutes. A series of experiments were made to show the effect of drying time of the membrane on the amount of SiO_2 dialyzed in 10 minutes. Every factor was the same except drying time. Results are shown in Table IV.

TABLE III

TOTAL AMOUNT OF SILICA DIALYZED OUT IN CONTINUOUS DIALYSIS IN RELATION TO AGE OF MIXTURE BEFORE START OF DIALYSIS

Dialysis continued 2000 hours. Time of set of original gel mixture, 288 hours.

Run	Time (hr.) before sample withdrawn	Wt. SiO_2 dialyzed, g.	SiO_2 dialyzed, %
2	0.00	0.1821	96.9
3	1.00	.0549	29.2
4	21.0	.0743	39.4
5	71.0	.0827	43.9
6	93	.0863	45.9
7	118	.0852	45.1
8	142	.0856	45.5
9	168	.0896	47.6

TABLE IV

EFFECT OF DRYING TIME OF COLLODION MEMBRANE ON AMOUNT OF SILICA DIALYZED IN 10 MINUTES

The smaller amount of SiO_2 dialyzing through the sacks, with longer drying time and smaller pore size, is evident.

Sample	Drying time, min.	Amount SiO_2 dialyzed, g.
1	15	0.0147
2	30	.0120
3	45	.0115
4	60	.0106
5	75	.0102
6	90	.0074
7	1180	.0068

Discussion

The results described here show that mixtures of solutions of sodium silicate and acetic acid contain silica in a form capable of dialyzing through collodion membranes. At first the solution probably contains simple silicic acid. This, being of small molecular size, dialyzes easily through collodion membranes, as shown by Fig. 1.

As the sol ages, less silicic acid is able to diffuse through the membrane in a given time, indicating the presence of smaller numbers of small molecules.

That the small molecules do not disappear completely is shown by the fact that some silicic acid is able to dialyze out, even if the original solution had formed a gel. That the smaller molecules are formed by a reaction which is the reverse of the condensation reaction is shown by the fact that more silicic acid can be dialyzed out each time the sack containing the gel mixture is placed in a fresh dialyzing receiving solution containing sodium acetate and acetic acid.

Table III shows that practically all of the silicic acid (97%) may be removed by continuous dialysis from the original mixture, while a mixture run 168 hours, whose setting time was 288 hours, lost 48% during continuous dialysis of 2000 hours. Probably, if sufficient time were available, essentially all of the silicic acid here could be removed.

Membranes with smaller pore size permitted less silicic acid to diffuse in a given time, since the number of molecules of size sufficient to pass through these smaller pores was smaller.

With hydrosols containing lower concentrations of SiO_2 it would appear that the smaller molecules of silicic acid are proportionally more plentiful.

To express these results by chemical equations, we may write, since sodium silicate is not made up of single species

$$(Na_2O)_a(SiO_2)_b + 2aCH_3COOH + (2b - a)\,H_2O \longrightarrow b\,Si(OH)_4 + 2aCH_3COONa$$

The condensation of simple monosilicic acid has been represented[7]

$$(HO)_3Si{-}O\boxed{H + HO}{-}Si(OH)_3$$

$$(HO)_3Si{-}O\boxed{H + HO}{-}\underset{\displaystyle OH}{\overset{\displaystyle OH}{Si}}{-}O{-}Si(OH)_3, \text{ etc.}$$

(7) C. B. Hurd, *Chem. Revs.*, **22**, 403 (1938).

Once a trisilicic acid has been formed, there are two different kinds of OH groups present, the 6 OH groups on the end Si atoms and the 2 OH groups on the Si atom not at the end. As the chains become longer, the number of OH groups on end Si atoms remains 6, but the number of the other kind increases. Condensations involving only OH groups on end Si atoms give linear polymers, while the other types of OH groups gives cross linkages. This explains why the gel is formed suddenly, the increasing number of OH groups not on end Si atoms compensating for the greater activity of OH groups on Si atoms on the end.

Table V shows by a few figures how this proportion changes.

TABLE V

RELATIVE PROPORTION OF OH GROUPS IN LINEAR POLYSILICIC ACIDS WHICH ARE ATTACHED TO Si ATOMS AT THE END OF THE CHAIN

No. Si atoms in chain	2	3	4	10	50
% OH groups on end Si atoms	100	75	60	21.4	5.5

Our data illustrate the reversibility of the reaction of condensation which produces polysilicic acids from simple silicic acids.

DISCUSSION

IRVING CLAPP.—Have you made any studies of silicic acid gels in alcohol?

CHARLES B. HURD.—About 95% of our attempts to form alcogels with silicic acid were unsuccessful. It is true, however, that *we* had some success using varied amounts of alcohol with tetraethyl orthosilicate, but only when water was present.

THE FORMATION AND TITRATION OF COLLOIDAL VANADIC ACID[1,2]

BY J. FRED HAZEL, WALLACE M. MCNABB AND RAFAEL SANTINI, JR.

Department of Chemistry, University of Pennsylvania, Philadelphia, Pa.

Received March 2, 1953

Vanadic acid and sodium vanadates prepared from ammonium metavanadate with the aid of ion-exchange resins have been titrated potentiometrically. The results indicate that the empirical formula of the low molecular weight isopoly acid which is in equilibrium with the high polymer, and about which there has been disagreement, is $H_4V_{10}O_{27}$. The results support those of Britton obtained with compounds prepared by conventional methods. The condensation polymerization of vanadates is discussed.

Introduction

Various formulas have been proposed for the isopoly acid of vanadium responsible for the first break in the titration of colloidal vanadic acid.[3-7] The present paper describes an attempt to clarify this point of disagreement employing the vanadic acid system prepared by ion exchange.[8] The application of ion exchange yields a relatively pure product without recourse to dialysis.

Experimental

Titration of Vanadic Acid with Sodium Hydroxide.—The data given in Fig. 1 are a clue as to why uncertainty has arisen about the formulas of the isopoly acids. Rapid titration with sodium hydroxide using a glass electrode assembly yielded the curve designated A. Although this curve had three inflections, it did not correspond to equilibrium conditions and only a fraction of the vanadium took part in the reaction. When *p*H readings were taken after five days, equilibrium had been established and three quantitative inflections, as shown in curve B of Fig. 1, resulted. The stoppers of the flasks were coated with paraffin and were not removed until the *p*H readings were made. Britton and Welford[9] have shown that the establishment of equilibrium in a similar system is aided by heating to boiling.

The results of the slow titration (Fig. 1, curve B) indicated that the colloidal vanadic acid was converted into the pyrovanadate ion, $V_2O_7^{-4}$, by the series of steps shown in Table I.

The formula $H_4V_{10}O_{27}$ supports the findings of Britton and Welford[9] who attributed the first inflection to the conversion

TABLE I

TITRATION OF COLLOIDAL VANADIC ACID

Vanadic acid
high polymer

$$H_4V_{10}O_{27} \rightleftharpoons V_{10}O_{27}^{-4} \rightleftharpoons VO_3^- \rightleftharpoons V_2O_7^{-4}$$

Inflection

$$H_4V_{10}O_{27} + 4OH^- = V_{10}O_{27}^{-4} + 4H_2O \quad (1)$$
$$V_{10}O_{27}^{-4} + 6OH^- = 10VO_3^- + 3H_2O \quad (2)$$
$$10VO_3^- + 10OH^- = 5V_2O_7^{-4} + 5H_2O \quad (3)$$

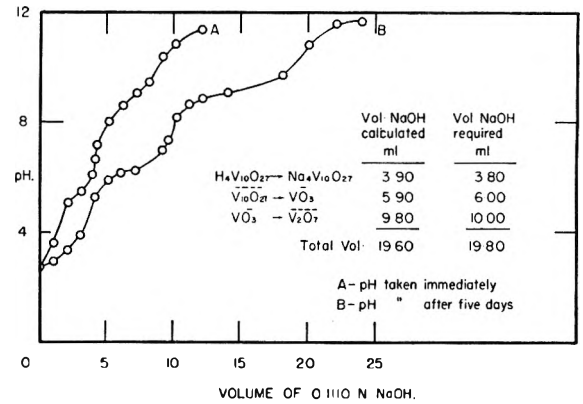

Fig. 1.

TABLE II

RESULTS COMPARED WITH THEORY

Inflection	Eq. of base (theory) $H_4V_6O_{17}$	Eq. of base (theory) $H_4V_{10}O_{27}$	Eq. of base found
First	4	4	3.9
Second	2	6	6.1
Third	6	10	10.2

of the acid into the sodium salt $Na_2O{\cdot}2.5V_2O_5$ (or $Na_4V_{10}O_{27}$). In Table II the equivalents of base required for the three inflections corresponding to the formulas $H_4V_6O_{17}$[8-5] and $H_4V_{10}O_{27}$ are compared with the experimental results.

Titration of Sodium Vanadates with Hydrochloric Acid.—Further confirmation of the formula of the complex polyvanadate ion was obtained by titrating sodium orthovanadate with hydrochloric acid. Colloidal vanadic acid sols prepared by ion exchange were mixed with calculated amounts of sodium hydroxide to prepare the following solutions: 0.005 *M* Na_3VO_4, 0.0025 *M* $Na_4V_2O_7$, 0.005 *M* $NaVO_3$, 0.005 *M* $Na_4V_{10}O_{27}$.

These different solutions were titrated potentiometrically, using 25 ml. of the different sodium vanadates in each flask, with 0.02 *N* HCl, the *p*H's being taken after five days. The results of this experiment are plotted in Fig. 2. All four solutions gave curves which could be superimposed. Other

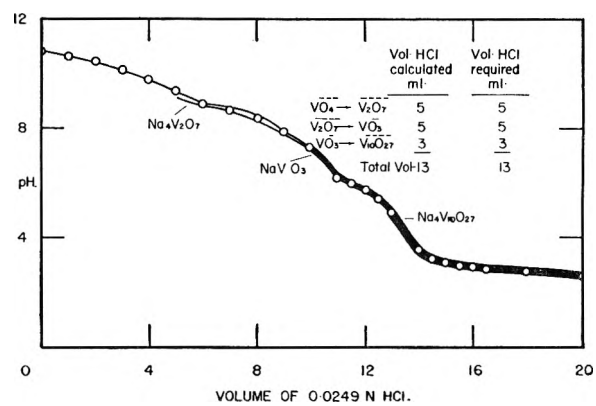

Fig. 2.

(1) This paper is based on a portion of the dissertation by Rafael Santini, Jr., presented to the faculty of the Graduate School of the University of Pennsylvania in partial fulfillment of the requirements for the degree of Doctor of Philosophy.

(2) The experimental data were presented before the Meeting-in-Miniature of the Philadelphia Section of the American Chemical Society, January 29, 1953.

(3) P. Dullberg, *Z. physik. Chem.*, **45**, 129 (1903).

(4) E. Carriere and H. Guiter, *Bull. soc. chim. France*, **12**, 329 (1945).

(5) G. Carpeni and P. Souchay, *ibid.*, **13**, 160 (1946); *J. chim. phys.*, **42**, 149 (1945).

(6) G. Jander and K. F. Jahr, *Z. anorg. Chem.*, **211**, 49 (1933); **212**, 1 (1933).

(7) H. T. S. Britton, *et al.*, *J. Chem. Soc.*, 1955 (1932); 764 (1940).

(8) J. F. Hazel, W. M. McNabb and J. Devlin, *J. Franklin Inst.*, **248**, 251 (1949).

(9) H. T. S. Britton and G. Welford, *J. Chem. Soc.*, 764 (1940).

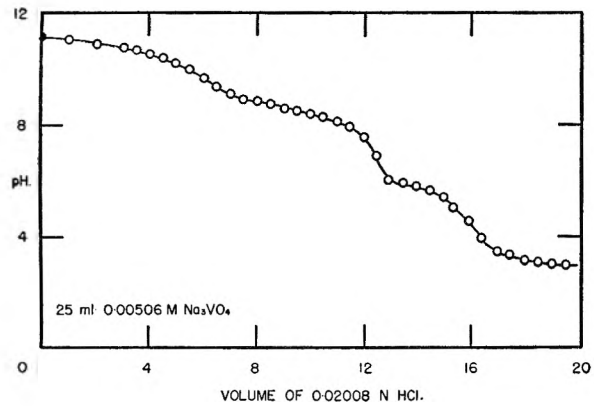

Fig. 3.

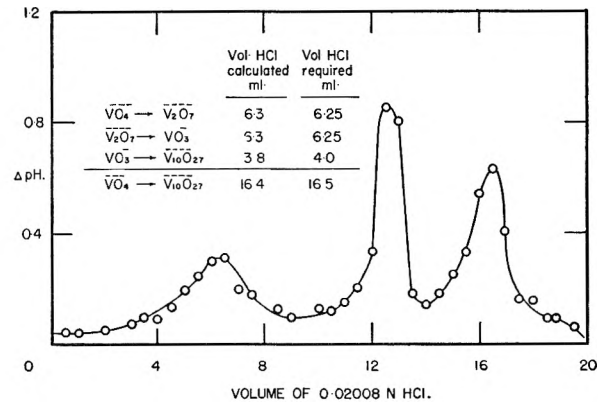

Fig. 4.

titrations of sodium vanadate were made with similar results. An example is given in Fig. 3. A differential plot of the data is shown in Fig. 4.

Discussion

The titration curves of vanadates show inflections similar to phosphates. The curves are characteristic of polyprotic acids having successive ionization constants with decreasing values. The stepwise polymerization of vanadates upon acidification can be treated as follows

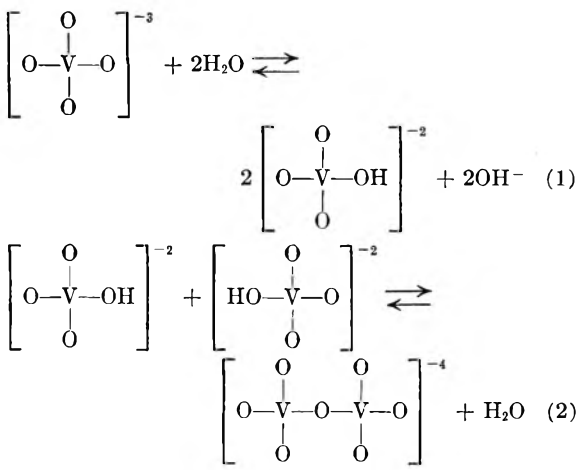

According to Britton and Robinson[10] hydrolysis of an 0.0833 *M* solution of orthovanadate occurs to an extent of 49%. The presence of the pyrovanadate has been indicated by diffusion measurements.[6] The condensation reaction occurs rapidly, hence the first step in the titration can be represented by the sum of reactions 1 and 2

$$2VO_4^{-3} + H_2O \rightleftharpoons V_2O_7^{-4} + 2OH^-$$

A similar condensation reaction with phosphorus does not occur at room temperature.

In seeking an explanation for the difference in the condensation tendencies of protonated phosphates and vanadates, a correlation may be made with the difference in the electronegativities of phosphorus and vanadium. Pauling[11] lists the electronegativities of oxygen, phosphorus and hydrogen as 3.5, 2.1 and 2.1, respectively. Comparison of the structures 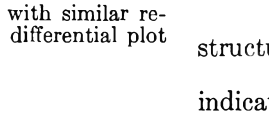 and 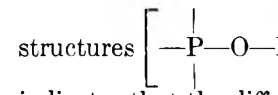 indicates that the differences in the electronegativities of the elements forming the bonds are the same, since both hydrogen and phosphorus have the same values. This condensation does not occur at room temperature.

The electronegativity of vanadium, a transition element, may be estimated to be about 1.6.[12] Since bond energies are qualitatively related to electronegativities and vanadium is more electropositive than hydrogen, the structure 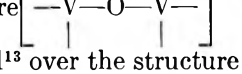 may be expected to be favored[13] over the structure 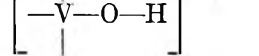 .

The next step in the polymerization on addition of acid involves the conversion of the pyrovanadate to the metavanadate. Molecular weights from diffusion data[6] suggest the $(VO_3)_4^{-4}$ formula although Souchay[14] supports the trimetavanadate formula. We are studying the ultraviolet absorption spectra of the vanadates in this Laboratory but are unable to give a clear interpretation of the results at the present time.

The titration data show that two protons react with each pyrovanadate ion in this step of the titration

$$V_2O_7^{-4} + 2H^+ = H_2V_2O_7^{-2}$$

The formula $H_2V_2O_7^{-2}$ is analogous to $H_2P_2O_7^{-2}$. The latter is formed in the titration of pyrophosphoric acid where the ratio of strong to weak titratable acid functions is 1:1.[15] Pyrophosphoric acid forms two sodium salts, $Na_4P_2O_7$ and $Na_2H_2P_2O_7$, while pyrovanadic acid forms $Na_4V_2O_7$. The metavanadate forms in preference to $Na_2H_2V_2O_7$ because

(10) H. T. S. Britton and R. A. Robinson, *J. Chem. Soc.*, 1955 (1932).

(11) L. Pauling, "The Nature of the Chemical Bond," 2nd Ed., Cornell University Press, Ithaca, N. Y., 1940, pp. 58-69.

(12) L. Pauling, "General Chemistry," W. H. Freeman and Co., San Francisco, Cal., 1947, p. 160.

(13) It is of interest to note that condensation reactions of the type

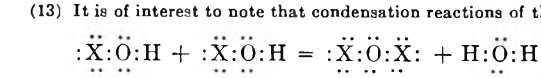

are common when the electronegativity of X is about 1.6 ± 0.2 Examples are found with chromium, silicon, tin and germanium.

(14) P. Souchay, *Bull. soc. chim., France*, **14**, 914 (1947).

(15) J. R. Van Wazer and K. A. Holst, *J. Am. Chem. Soc.*, **72**, 639 (1950).

the vanadate polymerizes as indicated by the reaction

$$H_2V_2O_7^{-2} + H_2V_2O_7^{-2} \rightleftharpoons (VO_3)_4^{-4} + 2H_2O$$

A structural formula may be suggested for the tetramer similar to that of tetrametaphosphate.[16]

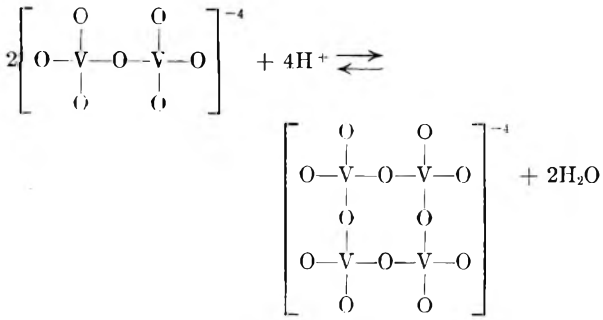

The tetrametavanadate ion is in equilibrium with the $H_2V_2O_7^{-2}$ ion as indicated above.

The clue to the product formed in the next step of the polymerization is given by the titration data. The empirical formula of the ion, $V_{10}O_{27}^{-4}$, or of the sodium salt, $Na_4V_{10}O_{27}$, deduced from the data supports the findings of Britton and coworkers.[7] The condensation may be summarized in the following equation.[17]

$$2(VO_3)_4^{-4} + H_2V_2O_7^{-2} + 6H^+ \rightleftharpoons V_{10}O_{27}^{-4} + 4H_2O$$

Further acidification leads to the formation of a linear polymer which is in equilibrium with low molecular weight decavanadic acid, $H_4V_{10}O_{27}$. Turkevich and Hillier[18] made electron micrographs of a vanadic acid sol and observed fibrils which were 27 Å. wide and 200–1000 Å. long. It is well known that aged vanadic acid sols show streaming double refraction due to the presence of rod-like particles. The equilibrium in the colloidal system can be represented as

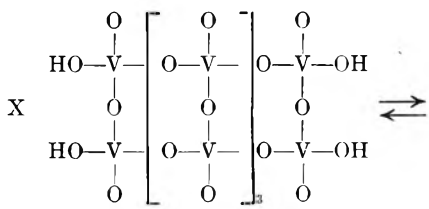

Decavanadic acid

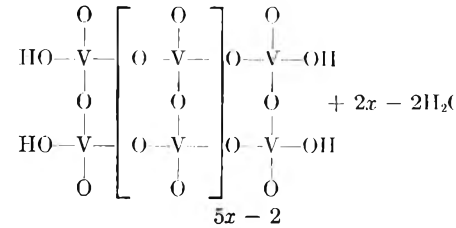

Linear polymer of vanadic acid

The isoelectric point of vanadic acid is about *p*H 2.2.[19] If the acidity is increased, the polymer is broken up and monomeric VO_2^+ and/or VO^{+3} ions are formed. At the isoelectric point the bond between the oxygen and vanadium in the H–O–V– group is weakened due to electrons being pulled away from vanadium toward the hydrogen. At still lower *p*H values the hydroxyl groups split off (and are neutralized) leaving the vanadium atoms with a positive ionic charge

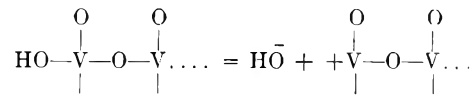

Electrons shift toward the positive vanadium and cleavage occurs leaving the adjacent vanadium atom with a positive charge

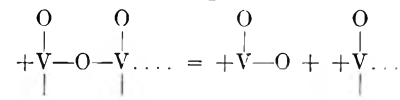

The cleavage of the linear polymer into monomeric cations results in consumption of protons. In the following the added proton is indicated by an arrow

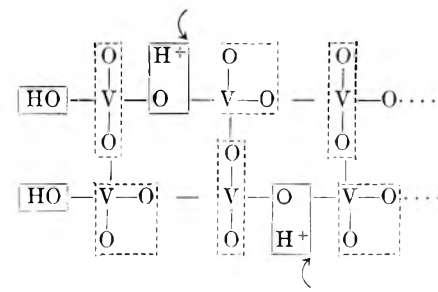

The products of the cleavage are OH^- ions, enclosed by solid lines and VO_2^+ ions[20] (hydrates of this ion as well as VO^{+3} ions may be formed).

$$PO_2^+ + 2H_2O = H_3PO_4^- + 2H^+$$

(16) T. Moeller, "Inorganic Chemistry," John Wiley and Sons, Inc., New York, N. Y., 1952, p. 645.

(17) Jander and Jahr[6] have suggested that two tetravanadate ions condense to form octavanadic acid which is unstable and undergoes slow hydrolysis to pentavanadic acid.

(18) J. Turkevich and J. Hillier, *Anal. Chem.*, **21**, 479 (1949).

(19) N. V. Sidgwick, "Chemical Elements and Their Compounds," Vol. 1, Oxford University Press, London, 1950, p. 809.

(20) Polyphosphates are slowly hydrolyzed to orthophosphates by H^+ ions but PO_2^+ ions are not a product of the cleavage of the –P–O–P– linkages. Phosphorus is more non-metallic than vanadium and this results in the complete hydrolysis.

THE INHIBITION OF FOAMING. V. SYNERGISTIC EFFECTS OF ANTIFOAMING AGENTS

BY SYDNEY ROSS, A. F. HUGHES, M. L. KENNEDY AND A. R. MARDOIAN

Department of Chemistry, Rensselaer Polytechnic Institute, Troy, N. Y.

Received March 2, 1953

Synergistic effects of antifoaming agents are investigated for foams of two synthetic detergents, Aerosol OT and Nacconol NRSF. The defoaming systems are (a) mixtures of Ucon 50-HB-3520 and 2-ethylhexanol and (b) mixtures of tributyl phosphate and methylisobutylcarbinol. The first of these shows a correspondence between antifoaming action and the free energy of spreading of the antifoam composition on the detergent solution. The second system shows no such correspondence, but a more complex effect related to the separate defoaming action of each constituent of the composition.

In the industrial use of antifoaming agents it has frequently been found that a mixture of two agents is more effective than either agent separately. This coöperative effect is known as *synergism*. In his report of industrial practices Ross[1] mentions a mixture of 2-ethylhexanol and diisobutylcarbinol, and again a mixture of Ucon lubricant 50-HB-3520 and heptanol-3, where this synergistic effect has been found. Despite its frequent use, there has not yet appeared any examination of this effect directed toward an understanding of its cause and a better basis for its further exploitation.

Two synergistic systems that have some general interest are reported in this paper. The first pair of agents is Ucon 50-HB-3520 and 2-ethylhexanol, which is a combination similar to one mentioned in reference (1). The second is a mixture of tributyl phosphate and methylisobutylcarbinol; these agents have already been investigated separately by Ross and Young[2] and shown to have widely differing effects. It was felt that mixtures of the two might, by a combination of their separate effects, display synergistic action. The first pair of agents was tried on a foaming solution containing 0.10% Aerosol OT. The second pair of agents was tried on a foaming solution containing 0.50% Nacconol NRSF and 0.75% sodium silicate (*cf.* reference 2).

Materials and Methods.—The materials and their sources are listed in Table I.

TABLE I

DESCRIPTIONS AND SOURCES OF MATERIALS USED

Trade name	Description	Source
Nacconol NRSF	Sodium alkyl aryl sulfonate, salt free	National Aniline Division, Allied Chemical and Dye Corporation
Aerosol OT	Dioctyl sodium sulfosuccinate	American Cyanamid Co.
Ucon 50-HB-3520	Polyalkylene glycol, water miscible	Carbide and Carbon Chemicals Corp.
Methylisobutylcarbinol	$(CH_3)_2CHCH_2CH(OH)CH_3$	Carbide and Carbon Chemicals Corp.
2-Ethylhexanol	$CH_3CH(C_2H_5)CH_2—(CH_2)_2—CHOH$	Carbide and Carbon Chemicals Corp.
Tributyl phosphate	$(C_4H_9O)_3P:O$	Commercial Solvents Corp.

The foam stabilities were measured as described in reference (2). Three indexes, designated L_l, L_g and L_t, are obtained from the data. Of the three, only L_t can properly be called the unit of foam stability, as it is actually a measure of the average time that 1 ml. of foam—*i.e.*, the mixture of the phases, not either one separately—has an existence of its own. The remaining two indexes, L_l and L_g, give an approximate account of the relative parts played in the total instability of the foam by drainage of liquid from the foam films and by rupture of the films to release gas, respectively. They give an approximate account only as these two factors are not measured in complete isolation even by this expedient.

The free energy of spreading of each solution of the two agents on the surface of the foaming system was calculated from surface and interfacial tensions by the equation

$$\Delta F_s = (\gamma_D + \gamma_{DF}) - \gamma_F$$

where γ_D is the surface tension of the solution of the two agents, γ_F is the surface tension of the foaming solution and γ_{DF} is the interfacial tension between the two liquids. The surface and interfacial tensions were measured using the Cenco–du Noüy precision form tensiometer and the Cenco–du Noüy interfacial tensiometer, using the ring corrections of Harkins and Jordan.[3]

Results.—The results obtained for the foam stabilities in the presence of different concentrations of the synergistic mixtures are depicted in Figs. 1 and 2. On each figure for comparison is given the corresponding free energy of spreading in ergs/cm.^{2}.

The antifoams of Fig. 1, 2-ethylhexanol and Ucon 50-HB-3520 on a foaming solution of 0.10% Aerosol OT, are used at a total concentration of 0.50% for each combination. The antifoams of Fig. 2, methylisobutylcarbinol and tributyl phosphate on a foaming solution of 0.50% Nacconol NRSF and 0.75% sodium silicate, are used at a total concentration of 2.0% for each combination.

Discussion.—An examination of the two figures shows that apparently a correspondence exists in one system between the foam stability, L_t, and the free energy of spreading of the antifoam on the foaming solution (Fig. 1), and that no such correspondence is observed in the other system (Fig. 2). The mechanisms by which the agents act are therefore deduced to differ.

(a) Correspondence between Foam Stability and Free Energy of Spreading.—A qualitative correspondence between defoaming action and the spreading coefficient (numerically equal but opposite in sign to the free energy of spreading) had already been pointed out for a majority of systems investigated by Robinson and Woods[4] and again by

(1) S. Ross, *Rensselaer Polytech. Inst. Bull.; Eng. Sci. Ser.*, No. 63.

(2) S. Ross and G. J. Young, *Ind. Eng. Chem.*, **43**, 2520 (1951).

(3) W. D. Harkins and H. F. Jordan, *J. Am. Chem. Soc.*, **52**, 1751 (1930).

(4) J. V. Robinson and W. W. Woods, *J. Soc. Chem. Ind. (London)*, **67**, 361 (1948).

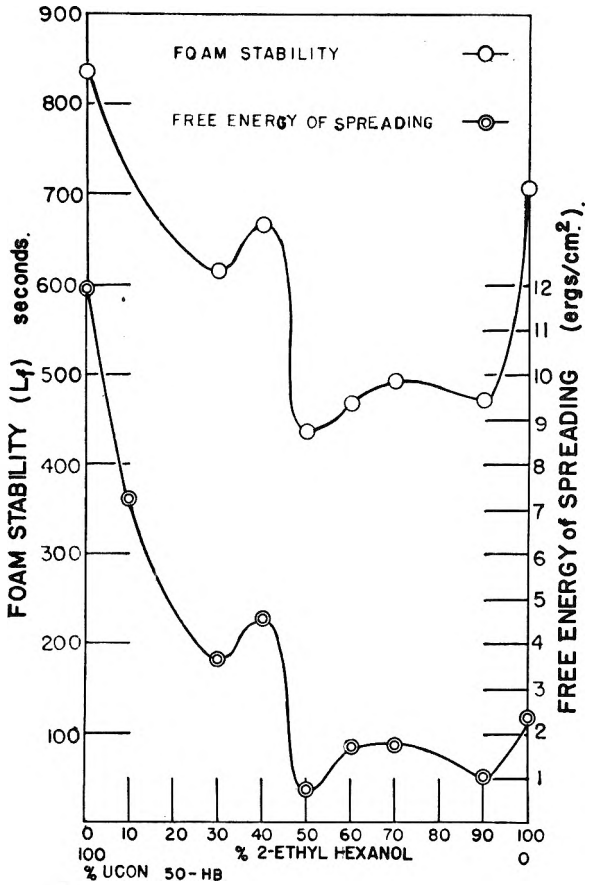

Fig. 1.—The effects of 0.50% of various mixtures of Ucon 50-HB-3520 and 2-ethylhexanol on a foam produced by 0.10% Aerosol OT, and the free energies of spreading of these mixtures on the detergent solution.

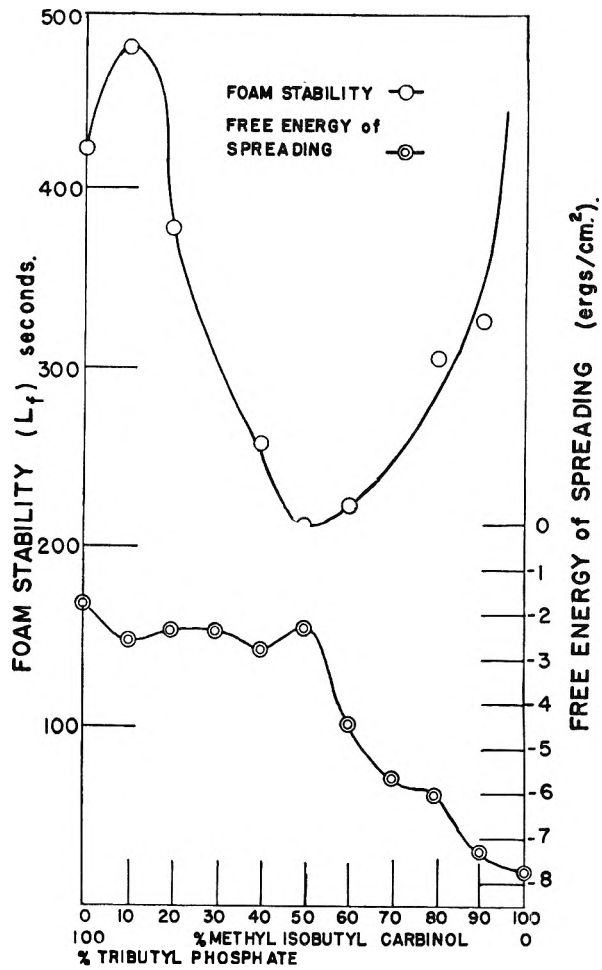

Fig. 2.—The effects of 2.0% of various mixtures of tributyl phosphate and methylisobutylcarbinol on a foam produced by a solution of 0.50% Nacconol NRSF and 0.75% sodium silicate, and the free energies of spreading of these mixtures on that solution.

Ross.[5] The spreading coefficient is one of several methods of estimating the degree of polarity of an organic liquid, or the hydrophilic–lipophilic balance of a mixture. This balance determines the surface activity of an agent, and has been reported to have an optimum value for antifoaming action on aqueous systems.[6] A similar effect was discovered by Morse and Moss[7] in an evaluation of defoamers for use during yeast manufacture. Tall oil (a source of fatty acids) condensed with different amounts of ethylene oxide was used as a series of defoamers, with a variable hydrophilic–lipophilic balance. The most effective defoaming occurred in the range of molar ratios around 1 to 1. The free energies of spreading were not measured for the varying composition of this system. It might be expected, however, that they would show a similar correspondence with defoaming action to that shown in Fig. 1.

It is significant for comparison with the next system to be discussed, that there is no clear separation of the functions of each of the two constituents.

The correspondence between good defoaming action and a large negative free energy of spreading could be interpreted as due to a displacement of the original foam-stabilizing surface layer by a more surface-active but less cohesive or resilient surface layer of antifoam.

(b) **Lack of Correspondence between Foam Stability and Free Energy of Spreading.**—Figure 2 presents an interesting example of a real synergistic effect that shows no correspondence with the free energy of spreading. The two agents concerned, methylisobutylcarbinol and tributyl phosphate, have already been studied separately (reference 2), and shown to affect foams in quite different ways. Tributyl phosphate greatly increases the rate of liquid drainage but has little direct effect in reducing the strength of the thinned liquid film. Methylisobutylcarbinol both increases the rate of liquid drainage, though not to the same extent as tributyl phosphate, and has also a pronounced weakening effect on the liquid films, which rupture while still

TABLE II

FOAM STABILITIES (SECONDS)

(Solution containing 0.50% Nacconol NRSF and 0.75% sodium silicate)

Agent	Concn., %	L_1	L_g	L_f
No agent		350	2080	1720
Methylisobutylcarbinol	6.00	135	180	170
Tributyl phosphate	4.00	95	1060	845

(5) S. Ross, THIS JOURNAL, **54**, 429 (1950).

(6) "Atlas Surface Active Agents," Atlas Powder Co., Wilmington, Del.

(7) R. E. Morse and H. V. Moss, *Ind. Eng. Chem.*, **44**, 346 (1952).

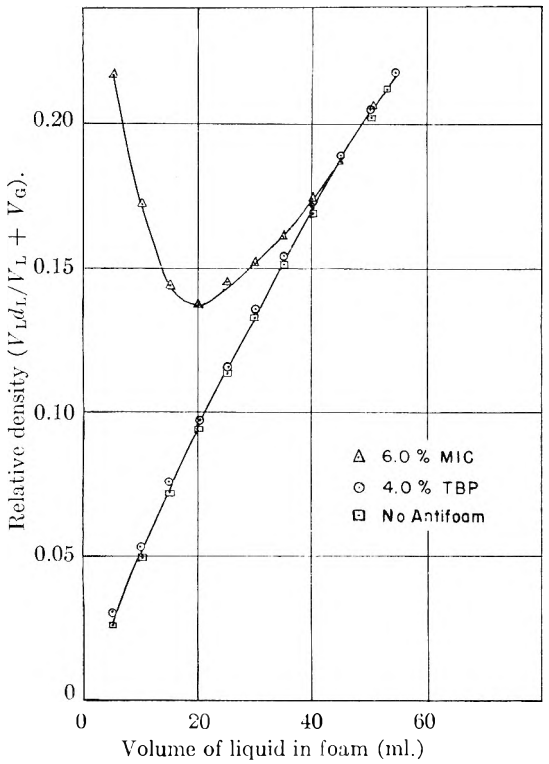

Fig. 3.—The effect of antifoaming agents on the variation of foam density with volume of liquid in the foam. The foaming solution contains 0.50% Nacconol NRSF and 0.75% sodium silicate. MIC = methylisobutylcarbinol; TBP = tributyl phosphate (data of G. J. Young).

relatively thick. The following results, from reference 2, reflect these modes of behavior.

Figure 3, based on data of G. J. Young, shows the variation of the density of the foam with the volume of liquid in the foam. Very low densities indicate a tenuous system of liquid films enclosing the gas phase. A rapidly increasing foam density (reading from right to left as the foam ages) indicates rupture of liquid films and loss of the gas phase. With tributyl phosphate present in the foam, the films drain to the same ultimate thickness before rupture, arriving at the condition of critical film thickness, however, in about half the time required in the absence of tributyl phosphate. With methylisobutylcarbinol in the foam, the foam

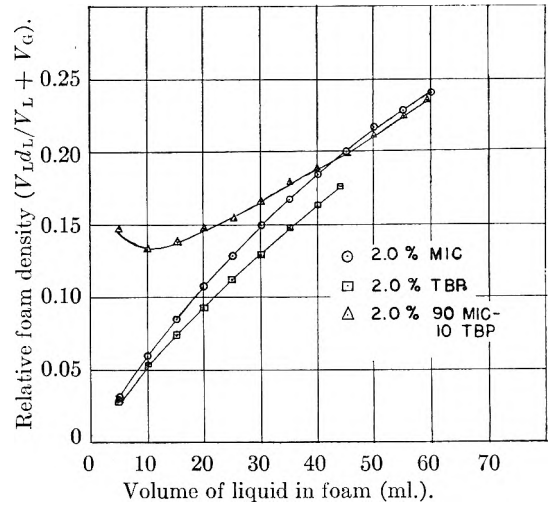

Fig. 4.—The effect of 2.0% of each of two antifoaming agents and of a mixture of the two on the variation of foam density with volume of liquid in the foam. 90 MIC-10 TBP represents a composition of 90% methylisobutylcarbinol and 10% tributyl phosphate.

density never reaches as low a value as in the absence of the agent. The minimum in this curve is produced by the rapid escape of gas from the foam, which proceeds at a greater rate than the escape of liquid.

Figure 4 shows the two effects in combination at total concentrations of 2%.

The action of methylisobutylcarbinol is probably related to its large negative free energy of spreading, by virtue of which it may at 6% concentration largely displace the original stabilizing film from the surfaces of the foam. The action of tributyl phosphate is probably related to its reduction of the surface viscosity of the original stabilizing film, reaching a maximum at 4% concentration, which then permits more rapid flow of interfilm liquid though without destroying the intrinsic strength of the film. The two agents are here combined at concentrations below their optimum effects (total of 2% concentration), so that one effect does not dwarf the other. The combination of these two effects is clearly a more complex phenomenon than is represented by the previous system, and can no longer be found to correspond with the measured free energies of spreading.

ELECTROMIGRATION IN A CATION-EXCHANGE RESIN. III. CORRELATION OF SELF-DIFFUSION COEFFICIENTS OF IONS IN A CATION-EXCHANGE MEMBRANE TO ITS ELECTRICAL CONDUCTANCE[1]

By K. S. Spiegler and C. D. Coryell[2]

Massachusetts Institute of Technology, Cambridge, Massachusetts, and Weizmann Institute of Science, Rehovoth, Israel

Received November 24, 1952

The self-diffusion coefficients of sodium, zinc and calcium ions in "Nepton CR-51" cation-exchange membranes were determined by observing the spread of radiotracers on the membranes. The values obtained by this method are compared to those calculated from the electrical conductance of the membranes by the Nernst–Einstein formula and to one value from the rate of isotopic exchange. The agreement is fairly good except for calcium and shows that the mechanisms of diffusion and electrical conductance in the membrane are similar; the observed discrepancies are believed to be due to electroösmosis.

Self-diffusion coefficients of ions in ion-exchange resins have been determined previously from the measurement of the rate of exchange of resin particles with solutions which were not in equilibrium with them.[3] This method involves assumptions about the rate-controlling process and the shape of the resin particles.

Since self-diffusion coefficients of ions in ionic crystals and in solutions are known to be related to the electrical conductance and since the measurement of the electrical conductance of ion-exchange resins is comparatively simple, it is of interest to compare diffusion and conductance data for resins.

Schulze[4] calculated diffusion coefficients of different ions in granular permutite from the rate of exchange and compared these values to the self-diffusion coefficients calculated from the electrical conductance of the permutite at 20°. A large discrepancy was found which was considered due to the porosity of the grains.

At the time of these investigations a direct determination of self-diffusion coefficients was not possible, because the isotopic tracer technique was not yet available. This technique was used in the present investigation in which the self-diffusion coefficients of sodium, zinc and calcium ions in a cation-exchange membrane were determined from the spread of absorbed radioactive tracer ions and compared to the values calculated from the electrical conductance of the membrane.

Theory.—The self-diffusion coefficient, D(cm.^{2} sec.$^{-1}$) of an ion of valency Z is related to its electrical mobility, m(cm.^{2} volt^{-1} sec.$^{-1}$) by the Nernst–Einstein formula[5]

$$D = \frac{RT}{ZF} m = \frac{RT}{ZF} \frac{1000kt}{cF} \qquad (1)$$

R is the gas constant (watt sec. deg.$^{-1}$ mole^{-1}), T the absolute temperature, F Faraday's constant (coul. eq.$^{-1}$), t the transference number of the ion, k the specific conductance (mho cm.$^{-1}$) and c the equivalent concentration of the solution (meq. ml.$^{-1}$).

This relation holds if the mechanism underlying diffusion is the same as that responsible for electrolytic conduction. Conversely, it has often been concluded that the two mechanisms are the same if agreement is found between the values of D calculated from equation (1) and those obtained by an independent method.

In ion-exchange resins one should expect the two mechanisms to be the same except for the fact that during electromigration electroösmotic flow of water occurs, which is not the case in the process of diffusion. In the absence of sufficient data on electroösmosis in ion-exchange resins, the authors have computed the diffusion coefficients of ions from the conductance without correcting for electroösmosis. The approximate agreement between computed and measured values seems to justify this procedure as a rough approximation.

In solutions of electrolytes, equation (1) holds strictly only at infinite dilution. At finite concentrations, the diffusion mobility and the electrical mobility are not the same, because the interaction between cations and anions is different when they migrate in a diffusion column with the same velocity in one direction and when they migrate in opposite directions under the influence of an external electrical field.[6] Thus if the diffusion coefficients of electrolytes in 0.1 N solution are calculated from the electrical mobilities corresponding to finite concentrations, these values are too low by several per cent.[7]

In cation-exchange resins in equilibrium with water, this problem does not exist because only the cations can migrate with respect to the hydrocarbon matrix in both diffusion and electromigration processes. The transference number of the cations with respect to this matrix is unity.[8,9] Therefore equation (1) reduces to

$$D_c = (2.66 \times 10^{-4}) \frac{k}{c_R \bar{Z}} = (2.66 \times 10^{-7}) \frac{\Lambda}{Z} \qquad (2)$$

at 25° where D_c is the self-diffusion coefficient as determined from the conductance, c_R the (volume) capacity (meq. ml.$^{-1}$), and Λ the equivalent conductance (mho cm.^{2} eq.$^{-1}$) of the resin.

Experimental

Capacity Determination.—Strips of "Nepton CR-51,"[10] a phenolsulfonic cation-exchange membrane, 10 × 1.9 ×

(1) The results of these studies have been presented at the A.A.A.S.-Gordon Conference on Ion Exchange in 1952; and also in the progress reports of the M.I.T. Laboratory for Nuclear Science.

(2) Department of Chemistry and Laboratory for Nuclear Science, M.I.T.

(3) G. E. Boyd, A. W. Adamson and L. S. Myers, Jr., *J. Am. Chem. Soc.*, **69**, 2836 (1947).

(4) G. Schulze, *Z. physik. Chem.*, **89**, 168 (1915).

(5) W. Jost, "Diffusion in Solids, Liquids and Gases," Academic Press, Inc., New York, N. Y., 1952.

(6) L. G. Longsworth, *Ann. N. Y. Acad. Sci.*, **46**, 211 (1945).

(7) G. S. Hartley, *Phil. Mag.*, **S.7.**, **12**, 473 (1931).

(8) K. S. Spiegler and C. D. Coryell, *Science*, **113**, 546 (1951).

(9) K. S. Spiegler and C. D. Coryell, This Journal, **56**, 106 (1952).

(10) A product of Ionics, Inc., Cambridge, Mass.

TABLE I

SPECIFIC CONDUCTANCE, k, OF NEPTON CR-51 IN THE SODIUM, CALCIUM AND ZINC FORM

Membrane no.	Cation	Date of measurement	Capacity, meq. ml.$^{-1}$	$k \times 10^3$, mho cm.$^{-1}$	Temp., °C.	Remarks
1	Na	1/29/52	0.98	8.4	24	
	Na	3/10/52	.94	7.7	25	After several Na–H cycles
2	Na	7/2/52	1.01	11.7	31.5	
	Na	7/3/52	1.01	11.37	31.5	
3	Ca	4/16/52	1.03	4.83	27	
	Ca	4/19/52	1.03	4.75	28.5	After new equilibration with $CaCl_2$
	Ca	5/8/52	1.03	4.19	26.3	
	Ca	6/12/52	1.03	4.09	26.5	After new equilibration with $CaCl_2$
4	Ca	7/2/52	1.02	5.57	31.5	This membrane had undergone several exchange cycles
	Ca	7/3/52	1.02	5.40	31.0	
	Ca	7/29/52	1.02	5.67	31.5	
	Ca	7/30/52	1.02	5.40	30.0	
5	Zn	4/16/52	1.02	4.21	28	
	Zn	4/19/52	1.02	3.75	29	After new equilibration with $Zn(NO_3)_2$
	Zn	5/8/52	1.02	3.35	26.5	
6	Zn	6/30/52	1.02	4.24	29.5	This membrane had undergone several exchange cycles
	Zn	6/31/52	1.02	4.54	32.9	
	Zn	8/1/52	1.02	4.07	29.7	

0.1 cm. were shaken vigorously with 60 ml. of 2 N hydrochloric acid for several hours, the liquid discarded and this procedure repeated several times. After leaching with distilled water, the membranes were transformed into the sodium, calcium and zinc forms by equilibration with 2 N solutions of NaCl, $CaCl_2$ and $Zn(NO_3)_2$, respectively. The cation in these solutions replaced hydrogen ion from the resin, which was titrated with standard 0.1 N sodium hydroxide.

Conductance Measurements.—The membrane strip was clamped between two platinized platinum electrodes on a "Lucite" support as described elsewhere,[11] and the whole assembly placed in a "Lucite" cell filled with deionized water in order to prevent drying and shrinkage of the membrane. The conductance of the membrane (60 cycles per second) was determined by means of a "Serfass" conductance bridge (A. H. Thomas Co., Philadelphia, Pa.) with an accuracy of 2%.

The conductance of different membrane samples was not quite equal and it was also found that the conductance changed as time went on. The zinc form of the resin was found to be covered with a thin white layer which may be $Zn(OH)_2$ due to partial hydrolysis. When the membranes were converted to the hydrogen form and then reconverted to the original form, the conductance was usually somewhat different than before.

The reason for the change of the conductance of the resins with time is not known. It is possible that some volume change occurred, but this could not be detected by a significant change of the length or width of the membrane strips. The capacity and specific conductance were calculated from the dimensions of the membrane in the appropriate form. The changes of membrane length on conversion from one form to the other were less than 3%, but it is not impossible that there were larger changes in the membrane thickness. It is known that phenolsulfonic membranes are not entirely insoluble and contain a certain amount of high-molecular weight diffusible fragments. This may at least partly account for the observed conductance changes.

The results of the capacity and conductance determinations are listed in Table I. The specific conductance, k, was calculated from the measured resistance and the geometrical dimensions of the membrane strips. The possible error in the determination of the membrane thickness was as high as 10%, but this error would not affect the determination of the diffusion coefficient by equation (2) because the equivalent conductance, Λ, of the membrane is determined from the ratio k/c_R and both k and c_R are equally affected by an error in the determination of the membrane thickness.

Determination of the Self-diffusion Coefficient by a Radiotracer Method.—The sodium membrane was superficially dried and about one-half of its length equilibrated for one hour with a 0.02 N solution of sodium chloride containing several hundred microcuries of 2.6y Na^{22}. The solution was stirred vigorously during this period. In order to obtain a sharp boundary between the traced and untraced portions of the membrane, the latter was covered with "Scotch" insulating tape. The membrane was then equilibrated with distilled water for about an hour and the tape removed.

An analogous procedure was adopted for the experiments with zinc and calcium ions. The radioactive tracers, 2.6y Na^{22} and 250d Zn^{65} were furnished by the M.I.T. cyclotron group. 152d Ca^{45} was obtained from the Isotope Division, U. S. Atomic Energy Commission, Oak Ridge, Tennessee.

The radioactive membranes were then wrapped in thin polystyrene film and autoradiographs taken on Kodak X-ray film ("No-screen"). The exposure periods varied between 10 and 25 minutes in the different experiments. The plates were developed with Kodak "D19" developer for five minutes.

After exposure, the membrane was allowed to stand in deionized water from which it was withdrawn at fixed intervals for short periods for further exposures. In this manner the spread of the radiotracer from the initially sharp boundary could be observed. In each experiment three to four autoradiographs, taken at different times, were evaluated.

The optical density of the autoradiographs was determined by means of a "Sinclair-Smith" recording microphotometer. Typical densitograms are shown in Fig. 1. From the values of the relative concentration, the diffusion coefficients were determined by a graphical method used by McCarthy and collaborators and described in detail elsewhere.[12] All evaluations of the autoradiographs showed reasonable straight lines on the "probability paper" plot,[12] showing conformity with the laws of one-dimensional diffusion from a long reservoir of constant concentration into a long region of zero initial concentration. The unavoidable small departure of the initial concentration—distribution curve from a sharp step was treated as a small addition to the time scale to give effective spread time. Three or four successive measurements at greatly different times indicated a precision of about 10% for the average value of D.

Results

Table II shows a comparison of the diffusion coefficients determined by the "spread" method with the values computed from the electrical conductance by means of equation (1). For comparison, there is tabulated the value determined by the usual kinetic method for another phenolsulfonic resin, Amberlite IR-1.[3]

(11) J. T. Clarke, J. A. Marinsky, W. Juda, N. W. Rosenberg and S. Alexander, THIS JOURNAL, **56**, 100 (1952).

(12) V. F. Felicetta, A. E. Markham, Q. P. Peniston and J. L. McCarthy, *J. Am. Chem. Soc.*, **71**, 2879 (1949).

TABLE II

SELF-DIFFUSION COEFFICIENTS, D, IN PHENOL-SULFONIC ION-EXCHANGE RESINS AS DETERMINED BY DIFFERENT METHODS

Cation	Resin	Capacity, meq. ml.$^{-1}$	Temp., °C.	Specific conductance, mho cm.$^{-1}$	Self-diffusion coefficient, $D \times 10^6$ cm.^{2} sec.$^{-1}$ Kinetic	Radioactive tracer spread	Electrical conductance
Sodium	Amberlite IR-1	..	30	.....	2.1	.....	.....
	Nepton CR-51	0.96	23	7.75×10^{-3}	...	1.95 ± 0.25	2.15 ± 0.20
Zinc	Nepton CR-51	1.02	27	3.69×10^{-3}	...	$0.41 \pm .05$	$0.48 \pm .05$
Calcium	Nepton CR-51	1.03	27	4.44×10^{-3}	...	$.31 \pm .05$	$.58 \pm .05$

The conductance values used for these calculations are the average values for membranes 1, 3 and 5 from Table I. The same membranes were used for the spread measurements, except in the case of sodium. The conductance values were reduced to the temperature of the spread measurement, assuming that the temperature coefficient of the conductance is 2.5% per deg.

The relatively large limit of error of the "spread" method is due to the large fluctuations in the densitographs. In general, the evaluation of the autoradiographs is much less accurate than the optical methods used for the concentration determinations[12] in transparent gels. The limit of error of 10% of the values of D_c calculated from the electrical conductance was estimated by taking into account the variations of the conductance as shown in Table I, the accuracy of the conductance bridge, the capacity determination and the measurement of the area of the membrane.

Discussion

It is seen that for sodium and zinc the values determined by the two methods agree within the limit of error, but in both cases the observed values are lower than the calculated. For calcium the value determined by the spread method is significantly lower. At any rate the calculation of the diffusion coefficient from the electrical conductance by means of equation (2) yields values of the right order of magnitude and this may be considered as a proof that the mechanism underlying diffusion in ion-exchange resins is roughly the same as the one underlying electrical conductance.

The fact that the observed values were lower than the computed ones is probably due to electroosmosis. When the mobile cations migrate under the action of an electric field they cause an electroosmotic flow of water in the same direction but at a lower linear velocity.[13] The linear velocity of the cations with respect to the fixed anions is then higher than with respect to the electroösmotic stream of water. Therefore the measured conconductance, k^*, is higher than the conductance, k, corresponding to a state where the water is at rest with respect to the fixed anions. When self-diffusion takes place in a resin, no electroösmosis occurs and hence if k^* instead of k is used to calculate the self-diffusion coefficient by equation (2), the computed values will be too high.

(13) G. Schmid, *Z. Elektrochem.*, **56**, 181 (1952).

A knowledge of the self-diffusion coefficients of ions is of limited practical importance, but could be useful if the coefficients of interdiffusion of different ions in a mixed resin could be calculated therefrom. In previous studies it has been assumed as a first approximation that the coefficient of interdiffusion is independent of the composition of the mixed resin. On the other hand, application of the classical Nernst theory of diffusion[5,14] of electrolytes leads to the conclusion that this is true only if the mobilities of the exchanging ions are equal. In general, the coefficient of interdiffusion, D_{AB}, of two univalent ions, A and B, is related to the composition by the equation

$$D_{AB} = 1/\left(\frac{X_A}{D_B} + \frac{X_B}{D_A}\right) \qquad (3)$$

provided the mobilities of the ions are independent of the composition. X_A and X_B are the mole fractions and D_A and D_B the self-diffusion coefficients of ions A and B, respectively. This relation was first derived[14] for interdiffusion in halide crystal systems such as AgCl-NaCl, at 280° which are somewhat analogous to cation-exchange resins because the anions are immobile. It was found in fair agreement with experimental results.[5]

In general, the variation of the interdiffusion co-

(14) C. Wagner, *Z. physik. Chem.*, **B11**, 139 (1930)

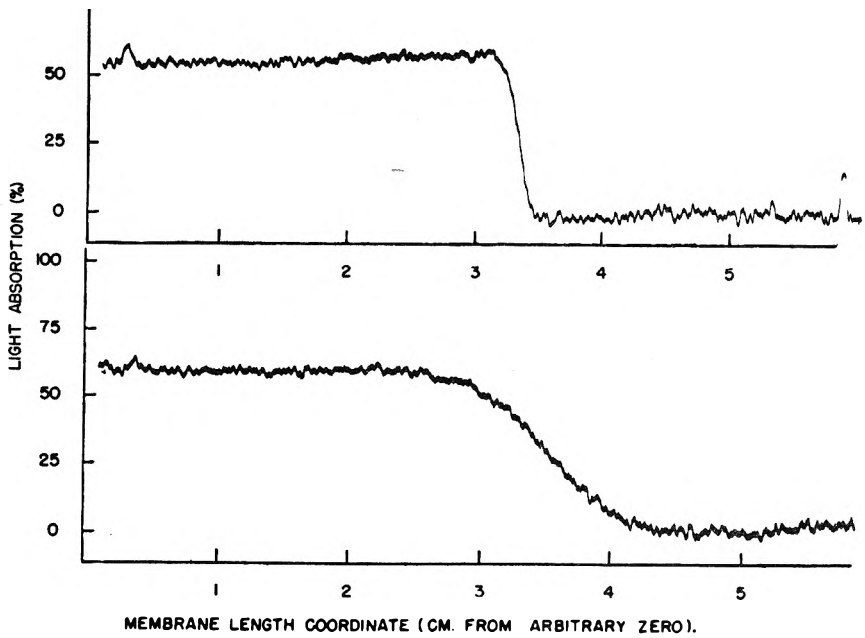

Fig. 1.—Self-diffusion of calcium in Nepton CR-51 membrane. Densitographic evaluation of autoradiographs showing spread of 152d Ca^{45} from an initially sharp boundary; temperature, 26.4°. Upper diagram, spread after 2.4 hours (effective spread time of 3.2 hours). Lower diagram, spread after 3 days and 7 hours.

efficient with composition may be expected to be somewhat less than by equation (3), which was derived on the assumption that the interaction of the ions is merely electrostatic and that the presence of one type of ion does not otherwise affect the mobility of the other. This is in general only approximately true. For instance, in a mixed sodium–hydrogen resin the ratio of the mobilities of hydrogen and sodium ions is smaller than that of their mobilities in the pure hydrogen and sodium forms, respectively.[9] Hence in this case the variation of the interdiffusion coefficient with the composition cannot be as large as expected from equation (3). If the ionic mobilities in a mixed resin are always less different than in the pure resin salts, equation (3) represents the upper limit of the dependence of the coefficient of interdiffusion on the concentration.

Acknowledgment.—The authors thank Miss M. Springer for her valuable help. The work described was supported in part by the U. S. Atomic Energy Commission. One of the authors (K. S. S.) is holder of a Weizmann Institute Postdoctoral Fellowship.

METAL CHELATING TENDENCIES OF GLUTAMIC AND ASPARTIC ACIDS[1]

BY R. F. LUMB AND A. E. MARTELL

Department of Chemistry of Clark University, Worcester, Mass.

Received January 12, 1953

The acid dissociation constants of glutamic and aspartic acids, and their interactions with the divalent ions of Mg, Ca, Sr, Ba and Cd were investigated potentiometrically with a cell consisting of glass and silver–silver chloride electrodes. The stability constants were calculated for the chelates consisting of one mole of ligand per mole of metal ion, and probable structures of the chelates are suggested. The measured chelating tendencies are compared to those reported for analogous amino acids, and the correlation of the calculated stability constants with the ionic radius of the metal is described.

Literature reports on the binding of the alkaline earth ions with glutamic and aspartic acids seem to be in disagreement on the nature and extent of the interaction. Miyamoto and Schmidt,[2] on the basis of transference numbers calculated from conductance measurements, could find no evidence for complexing of calcium and barium ions by glutamic and aspartic acids. Subsequently, however, Batchelder and Schmidt[3] studied the titration of aspartic acid in the presence of barium ion and concluded that complex formation possibly occurs. Also, a titrimetric study by Heinz[4] on calcium aspartate indicated that little or no binding occurs, and no stability constant was reported. On the other hand, recent quantitative studies have indicated definite interactions, and stability constants have been reported for calcium glutamate,[5] calcium and strontium aspartate,[6] and for radium aspartate.[7]

Since the existence of weak chelates of alkaline earth ions with glycine[5,8–11] are now known, it is to be expected that the additional carboxylate group in the glutamate and aspartate ions would render these more effective as ligands than the glycinate ion. The purpose of this research was to determine quantitatively the interaction of alkaline earth ions with aspartic and glutamic acids. The somewhat less basic cadmium ion was also included for investigation.

(1) Abstracted from a dissertation submitted by R. F. Lumb to the faculty of Clark University in partial fulfillment of the requirements for the degree of Doctor of Philosophy, June, 1951.

(2) S. Miyamoto and C. Schmidt, *J. Biol. Chem.*, **99**, 335 (1933).

(3) A. Batchelder and C. Schmidt, THIS JOURNAL, **44**, 893 (1940).

(4) E. Heinz, *Biochem. Z.*, **321**, 314 (1951).

(5) C. W. Davies and G. M. Waind, *J. Chem. Soc.*, 301 (1950).

(6) J. Schubert, THIS JOURNAL, **56**, 113 (1952).

(7) J. Schubert, E. Russell and L. Myers, *J. Biol. Chem.*, **185**, 387 (1950).

(8) A. Albert, *Biochem. J.*, **46**, Proc. of soc. xxxix (1950).

(9) C. B. Monk, *Trans. Faraday Soc.*, **47**, 297 (1951).

(10) C. B. Monk, *ibid.*, **47**, 1233 (1951).

(11) C. W. Davies, *J. Chem. Soc.*, 277 (1938).

Experimental

Method.—By means of potentiometric *p*H determinations, the ionization constants of glutamic and aspartic acids were measured in 0.1 *M* potassium chloride at 25°. Similar measurements were then made in solutions in which the metal ion being investigated was maintained at a concentration of about ten times that of the amino acid. In all cases there was maintained a very large excess of potassium chloride over all other ionic species present, so that the ionic strength was maintained relatively constant. The titrations were carried out by the addition of excess standard potassium hydroxide to the experimental solution containing the amino acid, potassium chloride and, in most cases, the metal chloride. The resulting solution was then back-titrated with small increments of standard hydrochloric acid.

Apparatus and Materials.—The conical reaction cell contained a large number of openings designed to accommodate a mercury seal stirrer, buret, glass, Ag–AgCl and hydrogen electrodes, hydrogen (or nitrogen) inlet and outlet. A number of electrodes of each type were employed in order to check the readings. The hydrogen and nitrogen used were purified and presaturated with a solution having the same composition as the experimental solution. The hydrogen electrodes were prepared as described by Weissberger.[12] The silver–silver chloride electrodes were prepared according to the directions of Shedlovsky and MacInnes.[13] Agreement among silver–silver chlorides was generally ±0.01 millivolt; those showing greater than ±0.1 millivolt deviation were discarded. Standard Beckmann #290 glass electrodes were adapted to the requirements of the investigation by shielding the lead with an insulated wire mesh sealed to the brass base and covered with amphenol. The cell potential was measured by means of a Leeds and Northrup thermionic amplifier of the type described by Cherry,[14] a Leeds and Northrup type K potentiometer, and sensitive galvanometer. The micro-buret used in the titrations could be read to 0.01 ml. with accuracy. The metal chloride solutions were prepared from J. T. Baker analyzed solutions and were standardized by titration with standard silver nitrate with fluorescein as indicator. The glutamic and aspartic acids were recrystallized several times from water and dried.

(12) A. Weissberger, "Physical Methods of Organic Chemistry," Vol. II, Interscience Publishers, Inc., New York, N. Y., 1946, p. 1058.

(13) T. Shedlovsky and D. A. MacInnes, *J. Am. Chem. Soc.*, **58**, 1970 (1936).

(14) R. H. Cherry, *Trans. Electrochem. Soc.*, **72**, 33 (1937).

Experimental Results

The pH was measured with the cell Ag, AgCl/0.1 M HCl/glass membrane/unknown solution/AgCl, Ag. This substitution of a glass electrode for the usual hydrogen electrode, resulted in greater stability and speed of measurement. The calibration of the glass electrode was carried out with experimental solutions by comparing the e.m.f. of the above cell with the following cell: Pt, H_2/unknown solution/AgCl, Ag. Two glass electrodes, used simultaneously in subsequent measurements, were calibrated in this manner and checked from time to time. By means of the calibration curves prepared from these data, the glass electrode measurements were converted to hydrogen electrode readings. Thus, the pH values measured in the present work may be defined as: $p\mathrm{H} = (1/0.05915)\ [E_m - (E^0 - 0.05915 \log f_{Cl^-} \cdot C_{Cl^-})]$, where E_m is the measured potential, E^0 is the standard potential of the silver–silver chloride electrode, and f and C represent activity coefficient and molar concentration, respectively.

In each titration curve obtained as outlined above, between 50 and 100 increments of standard hydrochloric acid were added. For the two glass electrodes employed, this involved an average of 150 potential readings for each run. In view of the fact that six runs were needed for each of the two amino acids, and that duplicate runs were made in each case, over 3000 measurements were made. The sample measurements given in Table I, representing only a very small fraction of the data, are selected near $N = 0.5$, the most significant region for the calculation of stability constants. When the pH is plotted *vs.* N for aspartic acid to give the usual type of titration curve, the alkaline earth titration curves appear to be barely resolvable from that of the free acid. However, the relative positions of the lines are readily apparent in the large scale plot given in Fig. 1. No curves are presented for glutamic acid since the curves are similar to those of aspartic acid, with the exception that the pH values of corresponding points are somewhat higher.

TABLE I

POTENTIOMETRIC MEASUREMENTS

Amino acid[a]	M^{++}[b]	μ	HCl, ml.	N[c]	E_m, mv.
G	None	0.09	3.20	0.494	−159.6
G	None	.09	3.50	.582	−151.0
G	Mg^{++}	.12	3.05	.451	−142.8
G	Mg^{++}	.12	3.46	.571	−131.4
G	Ca^{++}	.12	3.01	.515	−152.0
G	Ca^{++}	.13	3.23	.504	−141.2
G	Sr^{++}	.12	3.26	.512	−153.3
G	Sr^{++}	.12	3.10	.465	−146.2
G	Ba^{++}	.12	3.41	.557	−139.6
G	Ba^{++}	.12	3.36	.542	−139.7
G	Cd^{++}	.12	3.07	.476	− 28.6
G	Cd^{++}	.12	3.04	.468	− 29.5
A	None	.09	3.65	.526	−147.5
A	None	.09	3.75	.558	−145.2
A	Mg^{++}	.12	3.30	.482	−108.1
A	Mg^{++}	.12	3.55	.494	−105.2
A	Ca^{++}	.13	3.71	.544	−133.3
A	Ca^{++}	.13	3.72	.546	−131.2
A	Sr^{++}	.12	3.25	.466	−142.0
A	Sr^{++}	.12	3.20	.451	−146.5
A	Ba^{++}	.12	3.52	.486	−149.3
A	Ba^{++}	.12	3.51	.484	−145.2
A	Cd^{++}	.12	3.50	.482	+ 1.6
A	Cd^{++}	.12	3.30	.418	+ 5.6

[a] G = glutamic acid, A = aspartic acid; amino acid was 0.00300 M in all cases. [b] Concentration of bivalent metal was always 0.0300 M. [c] N = moles of acid added per mole of amino acid present.

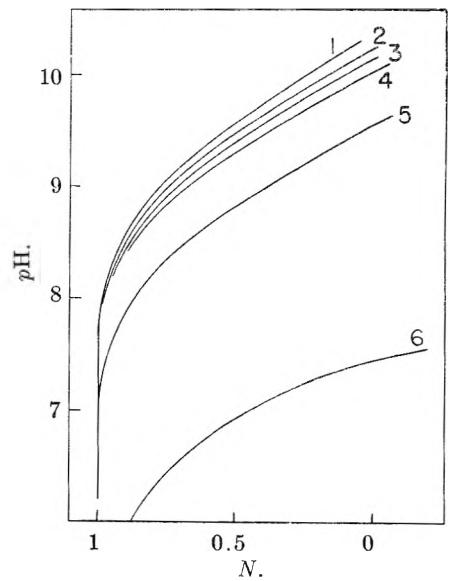

Fig. 1.—Magnified portion of potentiometric titration of aspartic acid in the presence of metal ions: 1, free aspartic acid; 2, $BaCl_2$; 3, $SrCl_2$; 4, $CaCl_2$; 5, $MgCl_2$; 6, $CdCl_2$. μ adjusted to 1.2 with potassium chloride. N = moles of acid added per mole of amino acid salt.

Calculations

The three acid dissociation constants of glutamic and aspartic acids may be defined by the equations

$$H_3A^+ \rightleftharpoons H_2A + H^+ \qquad k_1 = \frac{(H^+)(H_2A)}{(H_3A^+)} \quad (1)$$

$$H_2A \rightleftharpoons HA^- + H^+ \qquad k_2 = \frac{(H^+)(HA^-)}{(H_2A)} \quad (2)$$

$$HA^- \rightleftharpoons A^{-2} + H^+ \qquad k_3 = \frac{(H^+)(A^{-2})}{(HA^-)} \quad (3)$$

where H_2A represents aspartic and glutamic acids, and ( ) represents activities of the species involved. It is apparent from the titration curves that the first two reactions overlap, and that the calculations of k_1 and k_2 must be made simultaneously from data in the lower buffer region of the acid titration curves (not shown). If C_s represents the total molar concentration of amino acid species, it follows that at low pH, $C_s = C_{H_3A^+} + C_{H_2A} + C_{HA^-}$, and $NC_s = C_{H^+} + C_{HA^-} + 2C_{H_2A} + 3C_{H_3A^+}$. When these relationships are combined with equations 1 and 2, with the substitution of molar concentrations in place of activities for the amino acid species, the following relationship is obtained

$$k_2 = \frac{1}{k_1}\frac{(H^+)^2[C_s(N-3) - C_{H^+}]}{C_s(1-N) + C_{H^+}} + \frac{(H^+)[C_s(N-2) - C_{H^+}]}{C_s(1-N) + C_{H^+}} \quad (4)$$

Equation 4 may be solved directly near $N = 2$ under conditions whereby the difference between concentration and activity of hydrogen ion is relatively unimportant compared to C_s, since the measured pH values were used for both C_{H^+} and (H^+). The constants k_1 and k_2 were then obtained algebraically by using sets of data corresponding to different values of N. The dissociation constants thus calculated are the so-called "hybrid" concentration constants involving hydrogen ion activities.

In the calculation of the third acid dissociation constant, the stoichiometric relationships are: $C_s = C_{HA^-} + C_{A^{-2}}$ and $NC_s = C_{HA^-} - C_{OH^-}$. From these relationships it is possible to determine the values of C_{HA^-} and $C_{A^{-2}}$ directly since C_{OH^-} is very small compared to the other quantities, and it is possible to substitute the approximate quantity $K_w/(H^+)$ in its place. The resulting dissociation constant is also a hybrid constant in which activities of amino acid species in equation 3 are replaced by molar concentrations.

If it is assumed that only 1:1 metal chelates are formed, the relationships for the calculation of stability constants are relatively simple. The chelates involving more than one ligand per metal ion may be ruled out in view of the large excess of metal ion. Also, chelates of the type MHA^+ may be ruled out since all the measurements were made at pH values much higher than those at which proton complexes of amino acids usually occur. Thus in the presence of excess metal ion it is possible to set up the relationships

$$C_{A^{-2}} = [NC_s + (OH^-)]k_3/(H^+)$$
$$C_{MA} = C_s - [1 + k_3/(H^+)][NC_s + (OH^-)], \text{ and}$$
$$C_{M^{+2}} = C_{M_0{}^{+2}} - C_{MA}$$

where $C_{M^{+2}}$ and C_{MA} represent concentrations of metal ion and metal chelate, respectively, and $C_{M_0{}^{+2}}$ represents the total of the concentrations of metal species, and the other terms have the same definitions as are given above. Calculations of $C_{A^{-2}}$, C_{MA} and $C_{M^{+2}}$, by means of these equations allow the direct calculation of the concentration equilibrium constant k_1 for the formation of the metal chelate, MA. Inspection of these equations raises the question of the effect of employing pH for (H^+) on the calculated result. This difficulty is overcome if the hybrid constant described above is used for k_3 since this quantity contains a pH term which cancels out, leaving only concentration terms in the equations. The approximation introduced by substituting $K_w/(H^+)$ for C_{OH^-} becomes negligible under the experimental conditions employed where C_{OH^-} is small compared with NC_s.

Discussion of Results

Acid Dissociation Constants.—In Table II are listed the ionization constants, expressed in pk units, obtained in this investigation as well as the values obtained by previous investigators. The values in parentheses have been corrected to zero ionic strength by the method described by Neuberger.[15] The pk_2 and pk_3 values for glutamic and aspartic acids obtained in this research agree well with the results of Miyamoto and Schmidt[2] and of Neuberger.[15] There is also good agreement of our corrected values of pk_2 and pk_3 for aspartic acid with those of Batchelder and Schmidt.[3] The values of pk_1 are the least accurate because of the high hydrogen ion concentrations involved, and the results show somewhat less agreement in this case. In the measurement of interactions of these amino acids with metal ions, the value of pk_1 fortunately only seldom enters into the calculations. As it turned out, both k_1 and k_2 were eliminated from the calculation of stability constants of alkaline earth and Cd^{+2} ions in the present investigation because of the relatively high pH values necessary for appreciable interaction to occur. The relative values of the dissociation constants listed for glutamic and aspartic acids are in general what would be expected from the structural differences of these two amino acids.

TABLE II

IONIZATION CONSTANTS OF GLUTAMIC AND ASPARTIC ACIDS AT 25°

	Glutamic acid			Aspartic acid		
	pk_1	pk_2	pk_3	pk_1	pk_2	pk_3
Present investigation	2.30	4.28	9.67	1.94	3.70	9.62
	2.30[a]	4.51[a]	9.95[a]	1.94[a]	3.90[a]	9.90[a]
Schmidt, Kirk, Appleman[16]	2.10	4.07	9.47	1.91	3.63	9.47
Harris[17]	2.18	4.39	9.80	2.08	3.82	9.80
Miyamoto and Schmidt[2]	2.19	4.25	9.67	1.88	3.65	9.60
Neuberger[15]	2.155[a]	4.324[a]	9.960[a]	..	..	..
Batchelder and Schmidt[3]	..	..	..	2.01[b]	3.895[b]	9.842[b]

[a] Corrected to zero ionic strength by the method of Neuberger.[15] [b] Zero ionic strength.

Chelate Stability Constants.—The calculated values of the 1:1 chelate stability constants of the alkaline earth ions listed in Table III indicate definite, though weak, interactions which vary in a regular manner, the stabilities increasing with decreasing basicity of the metal ion. In cases where chelates are primarily ionic in nature, it has been pointed out by Martell and Calvin[18] that straight line correlation with the reciprocal of the radius of the gaseous ions is generally to be expected for metal ions of the same charge. In Fig. 2 the chelate stabilities (pk_1 values) are seen to vary in a linear

TABLE III

CHELATE STABILITY CONSTANTS AT 25°

Metal ion	log k_1			
	Glutamic acid	Aspartic acid	Glycine	Succinic acid
Mg^{+2}	1.9	2.43	..	1.0[d]
Ca^{+2}	1.43	1.60	1.43[b]	1.0[f]
Sr^{+2}	1.37	1.48	..	0.9[f]
Ba^{+2}	1.28	1.14	0.8[b]	1.0[e]
Ra^{+2}	..	0.86[a]	..	1.0[a]
Cd^{+2}	3.9	4.39	4.5[c]	..

$\mu = 0.1$ unless otherwise stated. [a] Reported by Schubert, *et al.*,[7] $\mu \leqq 0$. [b] Reported by Monk,[9] $\mu = 0$. [c] Estimated from Albert.[8] [d] Calculated from Simms,[19] $\mu = 0.07$. [e] Reported by Joseph,[20] $\mu = 0.15$. [f] Reported by Schubert,[6] $\mu = 0.16$.

(15) A. Neuberger, *Biochem. J.*, **30**, part 2, 2085 (1936).

(16) C. Schmidt, P. Kirk and W. Appleman, *J. Biol. Chem.*, **88**, 285 (1930).

(17) L. Harris, *Proc. Roy. Soc. (London)*, **95B**, 440 (1923).

(18) A. E. Martell and M. Calvin, "Chemistry of the Metal Chelate Compounds," Prentice-Hall, Inc., New York, N. Y., 1952, Chap. 5.

(19) H. Simms, THIS JOURNAL, **32**, 1121 (1928).

(20) N. Joseph, *J. Biol. Chem.*, **164**, 529 (1946).

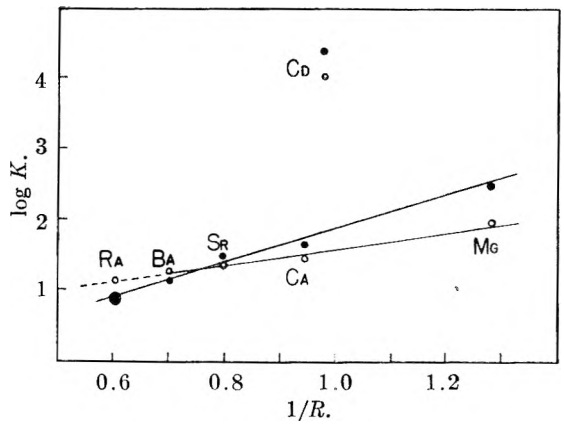

Fig. 2.—Correlation of stability constants with reciprocal of ionic radius: ● represents aspartic acid and ○ represents glutamic acid chelates.

fashion with the reciprocal of the ionic radius. It is further seen that the stability of the radium chelate, determined by Schubert, *et al.*,[7] by ion exchange measurements, correlate well with our results for the remaining alkaline earths. The value shown is slightly low since it was not corrected for ionization of aspartic acid. Correction to a slightly higher value apparently would improve the agreement. A similar correlation for the alkaline earth chelates of citric acid has been pointed out by Schubert, *et al.*[7] A correlation between chelate stability and the second ionization potential of the metal ion for transition metals has been noted by Calvin and Melchior.[13] An analogous correlation of chelate stability constants with the sum of the first and second ionization potentials for the alkaline earth metals has been pointed out by Schwarzenbach, *et al.*[21] Such correlations in the case of the alkaline earths amount to the same as that observed in Fig. 2, in view of the linear relationship between the reciprocal radius and sum of the ionization potentials for these metals. The comparisons pointed out by Calvin and Schwarzenbach are quite similar since the first ionization potential is nearly constant for the transition metals in question.

The difference in the slopes of the aspartate and glutamate lines in Fig. 2 is interesting since it is a reflection of the fact that the aspartate ion has the higher affinity for the less basic metal ions, while the glutamate ion is more effective than the aspartate in complexing the more basic metal ions. Thus it may be concluded that for most divalent metal ions, binding with aspartate will be greater than with glutamate, the differences decreasing with increasing basicity, and with a reversal in the effect for barium. As basicity increases beyond that point, it appears that the glutamate ion is increasingly more efficient. The seemingly anomalous position of the Cd^{+2} ion in Fig. 2 is merely a result of the fact that the type of chemical binding in this chelate is of a much higher order—involving more energy and an appreciably larger homopolar component than is the case for the alkaline earths.

A clearer picture of the structure of the aspartate and glutamate chelates is possible on the basis of the relative stabilities of other metal chelates listed in Table III. It is seen that the stability constants are reasonably close to those listed for the glycinate ion. The values are not only much higher than those of the succinate ion, but also behave in a different manner, the alkaline earth succinate chelates having approximate constant stability for the series magnesium through radium. Hence, it is possible to rule out participation of the second carboxylate ion in the binding of the metal ion, and it appears that structures I and II, analogous to the glycine chelates, are the most likely.

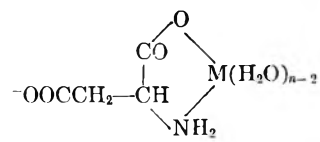

I, Aspartate chelate

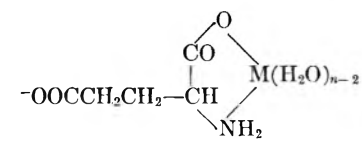

II, Glutamate chelate

It is noteworthy that although the additional carboxylate ion is probably not involved in the metal chelate bonds, it has an indirect influence on the stability of the chelate ring. The generally greater stability of the aspartate chelates indicates that the inductive effect of the negative carboxylate group in I lends stability to the structure (*i.e.*, increases basicity of the donor groups toward the metal ion). From the data available, it is not possible to determine if the weaker inductive effect of the analogous group in II has any appreciable influence on the stability of the chelate. In a recent publication Chaberek and Martell[22] suggested that aspartic acid is tridentate with respect to the first-row transition metal ions. This is apparently not the case with the alkaline earth and cadmium ions.

Acknowledgment.—The authors are indebted to Dr. S. Chaberek, Jr., for assistance in checking the calculations.

(21) G. Schwarzenbach, H. Ackermann and P. Ruckstuhl, *Helv. Chim. Acta*, **32**, 1175 (1949)

(22) S Chaberek, Jr., and A. E. Martell, *J. Am. Chem. Soc.*, **74**, 6021 (1952).

SPECTROPHOTOMETRIC DETERMINATION OF THE STABILITIES OF ETHYLENEDIAMINETETRAACETATE CHELATES

BY VINCENT L. HUGHES AND ARTHUR E. MARTELL

Contribution of the Department of Chemistry of Clark University, Worcester, Mass.

Received January 23, 1953

The interactions of colored metal chelates of ethylenediaminetetraacetic acid with various metal ions were determined by a direct spectrophotometric method in nitrate and perchlorate media. Under conditions such that the metal chelates are not appreciably dissociated and the chelate containing one metal ion per ligand was the important form, the measurements allowed calculation of the relative stability constants of the metal chelates investigated. The dissociation of the nickel(II)–ethylenediaminetetraacetate chelate was followed spectrophotometrically, the absolute value of the stability constant of this chelate was calculated, and the relative values for the other metals were converted to absolute stability constants. Studies were also made of the effect of ionic strength on the stabilities of the chelate compounds.

Although it is not possible to evaluate directly from potentiometric measurements of *p*H, the very large chelate stability constants for the transition and heavy metal ethylenediaminetetraacetates, a number of indirect methods have been developed in recent years. Schwarzenbach and Freitag[1] determined potentiometrically the position of the equilibrium in a system containing magnesium and transition metal chelates of β,β',β''-triaminotriethylamine and ethylenediaminetetraacetic acid. Also, the equilibrium between the ferrous and ferric chelates, determined by an oxidation–reduction method by Schwarzenbach and Heller,[2] and by a polarographic method by Kolthoff and Auerbach[3] has been useful in the calculation of chelate stability constants. Perhaps the most unusual method is that of Jones and Long,[4] wherein the kinetics of exchange of ferric ion with the ferric ethylenediaminetetraacetate chelate was studied. Extrapolation to zero time made possible the calculation of the concentration of free ferric ions, and, from this quantity, the chelate stability constant.

In recent publications,[5,6] a direct spectrophotometric method for the determination of relative stabilities of transition and rare earth metal chelates of ethylenediaminetetraacetic acid has been described in principle. However, the buffering agents employed to control *p*H also formed weak complexes with the metals being investigated. This method has now been investigated for solutions with no interfering buffers, and with an ionic atmosphere controlled with nitrates or perchlorates. Further, the relative chelate stability constants thus obtained have been placed on an absolute basis by spectrophotometric measurement of the degree of dissociation of the nickel chelate in sufficiently acidic solutions. The effect of ionic strength on the relative stability constants also was investigated.

Experimental Part

Materials and Equipment.—Absorption measurements were made with a Beckman model DU quartz spectrophotometer with 10.003-cm. cells. A Beckman Model G *p*H meter with extension electrodes was used to measure *p*H. It was calibrated with standard acetate buffer according to the method of Michaelis.[7]

The ethylenediaminetetraacetic acid employed was furnished through the courtesy of the Bersworth Chemical Company, Framingham, Mass., and was further purified by two successive recrystallizations from water. The metal nitrates were Baker's Analyzed and Mallinckrodt C.P. products. The metal perchlorates were prepared from the corresponding nitrates by precipitation as the metal hydroxide which was then washed by decantation with distilled water until free of soluble salts. The product was then dissolved in perchloric acid and the *p*H was adjusted to between 4.0 and 4.5 with perchloric acid. The metal salts were standardized by a metal chelate titration developed by Martell and Jones.[8]

The potassium nitrate, potassium perchlorate and perchloric acid were J. T. Baker Analyzed grade reagents. The label analysis listed maximum impurities to be less than 0.02% in each case. Carbonate-free potassium hydroxide was prepared by a modification of the method of Schwarzenbach and Biedermann.[9] A 0.1 *M* potassium chloride solution was allowed to react with two successive batches of silver oxide over an extended period of time with occasional shaking. The resulting potassium hydroxide solution contained no detectable amount of chloride ion.

All solutions were brought to equilibrium in a constant temperature bath at 30° before absorption measurements were made. The temperature of the absorption cell in the spectrophotometer was found to remain at 30 ± 1°.

The metal complex was prepared by mixing solutions of the metal nitrate and the potassium salt of the complexing agent, and the *p*H of the resulting solution was adjusted to 4.5.

For the determination of relative stability constants, solutions were made up which contained equimolar amounts of each of two metal ions and of the dipotassium salt of ethylenediaminetetraacetic acid. The *p*H of the resulting solution was considerably lower than the solutions used because of displacement of hydrogen ions from the complexing anion. These conditions were employed because it was found that equilibrium was obtained relatively rapidly at low *p*H, whereas a similar solution prepared in the *p*H range 4–5 required in certain cases a number of days before equilibrium was reached. After the acid solution had been allowed to remain in the constant temperature bath for a few hours, the *p*H and ionic strength were adjusted to the desired values. The solutions were checked for equilibrium by determination of absorption over a period of time at various concentrations. All mixtures were found to have reached equilibrium after standing in the constant temperature bath overnight.

The Cu(II)–Pb(II), Ni(II)–Pb(II) and Cu(II)–Ni(II) systems were studied as a function of ionic strength in potassium perchlorate while the first two were also studied in potassium nitrate.

Calculation of Relative Stabilities.—The solutions of the metal nitrates and perchlorates, the metal complexes, and mixtures of two metal salts with the complex of one of them,

(1) G. Schwarzenbach and E. Freitag, *Helv. Chim. Acta*, **34**, 1503 (1951).

(2) G. Schwarzenbach and J. Heller, *ibid.*, **34**, 576 (1951).

(3) I. M. Kolthoff and C. Auerbach, *J. Am. Chem. Soc.*, **74**, 1452 (1952).

(4) S. S. Jones and F. A. Long, THIS JOURNAL, **56**, 25 (1952).

(5) R. C. Plumb, A. E. Martell and F. C. Bersworth, *ibid.*, **54**, 1208 (1950).

(6) A. E. Martell and R. C. Plumb, *ibid.*, **56**, 993 (1952).

(7) L. Michaelis, "Physical Methods of Organic Chemistry," Vol. I, second edition, Interscience Publishers, Inc., New York, N. Y., 1950, p. 1727.

(8) L. A. Jones, Thesis, Clark University (1952).

(9) G. Schwarzenbach and W. Biedermann, *Helv. Chim. Acta*, **31**, 330 (1948).

at equilibrium, were all found to obey Beer's law. Hence, the optical density of a mixture in terms of its components may be expressed by

$$D = ecl + e'c'l + e_a c_a l + e_a' c_a' l \qquad (1)$$

where c and c' are the concentrations of uncomplexed metal ions M and M', while c_a and c_a' are the concentrations of the corresponding metal complexes, e represents the corresponding extinction coefficient, and l is the length of the light path.

Since it has been shown[1,6,10] that, under the reaction conditions employed, only the 1:1 metal chelates of ethylenediaminetetraacetic acid need be considered, the equilibrium constant may be expressed by

$$K_c = \frac{[MY][M']}{[M'Y][M]} = \frac{c_a \times c'}{c_a' \times c} \qquad (2)$$

where [] represents molar concentration, H_4Y represents ethylenediaminetetraacetic acid and M represents the metal ion. Ionic charges are omitted for convenience. It is apparent that $K_c = K/K'$, the ratio of the equilibrium formation constants of the respective metal chelates. The total concentrations of metal species, C_M and $C_{M'}$, and of the complexing agent, C_Y, are also known, hence

$$C_M = c + c_a \qquad (3)$$
$$C_{M'} = c' + c_a' \qquad (4)$$
$$C_Y = c_a + c_a' \qquad (5)$$

Equations (1), (3), (4) and (5) are sufficient to calculate the only four unknowns, c, c', c_a and c_a', from the experimental measurement of optical density at one wave length. These quantities were then used to calculate K_c from equation (2). The values of e, e', e_a and e_a' were obtained from absorption measurements on the pure substances.

Absolute Stability Constants.—In strongly acid solutions the summation of the major forms of ethylenediaminetetraacetic acid present under the reaction conditions may be expressed by

$$\Sigma Y = [H_4Y] + [H_3Y^{-1}] + [H_2Y^{-2}] + [Y^{-4}]\left(\frac{[H^+]^4}{k_1k_2k_3k_4} + \frac{[H^+]^3}{k_2k_3k_4} + \frac{[H^+]^2}{k_3k_4}\right) \qquad (6)$$

where k_1, k_1, k_3 and k_4 are the successive acid dissociation constants of H_4Y. If this equation is solved for $[Y^{-4}]$ and substituted into equation (3), the expression for the formation constant becomes

$$K = \frac{[MY][H^+]^2\left(1 + \frac{[H^+]}{k_2} + \frac{[H^+]^2}{k_1k_2}\right)}{[M](k_3k_4)\Sigma Y} \qquad (7)$$

The dissociation constants k_1, k_2, k_3 and k_4 have been determined previously by a number of workers.[11-13] The values given by Carini and Martell, $k_1 = 4.3 \times 10^{-3}$, $k_2 = 1.6 \times 10^{-3}$, $k_3 = 5.6 \times 10^{-7}$ and $k_4 = 1.8 \times 10^{-10}$, were used in the calculations. These values introduced some error since they were obtained at 25° and in 0.1 M KCl solution. The values listed above required correction for hydrogen ion activity, assuming that the value reported by Harned and Hamer[14] for HCl in KCl, $\gamma\pm = 0.781$ holds for hydrogen ion. Thus the "hybrid" constants were converted to the "concentration constants" needed in the present investigation.

Equation (7) was applied to the nickel(II) and copper(II) chelates. Appreciable dissociation was found to occur only when the hydrogen ion concentration was greater than 0.01 M. Solutions of the metal chelates, initially at ionic strength of 0.1, were diluted with various quantities of 0.1 M potassium perchlorate and 0.1 M perchloric acid. The optical density was then taken at four wave lengths, and the concentrations of the metal complex and free metal ion were calculated with the previously-measured values of extinction coefficients of these substances. The extinction coefficients of the metals and metal chelates were checked as a function of pH before being used in the more acid region. Neither the metals nor the metal complexes showed any change in absorption spectra from pH 7 to the point where dissociation began.

Experimental Results

Relative Stabilities.—Absorptions of the free metal ions and metal complexes were measured for copper(II), nickel(II) and cobalt(II), respectively. In all cases strict adherence to Beer's law was observed in the spectral region from 400 to 1000 mμ. The corresponding extinction coefficients were then employed in the calculation of the concentration of the species present in the equilibrium mixtures of metal pairs and ligand. The copper(II) complex was most useful for this purpose because of its intense absorption band at 700 mμ. However, in many cases it was necessary to employ the weaker cobalt(II) bands, since the very stable copper(II) and nickel(II) complexes do not interact sufficiently with certain metal ions.

Data for the system copper(II)–nickel(II)–copper(II) complex–nickel(II) complex, and for the system copper(II)–lead(II)–copper(II) complex and lead(II) complex are shown in graphic form in Fig. 1. It is not possible to present data obtained for mixtures in the form used for solutions containing a single species. Therefore a "formal" extinction coefficient, ϵ_m, defined as follows, was employed

$$\epsilon_m = D/l\Sigma c_i$$

where

D = optical density
l = length of light path
Σc_i = total concentration of one of the colored metal ions in both the complexed and uncomplexed forms

In the first region of Fig. 1, λ 700–760 mμ, the copper(II) complex shows its maximum absorption, while neither nickel(II), lead(II) ions, or the corresponding complexes, show any appreciable absorption. The formal extinction coefficient in this case is based on the total Cu(II) concentration. On a qualitative basis, these data indicate that the nickel(II) chelate is more stable than that of lead-

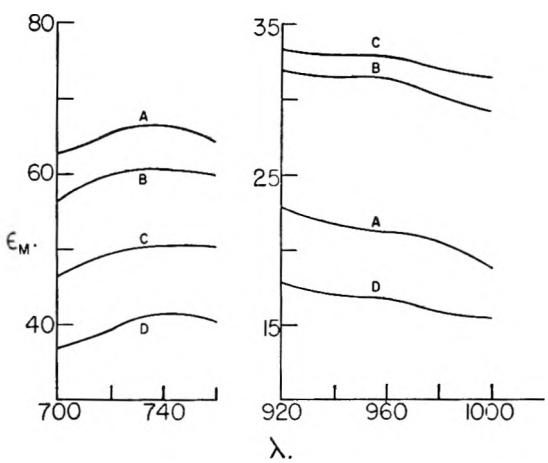

Fig. 1.—Formal extinction coefficient referred to the total Cu(II) concentration: (A) Cu(II)–Pb(II)–EDTA acid in the ratio 1:1:1; (B) Cu(II)–Ni(II)–EDTA acid, 1:1:1; (C) Cu(II)–Ni(II)–EDTA acid, 1:2:1; (D) Cu(II)–Pb(II)–EDTA acid, 2:3:1.

(10) See also a similar conclusion for the Nd(III) chelate by T. Moeller and Brantley, *J. Am. Chem. Soc.*, **72**, 5447 (1950).

(11) F. Carini and A. E. Martell, *ibid.*, **74**, 5745 (1952).

(12) G. Schwarzenbach and H. Ackermann, *Helv. Chim. Acta*, **30**, 1798 (1947).

(13) M. J. Cabell, A. E. R. E. Report C/R813, Ministry of Supply, Harwell, Berks., England, 1951.

(14) H. Harned and W. Hamer, *J. Am. Chem. Soc.*, **55**, 2194 (1933).

(II), since it displaces more copper(II) from the copper(II) complex, as evidenced by a greater lowering of the formal extinction coefficient of the copper species present. In the second region of Fig. 1, where the nickel(II) complex absorbs as strongly as the copper(II) complex, the relative stabilities are not apparent from absorption data. In this case various ratios of CuY/NiY give approximately the same optical density.

In Fig. 2, data are given for mixed complex systems of nickel(II)–zinc(II), nickel(II)–lead(II), and nickel(II)–cadmium(II), the formal extinction coefficients being calculated on the basis of total nickel content. The relative stabilities of the metal complexes for these metals is readily seen to be lead(II) >> zinc(II) > cadmium(II).

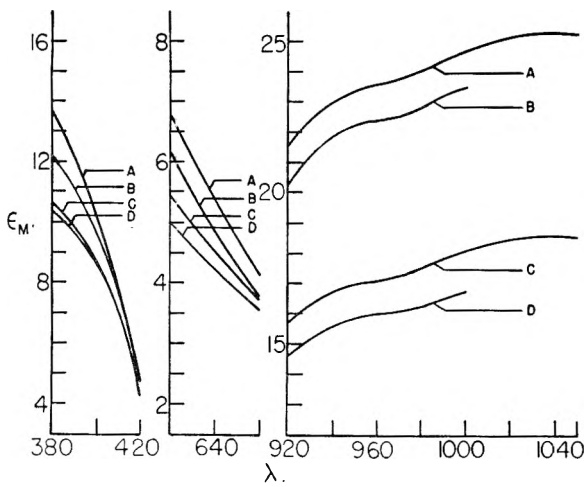

Fig. 2.—Formal extinction coefficient referred to total Ni(II) ion concentration: (A) Ni(II)–Cd(II)–EDTA in ratio of 1:2:1; (B) Ni(II)–Zn(II)–EDTA, of 1:2:1; (C) Ni(II)–Pb(II)–EDTA, of 1:1:1; (D) Ni(II)–Pb(II)–EDTA, of 2:3:2.

Not shown are the formal extinction coefficients based on the total Co(II) concentration after equilibration of the cobalt(II) complex with various proportions of lead(II), cadmium(II) and zinc(II) ions. Although the relationships were not as clear in this case, a visual comparison of the curves at 460 mμ, the cobalt complex maximum, indicated an increase in the interactions in the order cadmium(II) < zinc(II) < lead(II).

The results of the calculations of K_c by the method outlined above are listed in Table I. The relative stabilities at 30° in 0.1 *M* KNO_3 of the 1:1 ethylenediaminetetraacetate chelates are: Cu(II) > Ni(II) > Pb(II) > Co(II) > Zn(II) > Cd(II).

TABLE I

STABILITY CONSTANT RATIOS IN POTASSIUM NITRATE

$\mu = 0.1$; $t = \sim 30°$

Ratio	log K_c	Ratio	log K_c
CuY/NiY	0.315 ± 0.02	CoY/ZnY	0.07 ± 0.01
NiY/PbY	0.71 ± .02	CoY/CdY	0.30 ± .07
CuY/PbY	0.83 ± .03	NiY/CdY	2.46 ± .06
NiY/ZnY	2.20 ± .03	PbY/CoY	2

Effect of Ionic Strength.—The effects of decrease in ionic strength are given in graphic form in Figs. 3 and 4. In Fig. 3 it is seen that the ratio of stabilities of copper(II) to lead(II) chelates decreases sharply as the ionic strength of the potassium nitrate medium decreases. There is a somewhat less rapid decrease of stability constant ratio in potassium perchlorate solution. Both curves seem to approach the same value in dilute solutions, indicating a thermodynamic ratio of 2.3:1 at infinite dilution. The nickel(II)–lead(II) ratios in Fig. 4 show little change over the range of ionic strengths studied in both media. At lower ionic strengths, however, it seems that the ratios in potassium ni-

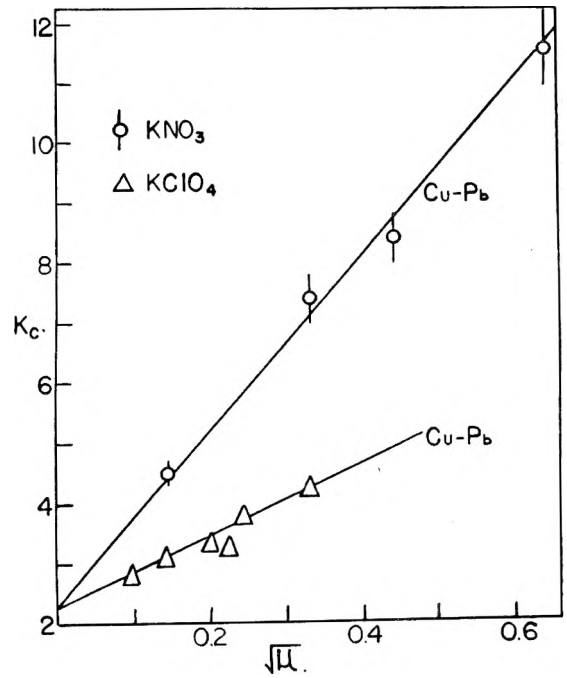

Fig. 3.—K_c for the ratio of Cu(II)–EDTA to Pb(II)–EDTA ions in potassium nitrate and potassium perchlorate at 30°.

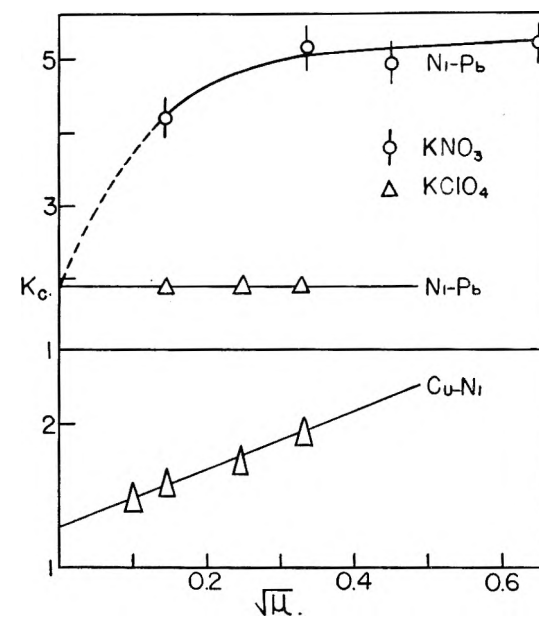

Fig. 4.—Upper graph, K_c for the ratio Ni(II)–EDTA to Pb(II)–EDTA ions in potassium nitrate and potassium perchlorate; lower graph, K_c for the ratio of the Cu(II)–EDTA to Ni(II)–EDTA ions in potassium perchlorate.

trate probably break sharply and become equal to the potassium perchlorate value at infinite dilution. The copper(II)–nickel(II) ratio in perchlorate solution, also shown in Fig. 4, has a definite slope analogous to that of the copper(II)–lead(II) system.

Absolute Stability Constants.—The results obtained for the stepwise dissociation of the nickel(II) complex at low *p*H are given graphically in Fig. 5. It is seen that as the hydrogen ion concentration is increased the intensity of absorption is greatly decreased, but the shape of the absorption band remains the same. The absolute stability constant for the NiY complex was calculated by the method outlined above, and from this the absolute stability constants were evaluated. The results are given in Table II.

TABLE II

METAL CHELATE FORMATION CONSTANTS

Metal	log *K*	Remarks	log *K* (Schwarzenbach) in 0.1 *M* chloride solution at 20°
Ni	17.5	Reference value	18.45
		Perchlorate sol.	
	17.5	Nitrate sol.	
Cu	17.8	Perchlorate sol.	18.34
	17.7	Nitrate sol.	
Pb	17.2	Perchlorate sol.	18.2
	16.8	Nitrate sol.	
		Reference value	
Co	15.4	Perchlorate sol.	
	15.4	Nitrate sol.	16.1
Zn	15.3	Perchlorate sol.	
	15.3	Nitrate sol.	16.2
Cd	15.0	Perchlorate sol.	
	15.0	Nitrate sol.	16.5

The dissociation of the copper(II) complex at low *p*H was also investigated. It may be seen that as the hydrogen ion concentration is increased, the curve shifts from its original shape. The maximum becomes broader at 700–760 mμ, and above 900 mμ the formal extinction coefficient rises above that of the normal complex. Apparently, therefore, one or more additional complex forms are present at low *p*H values. These may be hydrogen complexes similar to that described by Schwarzenbach and Heller[2] for the ferrous ethylenediaminetetraacetate complex.

Discussion

As a check on the self-consistency of the stability constant ratios, a series of interrelation tests were made by calculation of one ratio from two others involving a common metal. Thus the copper(II)–nickel(II) ratio is obtained by dividing the copper(II)–lead(II) ratio by the nickel(II)–lead(II) ratio. Results of such comparisons, given in Table III, show that the relative stabilities calculated by both the direct and indirect methods agree quite well. These results indicate that the spectrophotometric method is at least as sensitive as other methods previously employed for the determination of stabilities of transition metal–ethylenediaminetetraacetate chelates.

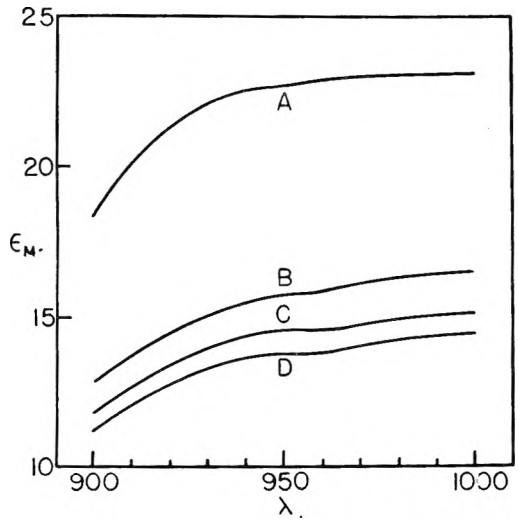

Fig. 5.—(A) Extinction coefficient of Ni(II) chelate at *p*H 4.5. Formal extinction coefficients of Ni(II) chelate in (B) 0.009 *M* $HClO_4$, (C) 0.018 *M* $HClO_4$ and (D) 0.025 *M* $HClO_4$.

TABLE III

RELATIVE STABILITIES CALCULATED BY DIRECT AND INDIRECT METHODS

Direct ratio	Indirect ratio	log *K* (direct)	log *K* (indirect)	Conditions
Cu/Pb	$\frac{Cu}{Ni}\cdot\frac{Ni}{Pb}$	0.63	0.55	$\mu = 0.1$ $KClO_4$
Cu/Pb	$\frac{Cu}{Ni}\cdot\frac{Ni}{Pb}$	0.38	0.37	$\mu = 0$
Cu/Ni	$\frac{Cu}{Pb}\Big/\frac{Ni}{Pb}$	0.29	0.37	$\mu = 0.1$ $KClO_4$
Cu/Ni	$\frac{Cu}{Pb}\Big/\frac{Ni}{Pb}$	0.37	0.38	$\mu = 0$
Ni/Pb	$\frac{Cu}{Pb}\Big/\frac{Cu}{Ni}$	0.34	0.26	$\mu = 0.1$ $KClO_4$
Ni/Pb	$\frac{Cu}{Pb}\Big/\frac{Cu}{Ni}$	0.27	0.26	$\mu = 0$
Ni/Cd	$\frac{Ni}{Zn}\cdot\frac{Co}{Cd}\Big/\frac{Co}{Zn}$	2.45	2.43	$\mu = 0.1$ KNO_3
Cu/Ni	$\frac{Cu}{Pb}\Big/\frac{Ni}{Pb}$	0.18	0.31	$\mu = 0.1$ KNO_3

The sharp drop in the relative stabilities of the copper(II) to lead(II) chelates in potassium nitrate as the ionic strength is decreased indicates the possibility of nitrate complexing. This idea is strengthened by the much lower slope for the same relative stabilities in potassium perchlorate solution, since the perchlorate ion is generally assumed not to form complexes with most bivalent metal ions. If consideration is restricted to the first nitrate complex of copper(II) and lead(II) ions, the corresponding formation constants K_{Cu} and K_{Pb} may be substituted into equation (2) to give

$$K'_c = \frac{[CuY]\left(\frac{\Sigma Pb}{1 + K_{Pb}[NO_3^-]}\right)}{[PbY]\left(\frac{\Sigma Cu}{1 + K_{Cu}[NO_3^-]}\right)} \qquad (8)$$

where ΣPb and ΣCu represent $[Pb^{+2}] + [PbNO_3^+]$ and $[Cu^{+2}] + [CuNO_3^+]$, respectively. These are the values obtained experimentally for the free metal ion. If it is assumed that there is no com-

plexing by perchlorate ion, K'_c can be evaluated from the K_c value obtained at the same ionic strength in perchlorate solution. Hence, for the nitrate solutions

$$K'_c = K_c \frac{1 + K_{Cu}[NO_3^-]}{1 + K_{Pb}[NO_3^-]} \quad (9)$$

This relationship may be rearranged to the linear form

$$K_{P_b} = \frac{K_c}{K'_c} K_{Cu} + \frac{K_c - K'_c}{K_c[NO_3^-]} \quad (10)$$

Substitution of experimental values of K_c, K'_c and $[NO_3^-]$ into this equation should give a series of straight lines intersecting at the common solutions for K_{Cu} and K_{Pb}. However, examination of the form of equation (9) indicates that the method is insensitive when the constants and nitrate concentration are small, since this would make the second term in both the numerator and denominator of the fraction small compared to unity. The equation is also insensitive when the nitrate complexing constants are nearly the same. Both sets of conditions apply in the present instance. Further, in order to solve (9) it was necessary to use data at very low nitrate concentration. The constants thus calculated varied by 50% and were several times the magnitude usually accepted for the metal ions investigated. On the other hand, the ratio of nitrate complexity constants determined from the data at 0.1 M nitrate concentration gives the ratio of nitrate complex formation constants as 6:3:2 for $PbNO_3^+$:$CuNO_3^+$: $NiNO_3^+$. It is believed that these relative values are fairly accurate. Although the measurement of the interaction of metals with nitrate ion is not the primary purpose of this research, it seems that evaluation of the absolute magnitude of the equilibrium constants would be possible by extension of the measurements to higher nitrate concentration.

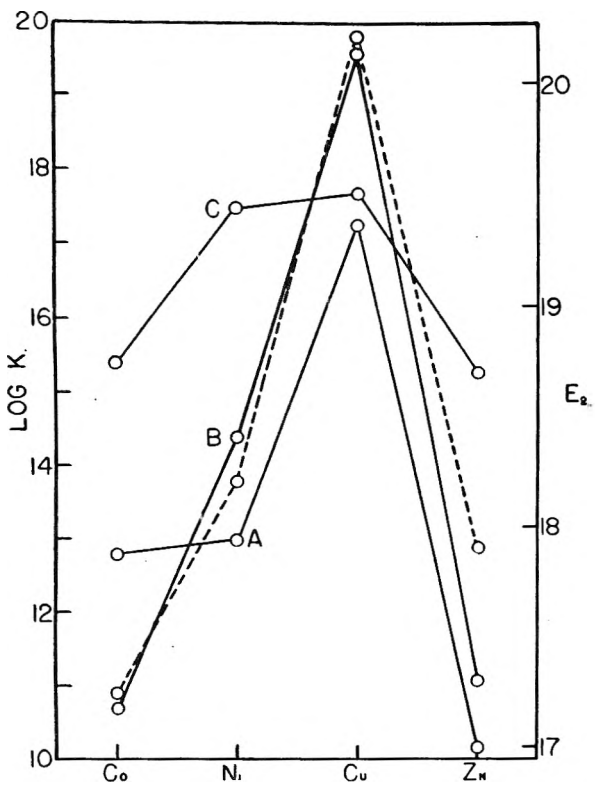

Fig. 6.—Chelate stability constants and ionization potential, as a function of atomic number. Solid lines: (A) log k_1k_2 of acetylacetone, (B) log k_1k_2 of ethylenediamine, and (C) log k of ethylenediaminetetraacetic acid chelates. Dotted line: second ionization potential (E_2).

The values of the absolute stability constants reported in Table II for nitrate solution were calculated from the measured relative stabilities and the absolute constant for the lead(II) nitrate complex calculated by the equation

$$K'_M = K_M (1 + K_{MNO_3}[NO_3^-])$$

where K'_M is the constant determined in perchlorate solution, K_M is the constant determined in nitrate solution without correcting for nitrate complexing, and K_{MNO_3} was assumed to be 15, the value reported by Harned and Owen[15] as the nitrate complex formation constant for lead(II) at 25° and 0.1 μ. Thus, the values reported in Table II for nitrate solution are uncorrected values, which may be employed directly to calculate metal ion concentrations in 0.1 M nitrate solution.

The perchlorate constants listed in Table II for Co(II), Zn(II) and Co(II) were calculated on the assumption that the ratios for these metals in perchlorate solution are the same as in nitrate solution. This assumption is justified by the form of equation (9) and the small nitrate complexity constants for these metals.

The effect of ionic strength on the stability constant ratios in perchlorate solution must ultimately be resolved in terms of the activity coefficients of the species involved, and so it would be well to consider the similarities and dissimilarities of the corresponding molecular structures. In the case of nickel and lead, the activity coefficients of the two metal ions would be expected to show about the same dependence on ionic strength. Thus, the ratio should be close to unity. The two complexes are probably hexadentate, and thus completely enclosed by the complexing anion. Since the structures and the charges are so similar, we might expect the activity coefficient ratio to remain close to unity. The over-all effect would then be small, and this is apparently the case experimentally.

The marked dependence on ionic strength of the copper(II)–lead(II) and copper(II)–nickel(II) systems is interesting in view of the fact that the metal ions involved are of the same valence type. A similar system,[16] copper(II) and nickel(II) sulfate, actually shows exactly the same dependence on ionic strength up to 0.7 molal. In each case one entity, the lead(II) or the nickel(II) complex, is hexadentate, while the copper(II) complex is square planar. A structural difference of this type would be expected to give rise to appreciable differences in the activity coefficient, except in an infinitely dilute solution.

Much of the discrepancy between stability constants obtained in this investigation and those reported by Schwarzenbach and Freitag[1] is due to the

(15) H. Harned and B. Owen, "The Physical Chemistry of Electrolytic Solutions," second edition, Reinhold Publ. Corp., New York, N. Y., 1950, p. 147.

(16) See reference 15, p. 427.

difference in the value employed for the fourth dissociation constant, k_4, of ethylenediaminetetraacetic acid. The insertion of Schwarzenbach's value of k_4 into equation (7) brings our results into better agreement with his: Ni, 18.0; Cu, 18.3; Pb, 17.7; Co, 15.9; Zn, 15.8; and Cd, 15.5. It is to be expected that some differences in the results would remain, in view of the fact that the present investigation was carried out at a higher temperature and in a different electrolyte. The order of stabilities obtained in this investigation also differs somewhat from that determined by Schwarzenbach and Freitag. However, these discrepancies are not surprising, in view of the strong effect of a supposedly inert electrolyte on the values of the relative stabilities of the chelate systems illustrated in Figs. 3 and 4.

It has been pointed out by Irving and Williams[17] that the divalent metal ions exhibit the same order of stability with a large number of ligands, *e.g.*, ethylenediamine, propylenediamine, ammonia and salicylaldehyde. This order of stability, Cu > Ni > Co, Zn > Cd, is the same as that obtained in the present investigation.

The stabilities of various chelates of a number of the first row transition metals are plotted *vs.* atomic number in Fig. 6. It is apparent that all the ligands show similar behavior with the metals in this series in that the stabilities increase as the atomic number increases, with a maximum at copper(II), followed by a sharp drop in stability for the zinc(II) complexes. The ethylenediaminetetraacetate chelate differs remarkably from the others shown in Fig. 6 in that the plot is much flatter, and the reagent is correspondingly much less selective for the transition metals.

The correlation of chelate stability constants of the transition metals with the second ionization potential of the metal, first suggested by Calvin and Melchior,[18] has been found to hold for a wide variety of ligands. The ionization potentials plotted in Fig. 6 as a function of atomic number, indicate that this correlation holds for all the metals and ligands shown. The correlation with ethylenediaminetetraacetate chelate stabilities differs from the others shown in that the properties of the metal ions, as measured by the ionization potentials, apparently have much less influence on chelate stability than is the case for the other ligands.

Acknowledgment.—The authors are indebted to the U. S. Navy Office of Naval Research for the support of this work under contract Nonr-596(00).

(17) H. Irving and R. Williams, *Nature*, **162**, 746 (1948).

(18) M. Calvin and N. C. Melchior, *J. Am. Chem. Soc.*, **70**, 3270 (1948).

THE STRUCTURE OF OXYGEN FLUORIDE

BY JAMES A. IBERS[1] AND VERNER SCHOMAKER

Contribution No. 1774 from the Gates and Crellin Laboratories of Chemistry, California Institute of Technology, Pasadena, California

Received January 26, 1953

A bond angle of 103.8 ± 1.5° and a bond length of 1.413 ± 0.019 Å. have been found for oxygen fluoride by the method of electron diffraction. Combining our data with the spectroscopic rotational constant reported by Bernstein and Powling,[2] we arrive at a bond angle of 103.2° and a bond length of 1.418 Å. as most probable values. Special attention was given the problem of weighting the measured ring diameters, and a simple adjustment was finally adopted which may prove useful in other electron diffraction work of this kind.

The bond length and bond angle in oxygen fluoride (OF_2) are of interest, especially in relation to the values for other simple compounds of the electronegative elements, but they have not been precisely determined. The best previous values are dependent on early electron diffraction results and on a single spectroscopically determined molecular constant.

For the present electron diffraction reinvestigation Professor L. Reed Brantley of Occidental College kindly gave us a one-to-one OF_2–O_2 mixture prepared by the usual method.[3] After nearly all the oxygen had been pumped off at liquid-nitrogen temperature,[4] the sample was fractionally distilled at about −160° through a 65-cm. vacuum-jacketed column; iodometric analyses of the product ranged from 98.5 to 99.4 mole % OF_2. Photographs were made and interpreted in the usual way,[5] except that in view of the simplicity of the problem the visual and radial distribution curves were not drawn. The camera distance and electron wave length were 10.91 cm. and 0.06056 Å., respectively.

Intensity curves were calculated for rigid, symmetrical OF_2 models with O—F = 1.42 Å. and F · · · F ranging from 2.10 to 2.32 Å., for various admixtures of O_2. Figure 1 shows three of the curves for pure OF_2 with critical marks[6] to indicate important comparisons with the photographs. The more sensitive features, important for the angle determination, are marked on curves A and C, and the less sensitive features on curve B. Finally, the measured ring positions were compared with

(1) National Science Foundation Predoctoral Fellow, 1952–1953.

(2) H. J. Bernstein and J. Powling, *J. Chem. Phys.*, 18, 685 (1950).

(3) P. Lebeau and A. Damiens, *Compt. rend.*, **188**, 1253 (1929); O. Ruff and W. Menzel, *Z. anorg. u. allgem. Chem.*, 190, 257 (1930); G. H. Cady, *J. Am. Chem. Soc.*, **57**, 246 (1935).

(4) The fact that OF_2 can be obtained in about 95% purity by pumping off the oxygen at liquid-nitrogen temperature has been confirmed by the recent work of J. G. Schnizlein, J. L. Sheard, R. C. Toole and T. D. O'Brien, THIS JOURNAL, **56**, 233 (1952).

(5) K. Hedberg and A. J. Stosick, *J. Am. Chem. Soc.*, **74**, 954 (1952).

(6) W. F. Sheehan, Jr., and V. Schomaker, *ibid.*, **74**, 4468 (1952).

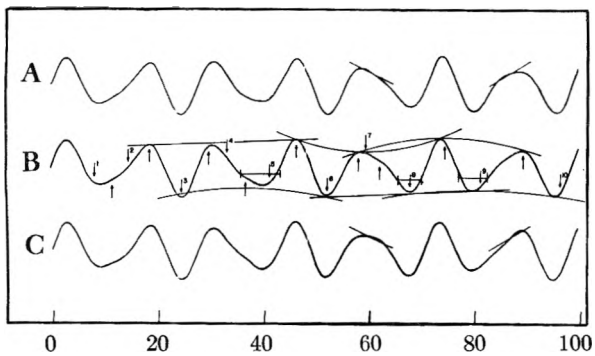

Fig. 1.—Theoretical intensity curves for rigid, symmetrical models of OF_2 with the O—F distance 1.42 Å. and the indicated bond angles: A, 102.8°; B, 103.8°; C, 104.8°.

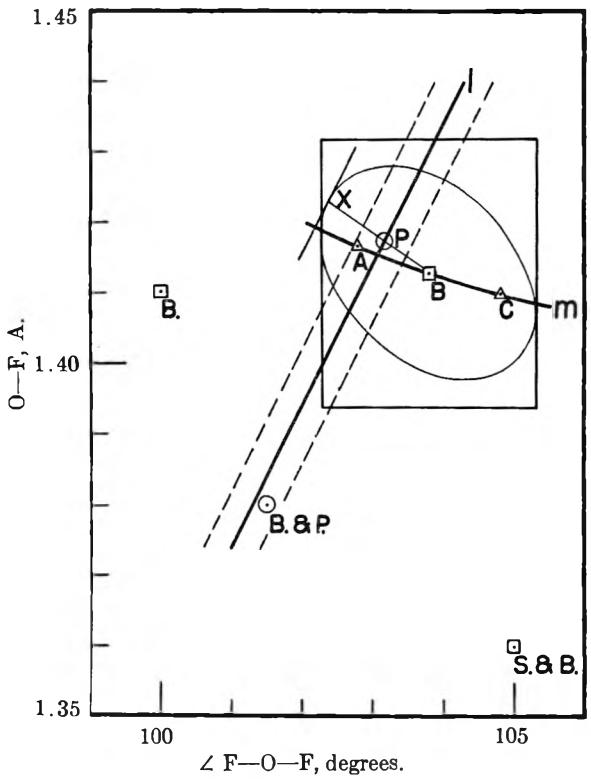

Fig. 2.—Bond length and bond angle values for OF_2. See text and Table II.

the positions read from curves A, B and C, with the results shown on curve m of Fig. 2. The details of the comparison are given for curve B by Table I.

In regard to Table I, some special remarks are in order. We give the unbiased estimate $s = \{\Sigma w_i(x_i - \bar{x})^2/(n-1)\}^{1/2}$ of the standard deviation of a $(q_{calc.}/q_{obs.})_i = x_i$ value of unit weight, as well as the weighted average deviation $\Sigma w_i|x_i - \bar{x}|/\Sigma w_i$, which, although quoted in our previous papers, seems to have no simple statistical meaning if the weights are not all equal.

Two related points confirm the belief, commonly held in this work, that truly random errors in the measurements of ring diameters are unimportant: the estimated standard deviation of the weighted mean $s/(\Sigma w_i)^{1/2}$ is about ±0.0015, considerably less than would correspond to the limit of error ±1.0% which, in accordance with our experience, had to be assigned to the scale factor; and even the deviations $(x_i - \bar{x})$ appear to represent mainly systematic error, since the four to thirteen individual measurements per ring by each observer lead to estimates of the standard deviations of the x_i that amount typically to only about a third of the values which correspond to s and the w_i as given in Table I.

TABLE I

ELECTRON DIFFRACTION DATA FOR OF_2

Min.	Max.	$q_{obs.}$	$q_B/q_{obs.}$	Wt. (w_i)
1		8.43	1.091	0
	1	11.71	1.016	0
2		14.79	0.960	0
	2	18.85	0.987	2
3		24.67	0.997	5
	3	30.09	1.017	0
4		33.32	1.035	0
	4	36.59	1.017	0
5		41.30	0.964	0
	5	46.44	0.997	10
6		52.23	0.998	10
	6	58.12	1.007	0
7		59.65	1.018	0
	7	62.20	1.013	0
8		67.94	0.999	10
	8	74.73	0.989	10
9		81.43	0.980	1
	9	89.51	0.993	1
10		96.59	0.990	2
Weighted mean:				0.9949
Estimated standard deviation of value of unit weight (s):				0.012
Weighted average deviation:				0.004

The weights were first assigned in about the usual way, *i.e.*, a smooth function of q rising from zero for the inner rings and falling toward zero again for the outermost rings was modified by factors of a half or a quarter for minor or for highly unsymmetrical features. The distribution of the resulting quantities $w_i(x_i - \bar{x})^2$ with respect to q and to classes of features—maxima *vs.* minima, the symmetrical *vs.* the unsymmetrical, etc.,—was satisfactory except that the weights for the unsymmetrical features (max. 1, 3, 4, 6, 7; min. 1, 2, 4, 5, 7) needed to be reduced by a factor of about one-tenth in order to equalize the estimates s to be obtained separately from them and from the symmetrical features. The final weights (Table I) were placed on a scale of ten and so vanish for all unsymmetrical features. This is satisfactory for the calculation of the average, but is hardly satisfactory for the estimation of the standard deviation. With this reservation, however, zero weights are indicated in most cases, as in reference 10, where fractional weights have been used for complex features. The above argument applies to the averaging of measurements by J. I. and V. S., but we have used only the simple averages.

We would emphasize that these remarks, despite their stress on other details are not intended to detract from the usual scrutiny of the $(q_{calc.}/q_{obs.})$ values for possible trends or for undue sensitivity of the average to reasonable variations of the weights. In this regard, the present average is somewhat more sensitive than usual.

The results from this and from previous electron diffraction investigations are given in the first three lines of Table II. The fourth entry represents Bernstein and Powling's adjustment of Boersch's result to the region between the dashed

TABLE II

THE STRUCTURE OF OF_2

O—F, Å.	∠ F–O–F, degrees	
1.36 ± 0.1	105 ± 5	Sutton and Brockway[7]
1.41 ± 0.05	100 ± 3	Boersch[8]
1.413 ± 0.019	103.8 ± 1.5	Present work
1.38 ± 0.03	101.5 ± 1.5	Bernstein and Powling[2]
1.418	103.2	Best value

(7) L. E. Sutton and L. O. Brockway, *J. Am. Chem. Soc.*, **57**, 473 (1935).

(8) H. Boersch, *Monatsh.*, **65**, 311 (1935).

lines in Fig. 2 defined for a rigid model by their value 1.60 ± 0.02 cm.$^{-1}$ for the rotational constant $A'' - B''$, and the last entry represents our related adjustment of the present result.

Our adjustment (see Fig. 2) differs from Bernstein and Powling's in that we take the point P lying on the line l defined by $A'' - B'' = 1.60$ cm.$^{-1}$ which seems most probable on the basis of the electron diffraction work. For this purpose we have assumed a probable error function which depends upon a sum of the squares of the errors in bond angle and in the scale factor, with coefficients such that the limiting errors in bond angle (±1.5°) and in the scale factor (±1.0%) correspond to the same probability. Plotted as a function of bond angle and bond length with the help of the linear relation between assumed bond angle and resultant bond length which is approximated at B by curve m, the corresponding ellipse takes the form shown; the indicated construction for P follows. (It is appropriate to place P exactly on l, since the indicated relative weights of the spectroscopic and diffraction data for the location of P along the line BX are about 20:1.) For their adjustment, on the other hand, Bernstein and Powling essentially used their result to reduce Boersch's limits of error and quoted only rounded values for a point symmetrically located with respect to the reduced limits.

It is notable that in OF_2 the bond angle is greater than in NF_3 (102°9′,[9] 102.5° [10]), whereas in H_2O (105°3′ [11]) it is less than in NH_3 (106°47′[11]). Nevertheless, the bond angle in OF_2 is somewhat less than in H_2O, in agreement with a discussion previously given for NF_3 and NH_3.[10] The new O—F bond length, being appreciably greater than Bernstein and Powling's value, is again in good agreement with the radius values and interpolation formula given previously.[12]

(9) J. Sheridan and W. Gordy, *Phys. Rev.*, **79**, 513 (1950).
(10) V. Schomaker and C. S. Lu, *J. Am. Chem. Soc.*, **72**, 1182 (1950).
(11) G. Herzberg, "Infrared and Raman Spectra of Polyatomic Molecules," D. Van Nostrand Co., Inc., New York, N. Y., 1945, pp. 489, 439.
(12) V. Schomaker and D. P. Stevenson, *J. Am. Chem. Soc.*, **63**, 37 (1941).

NON-STEADY STATE ELECTROLYSIS UNDER CONSTANT CURRENT[1]

By Lucien Gierst and Andre L. Juliard[2]

University of Brussels, Belgium, and Houdry Process Corporation, Marcus Hook, Pennsylvania

Received February 7, 1953

Valuable information about the kinetics of reactions occurring at the surface of an electrode can be obtained from the study of the time dependence of the potential of a working electrode during the non-steady state electrolysis which follows the forcing through the cell of a constant high current density. When the rate of the electrolysis depends solely upon the speed of diffusion of the depolarizer, the product $iT^{1/2}$, of the constant current and the square root of the transition time, remains constant. When the rate of electrolysis is also controlled by a chemical reaction, the product $iT^{1/2}$ decreases linearly with the current density. This product acquires abnormally high values when the electrolysis process is accompanied by electrocapillary convection. The study of the relation between the product $iT^{1/2}$ and the current i may also give a better understanding of the action upon the mechanism of electrolysis of substances adsorbed on the electrode.

Introduction

Non-steady state electrolysis under constant current was investigated more than half a century ago by Weber[3] and Sand[4] as a method for determining diffusion constants. More recently this type of electrolysis has been used by Muller and Schwabe[5] as a procedure to study anodic polarization of metals, and by Rius, *et al.*,[6] as an analytical tool.

This type of electrolysis appears furthermore to be a convenient method for elucidating the mechanism of electrochemical reactions.[7]

Constant current non-steady state electrolysis occurs during the short time following the connecting of a cell to a high d.c. voltage supply through a current limiting resistance. When the cell contains a micro working-electrode (approximately 1 sq. mm.) and a large reversible counter-electrode (approximately 300 sq. mm.), the potential of the working electrode varies with the time during the transient-time ($t_3 - t_0$) according to one of the three curves of Fig. 1.

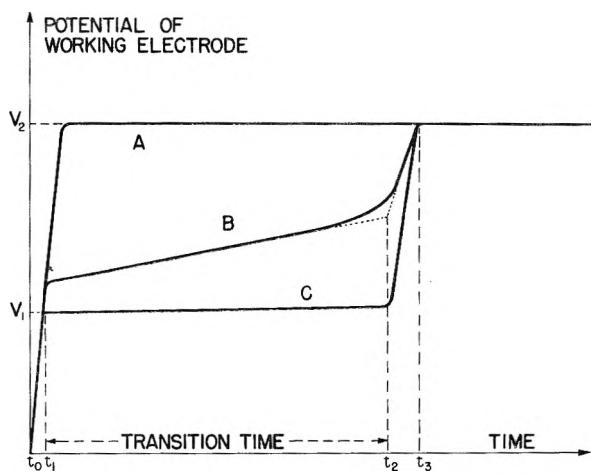

Fig. 1.—Voltage–time curves during transient electrolysis under constant current: A, supporting electrolyte alone; B, supporting electrolyte plus "non-reversible" depolarizer; C, supporting electrolyte plus "reversible" depolarizer.

Curve A is recorded when the cell contains only a supporting electrolyte.

Curve C appears when a small amount of a "reversible" depolarizer is added to the supporting

(1) This paper, presented at the Miniature Meeting of the Philadelphia Section of the American Chemical Society, January 29, 1953, is a summary of the thesis presented by Dr. Lucien Gierst in partial fulfillment of the requirement for the Doctor's degree at the University of Brussels in 1952.
(2) Houdry Process Corporation, Marcus Hook, Penna.
(3) H. F. Weber, *Wied. Ann.*, **7**, 537 (1879).
(4) H. J. S. Sand, *Phil. Mag.*, [6] **1**, 45 (1901).
(5) E. Muller and K. Schwabe, *Z. Elektrochem.*, **39**, 414 (1933).
(6) A. Rius, J. Llopis and S. Polo, *Anales fis. quim. Esp.*, **45B**, 469 (1949).
(7) L. Gierst and A. Juliard, "Proceedings of the 2nd Meeting of the International Committee of Electrochemical Thermodynamics and Kinetics," Tamburini, Milan, 1950, pp. 117 and 279.

electrolyte. In such a case, the transient time is composed of three different periods:

A. The capacity-controlled period ($t_1 - t_0$), during which the potential increases practically linearly with time until a value at which the depolarizer begins to be reduced at a measurable speed is reached.

B. The depolarization-controlled period or **transition time** ($t_2 - t_1$), during which the potential of the working electrode is "buffered" by the depolarizer. This buffering effect lasts as long as the current is primarily consumed by the depolarizing process. *The length of this time interval depends on the kinetic characteristics of the over-all reaction*, being shorter when the rate of the electrolysis is limited by the speed of an intermediate chemical step, or lengthened when the electrolysis is accompanied by electrocapillary convection.

C. The mixed process-controlled period ($t_3 - t_2$), during which the potential increases again quite rapidly with time, but at a slower rate than during the capacity controlled period. In this last period only a fraction of the current is used by the electrolysis process, the residual current is consumed by the charging of the double layer until the potential reaches V_2, at which the cation of the supporting electrolyte undergoes reduction.

Curve B shows the characteristics of the non-steady electrolysis when the depolarizer is a "non-reversible" one, requiring an activation over-voltage for reduction. With such a depolarizer the voltage may substantially increase during the transition time, especially at the end of this period. The end of the transition time is not as sharply defined as with a "reversible" depolarizer. The transition time can, however, be exactly measured by extrapolating the two segments of the voltage–time curve which correspond, respectively, to the depolarization and to the mixed process-controlled periods.

The duration of the transition time: (a) increases with the concentration of the depolarizer and, at equal concentration, with the diffusion coefficient; (b) decreases with increasing current density; (c) depends upon the speed of the surface reaction or upon the speed of transformation of the depolarizer into a more readily reducible molecule or ion, when these speeds are lower than the diffusion rate.

This paper will show what kind of information regarding the kinetics of electrode processes can be obtained from the study of the relation between the transition time and the value of the constant current.

Experimental

A. Electrolytic Cell.—The cell is a double-walled Pyrex vessel of 2 cm. internal diameter and 10 cm. height, thermostated with circulating water controlled at 25.0 ± 0.1°. The thermostat water contains an electrolyte and is grounded in order to screen the cell from any induced current.

The working-electrode is a freshly formed small drop of mercury which grows very slowly, at a constant speed, at the bottom of a capillary tube. The speed of growth of the drop is controlled by a 20-cm. "marine barometer tubing" capillary having 0.05 mm. internal diameter. This tube is slightly constructed in its central part in order to provide drops of a lifetime of about sixty seconds at 80 cm. Hg pressure. The electrolysis starts about 20 seconds after the appearance of a new drop, and is completed in a fraction of a second. Under these conditions, the electrolysis occurs on an electrode of practically constant area.

The surface of the electrode is determined with high precision by the drop controlling capillary and by an electronic circuit which starts the electrolysis at a selected time after the appearance of a new drop.

Switching this circuit: (a) activates a relay which causes a hammer to knock against the capillary drop controlling tube. The shock detaches the drop already formed at the bottom of the capillary. At that very moment, a drop starts to grow.

(b) Disconnects the grid of a Thyratron (type 2D21) from the negative pole of an auxiliary battery. From that time, the potential of the control grid, previously at −20 to −80 v., becomes more positive. The rate of increase of the grid potential is controlled at about 2 volts per second by a resistance capacity circuit.

When the Thyratron fires, a second relay cuts out the short circuit across the electrolytic cell, starting abruptly the electrolysis at a definite time after the birth of the drop. Keeping constant all the other growth controlling factors, the reproducibility of the area of the electrode depends only on the reproducibility of the circuit delay. Oscillographic measurements have shown that by using stabilized voltages and a preheating time of half an hour, this delay is reproducible within less than 0.2%.

B. Polarizing Circuit.—In order to determine with accuracy the value of the current density applied to the working-electrode, not only the area of the electrode but also the values of the applied voltage and the limiting-resistance must be exactly known.

The voltage applied to the resistance-cell circuit is obtained from a 400-volt stabilized power supply of conventional design. The voltage is set at any desired value between 200 and 100 volts by means of a voltage divider, and is measured with a potentiometer.

The limiting-resistances are high quality 10 watt 25, 50, 100 and 200 kilohm resistances, whose exact values were checked at regular intervals with a Cambridge precision potentiometer.

The variation of the counter-electromotive force of the cell that occurs during the electrolysis would depress the current to about 1% of its initial value. This effect is reduced to less than 0.1% by placing a 20-ohm potentiometer in series with the cell. This potentiometer is adjusted before the electrolysis to the previously determined value corresponding to the back electromotive force of the cell during the transition time.

C. Potential Time Recorder.—The potential *versus* time curve is recorded by means of a large (30 cm. diameter) magnetically deflected cathode ray tube. The change of potential of the working electrode produces, through a d.c. amplifier, a radial deflection of the electron beam, while the time is recorded by the angle of rotation of the beam. The voltage scale is adjusted in such a manner that the voltage is recorded sweeping from the periphery inwards. By adjusting the speed of rotation of the deflecting electromagnets, the fraction of the voltage–time curve corresponding to the transition time may be stretched over a complete circumference, the length of which corresponds in this case to about 70 cm.

The voltage scale is checked before each experiment by tracing on the screen, by means of a voltage divider, concentric reference voltage circles in 0.25-volt steps.

The time is roughly measured by the value of the angle of rotation of the spot as related to the speed of rotation of the deflecting coils. Very accurate time intervals (accuracy better than 0.01 millisecond) were determined by modulating the intensity of the electron beam with a constant frequency. This frequency was checked against that of a tuning fork (frequency 1,024 c.p.s.), used as standard. The time measuring scale can be magnified for short transient electrolysis by increasing simultaneously the speed of rotation of the deflecting coil and the frequency of the impulse generator which modulates the electron beam.

Because of the persistence of the luminescence of the screen, the trace of the voltage–time curve remains clearly visible during about one minute. This allows visual measurement of the transition time simply by adding the pulsed luminous points along the constant voltage line.

D. Reagents.—All reagents were Merck Analytical Grade products. The absence of any reducible impurities

at a concentration higher than one thousandth of the concentration of the depolarizer has been checked for each solution by polarographic analysis.

Conventional procedures were used to eliminate oxygen dissolved in the solution and impurities present in the mercury.

E. Reproducibility of Measurements. 1.—In sets of successive determinations of transition-times of the range of 100 milliseconds, the *maximum* deviation was less than 0.4% of the average value. The surface of the mercury electrode, which depends primarily on this factor, may thus be reproduced within these limits.

2.—The drift of the average value of five determinations during an interval of time of ¾ of an hour was less than 0.3%.

As the complete investigation of the non-steady electrolysis of a solution under different current densities can be made in triplicate in less than 15 minutes, the term $T^{1/2}$ may be known to within 0.2%.

Description and Discussion of the Results

A simple mathematical equation can be deduced from Fick's diffusion equation[4,8] which relates the transition time, T, to the current, i, by assuming that during this period, the following conditions are fulfilled: 1. The current remains practically constant; 2. The current is almost exclusively consumed by the reduction of the depolarizer; 3. The depolarizer reaches the working-electrode exclusively by diffusion; 4. The concentration of the depolarizer at the beginning of the electrolysis is the same throughout the solution; 5. The rapidity of the depolarizing process must be great compared to the diffusion rate.

In order to satisfy: *Condition 1:* The current-limiting resistance must be several hundred times greater than the cell resistance. *Condition 2:* The concentration of the depolarizer must be high enough so that even with electrolysis performed at high current densities the capacity component of the current during the transition-time remains less than 1% of the total current. This condition is fulfilled even for current densities in the range of 500 milliamperes per square cm. when the concentration of the depolarizer is higher than 10 milliequivalents ion per liter. *Condition 3:* The electrolysis must be performed under normal polarographic conditions, in the absence of any migration, and thermal, gravitational, mechanical or electrocapillary convection. When using as working-electrode a stationary mercury drop, the transient time must be short enough (less than 1 second) to keep the thickness of the diffusion controlling layer covering the electrode a negligible fraction of the radius of curvature of the electrode. *Condition 4:* The solution must be homogeneous, and the working electrode must be free from any foreign adsorbed substance. *Condition 5:* The depolarizer must be rapidly reduced at the surface of the electrode, without any slow intermediate reaction step.

A. Diffusion-controlled Electrolysis.—When all the above five specified conditions are fulfilled, the following equation[6,8] gives the relation between the time of the non-steady electrolysis and the concentration of the depolarizer at the surface of the electrode

$$C - C(x,t) = 2i(t/\pi D)^{1/2}/nF \qquad (1)$$

(8) T. R. Rosebrugh and W. L. Miller, THIS JOURNAL, 14, 816 (1910).

where

C = concn. of the depolarizer in the bulk of the sol., mmoles per l.
$C(x,t)$ = concn. of the depolarizer at the surface of the electrode after t sec.
i = controlled constant current density, milliamp. per sq. cm.
D = diffusion coefficient of the depolarizer, cm.^{2} sec.$^{-1}$
n = no. of electrons involved in the electrochemical process
F = Faraday constant, coulombs

If the electrolysis is exclusively controlled by the diffusion of the depolarizer, the end of the transition time is the moment at which the concentration of the depolarizer in the vicinity of the surface of the electrode falls close to zero.

In this case equation 1 becomes

$$iT^{1/2} = nFC(\pi D)^{1/2}/2 = KD^{1/2}C \ (K = nF\pi^{1/2}/2) \qquad (2)$$

where T = transition time, millisec.

The product $iT^{1/2}$ is thus linearly proportional to the square root of the diffusion coefficient and to the concentration of the depolarizer, the factor of proportionality, K, being a product of universal constants.

When $iT^{1/2}$ is plotted against i, a straight line is obtained. The intercept with the $iT^{1/2}$ axis is $KD^{1/2}C$. *The diffusion coefficient D or the concentration C of the depolarizer can be determined with a fairly good accuracy from this intercept.* The square proportionality between the transition time and the concentration emphasizes the importance of transition time measurement as an analytical method for accurate determination of depolarizers.

The non-steady electrolysis of cadmium ion in potassium chloride solution on a mercury electrode belongs to this type of diffusion-controlled electrolysis. Table I shows that in this electrolysis the product $iT^{1/2}$ remains constant within 0.6% even when the current density changes tenfold (from 0.18 to 1.18 milliamp. per square mm.) and the transition time almost a hundred-fold (from 1.4 to 125 milliseconds).

TABLE I

VALUE OF THE PRODUCT $iT^{1/2}$ IN FUNCTION OF i IN THE NON-STEADY STATE ELECTROLYSIS OF CADMIUM IN PRESENCE OF CHLORIDE IONS AT 25.0 ± 0.1°

Depolarizer, 2.46 ± 0.01 × 10^{-2} N Cd(II); potential, −0.64 v./S.C.E.; supporting electrolyte, N KCl plus 1 × 10^{-4} N HCl; surface of the electrode, 1.72 mm.^{2}

Current, i, milliamp. per 1.72 square mm.	Transition time, T, 1/1024 sec. (n = 4)	Product $iT^{1/2}$ 55.1 milliamp. sec.$^{1/2}$ mm.$^{-2}$
0.300	124.1 ± 0.1	3.34
0.600	30.3 ± .1	3.30
0.900	13.3 ± .1	3.28
1.200	7.50 ± .08	3.29
1.800	3.38 ± .02	3.31
2.200	2.24 ± .02	3.29
2.800	1.38 ± .01	3.29
0.300	122.8 ± .8	3.33
	Av.	3.30 ± 0.02

The transition time and the constant current density are likewise related (according to equation 2) in the following "reversible" systems: Cd(II) in 1 M KI, or in 1 M NH_4OH + 1 M H_4NCl; Pb(II)

in 1 M NaOH, or in 1 M KNO_3; Zn(II) in 1 M H_4NOH + 1 M H_4NCl; IO_3^- in 1 M KCl; and H_3O^+ (HCl 1.10^{-2} M) in 1.5 M KCl.

In all these "reversible" systems the speed of the non-steady state electrolysis is thus exclusively determined by the diffusion rate of the depolarizer.

The same process occurs with some "semi-reversible" systems, like Ni(II) or Co(II) in 1 M KCl solution, for which the product $iT^{1/2}$ is also independent of the value of the constant current.

B. Reaction Rate-controlled Electrolysis.—In some cases the transition time comes to an end before the concentration of the depolarizer at the surface of the electrode is reduced to zero. This occurs, for instance, when the depolarizer is not immediately reduced on the electrode, but undergoes beforehand a reaction giving rise to a more reducible species P'

$$P \xrightarrow{k} P' \qquad (3)$$

which proceeds with a lower speed than that with which the depolarizer diffuses to the electrode.

Assuming that the rate of formation of the readily reducible species is directly proportional with coefficient k to the concentration of the depolarizer, the transition time ends when the concentration of the depolarizer on the electrode is

$$C(o,T) = i/nFk \qquad (4)$$

Substituting this value for $C(x, t)$ in 1 we get

$$C - i/nFk = 2i(T/D)^{1/2}/nF^{1/2}$$

or

$$iT^{1/2} = (\pi D)^{1/2}(nFC - i/k)/2 = KD^{1/2}C - K'i$$
$$(K = nF^{1/2}/2 \text{ and } K' = 1/2K) \qquad (5)$$

where k represents a kinetic "surface" coefficient, closely related to the kinetic "volume" constant of reaction.[3] The constant k measures the maximum number of P' species which can be formed per unit time on a surface of one square cm. from a solution containing one millimole of depolarizer per liter.

Inspection of equation 5 shows that in a reaction rate-controlled electrolysis the product $iT^{1/2}$ is not independent of the constant current. When the rate controlling reaction is of the first order, this product decreases linearly with increasing current (curve C of Fig. 2).

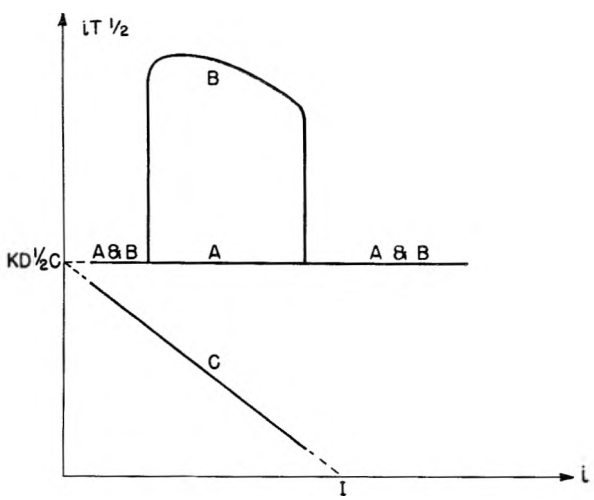

Fig. 2.—Relation between the product $iT^{1/2}$ and the constant current densities in non-steady state electrolysis.

The intercept on the i axis of the plot of $iT^{1/2}$ *vs.* i defines a *critical limiting current density* I at which, from equation 5

$$nFC = I/k \qquad (6)$$

The critical limiting current density represents the density beyond which the transition time disappears from the potential time curve. The reaction rate constant k may thus be evaluated from this initial density (equation 6).

The non-steady electrolysis of $Cd(CN)_4^{2-}$ in KSCN, in NaOH or in KI solution occurs according to equation 5. We may therefore conclude that the speed of these non-steady state electrolysis is controlled by the rate of a slow reaction, and not by the rate of a diffusion process.

The non-steady state electrolysis of cobalt(II) in 1 M KSCN solution offers a striking example of a two-stage reduction, the first one being controlled by a slow chemical reaction, the second one by a diffusion process. The potential time curves of this solution for current densities between 20 and 60 milliamp. per square cm. indicate, indeed, two plateaus with levels, respectively, at −0.103 and −1.25 v. *vs.* S.C.E. Figure 3 shows, indeed, that the product $iT^{1/2}$ corresponding to the duration of the first plateau decreases linearly with increasing current.[9]

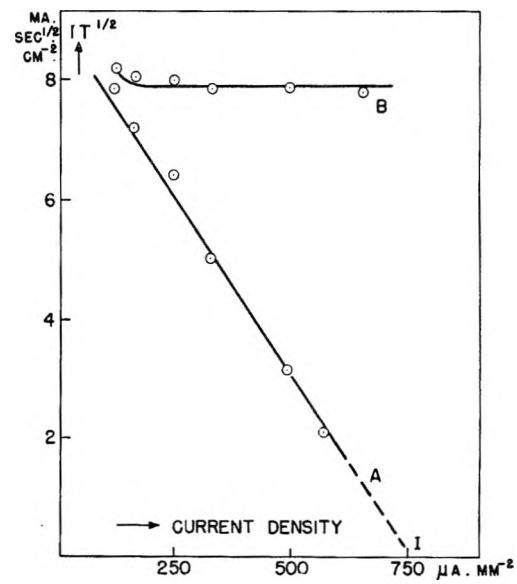

Fig. 3.—Relation between $iT^{1/2}$ and i of 3.5×10^{-2} N cobalt in 1 M KSCN: A, transition time T measured at −1.03 v./S.C.E.; B, sum of transition time at −1.03 and −1.25 v./S.C.E.

As Brönsted's theory concerning the influence of the ionic strength on the kinetics of homogeneous reaction[10] predicts, the addition of electrolytes has a marked action on the value of the critical limiting current density. The critical density of $Cd(CN)_4^{2-}$ solutions increases, indeed, approximately in linear proportion to the ionic strength of added electrolytes, whether the electrolyte is KCl, NaOH, KI or KSCN at concentrations from 0.3 to 2.4

(9) The critical density of a 35 milliequivalent Co(II) solution is equal to 75 milliamp. per square cm. The rate constant of the first-stage reduction is equal to 2.1 milliamp./square cm. per milliequivalent.

(10) J. Brönsted, *Z. physik. Chem.*, 102, 169 (1910).

moles per liter. *No specific catalytic activity seems to be related to the nature of the halogen ion or to the* pH. This confirms, indirectly, that the rate of electrolysis of $Cd(CN)_4^{2-}$ is more reasonably related to a "volume" reaction process than to "surface" electron transfer process, which would be more specifically dependent on the nature of foreign substances.

C. Influence of Adsorbable Substances.—The transition time may also end before the concentration of the depolarizer at the electrode falls near to zero when the rate of transfer of electrons at the solution-electrode interface is hindered by the presence of a poorly conducting adsorbed film.

This happens, perhaps, when small amounts of gelatin are added to a 3×10^{-2} *N* cadmium solution in 1 *M* KCl. Figure 4 shows the tremendous effect of traces of gelatin, in the range of a tenth of a milligram per liter, on the kinetics of this electrolysis. In the absence of gelatin, the speed of the electrode process is so great that the electrolysis appears to be exclusively diffusion controlled. In the presence of 0.03 mg. of gelatin per liter, the non-steady state electrolysis is no longer controlled by diffusion when the current exceeds the critical limiting current density of 55 milliamp. per square cm. (value extrapolated from curve B of Fig. 4).

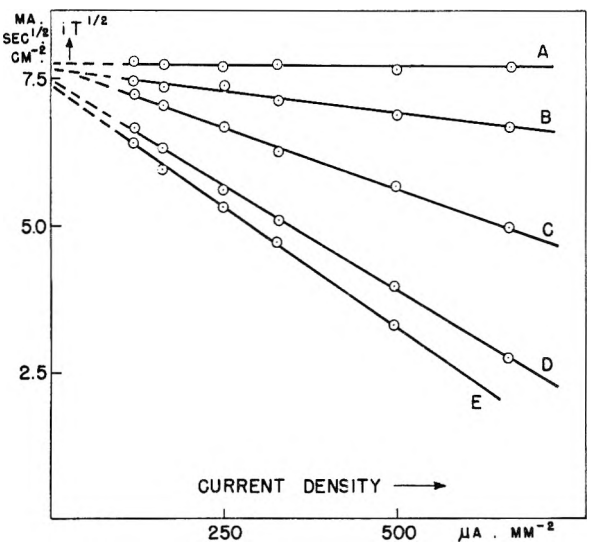

Fig. 4.—Action of gelatin on the electrolysis of 3.1×10^{-2} *N* cadmium in 1 *N* KCl: A, without gelatin; B, with 3×10^{-5} g. per l. gelatin; C, with 8×10^{-5} g. per l. gelatin; D, with 16×10^{-5} g. per l. gelatin; E, with 25×10^{-5} g. per l. gelatin; transition potential, −0.64 v./S.C.E.; electrode surface area, 1.52 mm.^{2}.

Table II shows that, as a first approximation, the product of the critical limiting current density and the concentration of the gelatin remains constant.

TABLE II

RELATION BETWEEN THE CRITICAL LIMITING CURRENT DENSITY, *I*, OF Cd(II) IN KCl SOLUTION, AND THE CONCENTRATION OF ADDED GELATIN

Gelatin concn., 10^{-5} g. per l.	Critical limiting current density, *I*, milliamp. cm.$^{-2}$	Products IC_a
30	55.0	165
80	18.5	148
160	10.5	168
250	8.5	212

This example of interference of a foreign substance on transition time shows that the study of non-steady electrolysis under constant current could be a convenient method for investigating the mechanism of action of inhibitors on electrode processes.

D. Influence of Electrocapillary Convection.—When the electrolysis is accompanied by convection phenomena, condition 3 is not satisfied, and the product $iT^{1/2}$ acquires values many times greater than the theoretical value given by equation 2.

If the convection is due to the electrocapillary phenomenon which is responsible for maxima in polarographic waves, the product $iT^{1/2}$ generally passes abruptly from normal to high abnormal values for characteristic current densities depending on the nature and the concentration of the depolarizer and the foreign substances (curve B of Fig. 2).

This happens, for instance, during the electrolysis of zinc solution in 1 *M* NH_4OH + 1 *M* NH_4Cl (Fig. 5).

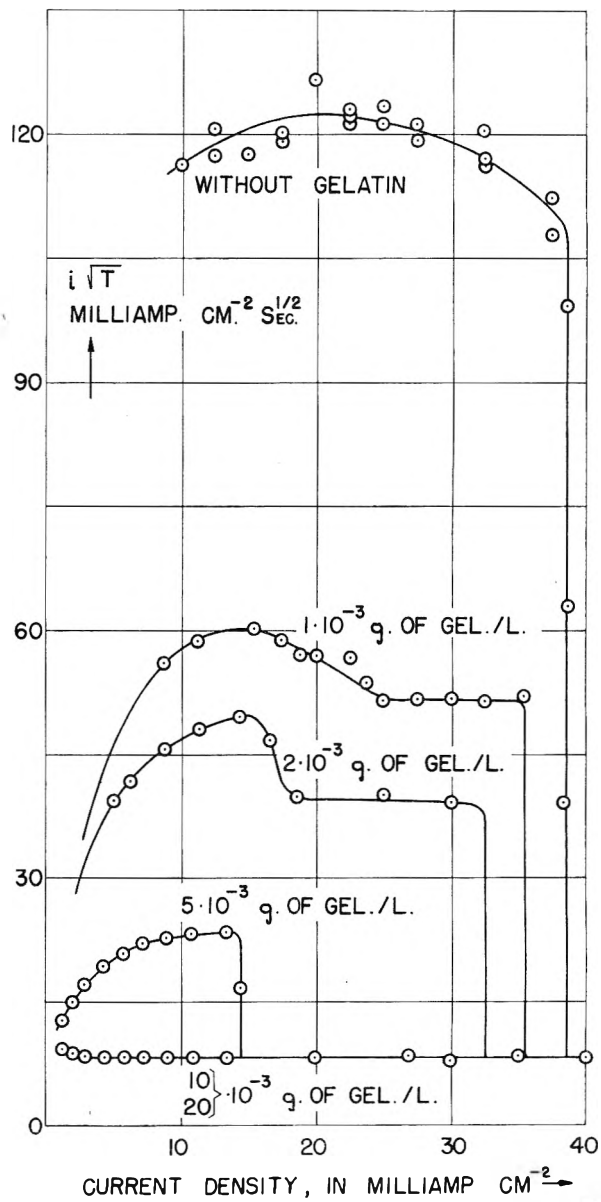

Fig. 5.—Action of gelatin on the electrolysis of 3.1×10^{-2} *N* zinc plus 1 *M* NH_4OH and 1 *M* NH_4Cl.

Without gelatin, the product $iT^{1/2}$ is about ten times greater than the theoretical value which could be expected in the absence of any convection. The addition of 1 milligram per liter of gelatin reduces this product to about half of its original too high value. With 20 to 40 mg. per liter, the non-steady state electrolysis of zinc ions occurs as a normal simple diffusion controlled electrolysis. At that concentration level, gelatin has no effect on the kinetics of reduction of zinc, though it reduces the speed of reduction of cadmium in KCl solution, which occurs at a less negative potential, even at a concentration of 30 micrograms per liter (curve B of Fig. 4).

The study of non-steady state electrolysis under constant current offers thus a valuable method of determining whenever the electrolysis is controlled either by a diffusion or a convection process, by a chemical reaction in the liquid phase or by an electron transfer at the surface of the electrode.

We wish to express our gratitude to Dr. Joseph J. Donovan of Houdry Process Corporation, to Dr. Erwin Sterling of Carnegie Institute of Technology and to Dr. Paul Delahay of Louisiana State University for their courteous criticism and suggestions concerning the present paper.

Acknowledgment with gratitude is also expressed to the Belgian National Scientific Research Foundation which granted a fellowship to one of the authors during part of the time devoted to this research.

CHEMICAL NATURE OF SILICA CARRIED BY STEAM

BY EDWARD L. BRADY

General Electric Research Laboratory, Schenectady, New York

Received February 12, 1953

The existing literature reporting the concentration of silica in the vapor phase when steam is equilibrated with a siliceous molecule has been surveyed and reinterpreted in an attempt to determine the chemical nature of the volatile species in the steam. It is inferred that orthosilicic acid, $Si(OH)_4$, is the volatile species at steam pressures above a few hundred atmospheres, while at lower pressures a higher molecular weight molecule, perhaps the dimer, $Si_2O(OH)_6$, exists in the vapor phase. Explanations are given for the lack of reproducibility in some of the experimental results in the literature.

Introduction

The fact that steam will carry silica as a volatile compound was conclusively established by van Nieuwenburg and co-workers.[1] The effect has been studied both qualitatively and quantitatively by a number of other investigators[2-5] but the chemical identity of the volatile species has never been established. Straub[2] has suggested that the volatile compound is silicic acid, but his data are inadequate to prove this contention. The purpose of this note is to contribute to the interpretation of the results obtained by Straub,[2] Morey and Hesselgesser,[3] Kennedy,[4] and Jacklin and Browar,[5] and to suggest that orthosilicic acid, $Si(OH)_4$, is the volatile species at steam pressures of a few hundred atmospheres while at lower pressures a higher molecular weight molecule, perhaps the dimer $Si_2O(OH)_6$, exists in the vapor phase. Explanations will be given for the lack of reproducibility of some of the experimental results.

Molecular Species of Silica in Steam.—Since SiO_2 has such a low vapor pressure at the temperature of the experiments, the volatile species almost certainly contains water combined in some way with the SiO_2 molecule. For simplicity and definiteness let us consider a system which consists of only two components and two phases: crystalline quartz and water vapor together with the volatile silica-containing compound. Reasonable chemical equilibria involving the two components are represented by the equations

$$SiO_2\ (\text{quartz}) + H_2O\ (\text{gas}) \rightleftarrows SiO(OH)_2\ (\text{gas}) \quad (1)$$

$$SiO_2\ (\text{quartz}) + 2H_2O\ (\text{gas}) \rightleftarrows Si(OH)_4\ (\text{gas}) \quad (2)$$

$$2SiO_2\ (\text{quartz}) + 3H_2O\ (\text{gas}) \rightleftarrows Si_2O(OH)_6\ (\text{gas}) \quad (3)$$

The product of reaction (1) is metasilicic acid and the product of reaction (2) is orthosilicic acid. The dimer which is the product of reaction (3) has been claimed to exist in aqueous solution in appreciable quantity under certain conditions[6-7] and is the first stage in the polymerization of silicic acid to silica. The mass action expressions obtained from equations (1), (2), and (3) are given by

$$\frac{[SiO(OH)_2]}{[H_2O]\,[SiO_2]} = K_1 \quad (4)$$

$$\frac{[Si(OH)_4]}{[H_2O]^2\,[SiO_2]} = K_2 \quad (5)$$

$$\frac{[Si_2O(OH)_6]}{[H_2O]^3\,[SiO_2]^2} = K_3 \quad (6)$$

in which the bracketed quantities represent thermodynamic activities. Hence, if the fugacities of all species involved in equations (4), (5) and (6) are known, evaluation of K_1, K_2 and K_3 (as a function of steam pressure) will enable a decision to be made regarding which of the equilibria represented by equations (1), (2) and (3) is most likely to exist in the system. Data to test the constancy of K_1,

(1) C. J. van Nieuwenburg and P. M. van Zon, *Rec. trav. chim.*, **54**, 129 (1935).

(2) F. G. Straub, Univ. of Illinois Engineering Experiment Station—Bulletin Series 364 (1946).

(3) G. W. Morey and J. M. Hesselgesser, *Trans. Am. Soc. Mech. Engrs.*, **73**, 865 (1951).

(4) G. C. Kennedy, *Econ. Geol.*, **45**, 629 (1950); **46**, 821 (1951).

(5) C. Jacklin and S. R. Browar, paper presented at the Annual Meeting, Am. Soc. Mechanical Engineers, November, 1951.

(6) W. Eitel, "Physikalische Chemie der Silikate," Barth Verlag, Leipzig, 1941, p. 226-227; republished by J. W. Edwards, Ann Arbor, Mich., 1944.

(7) P. A. Thiessen and O. Koerner, *Z. anorg. allgem. Chem.*, **182**, 343 (1929).

K_2 and K_3 are scarce in the literature. Of the investigators mentioned above, only Morey and Hesselgesser[3] and Kennedy[4] have obtained suitable data. Morey and Hesselgesser measured the concentration of silica in steam in equilibrium with quartz at 400, 500 and 600° over a range of pressures from about 33 to 2000 atmospheres, and Kennedy measured the weight loss of quartz disks equilibrated with water or steam in a closed system over a range of temperatures and pressures up to about 500° and 2000 atmospheres.

At these temperatures and pressures the steam pressure is not an accurate measure of the fugacity but the ratio of fugacity to pressure, f/p, can be calculated if the equation of state is known. Newton[8] has calculated the ratio f/p for gases which obey the van der Waals equation of state in reduced form. These values have been used in the calculations which follow. Although more accurate values of f/p could be calculated from the known equation of state of water vapor, the labor of performing the calculations was thought not worthwhile since nothing at all is known about the relationship of total pressure to the fugacity of the silica-containing molecule. The fugacity of SiO_2 (quartz) as a function of pressure was obtained from the relationship

$$\ln (f_B/f_A) = \int_{P_A}^{P_B} (V/RT')dp \qquad (7)$$

in which f_B/f_A is the ratio of the fugacities in the two states A and B in which the pressures are P_A and P_B, and V is the molal volume. In the calculations the molal volume of quartz was assumed constant at 22.65 cm.^{3}/mole. Since ΔP amounts to as much as 2000 atmospheres, the change in activity of the quartz cannot be neglected.

From the available data neither the fugacity of the silica-containing species nor the partial pressure can be calculated. It must be assumed that the partial pressure is equal to the product of mole ratio and total pressure. Two approximations for the fugacity of the siliceous species were used: (1) that the fugacity is equal to the partial pressure, and (2) that it is equal to the partial pressure multiplied by the value of f/p for water vapor at the same temperature and total pressure. Values of K_2 and K_3 were calculated for each assumption. Inspection of the data of Morey and Hesselgesser and of Kennedy indicate that the equilibrium denoted by equation (4) cannot represent the situation. In this equation, the concentration of the silica-containing species in the gas phase would be roughly linear with the steam pressure, and this is very obviously not the case. Hence, values of K_1 were not calculated.

Tables I–VI present the working data as well as the results of the calculations of K_2 and K_3 (of equations (5) and (6)). The first column contains the observed steam pressure, with the approximation that bars equal atmospheres, since the original data were recorded in bars. The second column presents the result of multiplying the pressure by the ratio of fugacity to pressure given by Newton.[8] The third column contains the experimental value of the concentration of the volatile silica-containing species in weight per cent. while the fourth column shows the result of multiplying the total pressure of the system by the mole ratio of silica-containing species, assuming the volatile species is $Si(OH)_4$. The fifth column indicates the fugacity of quartz with the fugacity at one atmosphere taken as unity. The sixth column presents the calculated value of K_2 based on the assumption that the fugacity of the silica-containing species is equal to its partial pressure (column 4), while the seventh column represents the value of the mass action constant if the assumption is made that the fugacity of the silica-containing species equals its partial pressure multiplied by the f/p ratio for steam. The eighth column represents the partial pressure of the silica-containing species if the volatile molecule is $Si_2O(OH)_6$. The ninth and tenth columns present the mass action constant of equation (6) calculated on the assumptions that the fugacity is equal to the partial pressure in the first case and in the second case is equal to the product of the partial pressure and the f/p ratio for steam.

An inspection of columns 6, 7, 9 and 10 of all the tables shows that no clear-cut choice among the possibilities can be made. Some general trends can be observed, however. At the lower pressures (below about 300–400 atmospheres) and at 400–500°, K_3 seems to be somewhat more constant than K_2, while at the higher pressures K_2 seems to be more constant. The constancy of neither K_2 nor K_3 is improved by multiplying by the ratio $(f/p)_{H_2O}$. At 600° sufficient data are not available to enable a choice to be made; K_2 and K_3 seem about equally constant with the largest deviation for K_2 occurring at the lowest pressure, while the largest deviation for K_3 occurs at the highest pressure.

This analysis of the results indicates that the equilibria of both equations (2) and (3) were of importance under the conditions of the experiments. Equilibrium (3) would predominate at lower pressures, while equilibrium (2), which involves more water per SiO_2 molecule, would predominate at higher pressures.

There is no reason to suppose that polymerization in the vapor phase occurs only as far as the dimer. As the water activity is lowered, polymerization may continue several steps further, with the equilibrium vapor pressure decreasing rapidly with increasing molecular weight.

Interpretation of data would be greatly simplified if the experiments had been performed under conditions further removed from the critical conditions for water, so that the pressure would be a more accurate measure of the fugacity. In any experiment the relation between fugacity and concentration of the siliceous species would be difficult to determine.

Volatility of Silica from Freshly Precipitated Silicic Acid.—Straub[2] has measured the concentration of silica in steam equilibrated with freshly precipitated silicic acid, made by acidifying sodium silicate solution, Na_2SiO_3. Under these conditions the solid phase is amorphous, and can be thought of as polymerized, dehydrated $Si(OH)_4$. The degree

(8) R. H. Newton, *Ind. Eng. Chem.*, **27**, 302 (1935).

TABLE I

BASED ON DATA OF MOREY AHD HESSELGESSER AT 400°

P_{H_2O} (atm.)	f_{H_2O} (atm.)	Wt. % SiO_2 in steam	P_{SiO_2} in steam (atm.)	f_{SiO_2} (quartz)	K_2	$K_2(f/p)_{H_2O}$	$P_{Si_2O(OH)_6}$ in steam (atm.)	K_3	$K_3(f/p)_{H_2O}$
33	31.3	0.0001	1.0×10^{-5}	1.00	1.02×10^{-8}	0.97×10^{-8}	0.5×10^{-5}	1.63×10^{-10}	1.55×10^{-10}
67	61.0	.0003	6.0×10^{-5}	1.02	1.59×10^{-8}	1.45×10^{-8}	3.0×10^{-5}	1.28×10^{-10}	1.16×10^{-10}
133	108	.0005	2.0×10^{-4}	1.06	1.62×10^{-8}	1.31×10^{-8}	1.0×10^{-4}	0.71×10^{-10}	0.58×10^{-10}
333	183	.064	6.4×10^{-2}	1.15	1.66×10^{-6}	9.13×10^{-7}	3.2×10^{-2}	4.0×10^{-9}	2.20×10^{-9}
667	234	.126	0.252	1.32	3.48×10^{-6}	1.22×10^{-6}	0.126	5.6×10^{-9}	1.98×10^{-9}
1000	290	.155	0.465	1.51	3.54×10^{-6}	1.02×10^{-6}	.233	4.2×10^{-9}	1.21×10^{-9}
1500	405	.206	0.928	1.86	3.04×10^{-6}	0.82×10^{-6}	.464	2.02×10^{-9}	5.5×10^{-10}
2000	500	.231	1.39	2.28	2.44×10^{-6}	0.61×10^{-6}	.695	1.07×10^{-9}	2.68×10^{-10}

TABLE II

BASED ON DATA OF MOREY AND HESSELGESSER AT 500°

P_{H_2O} (atm.)	f_{H_2O} (atm.)	Wt. % SiO_2 in steam	P_{SiO_2} in steam (atm.)	f_{SiO_2} (quartz)	K_2	$K_2(f/p)_{H_2O}$	$P_{Si_2O(OH)_6}$ in steam (atm.)	K_3	$K_3(f/p)_{H_2O}$
67	63	0.0014	2.8×10^{-4}	1.02	6.9×10^{-8}	6.6×10^{-8}	1.4×10^{-4}	5.4×10^{-10}	5.1×10^{-10}
133	117	.0036	1.44×10^{-3}	1.05	1.10×10^{-7}	9.7×10^{-8}	0.72×10^{-3}	4.1×10^{-10}	3.6×10^{-10}
333	243	.022	2.2×10^{-2}	1.13	3.30×10^{-7}	2.4×10^{-7}	1.1×10^{-2}	6.0×10^{-10}	4.4×10^{-10}
667	367	.135	0.27	1.26	1.59×10^{-6}	8.8×10^{-7}	0.135	1.73×10^{-9}	9.5×10^{-10}
1000	470	.260	0.78	1.42	2.48×10^{-6}	1.16×10^{-6}	0.39	1.86×10^{-9}	8.3×10^{-10}
1500	645	.404	1.82	1.71	2.56×10^{-6}	1.10×10^{-6}	0.91	1.17×10^{-9}	5.0×10^{-10}
2000	860	.499	3.00	2.04	1.99×10^{-6}	8.6×10^{-7}	1.50	5.67×10^{-10}	2.44×10^{-10}

TABLE III

BASED ON DATA OF MOREY AND HESSELGESSER AT 600°

P_{H_2O} (atm.)	f_{H_2O} (atm.)	Wt. % SiO_2 in steam	P_{SiO_2} in steam (atm.)	f_{SiO_2} (quartz)	K_2	$K_2(f/p)_{H_2O}$	$P_{Si_2O(OH)_6}$ in steam (atm.)	K_3	$K_3(f/p)_{H_2O}$
333	280	0.036	0.036	1.11	4.1×10^{-7}	3.48×10^{-7}	0.018	6.7×10^{-10}	5.6×10^{-10}
1000	620	.296	0.888	1.37	1.68×10^{-6}	1.04×10^{-6}	0.444	10.0×10^{-10}	6.2×10^{-10}
1500	870	.559	2.52	1.61	2.07×10^{-6}	1.20×10^{-6}	1.26	7.4×10^{-10}	4.3×10^{-10}
2000	1160	.765	4.55	1.88	1.97×10^{-6}	1.14×10^{-6}	2.28	4.1×10^{-10}	2.40×10^{-10}

TABLE IV

BASED ON DATA OF KENNEDY AT 400°

P_{H_2O} (atm.)	f_{H_2O} (atm.)	Wt. % SiO_2 in steam	P_{SiO_2} in steam (atm.)	f_{SiO_2} (quartz)	K_2	$K_2(f/p)_{H_2O}$	$P_{Si_2O(OH)_6}$ in steam (atm.)	K_3	$K_3(f/p)_{H_2O}$
300	171	0.040	0.036	1.14	1.08×10^{-6}	0.62×10^{-6}	0.018	2.77×10^{-9}	1.58×10^{-9}
350	185	.076	.080	1.16	2.01×10^{-6}	1.17×10^{-6}	.040	4.74×10^{-9}	2.51×10^{-9}
400	196	.096	.115	1.18	2.54×10^{-6}	1.24×10^{-6}	.0575	5.51×10^{-9}	2.70×10^{-9}
500	210	.118	.177	1.23	3.26×10^{-6}	1.37×10^{-6}	.0885	6.34×10^{-9}	2.66×10^{-9}
600	228	.136	.245	1.28	3.68×10^{-6}	1.40×10^{-6}	.123	6.36×10^{-9}	2.42×10^{-9}
750	248	.151	.340	1.36	4.18×10^{-6}	1.38×10^{-6}	.170	6.05×10^{-9}	2.00×10^{-9}
1000	290	.175	.525	1.51	4.14×10^{-6}	1.20×10^{-6}	.263	4.75×10^{-9}	1.38×10^{-9}
1250	338	.195	.732	1.68	3.81×10^{-6}	1.03×10^{-6}	.366	3.36×10^{-9}	0.91×10^{-9}
1500	375	.217	.977	1.86	3.74×10^{-6}	0.94×10^{-6}	.489	2.69×10^{-9}	0.67×10^{-9}
1750	438	.230	1.21	2.05	3.08×10^{-6}	0.77×10^{-6}	.605	1.71×10^{-9}	0.43×10^{-9}

TABLE V

BASED ON DATA OF KENNEDY AT 450°

P_{H_2O} (atm.)	f_{H_2O} (atm.)	Wt. % SiO_2 in steam	P_{SiO_2} in steam (atm.)	f_{SiO_2} (quartz)	K_2	$K_2(f/p)_{H_2O}$	$P_{Si_2O(OH)_6}$ in steam (atm.)	K_3	$K_3(f/p)_{H_2O}$
400	256	0.047	0.0552	1.17	7.2×10^{-7}	4.61×10^{-7}	0.0276	1.23×10^{-9}	7.8×10^{-10}
500	270	.095	.142	1.21	1.61×10^{-6}	8.7×10^{-7}	.071	2.48×10^{-9}	13.4×10^{-10}
600	288	.128	.230	1.26	2.20×10^{-6}	1.06×10^{-6}	.115	3.05×10^{-9}	14.6×10^{-10}
750	315	.160	.360	1.33	2.73×10^{-6}	1.15×10^{-6}	.180	3.26×10^{-9}	13.7×10^{-10}
1000	370	.210	.630	1.46	3.15×10^{-6}	1.16×10^{-6}	.315	2.92×10^{-9}	10.8×10^{-10}
1250	425	.248	.930	1.61	3.20×10^{-6}	1.09×10^{-6}	.465	2.35×10^{-9}	8.0×10^{-10}
1500	495	.290	1.31	1.77	3.01×10^{-6}	0.99×10^{-6}	.653	1.46×10^{-9}	4.8×10^{-10}
1750	577	.343	1.80	1.95	2.77×10^{-6}	0.91×10^{-6}	.900	1.23×10^{-9}	4.1×10^{-10}

TABLE VI

BASED ON DATA OF KENNEDY AT 500°

P_{H_2O} (atm.)	f_{H_2O} (atm.)	Wt. % SiO_2 in steam	P_{SiO_2} in steam (atm.)	f_{SiO_2} (quartz)	K_2	$K_2(f/p)_{H_2O}$	$P_{Si_2O(OH)_6}$ in steam (atm.)	K_3	$K_3(f/p)_{H_2O}$
500	310	0.069	0.103	1.19	8.9×10^{-7}	5.5×10^{-7}	0.0515	1.22×10^{-9}	7.6×10^{-10}
600	336	.108	.194	1.24	1.39×10^{-6}	7.8×10^{-7}	.097	1.66×10^{-9}	9.3×10^{-10}
750	383	.164	.369	1.31	1.92×10^{-6}	9.8×10^{-7}	.185	1.92×10^{-9}	9.8×10^{-10}
1000	460	.238	.714	1.42	2.37×10^{-6}	10.9×10^{-7}	.357	2.03×10^{-9}	9.4×10^{-10}
1250	537	.300	1.13	1.56	2.51×10^{-6}	10.8×10^{-7}	.565	1.50×10^{-9}	6.5×10^{-10}

of polymerization and dehydration depends on the temperature, pressure and duration of the experiment. Hence, Straub's starting material was not clearly defined; several solid phases may have been present.

If we assume that the volatile species is $Si_2O(OH)_6$ or $Si(OH)_4$, some of the possible reactions involved in his experiment can be written as

$$SiO(OH)_2(amorph) + H_2O(g) \rightleftarrows Si(OH)_4(g) \quad (7)$$

$$2SiO(OH)_2(amorph) + H_2O(g) \rightleftarrows Si_2O(OH)_6(g) \quad (8)$$

$$SiO_2(amorph) + 2H_2O(g) \rightleftarrows Si(OH)_4(g) \quad (9)$$

$$2SiO_2(amorph) + 3H_2O(g) \rightleftarrows Si_2O(OH)_6(g) \quad (10)$$

$$Si_2O(OH)_6(amorph) + H_2O(g) \rightleftarrows 2Si(OH)_4(g) \quad (11)$$

$$Si_2O(OH)_6(amorph) \rightleftarrows Si_2O(OH)_6(g) \quad (12)$$

If we neglect the change in fugacity with pressure (which can be done more readily since the pressure in these experiments was not higher than 30 atmospheres) and plot the logarithm of the partial pressure of the gaseous siliceous species *vs.* the logarithm of the steam pressure, the slope of the curve obtained should be intermediate between 0 and 3, if several of the equilibria (7)–(12) are simultaneously involved. When Straub's data at 260 and 316° over the pressure range 67–420 p.s.i. are plotted in this way, a slope of 2.4 is obtained for both temperatures. This result is consistent with the picture developed above.

Volatility of Silica from Silica Glass.—Morey and Hesselgesser also obtained data for the volatility of silica in steam in contact with silica glass. As expected, the concentration in the vapor phase was considerably greater than when quartz was the solid phase, but no quantitative estimate of the expected increase was made. An estimate of the difference can be obtained from the relation

$$\Delta F = -2.3RT \log(P_2/P_1) \quad (13)$$

in which ΔF is the free energy change accompanying the transition from silica glass to quartz and P_2 and P_1 are the vapor pressures of the volatile silica-containing species when in equilibrium with glass and quartz, respectively, with the pressure of water vapor maintained constant. At 25° the value of ΔF for the glass to quartz transition is -1.5 kcal./mole[9]; this value would not change greatly with increase in temperature up to 400 or 500°. At 400° we obtain

$$\log \frac{P_2}{P_1} = \frac{1.5 \times 10^3}{(2.3)(1.986)(673)} = 0.49$$

$$P_2/P_1 = 3.1$$

This result indicates that the concentration in the vapor above the glass should be the order of three times that above the quartz. The observed ratio of vapor pressures is about two to one, except at 2000 p.s.i. where it is seven. Since the ratio of vapor pressures is very sensitive to small changes in ΔF, the calculated ratio of 3 to 1 may be too low because of the use of an inaccurate value for ΔF. Also, experimental error in the value of one of the measured vapor concentrations may be responsible for the high value. Since Morey and Hesselgesser obtained indications that crystallization to quartz occurred during the experiment, their conditions did not represent a metastable equilibrium between the glass and the vapor phases. Therefore, in accord with the observation, the measured concentration of the vapor phase would be expected to be somewhat lower than that corresponding to the metastable equilibrium conditions.

Volatility of Silica from Aqueous Solution.—Data which have been obtained for the equilibrium of silica between the vapor phase and a liquid solution phase are not nearly so clear-cut as data obtained for a solid. The results of Jacklin and Browar[5] illustrate this quite clearly. Figure 1 is taken from their paper and "shows the ratio of silica in the steam to silica in the boiler water, expressed in per cent., plotted against the silica concentration in the boiler water. The *p*H of the boiler water was in the range of 10–11 and the pressure was 1500 p.s.i." A possible explanation for the wide variability in the results is given below.

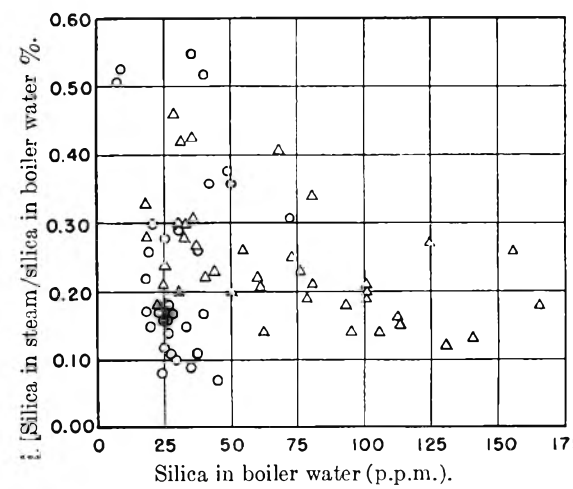

Fig. 1.—Ratio of silica in steam to silica in boiler water as a function of boiler water silica concentration.

The equilibria in the aqueous solution can be represented by the equations

(9) National Bureau of Standards, Circular 500, "Selected Values of Chemical Thermodynamic Properties," U. S. Government Printing Office, 1952, p. 148.

$$Si(OH)_4(soln) \rightleftharpoons Si(OH)_4(gas) \quad (14)$$

$$Si_2O(OH)_6(soln) \rightleftharpoons Si_2O(OH)_6(gas) \quad (15)$$

$$Si(OH)_4(soln) \rightleftharpoons SiO(OH)_3^-(soln) + H^+(soln) \quad (16)$$

$$Si_2O(OH)_6(soln) + H_2O \rightleftharpoons 2SiO(OH)_3^-(soln) + 2H^+ \quad (17)$$

It is seen that if equation (16) or (17) is driven to the right by removing the hydrogen ion, as in a basic solution, the equilibrium (14) or (15) will be shifted to the left, thereby reducing the silica in the gas phase. A rough estimate of the magnitude of the effect of changing the *p*H from 10 to 11 can be obtained by using the reported value of the ionization constant of orthosilicic acid at 25°. The value will certainly be quite different under the actual conditions of the experiment, so only a semiquantitative answer can be expected. The equilibrium constant of reaction (15) above, given by

$$K = \frac{[H^+][SiO(OH)_3^-]}{[Si(OH)_4]} \quad (18)$$

is reported[10] to be $K = 2.2 \times 10^{-10}$. Let us choose the following conditions: *p*H = 10; total silica concentration in solution = 25 p.p.m.; let $SiO(OH)_3^- = x$. Ignoring activity coefficients, equation (18) becomes

$$\frac{[10^{-10}][x]}{\left[\frac{25 \times 10^{-3}}{60} - x\right]} = 2.2 \times 10^{-10}$$

Solving, we obtain

$$x = 2.9 \times 10^{-4} \text{ mole/liter, and}$$

$$[Si(OH)_4] = (4.2 \times 10^{-4}) - x = 1.3 \times 10^{-4} \text{ mole/liter}$$

(10) Landolt-Börnstein, "Physikalish-Chemische Tabellen," 5th Edition, 2nd Supplement, Julius Springer, Berlin, 1931, p. 1080; republished by Edwards Bros., Inc., Ann Arbor, Michigan, 1943.

For the same total silica concentration and a *p*H of 11, we obtain $x = 4.0 \times 10^{-4}$ mole/liter and $[Si(OH)_4] = 4.2 \times 10^{-4} - x = 0.2 \times 10^{-4}$ mole/liter. This means that for the same total silica, the concentration of $Si(OH)_4$ in solution and hence in the gas phase is 6.5 times as great when the *p*H is 10 than it is when the *p*H is 11. It must be emphasized that this estimate is based on data obtained at 25° but is expected to be of the correct order of magnitude for the experimental conditions. This variation easily accounts for the spread in the data of Fig. 1. For reproducible results, the *p*H must be maintained constant.

Conclusions

The conclusions to be obtained from the above discussion are the following.

(1) The volatile silica-containing molecular species obtained from the reaction of steam with silica are most probably both $Si(OH)_4$ and $Si_2O(OH)_6$ with the former predominating at higher pressures and the latter at pressures below about 300–400 atmospheres. The data can undoubtedly be fitted with other assumptions for the volatile species, but $Si(OH)_4$ and $Si_2O(OH)_6$ are considered to be the most reasonable chemically.

(2) Experiments to establish the formula should involve the equilibration of water vapor with crystalline quartz, and the temperature and pressure should be far enough away from critical conditions so that the vapor pressure is a reasonable measure of the activity.

(3) In any experiments carried out with a siliceous species in solution, the *p*H of the solution should be accurately controlled.

SELECTIVE ADSORPTION—2,4-DIMETHYLPENTANE–BENZENE–SILICA GEL AT 65.6°

BY M. R. CINES AND F. N. RUEHLEN

Phillips Petroleum Company, Research and Development Department, Research Division, Bartlesville, Oklahoma

Received February 18, 1953

Liquid phase studies of selective adsorption as a means of separation of hydrocarbons by type do not yield any indication of the variation of selectivity with surface coverage. Therefore, a study was made of the selective adsorption of mixtures of 2,4-dimethylpentane–benzene vapors on silica gels. Four isotherms were established at 65.6° using two silica gels of different pore size distribution in a system which circulated mixed vapor of constant composition over the adsorbent. The results showed that, for the gel with essentially monomolecular adsorption, the selective action of the surface increased quite regularly with increasing pressure up to the saturation value. In contrast, the gel yielding a sigmoid isotherm had a maximum selectivity at a pressure of about 140 mm. Thereafter, the selectivity decreased rapidly as the pressure approached saturation. Thus, although some selective action persists in the multilayers, the efficacy of such selective action is of a lower magnitude than that occurring in the monolayer.

Introduction

Since the demonstration[1] that selective adsorption could separate hydrocarbons by type, considerable interest has developed in the phenomenon both as an analytical technique and, more recently, as a commercial operation. Because these processes involve adsorption from the liquid phase, they give no indication of the variation of the selective action of the adsorbent as a function either of surface coverage or of multilayer buildup. There is no information as to how the separation efficiency changes during the approach to saturation, for such data must be obtained through vapor phase adsorption studies.

The older literature on mixed adsorption[2] does not contain systems analogous to the hydrocarbon separation. Most of the systems were studied far from saturation conditions. Those which did survey the approach to saturation utilized two widely different molecular species. The more

(1) B. J. Mair and A. F. Forziati, *J. Research Natl. Bur. Standards*, 32, 165 (1944).

(2) S. Brunauer, "The Adsorption of Gases and Vapors," Princeton University Press, Princeton, N. J., 1945.

recent work of Innes and Rowley[3] was done under conditions of constant surface composition. There are not sufficient data presented to convert to constant vapor composition so that the selective behavior can be studied. Arnold's study[4] of O_2–N_2 mixtures represents the type of investigation of the surface variation of selectivity which is of interest in hydrocarbon separation. The pronounced selectivity of the anatase surface for N_2 at low surface coverage is quite obvious. Examination of Arnold's results shows, at relative pressures at least as low as 0.05, that the selective action of the adsorbent decreases continuously and quite markedly with increasing adsorption. It appears from those results that nitrogen is much more strongly adsorbed at very low coverage than oxygen. Whether or not the behavior of hydrocarbon mixtures would follow this same pattern could not be predicted.

To observe the effect of both surface coverage and multilayer buildup, it was obvious that two different silica gels should be used, one having Type I isotherm and the other Type II. Selectivity as a function of surface coverage could best be studied using the Type I gel which exhibited only monolayer adsorption. Conversely, selectivity beyond the monolayer could only be observed with the Sigmoid isotherm of the Type II gel. To eliminate, as far as possible, differences in vapor pressure, the aromatic and paraffinic hydrocarbons selected were benzene and 2,4-dimethylpentane, which have identical vapor pressures at 65.6°.

Experimental

Materials.—Benzene—"pure grade" supplied by Phillips Petroleum Company. Purity guaranteed greater than 99% R.I.^{20}D 1.50122, d^{20} 0.87912. Corresponding API Project 44 values[5] for pure material are R.I.^{20}D 1.50110, and d^{20} 0.87903.

2,4-Dimethylpentane—"pure grade" supplied by Phillips Petroleum Company. Purity guaranteed greater than 99% R.I.^{20}D 1.38157, d^{20} 0.67285. Corresponding API Project 44 values[5] for pure material are R.I.^{20}D 1.38145 and d^{20} 0.67270.

Silica Gel—Type I—Davison Silica Gel #08-08-237, 14–30 mesh. Type II—Mallinckrodt Silicic Acid—200 mesh. To eliminate pressure drop in the adsorption cell, this gel was cast into small pellets using a gel–distilled-water paste without any binder.

Apparatus.—The adsorption apparatus utilized a recirculation principle. A separate thermostated liquid reservoir set the system pressure and the vapor phase composition. Two Toepler pumps operating 180° out of phase, circulated vapor from the vapor space in the liquid reservoir through the adsorbent and back through the liquid in the reservoir. Pressure in the system was measured either by a Zimmerli gage, up to 100 mm., or by an external manometer operating through a pressure balance. The adsorption cell, Toepler pumps, Zimmerli gage and pressure balance were all enclosed in a thermostated air-bath maintained at 65.6 ± 0.05°. The lines connecting apparatus in the air-bath and the liquid reservoir were traced with electrical heaters to prevent condensation. Provision was made for obtaining liquid samples from the reservoir without introducing air into the system.

Procedure.—Before admitting the desired 2,4-dimethylpentane–benzene liquid mixture to the reservoir, the entire system was evacuated. During this pumping period the adsorbent was heated to 205°. When the liquid entered the reservoir, a small amount was allowed to vaporize to remove any air admitted. The vapor in equilibrium with the liquid reservoir was then circulated over the absorbent, now at 65.6°, for 1.5 to 2.5 hours to establish equilibrium. (By experiment, it was found that there was no significant difference in results between 1.5- and 5.5-hour equilibration periods). The adsorption cell and the liquid reservoir were then isolated from the rest of the system which was evacuated. Thereafter, the adsorbate was desorbed at 205° and condensed in sample collecting ampoules at liquid nitrogen temperatures. Liquid samples were collected directly from the reservoir. The adsorbate was weighed and both the adsorbate and liquid reservoir samples were analyzed by refractive index measurements using the 5-place Precision Bausch and Lomb refractometer. In the early stages of this investigation, vapor samples were collected and analyzed by ultraviolet adsorption. However, it was found to be more reliable to analyze the liquid phase and then determine the vapor phase from the vapor–liquid equilibria measured for this system.

Results and Discussions

Vapor–Liquid Equilibria.—The adsorption apparatus was used to determine vapor–liquid equilibria in the 2,4-dimethylpentane–benzene system by operating the unit without adsorbent. The results obtained in Table I were extrapolated to to 65.6° to yield the phase diagram in Fig. 1. According to these results the azeotropic composition at 65.6° and 550 mm. is 55 mole per cent. benzene. Horsley[6] reports the azeotrope as 56.6 mole per cent. benzene at 760 mm. and 75.2°.

TABLE I

VAPOR LIQUID EQUILIBRIA FOR 2,4-DIMETHYLPENTANE–BENZENE MIXTURES

Temp., °C.	Pressure, mm.	Mole per cent. benzene Liquid	Vapor
8.2	49.1	22.8	28.7
8.2	49.6	22.7	28.8
42.1	220.8	22.3	28.8
60.3	419.3	21.8	28.8
7.9	50.3	41.7	43.8
41.5	220.8	41.9	45.6
59.1	419.7	40.9	45.9
4.5	42.6	63.2	59.0
40.7	217.5	62.9	60.6
58.1	411.9	63.1	61.3
6.9	46.3	82.0	73.6
41.3	216.9	82.0	75.1
41.4	216.9	83.0	76.4
58.8	412.8	83.4	76.7

Adsorption.—The adsorption of the individual components, benzene and 2,4-dimethylpentane, on the Type I gel is shown as the upper and lower curves, respectively, of Fig. 2. The isotherms for these two pure hydrocarbons were found to be fitted quite well by the Langmuir equation. From the straight lines obtained on plotting p/v *vs.* p, V_m values of 4.64 and 2.85 millimoles per gram were found for benzene and 2,4-dimethylpentane, respectively. The behavior of these two hydrocarbons is in line with their molecular areas calculated from the equation $(M/N\rho)^{2/3}$ where M is molecular weight, N is Avogadro's number and ρ is the liquid density at the equilibrium temperature. However, because the heptane's symmetry is lower than benzene's, the monolayer contained roughly 13% less heptane than was calculated from

(3) W. B. Innes and H. H. Rowley, THIS JOURNAL, 51, 1172 (1947).

(4) J. R. Arnold, *J. Am. Chem. Soc.*, 71, 104 (1949).

(5) "Selected Values of Properties of Hydrocarbons," Circular Natl. Bur. Standards C461 (1947).

(6) L. H. Horsley, *Ind. Eng. Chem., Anal. Ed.*, 19, 508 (1947).

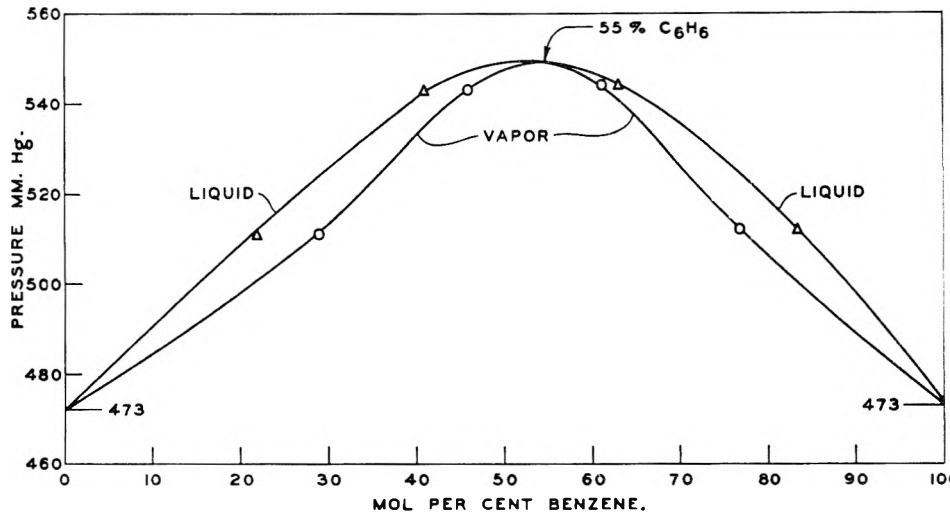

Fig. 1.—Liquid–vapor equilibria at 65.6°.

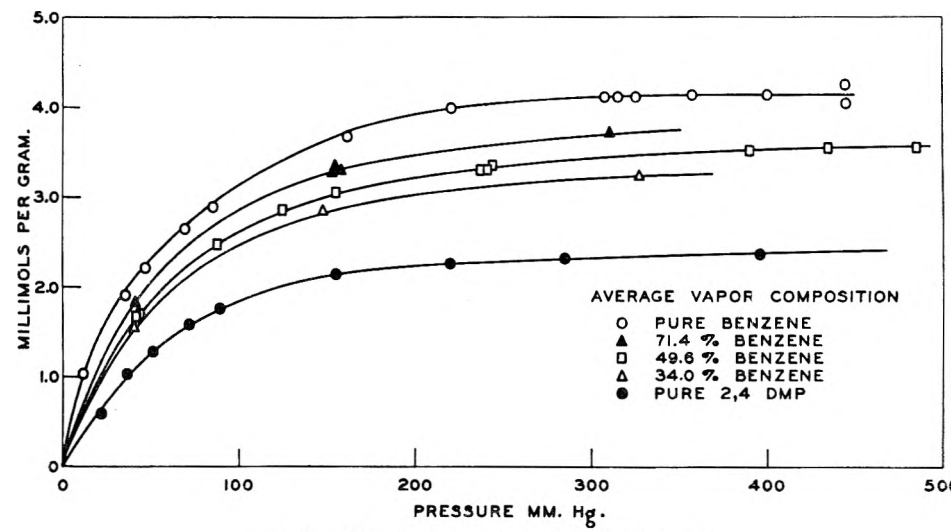

Fig. 2.—Mixed vapor adsorption, 65.6°, Gel I.

the benzene adsorption and the ratio of the molecular areas. Nitrogen surface area of this Type I gel was 618 m.²/g.; for the Type II gel the corresponding area was 637 m.²/g. The pure component isotherms were not determined on Gel II.

In the study of mixed adsorbates, three isotherms were measured for Type I gel and one for the Type II gel at as nearly constant vapor phase composition as practical. The Type I gel results are the three curves lying between the pure component isotherms in Fig. 2. As might be expected, the total number of millimoles adsorbed increases quite regularly with increasing benzene concentration in the equilibrium vapor. The behavior of the two components over the pressure range studied is shown quite clearly for a single isotherm in Fig. 3. While the total adsorption curves in Fig. 2 give no indication that actual replacement of heptane by benzene occurs as the saturation pressure is approached, the component isotherms in Fig. 3 demonstrate the phenomenon vividly. The selective adsorption can be shown more lucidly by considering the vapor–adsorbate relative distribution coefficient (K_R) which is defined as the ratio of the distribution coefficient for benzene to that for 2,4-dimethylpentane. Figure 4 shows the variation of K_R as a function of pressure, *i.e.*, surface coverage, for the three mixed adsorption isotherms. The increasing values of K_R as saturation is approached indicate the higher selectivity for benzene. The rise in the value of K_R with decreasing benzene concentration in the vapor phase is in accord with similar results found in other separation processes.[7,8]

Langmuir-type equations for mixed adsorption developed by Markham and Benton[9] are

$$\theta_1 = \frac{b_1 p_1}{1 - b_1 p_1 + b_2 p_2} \quad \text{and}$$

$$\theta_2 = \frac{b_2 p_2}{1 + b_1 p_1 + b_2 p_2}$$

where θ_1 is the fractional surface coverage for component 1, p_1 is partial pressure of component 1 and b_1 is a constant obtained from the isotherm of

(7) R. E. Treybal, "Liquid Extraction," McGraw-Hill Book Co., Inc., New York, N. Y., 1951, p. 90.

(8) M. R. Cines, J. T. Roach, R. J. Hogan and C. H. Roland, *Chem. Engr. Progress*, to be published.

(9) E. C. Markham and A. F. Benton, *J. Am. Chem. Soc.*, 53, 497 (1931).

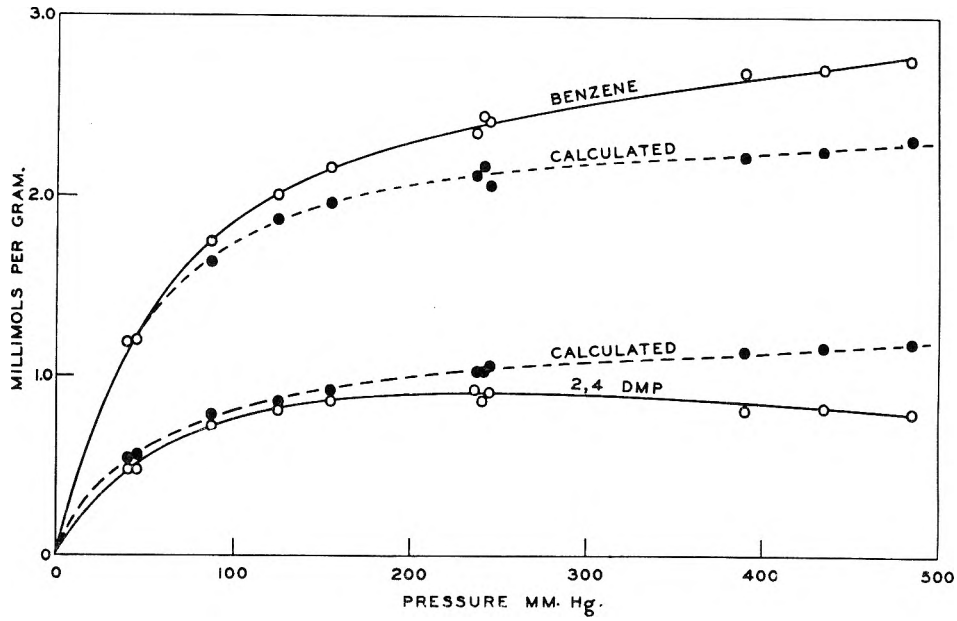

Fig. 3.—Component distribution on Gel I; av. vapor 49.6 mole % benzene, $t = 65.6°$, $p_0 = 549$ mm.

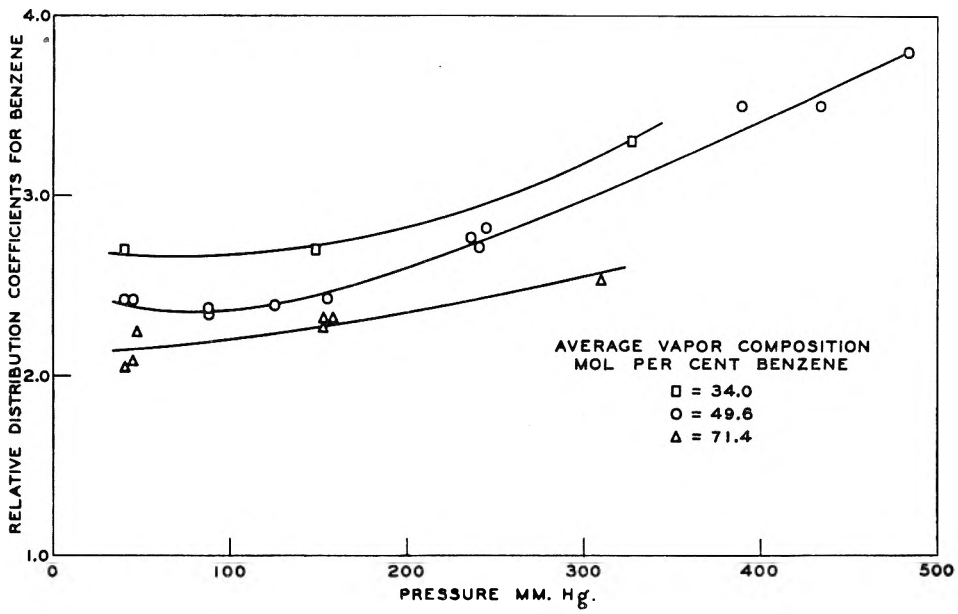

Fig. 4.—Pressure–selectivity relationship, 65.6°, Gel I.

pure component 1. The results of applying these relations to the mixed adsorption isotherm at 49.6% benzene in the vapor phase are given in Fig. 3 as the dotted curves. While the Langmuir equation is applicable to the single adsorbate studies, it is obviously inadequate to present the behavior in this mixed adsorbate system. From this comparison, the adsorption of benzene appears to exceed theoretical values while heptane falls considerably short of theoretical. However, these equations do yield a correct representation of total adsorption. The sums of the two calculated values give results which are in reasonable agreement with experimental values; average deviation of sums of the calculated points from the experimental results is approximately 4%.

The mixed adsorption isotherm for the Type II gel is shown in Fig. 5. The isotherms for each component adsorbed from the mixture are also included. The replacement of 2,4-dimethylpentane by benzene as found with the Type I gel is not apparent in this case. Limitations in the apparatus prevented measurements at pressures low enough to study the portion of the isotherm where monolayer coverage predominates. If, once again, the selectivity of the adsorption is represented by the relative distribution coefficient, K_R, the relationship with pressure is quite different from the previous observation. In Fig. 6, the curves of K_R *vs.* pressure are shown for both gels at approximately 50% benzene vapor composition. The value of K_R for the Type II gel appears to go through a maximum value at approximately 140 mm. pressure, or a relative pressure of 0.25. According to a

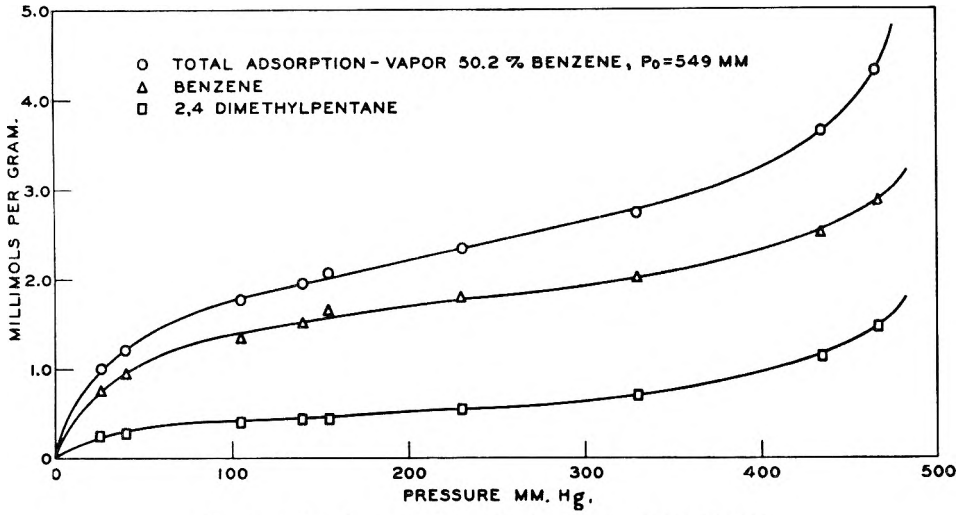

Fig. 5.—Mixed vapor adsorption isotherm, 65.6°, Gel II.

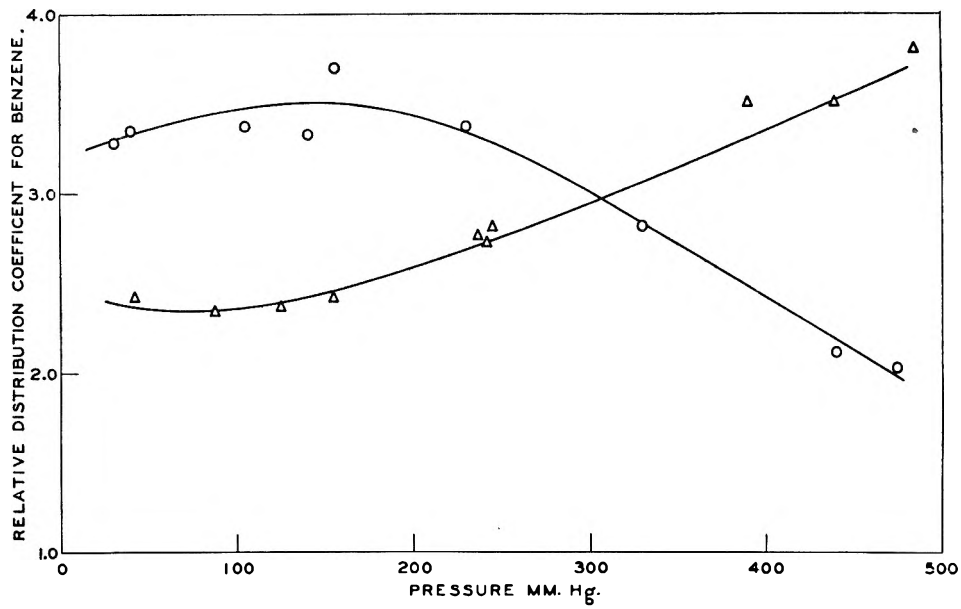

Fig. 6.—Pressure–selectivity relationship: Δ, Gel I; O, Gel II; t = 65.6°, p_0 = 549 mm., vapor approx. 50% benzene.

BET[10] plot, the V_m value is 1.57 millimoles per gram at 70 mm. Because calculated values of K_R are quite sensitive to the composition of the phases,[11] the exact shape of the curve of K_R *vs.* pressure is somewhat uncertain. Therefore, although the maximum indicated in Fig. 6 corresponds to a pressure somewhat higher than that calculated for monolayer coverage, there is sufficient uncertainty to allow an assumption that maximum selectivity occurs at the completion of the monolayer. Furthermore, this maximum value approximates closely the value which the Type I gel approaches at saturation. Thus, K_R of the order of 3.5 is probably representative of the separation efficiency of the monolayer. It should be understood that K_R represents an integrated selectivity. It is based on the composition of the adsorbed phase at a given set of conditions. Therefore, even though adsorption beyond the monolayer were non-selective, K_R values would not fall to unity immediately. Selectivity of multilayer adsorption can be evaluated only from the slope of the K_R *vs.* pressure curve. If non-selectivity is assumed for the second and successive layers, calculations show that the slope of the curve would be somewhat greater than the experimental results in Fig. 6 show to be the case. Thus, although some selectivity persists in the multilayers, it seems evident that selectivity is vested primarily in the monolayer and the efficacy of the separation in the multilayers is of lower magnitude.

(10) S. Brunauer, P. H. Emmett and E. Teller, *J. Am. Chem. Soc.*, 60, 309 (1938).

(11) The values of K_R magnify any uncertainties in the analysis of the phases. Accordingly the scatter in K_R values increases as the values themselves increase. Thus, for the region of K_R = 3.0, an uncertainty of 1% in the adsorbate composition produces a corresponding uncertainty of approximately 5% in K_R.

THE PRECIPITATION OF NICKEL OXALATE

BY J. A. ALLEN

Department of Chemistry, University of Tasmania, Hobart, Tasmania, Australia

Received February 16, 1953

The rate of formation of precipitates of nickel oxalate in solutions containing nickel sulfate and oxalic acid has been studied by turbidimetric and dilatometric techniques which cover successive stages of the reaction. Equations have been derived relating the rate of formation to the initial concentrations of nickel sulfate and oxalic acid in the solution. A mechanism based on the formation and subsequent rearrangement of a complex ion is suggested.

The work described in this paper is part of a general study of the properties of the oxalates of divalent heavy metals in the solid state. Nickel oxalate is an example of this class of compounds and may be prepared by the reaction in solution between a soluble nickel salt and oxalic acid.[1] This reaction does not, however, proceed by a simple ionic double decomposition mechanism; an induction period is observed and the rate of precipitation depends markedly on the concentrations of the reactants in solution. The present work was undertaken to establish these relationships.

Experimental

Stock solutions of nickel sulfate and oxalic acid of normal strength were prepared from high grade chemicals and diluted as required. When a solution of nickel sulfate of, say, 0.3 *N* is added to one of oxalic acid of the same strength —the order of addition is immaterial—no precipitate at first appears. After some minutes the solution becomes cloudy, the solid particles increase in size and subsequently settle out. Two techniques have been employed to follow these processes.

(i) **Turbidimetric Method.**—This method is useful for following the very early stages of the reaction which is carried out in the cell of a photoelectric colorimeter. The instrument scale, graduated logarithmically from 0 to 100, gave directly the percentage of light cut off by the solution. A green filter was used throughout and the instrument was adjusted to read zero with distilled water in the cell. The solutions were mixed in the required amounts to make up a total volume of 10 ml., the cell inserted in the colorimeter and the scale reading followed with time as the optical density of the solution increased.

As it is not possible to relate the scale reading, R, directly to the amount of precipitate present, the assumption was made that dR/dt was proportional to the rate of formation of the precipitate. The method was used only for the very early part of the reaction when no visible settling took place.

(ii) **Dilatometric Method.**—The required solutions were mixed and drawn rapidly into a dilatometer. The rate of change in volume of the reaction system as the precipitation proceeded, which is proportional to dH/dt where H is the reading of the liquid level in the capillary, was taken as a measure of the rate of precipitation. The volume of the bulb of the dilatometer was 93 ml. and the capillary diameter was 0.8 mm. The solutions and dilatometer were maintained at 20 ± 0.05°.

These two methods are complementary in that the part of the reaction measured in the colorimeter precedes that which causes a significant increase in volume in the dilatometer.

Results

In the turbidimetric experiments, the graph of the scale reading against time gave an s-shaped curve with a long central straight portion, the slope of which, S_t, was taken as the rate of formation of the precipitate. Measurements were made at five different oxalic acid concentrations. The slopes, S_t, plotted against the excess concentration of oxalic acid, C, are shown in Fig. 1. For concentrations of oxalic acid equal to or greater than those of nickel sulfate

$$S_t = h_1C + h_2 \quad (1)$$

where h_1 and h_2 are both functions of the concentration of nickel salt, E, given by

$$h_1 = k_1E^3 \quad (2)$$

$$h_2 = k_2E^{3/2} \quad (3)$$

The over-all equation is, therefore

$$S_t = k_1E^3C + k_2E^{3/2} \quad (4)$$

where $k_1 = 2820$ and $k_2 = 43.6$ when C and E are expressed as normalities and S_t as the number of scale divisions per minute.

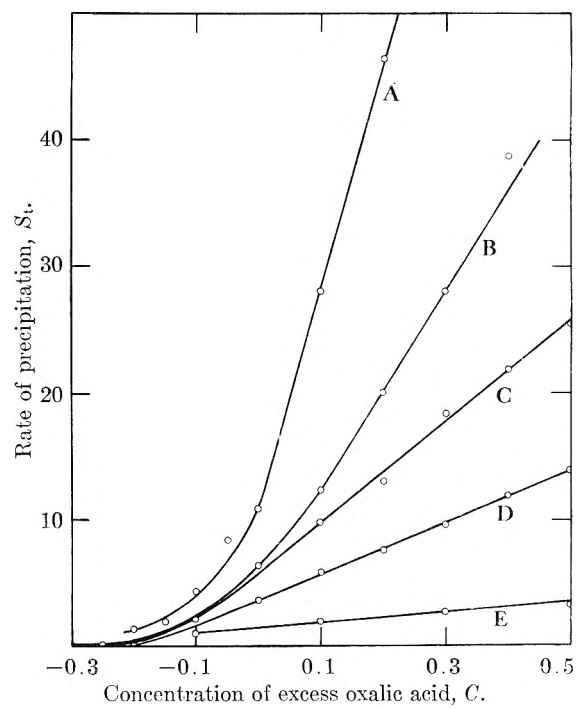

Fig. 1.—A, 0.4 *N*; B, 0.3 *N*; C, 0.25 *N*; D, 0.2 *N*; E, 0.15 *N*.

The dilatometric experiments were carried out on the same plan. The graph of the capillary reading against time again gave an s-shaped curve with a long central straight portion, the slope of which, S_d, was taken as the rate of formation of the precipitate. The results are shown in Fig. 2 in a manner analogous to Fig. 1. For concentrations of oxalic acid equal to or greater than those of nickel sulfate

$$S_d = h_3C + h_4 \quad (5)$$

(1) N. V. Sidgwick, "The Chemical Elements and their Compounds," Vol. 2, Oxford University Press, London, 1950, p. 1435.

where h_3 and h_4 are both functions of the concentration of the nickel salt, E, given by

$$h_3 = k_3E - k_4 \quad (6)$$

and

$$h_4 = k_5E^3 \quad (7)$$

The over-all equation is therefore

$$S_d = (k_3E - k_4)C + k_5E^3 \quad (8)$$

where $k_3 = 16.15$, $k_4 = 2.0$ and $k_5 = 8.4$ when C and E are expressed as normalities and S_d in cm. min.$^{-1}$.

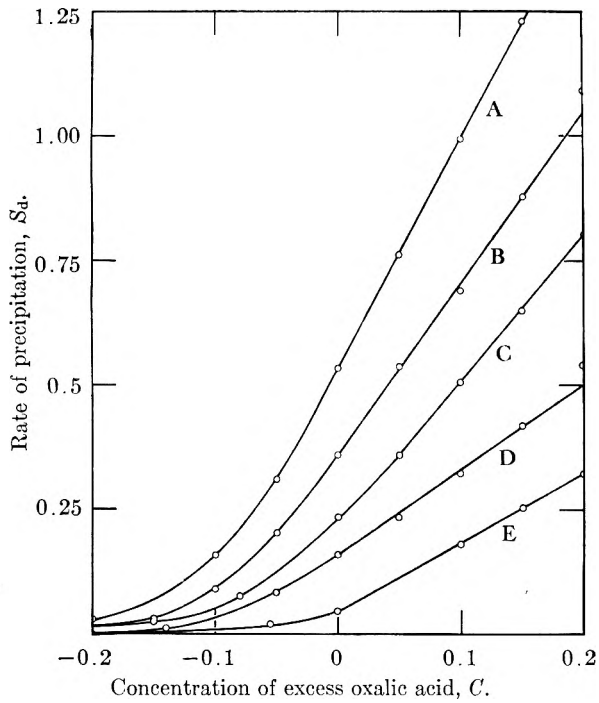

Fig. 2.—A, 0.4 N; B, 0.35 N; C, 0.3 N; D, 0.25 N; E, 0.2 N.

Equations 4 and 8 do not hold when the nickel sulfate is in excess. In these circumstances the rates tail off asymptotically with decreasing acid concentration; the induction period increases with decreasing salt and acid concentration and is considerable at the lower concentrations, especially when the salt is in excess.

Discussion

Nickel oxalate is known to exhibit a strong tendency to self-complex formation[2,3]; it is suggested, therefore, that the first step in the reaction involves the formation of a soluble complex represented by the equation

$$2NiSO_4\,(aq) + 2H_2C_2O_4\,(aq) \rightleftharpoons [Ni(C_2O_4)_2]^{=}\,Ni^{++}\,(aq) + 2H_2SO_4\,(aq)$$

The equilibrium constant is $\sim 10^{13}$,[4] so that formation of the favored complex ion would account for the existence of an induction period and for the longer periods and slower rates of precipitation in the presence of excess nickel sulfate.

In the early part of reaction studied turbidimetrically, for equinormal conditions the direct rearrangement

$$[Ni(C_2O_4)_2]^{=}\,Ni^{++}(aq) \longrightarrow 2Ni\,C_2O_4{\cdot}2H_2O(s) \quad (5)$$

would give rise to a term in the rate equation proportional to the square root of the complex ion concentration, that is, to $E^{3/2}$. There is good evidence that this step proceeds heterogeneously on the walls of the vessel. In the presence of excess oxalic acid the complex is rendered less stable, the decomposition yielding an additional term proportional to the product of the concentration of the complex ion, E^3, and the excess oxalic acid concentration, C. These two steps account for the experimental equation 4.

In the dilatometric range the solution is already cloudy with small crystals of solid oxalate dispersed in the solution. Growth may proceed by the breakdown of the complex ion at the surface of existing crystals, giving rise to a term proportional to the concentration of the complex ion, E^3, and, in the presence of excess oxalic acid, by direct ionic addition to the existing crystals yielding a term proportional to EC. The additional retardation term, $-k_4C$ in 8 is attributed to the solubility of the freshly deposited oxalate in the solution containing excess oxalic acid. These three processes would account for the experimental equation 8.

(2) R. Scholder, E. Gadenne and H. Niemann, *Ber.*, **60**, 1510 (1927).
(3) R. Scholder, *ibid.*, **60**, 1525 (1927).
(4) G. Sartori, *Gazz. chim. ital.*, **64**, 3 (1934).

EQUILIBRIA BETWEEN 18 AND 114° IN THE AQUEOUS TERNARY SYSTEM CONTAINING Ca^{2+}, Sr^{2+} AND Cl^-

BY GUNNAR O. ASSARSSON AND AINO BALDER

Chemical Laboratory of The Geological Survey of Sweden, Stockholm

Received February 16, 1953

The system strontium chloride–calcium chloride–water has been investigated between 18 and 114°. No double salt has been found within this temperature range. The hexahydrates of the chlorides form solid solution crystals of complete miscibility belonging to Roozeboom's type I, the cell axes of these crystals being slightly shorter than those calculated from Vegard's law. The dehydrating properties of the concentrated calcium chloride solutions cause an appreciable lowering of the transition temperature strontium chloride hexahydrate–dihydrate so that the field of stable existence of strontium chloride dihydrate overlaps the region of stability of the solid solution of the hexahydrates. In this way a new type of isothermal solid solution diagram appears: a continuous miscibility of the end phases is interrupted by a gap within which the stable phase is a compound not belonging to the end phases. The boundary curve between strontium calcium chloride hexahydrate (solid solution) and strontium chloride dihydrate has a temperature minimum at 28.2 ± 0.2°. The invariant point at which strontium calcium chloride hexahydrate (solid solution) is in equilibrium with α-calcium chloride tetrahydrate, strontium dihydrate and liquid is at 29.4 ± 0.1°. Another invariant point occurs at 44.9 ± 0.2° at which temperature α-calcium chloride tetrahydrate may exist in equilibrium with calcium chloride dihydrate, strontium chloride dihydrate and liquid. At higher temperatures strontium chloride monohydrate is deposited, its lowest formation temperature being at 76 ± 1°. The X-ray interferences of this new compound are given. The observations on the system are combined in a synopsis diagram.

In an earlier paper,[1] the results were reported of an investigation on the equilibrium between strontium chloride and alkali chlorides in aqueous solutions, with regard to the crystallization of salt from certain brines. Calcium chloride is also a usual component of such brines. Among the crystalline phases in salt deposits strontium chloride should occur either as a pure compound or in phases in which it could be combined with other components, although these phases have not yet been observed and recorded. It may be suggested that the phases containing strontium chloride could be utilized as temperature indicators for the crystallization of the salt deposits and it would therefore be of considerable interest to know the equilibria in the systems containing the chlorides of the alkalies as well as those of calcium and strontium.

Experimental

The experiments were performed as described in the earlier papers. Some difficulty was encountered in finding a rapid and accurate method for the determination of calcium and strontium chloride when occurring together. An indirect physical chemical method, based on the electrical conductivity of the aqueous solutions, was tried and worked out; it is described elsewhere.[2] For the elucidation of the character of the crystal phases the methods of optical microscopy, of thermal analysis, and of X-ray identification were used. In this work the equilibria between 18 and 114° were studied.

In the tables all determinations are given as weight per cent.

Discussion of the Results

It can be expected that the calcium chloride in the solutions will depress the solubility of strontium chloride. This appears in fact in the isotherms; the solubility of strontium chloride in concentrated calcium chloride solutions is very low (about 1–2%). As the water of crystallization of strontium chloride hexahydrate is partly loosely bound, the transition temperature of strontium chloride hexahydrate–dihydrate should be lowered appreciably with increasing calcium chloride content.

The transition temperature strontium chloride hexahydrate–dihydrate is at 61.3° in the binary system strontium chloride–water, and in the present ternary system the strontium chloride dihydrate has its lowest formation temperature at 28.2°. The transition temperature of calcium chloride α-tetrahydrate-dihydrate is insignificantly affected by the presence of strontium chloride; the temperatures are 45.3 and 44.9°, respectively, in the binary system calcium chloride–water and in the present ternary system (Table I, point E).

The equilibria in which the hexahydrates of calcium and strontium chlorides are present have a certain interest. Eppler[3] has shown by goniometrical measurements that the hexahydrates are isomorphous and trigonal. Herrmann[4] and later Tovborg-Jensen[5] have recorded that the two phases mentioned have a unit cell of almost the same dimensions. Because the hexahydrates are isomorphous and there is no considerable difference between the ionic radii of Ca^{2+} and Sr^{2+}, they should be able to form solid solution (mixed crystals). The study of the isothermal equilibria in the present investigation has shown the conditions for the formation of the solid solution. The isotherms between 18.0 and 28.0° have no breaks indicating isothermal invariant points. Instead of the break there is a flexure on the curves, which are S-shaped close to the calcium chloride axis of the diagrams (see Table I and Fig. 1, the isotherms at 18.0 and 28.0°), and the composition of the solid phase changes successively with the concentration of the mother liquor, two characteristic phenomena shown when a solid solution crystallizes. It can be estimated from the tie-lines of Fig. 1 that a solid solution containing equal parts of the two hexahydrates requires a mother liquor containing 1.4–2.1% strontium chloride and 39–42% calcium chloride between 18.0 and 28.0°. The distribution diagram according to Roozeboom (Fig. 2, 28.0°) illustrates the dependence of the composition of the solid solution on the concentration of the solutions. As the curve first follows very close to one of the axes of the distribution

(1) G. O. Assarsson, THIS JOURNAL, 57, 207 (1953).

(2) G. O. Assarsson and A. Balder, *Anal. Chem.*, 24, 1679 (1952)

(3) A. Eppler, *Z. Krist.*, 30, 149 (1899).

(4) L. Herrmann, *Z. anorg. allgem. Chem.*, 197, 212 (1931).

(5) A. Tovborg-Jensen, *Danske Videnskab. Selskab., Mat.-fys. Medd.*, XVII, 9 (1940), (Copenhagen) (English).

TABLE I

THE TERNARY SYSTEM $SrCl_2$–$CaCl_2$–H_2O

Symbols for the solid phases, used in the tables: a, $SrCl_2 \cdot 6H_2O$; b, $SrCl_2 \cdot 2H_2O$; c, $CaCl_2 \cdot 6H_2O$; d, α-$CaCl_2 \cdot 4H_2O$; e, $CaCl_2 \cdot 2H_2O$; f, solid solution of $SrCl_2 \cdot 6H_2O$ and $CaCl_2 \cdot 6H_2O$; g, $SrCl_2 \cdot H_2O$. Some isotherms between 18 and 45°.

Solution $SrCl_2$	Solution $CaCl_2$	Wet residue $SrCl_2$	Wet residue $CaCl_2$	Solid phase
		18°		
34.15	...	..	..	a
26.9	6.6	..	..	f
18.0	14.6	..	..	f
4.0	31.2	42.0	10.5	f
3.0	33.3	41.2	12.2	f
2.1	35.5	40.3	13.6	f
1.9	37.7	27.6	22.4	f
1.4	38.7	22.5	28.4	f
1.1	39.7	18.9	31.2	f
0.7	40.4	10.0	40.6	f
0.5	40.6	5.0	43.0	f
0.4	41.2	1.5	46.0	f
0.3	41.4	1.0	48.9	f
...	42.05	..	..	c
		28.0°		
36.6	...	..	..	a
17.6	17.2	44.8	6.3	f
6.0	30.7	39.0	7.0	f
3.4	35.4	35.7	16.0	f
2.7	40.1	34.6	19.0	f
2.2	41.7	20.4	31.4	f
2.1	42.3	15.9	35.4	f
1.7	43.6	11.1	39.4	f
1.5	44.3	5.3	44.0	f
1.0	45.2	5.7	44.7	f
1.1	45.9	2.9	47.1	f
1.0	46.1	2.4	47.3	f
0.6	46.6	1.6	48.3	f
...	47.2	..	..	c
		28.5°		
2.6	40.3	33.6	20.3	f
2.6	40.9	22.8	29.0	f
2.4	42.2	52.9	16.1	b
2.3	42.7	52.5	17.0	b
1.7	44.1	52.1	17.6	b
1.6	44.2	8.7	41.1	f
1.3	44.6	8.2	42.1	f
1.2	45.2	6.6	43.9	f
1.0	46.0	3.5	46.0	f
0.8	46.9	2.9	47.1	f
...	47.9	..	49.5	c
		29.0°		
36.8	...	..	..	a
20.0	16.0	55.0	2.0	f
6.4	30.6	39.1	12.0	f
2.8	39.1	34.9	19.1	f
2.9	40.6	33.0	21.0	f
2.9	41.6	58.7	13.1	b
2.5	42.0	55.0	15.0	b
2.5	42.5	57.7	14.5	b
1.7	44.0	59.7	11.7	b
1.7	44.3	54.6	15.5	b
1.6	44.6	9.6	41.2	f
1.4	45.2	8.2	42.6	f
1.4	45.8	5.8	44.8	f
1.1	46.8	2.6	47.2	f
0.9	47.7	1.9	48.7	f
0.2	48.7	0.5	49.0	f
...	49.2	..	49.8	c
		29.3°		
3.7	38.5	41.5	14.2	f
3.5	39.9	35.9	18.3	f
3.4	40.2	50.0	11.6	b + f
2.7	41.6	55.3	14.3	b
2.5	42.4	54.7	15.1	b
2.3	42.8	55.5	14.9	b
1.9	44.8	54.5	16.0	b
1.7	46.5	9.0	42.0	f
1.4	47.4	4.5	46.7	f
0.7	48.7	1.8	48.7	f
0.3	49.1	0.9	49.6	f
...	49.6	..	49.8	c
		29.7°		
37.0	...	..	..	a
28.7	7.5	57.0	1.0	f
13.5	21.9	56.3	1.6	f
7.4	29.5	42.0	10.6	f
3.1	39.4	35.5	19.0	f
3.0	40.4	48.4	11.2	b + f
2.0	42.2	54.1	14.9	b
1.4	44.6	52.7	16.9	b
1.3	46.6	54.8	16.2	b
1.4	46.9	47.0	21.4	b
1.2	47.7	47.0	21.7	b
1.2	48.2	47.5	22.0	b
1.0	49.2	6.0	49.0	b + d
1.0	49.0	0.7	57.4	d
0.8	49.2	0.5	57.7	d
...	50.2	..	56.7	d
		44.3°		
9.6	31.6	45.7	10.4	f
7.2	34.4	53.5	13.5	b
1.0	55.2	0.4	59.7	d
		44.7°		
1.0	55.0	35.1	31.9	b
0.9	55.6	0.4	59.0	d
		45.3°		
0.9	56.0	34.0	33.6	b
0.9	56.3	0.1	69.2	e

For the invariant points (C, D, E, in Fig. 5)

	Solution $SrCl_2$	Solution $CaCl_2$	
C 28.2 ± 0.2°	2.0	42.2	b + f
D 29.4 ± 0.1°	1.0	48.5	b + d + f
E 44.9 ± 0.2°	1.0	55.7	b + d + e

diagram up to a very high concentration of one of the components, and then follows the direction of the other axis, it can be concluded that the formation of the solid phase is connected with extraordinary properties of the liquid phase. Other plotting methods point to the same conclusion.

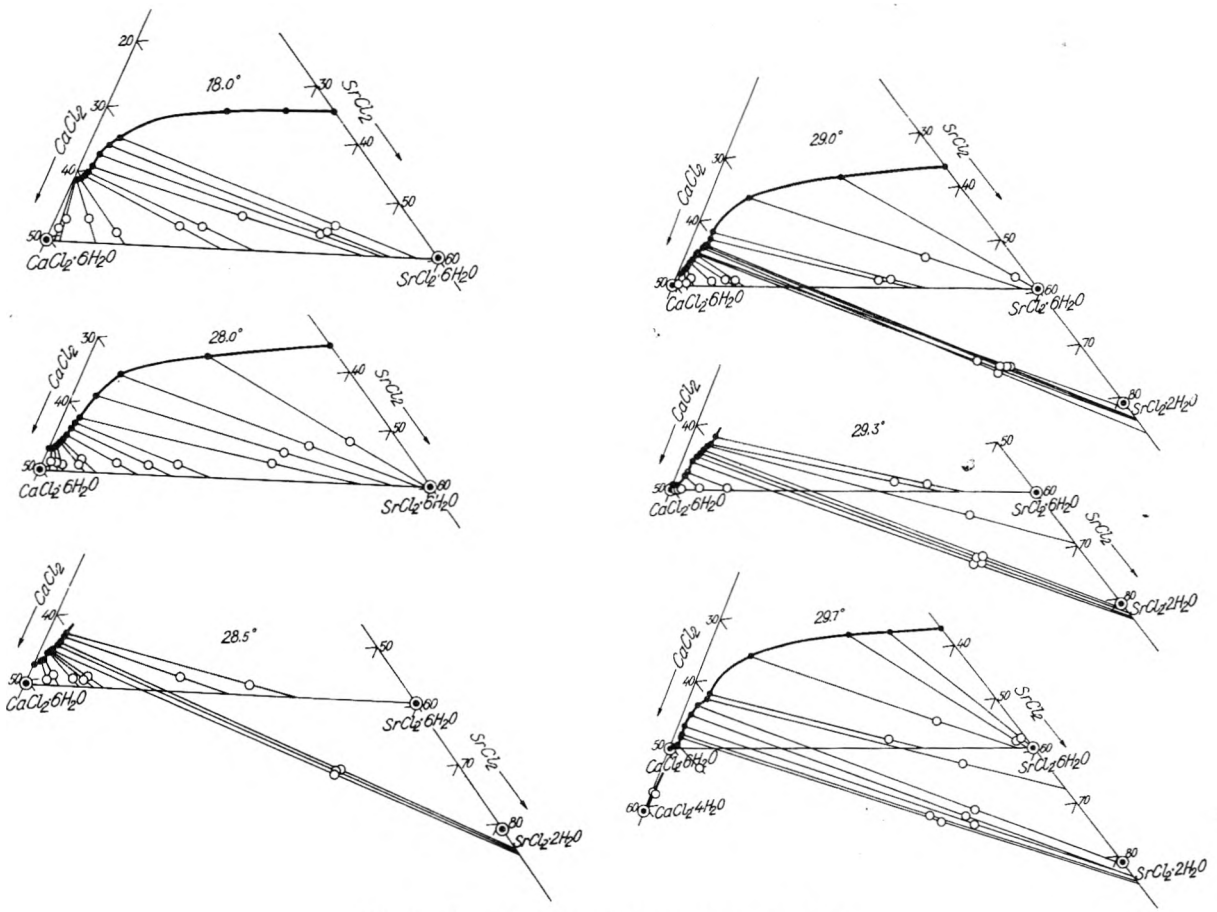

Fig. 1.—Some isotherms between 18.0 and 29.7°.

The plot of log R_l against R_s (R_l = mole ratio of the dissolved salts, R_s = mole ratio of the solid phase) and the plot of log (R_l/R_s) against the mole fraction in the solid are not linear, so that the distribution coefficient is not constant and the solid solution is not "regular."[6] It can hardly be expected that the concentrated solutions in which the solid solution in question is formed, would correspond to the more "ideal" solution presumed in such calculations, since the reactions of concentrated calcium chloride solutions obviously indicate that the solutions contain hydrated aggregates.

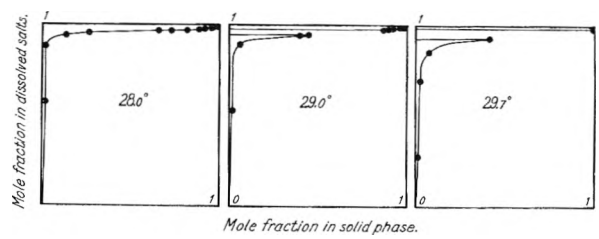

Fig. 2.—Distribution diagrams according to Roozeboom: in solid solution $(CaSr)Cl_2 \cdot 6H_2O$ and mother liquor mole fraction 1 = 100% $CaCl_2$.

TABLE II

CALCULATED AND OBSERVED INTERFERENCES IN POWDER DIAGRAMS OF $CaCl_2 \cdot 6H_2O$, $SrCl_2 \cdot 6H_2O$, AND A SOLID SOLUTION CONTAINING 50% OF EACH; $CuK\alpha$ RADIATION

	$SrCl_2 \cdot 6H_2O$		Solid solution $(Ca_{0.5}Sr_{0.5})Cl_2 \cdot 6H_2O$		$CaCl_2 \cdot 6H_2O$		
	Sin^2		Sin^2		Sin^2		
Int.	calcd.	obsd.	calcd.	obsd.	calcd.	obsd.	Miller indices
s	0.0127	0.0130	0.0127	0.0127	0.0128	0.0130	100
s	.0375	.0375	.0380	.0380	.0380	.0382	110
s	.0474	.0477	.0496	.0500	.0513	.0509	101
w	.0500	..	.0507	..	.0510	..	200
m	.0725	.0727	.0750	.0751	.0767	.0760	111
s	.0843	.0850	.0876	.0875	.0895	.0894	201
w	.0878	..	.0887	..	.0893	..	210
s	.1124	.1125	.1140	.1140	.1148	.1154	300
s	.1224	.1229	.1256	.1260	.1277	.1280	211
w-m	.1397	.1400	.1477	.1480	.1528	.1536	002
w	.1474	.1480	.1509	..	.1533	..	301
m	.1504	.1510	.1520	..	.1551	..	220
w-m	.1626	.1625	.1647	.1620	.1659	.1662	310
w-m	.1771	.1775	.1858	.1860	.1920	.1921	112
w	.1897	.1900	.1989	.1980	.2048	.2045	202
m	.1971	.1972	.2016	.2011	.2044	..	311
w	.2000	..	.2027	..	.2045	..	400
m	.2267	.2270	.2364	.2363	.2432	.2431	212
m	.2348	.2350	.2396	..	.2426	..	401
m	.2519	.2519	.2618	.2610	.2688	.2683	302
m	.2622	.2626	.2661	.2672	.2681	..	410
m	.2726	.2726	.2777	.2794	.2809	.2806	312

The relation between the cell dimensions of the solid solution crystals and their composition could be of some interest. X-Ray photographs (powder) of some preparations were made. The samples were exposed to $CuK\alpha$ radiation and the cameras used had a diameter of 114.7 mm. The interference measurements of a preparation containing 50% of each component are listed in Table II together with the measurements for the pure hexahydrates: these last are calculated from measurements earlier

(6) J. E. Ricci and J. Fischer, *J. Am. Chem. Soc.*, **74**, 1443 (1952), and their cited literature.

published.[5] The calculated axial lengths of two other preparations are listed in Table III together with those above mentioned. The hexahydrates

TABLE III

RELATION BETWEEN THE UNIT CELL DIMENSIONS AND THE COMPOSITION OF THE SOLID SOLUTION $(CaSr)Cl_2 \cdot 6H_2O$, Å. UNITS

Content of $CaCl_2 \cdot 6H_2O$	100	78	50	33	0
a-axis	7.880	7.890	7.905	7.920	7.960
c-axis	3.930	3.970	4.010	4.045	4.130

form solid solution crystals, with axes slightly shorter than those calculated on the assumption that they depend only on the relative length of the integral components, represented in Fig. 3 by the tie-line between the values of the pure phases (Vegard's law). The largest negative deviation appears to be shown by the crystals containing equal parts of the components.

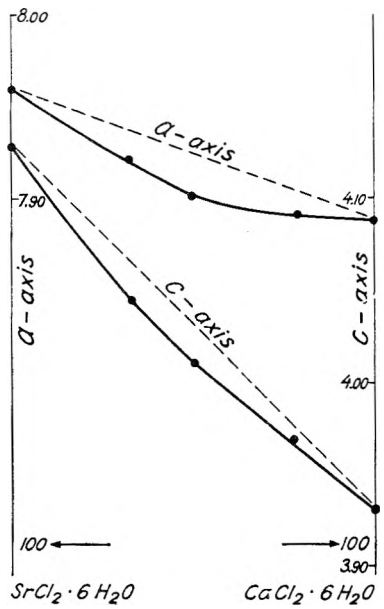

Fig. 3.—The relation between the axial lengths of the unit cells and the composition of the solid solution $(CaSr)Cl_2 \cdot 6H_2O$.

Between 28.0 and 30.0° the system shows some interesting traits. In the binary system calcium chloride–water the transition temperature calcium chloride hexahydrate–α-tetrahydrate is at 29.5°.[7] In the present ternary system, however, the dihydrate of the strontium chloride is the stable phase in saturated calcium chloride solution at this temperature. This dihydrate is monoclinic and α-calcium chloride tetrahydrate is triclinic.[8] The hexahydrates of calcium and strontium chlorides are isomorphous and form crystals of complete miscibility as shown above. Therefore, the stability area of strontium chloride dihydrate overlaps the area of solid solution of the hexahydrates.

When studying in more detail the isotherms from 28.0 to 29.7°, the following observations can be made (see Table I and Fig. 1). The isotherm at 28.0° shows the hexhydrates forming solid solution continuously without any gap. Between 28.5 and 29.3°, when the solutions contain pure calcium chloride, the solid phase is the hexahydrate. On adding small quantities of strontium chloride, solid solution of the two hexahydrates is deposited, the crystals being rich in calcium chloride. As the proportion of strontium chloride is further increased, the solid phase undergoes continuous change in composition, the crystals containing successively more strontium chloride and less calcium chloride. The calcium chloride concentration can be lowered in this way to a certain value, after which the solid phase suddenly changes its character. A deposition of strontium chloride dihydrate now begins. The transition concentration, however, is not discernible as a break in the isotherm. As the calcium chloride concentration is lowered still further, deposition of strontium chloride dihydrate continues. During the first part of this crystallization the strontium chloride concentration of the solutions is almost constant and during the later part the concentration increases. With continued decrease in calcium chloride content the solid phase again changes its character and the solid solution is formed once more. Here the curves show a distinct break. The crystals are now poorer in calcium chloride than those formed within the solid solution zone immediately before the described transition to strontium dihydrate. As the curves representing the solutions in equilibrium are S-shaped and have no discernible break where the solutions are very rich in calcium chloride, it is to be suggested that the transition of the solid phase in this case is caused by only a small change of entropy of the system compared with the change in concentration. At that part of the curves where the break is distinct the entropy change must be greater. If the isotherms are compared it is apparent that the higher the temperature, the higher the calcium chloride content in the solutions at the isothermal invariant point strontium dihydrate–solid solution of the hexahydrates rich in calcium chloride. The solid solution occurs in this part of the 29.3° isotherm but cannot occur in the same part of the 29.7° isotherm containing the transition point calcium chloride hexahydrate–α-tetrahydrate in pure water, therefore the invariant point strontium chloride dihydrate–α-calcium chloride tetrahydrate–solid solution of the hexahydrates is estimated to be at 29.4°. As the dihydrate crystallizes in the described way along the isotherm at 28.5° but does not do so along the isotherm 28.0°, the lowest temperature of its formation is estimated to be 28.2 ± 0.2°.

The solid solution of the hexahydrates formed at both sides of the dihydrate interval, changes in composition in the same continuous way as already described for temperatures lower than 28.0°. In the distribution diagrams (Fig. 2) the change in composition of the solids [solid solution (hexahydrate)–strontium chloride dihydrate–solid solution (hexahydrate)] appears as a continuous curve

(7) H. W. B. Roozeboom, *Z. physik. Chem.*, **4**, 31 (1889), has recorded 29.8°. A. Lannung, *Z. anorg. allgem. Chem.*, **228**, 1 (1936), reports 29.5° as transition temperature, which value has been confirmed and will be used here.

(8) H. Basset, H. F. Gordon and J. Heinshall, *J. Chem. Soc.*, 972 (1937).

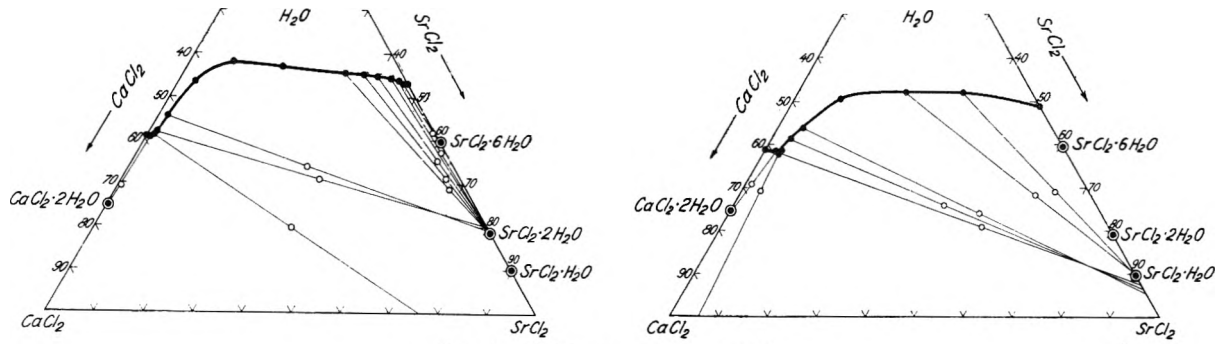

Fig. 4. Isotherms at 60 and 100°.

representing solid solution, interrupted by a gap corresponding to the dihydrate. Thus, the formation of solid solution mentioned above is characterized by the fact that a continuous crystallization occurs, having the behavior of a solid solution with complete miscibility of the end phases, but showing a gap in which there crystallizes out a new phase not belonging to the miscible phases. This type of crystallization of a solid solution with a gap in which is deposited another compound has not been described before, as far as is known to the authors. It could perhaps be classified as a seventh type of system forming solid solutions after Roozeboom,—a sixth type has been recorded by Ricci[9]—but in the authors' opinion the case described above should be considered as an infrequent and special one of Roozeboom's type I, as the solid solution shows a continuous miscibility and the intermediate phase does not contain the end phases.

At higher temperatures, too, the system shows some interesting characteristics. The isotherm at 60° (Table IV, Fig. 4) shows no double salt but it is noteworthy that even a small amount of calcium chloride (1.4%) in the solution causes a transition of the strontium chloride hexahydrate into the dihydrate.

It is known from some earlier investigations, that strontium chloride monohydrate is formed above 100° (Etard,[10] Hüttig and Slonim[11]). Benrath[12] has determined the transition temperature of this reaction in the binary system chloride–water and found it to be at as high a temperature as 230°. The very strongly dehydrating properties of saturated calcium chloride solutions must influence the transition temperature considerably. For the 100° isotherm (Table IV, Fig. 4) it is shown that the solid phase is the monohydrate over the greater part of the strontium chloride branch. Because of the experimental conditions it is difficult to determine the calcium chloride concentration at which the transformation of the di- and monohydrate takes place at 100°; it has no special significance in the present investigation but it must have a low value. In order to determine the invariant point in the ternary system some other isotherms were investigated. An extract of the observations are listed in Table V. The lowest formation temperature of strontium chloride mono-

(9) J. E. Ricci, *J. Am. Chem. Soc.*, **57**, 805 (1935).
(10) A. L. Etard, *Ann. chim. phys.*, [7] **2**, 533 (1894).
(11) G. I. Hüttig and Chr. Slonim, *Z. anorg. allgem Chem.*, **181**, 66 (1929).
(12) A. Benrath, *ibid.*, **247**, 147 (1941).

TABLE IV

THE TERNARY SYSTEM $SrCl_2$–$CaCl_2$–H_2O

Solution $SrCl_2$	Solution $CaCl_2$	Wet residue $SrCl_2$	Wet residue $CaCl_2$	Solid phase
		Isotherm at 60.0°		
46.2	..	..	..	a
45.5	0.8	58.0	0.2	f
45.0	1.4	62.4	0.2	f + b
43.3	2.9	72.1	0.5	b
40.0	5.6	62.0	2.6	b
37.0	8.0	66.0	2.5	b
33.0	11.4	68.2	3.3	b
18.8	23.7	..	..	b
8.5	34.3	..	..	b
3.3	43.2	..	..	b
1.7	52.5	36.0	30.0	b
1.0	57.0	39.9	29.0	b
1.0	57.1	38.2	40.6	b + e
0.8	57.6	0.6	70.3	e
..	58.2	..	69.7	e
		Isotherm at 100°		
50.8	..	..	..	b
33.7	15.2	63.8	7.0	g
22.4	26.0	60.2	11.2	g
9.5	39.8	..	..	g
5.1	51.0	51.3	25.2	g
3.9	54.4	42.6	31.1	g
2.9	58.7	53.1	26.2	g
2.7	59.1	3.6	67.1	e + g
2.5	59.4	1.4	68.1	e
..	61.3	..	70.0	e

TABLE V

THE TERNARY SYSTEM $SrCl_2$–$CaCl_2$–H_2O; SOME EQUILIBRIA BETWEEN 50 AND 114°

Temp., °C.	Solution $SrCl_2$	Solution $CaCl_2$	Wet residue $SrCl_2$	Wet residue $CaCl_2$	Solid phase
50	0.9	56.7	..	..	b + e
60	1.0	57.0	..	..	b + e
70	1.5	57.0	..	..	b + e
75	2.6	56.5	46.4	26.0	b
	2.5	56.8	2.0	66.5	e
77	3.0	55.6	47.2	25.7	b
	2.9	56.1	36.5	35.4	g
	2.4	57.1	1.6	57.1	e
90	2.5	58.2	..	..	e + g
100	2.7	59.1	..	..	e + g
114	3.5	59.6	..	..	e + g
		For the invariant point (I, Fig. 5)			
76	2.5	57.0	b + e + g		

hydrate was found to be 76°. The univariant curve as defined by the series of isothermal invariant points is drawn in Fig. 5, but no distinct break can be observed in this curve at 76°.

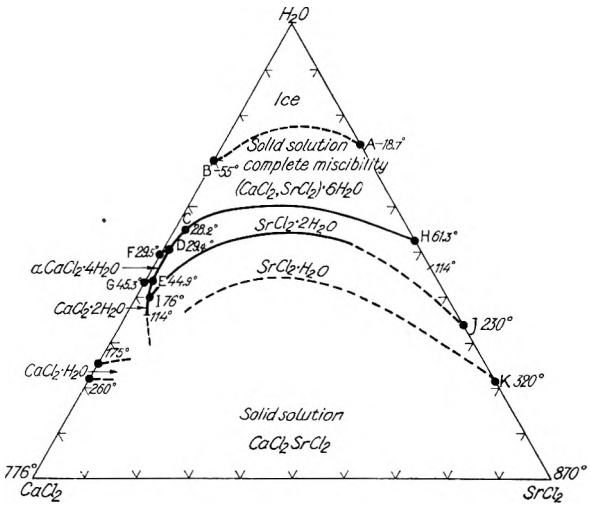

Fig. 5.—Synopsis of the composition of the solutions at the invariant and univariant equilibria of the ternary system $SrCl_2$–$CaCl_2$–H_2O.

Some other experiments were performed in order to determine the character of the solid phase. The direct preparation of pure solid phase according to a method earlier used,[1] was not successful because of the necessity of working at high temperatures and with mother liquors rich in calcium chloride. Differential thermal analysis, mentioned in the earlier paper[1] was performed on a mixture of three parts strontium chloride dihydrate and two parts calcium chloride tetrahydrate and showed a distinctly marked endothermic peak beginning at about 80°. As the transition takes place slowly, it was of importance to conduct the analysis under conditions of very slowly increasing temperature, which resulted in the heat absorption being delayed.

A preparation of strontium chloride dihydrate was mixed with 10% α-calcium chloride tetrahydrate and exposed in a Lindemann glass capillary in a heat X-ray camera at 110°. At another preparation strontium chloride hexahydrate was dried in an air-bath at 95° to constant weight (89.5% chloride) and exposed in a common X-ray camera of 114.7 mm. diameter. The interference measurements of both preparations are listed in Table VI and agree very well with one another and are quite different from those of strontium chloride dihydrate.[13] As the preparation at the heat camera corresponds to the solid phases precipitated from the saturated calcium chloride solutions at 110°, both of the preparations contain the same phase, which must be a monohydrate. An examination of the crystals in a polarization microscope with heated stage was not successful because of the difficulty in handling the solutions.

(13) A. Tovborg-Jensen, *Kgl. Danske Videnskafs Selskab. Mat.-fys. Medd.*, **XX**, nr 5, Copenhagen 1942 (English).

TABLE VI

X-RAY INTERFERENCES OF $SrCl_2·H_2O$; Cu Kα RADIATION

Preparation: a, $SrCl_2·6H_2O$, dried in an air-bath at 95°, 89.5% $SrCl_2$; b, $SrCl_2·2H_2O$, containing 10% $CaCl_2·4H_2O$, exp. at 110° in X-ray heat camera.

Int.	Prep. a Sin^2	Prep. b Sin^2	d, Å.	Int.	Prep. a Sin^2	Prep. b Sin^2	d, Å.
s	0.0119	0.0119	7.00	s	0.0716	0.0714	2.882
m-w	.0130	.0130	6.74	m	.0771	.0769	2.774
w	.0150	..	6.27	m	.0820	.0813	2.696
m	.0199	.0198	5.47	m	.0870	.0865	2.615
w	.0225	..	5.11	w	..	.0895	2.572
w	.0247	..	4.88	m	.0995	.0981	2.456
m	.0275	.0273	4.62	m	.1050	.1042	2.384
m-w	..	.0288	4.518	s	.1124	.1118	2.301
w	.0340	.0347	4.132	m	.1154	.1151	2.259
m	.0366	.0360	4.047	w	.1186	..	2.228
w	.0428	.0427	3.721	m	.1240	.1233	2.191
m	.0483	.0478	3.526	w	.1285	.1273	2.156
w	.0535	.0535	3.325	m	.1393	.1391	2.062
w	.0580	.0576	3.202	w	.1510	.1501	1.986
w	.0640	.0627	3.066				

The only observation which was made concerning the crystallographic properties was that the monohydrate crystallizes in plates and needles of apparently low degree of symmetry. As the strontium chloride monohydrate is formed at 230° in the binary system[12] and its lowest formation temperature in present ternary system is at 76° (Table V) the saturated calcium chloride solution lowers the transition temperature 154°.

Figure 5 is intended to give a synopsis of the univariant and invariant equilibria of the system. The equilibria at low temperature with ice as one of the solid phases are known only in the case of the binary systems, where the second phase is the respective hexahydrate. It is evident, however, that in the present ternary system the other solid phase must be solid solution of the hexahydrates. The bivariant equilibria containing the solid solution cover the area up to the line FDCH (Fig. 5), bounding the area within which strontium chloride dihydrate is a stable phase. Strontium chloride monohydrate crystallizes at temperatures higher than 76° (boundary I-J) and at very high temperatures, at which the mother liquor is very poor in water, a solid solution of anhydrous calcium and strontium chloride must crystallize.[12,14]

(14) C. Sandonnini, *Atti Acad. Lincei.*, [5] **20**, II, 497 (1911).

THE EXCHANGE REACTION OF HYDROGEN AND TRITIUM[1,2]

BY LEON M. DORFMAN AND H. C. MATTRAW

Contribution from the Knolls Atomic Power Laboratory, The General Electric Company, Schenectady, N. Y.

Received February 19, 1953

The rate of exchange of hydrogen and tritium, initiated by the tritium β-radiation, has been investigated at room temperature. Over the range of conditions studied, half-times of from 260 to 818 minutes have been obtained. G values for the initial rate of formation of tritium hydride range as high as 450 molecules/100 e.v., indicating the reaction to be a chain process. The initial rate was found to be directly proportional to the total pressure and to the square-root of the absorbed β-intensity.

Introduction

The exchange reaction of hydrogen and deuterium has been the subject of a number of previous investigations. Extensive studies of the rate of the thermal exchange reaction have been made by Farkas and Farkas[3] and more recently by Van Meersche.[4] These studies have established that the mechanism of the thermal exchange is a chain process involving atom–molecule interactions. Mund, *et al.*,[5] have reported results of the radiation-induced exchange of hydrogen and deuterium initiated by α-particles from radon. In all these cases analyses have been carried out by the thermal conductivity method.

We have investigated the rate of the hydrogen–tritium exchange

$$H_2 + T_2 = 2HT$$

This reaction, initiated by the tritium β-radiation, has been studied at room temperature using a mass spectrometer as the analytical instrument.

Experimental

A series of runs has been carried out extending over a range of total pressures from 59.0 to 399.9 mm. with tritium pressures between 33.2 and 147.7 mm. Hydrogen was purified by absorption on a uranium bed followed by pumping and subsequent desorption. The hydrogen was stored over a Fugassi valve to avoid any contamination by grease. Tritium, containing approximately 95% tritium and 5% hydrogen, was separated from impurities prior to each run by diffusion through a palladium thimble.

Runs were carried out in spherical Pyrex bulbs with a total volume of 109.5 ± 0.5 cc., at a temperature of 28.0 ± 1.0°. Each bulb was fitted with two vacuum stopcocks in series enclosing a capillary lock to permit removal from time to time of a small analytical sample. The volume of the capillary lock was approximately 0.13 cc. so that removal of a sample for analysis resulted in a negligible pressure decrease in the reaction bulb. Fluorothene grease was used as the lubricant to minimize any exchange or interaction with the tritium. A new reaction bulb was used for each run. Prior to the run the bulb was pumped out and thoroughly degassed for several hours after which tritium was introduced by means of a Toepler pump. The run was started by adding hydrogen. The bulb was then connected to the sample manifold of the mass spectrometer by means of a ground joint lubricated with Fluorothene grease. The gas present in the capillary lock at the start of the run was discarded and analytical samples were taken from the reaction bulb.

A General Electric analytical mass spectrometer was used for the analyses. Sensitivity calibrations[6] showed that hydrogen and tritium have equal mass spectrometric sensitivities. A test of a H_2–T_2 sample at approximately 50 microns pressure in the expansion bulb of the mass spectrometer showed that the composition of the analytical sample remained constant for over half-an-hour, a considerably longer time than that required for an analysis. Some six to ten analyses were done on each run over a period of 10 to 40 hours depending on the composition of a particular run.

Results and Discussion

The progress of the reaction, as in the thermal H_2–D_2 exchange,[3] may be represented by the exponential equation

$$(HT)_\infty - (HT)_t = (HT)_\infty e^{-kt} \qquad (I)$$

where $(HT)_t$ and $(HT)_\infty$ denote the concentrations of tritium hydride at time t and at equilibrium, respectively. The concentration of HT is not zero at the start of a run since the initial tritium contained some 10% of tritium hydride. The constant k is fixed for a given run by the composition and pressure. $(HT)_\infty$ has been determined experimentally[6] for a number of compositions and pressures. The experimental values are slightly higher than the theoretical values. The differences are of significance in the determination of the equilibrium constant; their effect is negligible in the calculation of exchange rates based on equation I. The calculated value of the equilibrium constant is 2.57 at 25°. We have obtained[6] an experimental value of 2.87 ± 0.06.

The validity of equation I in representing the progress of the exchange may be seen from Fig. 1 which shows a plot for some of the runs of $1 - (HT)_t/(HT)_\infty$ *vs.* time in minutes, on a semi-logarithmic scale. The rate of exchange at time t is then given by

$$\frac{d(HT)_t}{dt} = k(HT)_\infty e^{-kt} \qquad (II)$$

and the true initial rate of HT formation is given by

$$\left(\frac{d(HT)_t}{dt}\right)_{t=0} = k(HT)_\infty \qquad (III)$$

The half-time, τ, of the reaction is given by

$$\tau = 0.693/k \qquad (IV)$$

where k is obtained from the slope of the straight lines in Fig. 1. The values of k and the half-times in minutes are shown in Table I in which the data for the series of six runs are tabulated.

A correlation of the exchange rate as a function of pressure and absorbed β-intensity is dependent on a knowledge of the fraction of the β-energy absorbed by the gas in the spherical reaction bulb The

(1) The Knolls Atomic Power Laboratory is operated by the General Electric Co. for the Atomic Energy Commission. The work reported here was carried out under Contract No. W-31-109 Eng.-52.

(2) Presented at the 122nd meeting of the American Chemical Society in Atlantic City, N. J., September, 1952.

(3) A. Farkas and L. Farkas, *Proc. Roy. Soc.* (*London*), **152A**, 124 (1935).

(4) M. Van Meersche, *Bull. soc. chim. Belg.*, **50**, 99 (1951).

(5) W. Mund, T. de Menten de Hornes and M. Van Meersche, *ibid.*, **56**, 386 (1947).

(6) H. C. Mattraw, C. F. Pachucki and L. M. Dorfman, *J. Chem. Phys.*, **20**, 926 (1952).

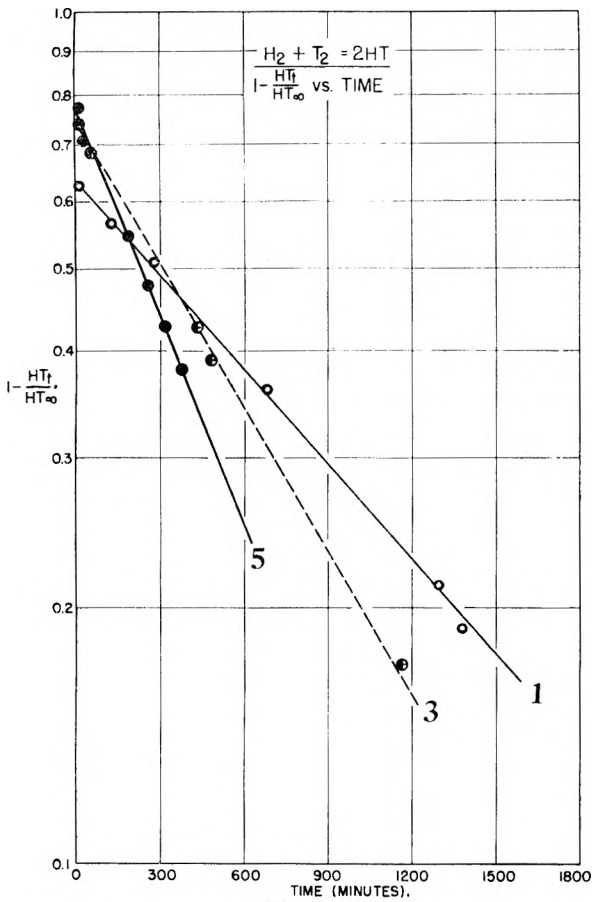

Fig. 1.

percentage absorption has therefore been estimated in the following manner.

Tritium has a half-life of 12.46 years[7] with a β-spectrum[8,9] having an end-point energy of 18 kev. and an average energy of 5.69 kev. The mass absorption coefficient for nuclear β-particles in aluminum is given by the equation[10]

$$\mu/\rho = 22/E_0^{1.33} \qquad (V)$$

for $0.1 < E_0 < 3.0$, E_0 being the end-point energy in mev.; or it may be obtained from the half-thickness curve[11] for nuclear β-particles. Equation V and extrapolation of the half-thickness curve, which is very nearly linear at the low-energy end, give a value of $\mu/\rho = 4.7$ cm.^{2}/mg. for tritium β-particles in aluminum. Examination of the range energy curve[12] (which requires no extrapolation) on the basis that the half-thickness is one-tenth the range, indicates that this estimated value for μ/ρ is at least of the right order of magnitude.

The mass absorption coefficient for different absorbers is very nearly proportional to Z/A. This gives a value, for nuclear β-particles in hydrogen, of $(\mu/\rho)_H = 2.1(\mu/\rho)_{Al}$, and in tritium of $(\mu/\rho)_T = 0.69(\mu/\rho)_{Al}$. Calculation of this ratio for hydrogen on the basis of the Bethe–Block equation[13,14] shows agreement within 19% with the value based on proportionality in Z/A. Comparison[15] of calculated with experimental values for absorbers of low atomic number indicates that the absolute values agree within 20%. The fraction of the β-energy absorbed has therefore been calculated from

$$\frac{I_{abs}}{I_0} = 1 - e^{-(\mu/\rho)x} \qquad (VI)$$

where x is the absorber thickness in mg./cm.^{2}. The average energy, 5.69 kev., has been used in calculating the amount of absorbed energy. The source of radiation in this case is uniformly distributed throughout a spherical bulb. Lind[16] has calculated that the average distance from all points within a sphere to the walls is 0.814 times the radius. The diameter of the reaction bulbs is 5.8 cm., so that the average path length through the gas is 2.36 cm.

The initial rates of formation of tritium hydride are shown in col. 7 of Table I. Column 8 lists the estimated fraction of the incident β-energy absorbed for each run. G-Values for the initial rate of formation of HT have been calculated and are listed in the last column. It is evident from these G-values which range as high as 450 molecules/100 ev. (corresponding to an ion-yield of 150 molecules/ion pair) that the exchange reaction involves a chain process.

TABLE I

Run no.	Total pressure, mm.	Tritium pressure, mm.	$M_{HT\infty}$	k, min.$^{-1}$ × 10^4	Half time, min.	$\left(\frac{d(HT)_t}{dt}\right)_{t=0}$ moles/l./min. × 10^7	I_a/I_0	$K' = \frac{kM_{HT\infty}}{\left(\frac{I_a}{I_0} \times [T_2]\right)^{1/2}}$ min.$^{-1}$ moles$^{-1/2}$ liters$^{-1/2}$ × 10^2	Initial HT yield, Molec./100 ev.
1	59.0	46.1	0.320	8.47	818	8.55	0.13	1.52	220
2	119.3	64.6	.454	12.6	550	36.4	.25	1.95	350
3	123.7	81.6	.418	13.3	522	36.7	.26	1.65	270
4	213.2	33.2	.248	13.7	504	38.7	.40	1.28	450
5	295.4	147.7	.458	19.5	355	140.6	.51	1.41	290
6	399.9	133.6	.411	26.7	260	233.9	.62	1.65	440
								Mean 1.58	

It may be shown from these data that the initial rate of exchange is proportional to the total pressure and to the square root of the absorbed β-intensity. This relationship

(7) G. H. Jenks, F. N. Sweeton and J. A. Ghormley, *Phys. Rev.*, **80**, 990 (1950).

(8) G. C. Hanna and B. Pontecorvo, *ibid.*, **75**, 983 (1949).

(9) E. R. Graves and D. I. Meyer, *ibid.*, **76**, 183 (1949).

(10) R. D. Evans, "The Science and Engineering of Nuclear Power," Vol. I, Addison-Wesley Press, Inc., Cambridge, Mass., 1947, p. 53.

(11) C. D. Coryell and N. Sugarman, "Radiochemical Studies: The Fission Products," McGraw-Hill Inc., New York, N. Y., 1951, Book 1, p. 18.

(12) L. E. Glendenin, *Nucleonics*, 2 (No. 1), 12 (1948).

(13) H. Bethe, *Z. Physik*, **76**, 293 (1932).

(14) H. Block, *ibid.*, **81**, 363 (1933).

(15) G. L. Brownell, "Conference on Absolute Beta-Counting," Preliminary Report No. 8, Nuclear Science Series, Paper 6 (1950).

(16) S. C. Lind, *J. Am. Chem. Soc.*, **41**, 531 (1919).

$$\left(\frac{d(HT)_t}{dt}\right)_{t=0} = K(I_{abs})^{1/2}P \qquad (VII)$$

may be tested in the following manner. From equations III and VII

$$k(HT)_\infty = K(I_{abs})^{1/2}P \qquad (VIII)$$

and since the incident β-intensity is directly proportional to the tritium concentration this may be written

$$K' = \frac{kM_{HT\infty}}{(I_{abs}/I_0[T_2])^{1/2}} \qquad (IX)$$

Where $M_{HT\infty}$ is the mole fraction of HT at equilibrium. The values of K' obtained in this correlation are shown in col. 9 of Table I. Reasonably good constancy obtains over a wide range of pressures and absorbed intensities. The mean value is $K' = 1.58 \times 10^{-2}$ (min.$^{-1}$ mole$^{-1/2}$ liter$^{-1/2}$). The individual values have an average deviation of 0.17×10^{-2}, or a standard deviation of 0.23×10^{-2}.

The kinetic expression for this radiation-induced exchange differs from that obtained in the thermal H_2–D_2 exchange,[3] in which the order of the reaction was found to be 3/2, in that $\sqrt{P}$ in the latter case is replaced by $\sqrt{I_{abs}}$. This difference stems from the different primary processes. In the thermal exchange reaction the primary dissociation at a given temperature is pressure dependent. In the H_2–T_2 exchange at room temperature the primary dissociation is dependent on the radiation intensity, or in other words on the tritium pressure. The square-root dependence in both cases indicates that the exchange proceeds by way of atom–molecule interactions. The mechanism may be written

$$H_2 \xrightarrow{\sim} 2H \qquad (1)$$
$$T_2 \xrightarrow{\sim} 2T \qquad (2)$$
$$HT \xrightarrow{\sim} H + T \qquad (3)$$
$$H + T_2 \rightleftharpoons HT + T \qquad (4)$$
$$T + H_2 \rightleftharpoons HT + H \qquad (5)$$
$$2H \longrightarrow H_2 \qquad (6)$$
$$2T \longrightarrow T_2 \qquad (7)$$
$$H + T \longrightarrow HT \qquad (8)$$

The exchange occurs chiefly by way of reactions (4) and (5) rather than reaction (8) as indicated by the high ion yields.

The ion yield is inversely proportional to the square-root of the radiation intensity. Mund, *et al.*,[5] in one of their two runs have obtained an ion yield for HD formation greater than 10^3. This may be explained by the fact that their ionization intensity was on the order of 1/200th of the intensity in these H_2–T_2 runs.

Acknowledgment.—We are indebted to Mr. C. F. Pachucki for his assistance in carrying out the mass spectrometric analyses, and to Dr. D. L. Douglas with whom we have had many helpful discussions.

KINETICS OF THE REACTION BETWEEN SILVER BROMIDE AND AN ADSORBED LAYER OF ALLYLTHIOUREA

BY T. H. JAMES AND W. VANSELOW

Communication No. 1544 from the Kodak Research Laboratories

Received February 25, 1953

Allylthiourea is strongly adsorbed by silver bromide to form a monolayer. The adsorbed allylthiourea prevents adsorption of certain dye ions, *e.g.*, phenosafranin and 3,3′-diethyloxacarbocyanine, but the dyes are rapidly adsorbed after reaction between the allylthiourea and silver bromide occurs. Use is made of this fact to measure the rate of reaction in the adsorbed layer. The rate of reaction varies as the logarithm of the reciprocal of the bromide ion concentration in the surrounding solution. The rate varies as the 1.5 to 2 power of the hydroxyl ion concentration, depending on the bromide ion concentration. The reaction curve is not autocatalytic in shape, but reaction occurs faster on a silver bromide surface which contains sulfide, either from previous reaction with allylthiourea or from reaction with sodium sulfide. Chromatographic experiments indicate that the surface after reaction with one layer of allylthiourea is intermediate in adsorptive properties between a pure silver bromide surface and a silver sulfide surface, but more closely resembles the former. The rate of reaction of subsequently adsorbed layers of allylthiourea continues to increase with increasing amount of sulfide formed in previous reaction, far beyond the amount of sulfide which corresponds to a uniform layer one molecule thick. The rate of the sulfide-catalyzed reaction varies as the first power of the hydroxyl ion concentration. The over-all energy of activation of the uncatalyzed reaction is 32 kcal./mole in the absence of excess bromide, and 40 kcal./mole in the presence of 0.0001 *M* bromide ion. The activation energy of the sulfide-catalyzed reaction is 22 kcal./mole. The mechanism of the reaction is discussed on the basis of the kinetic results. The rate of reaction of derivatives of thiourea at *p*H 7.2 increases in the order: 1,3-diethyl, 1,1-dimethyl, methyl, (thiourea), allyl, phenyl, acetyl. 1,1,3,3-Tetramethylthiourea is inactive.

Introduction

Thiourea and many of its derivatives are strongly adsorbed by silver bromide. The adsorbed layer prevents adsorption of certain dye ions, such as the phenosafranin and 3,3′-diethyloxacarbocyanine cations. Under suitable conditions of temperature and *p*H, the adsorbed thioureas react with the silver bromide to form silver sulfide, and the surface formed by this reaction very rapidly adsorbs the dye cations. Use has been made of these facts to study the kinetics of the reaction of adsorbed thioureas, particularly allylthiourea, with silver bromide. Probably the technique can be extended to other reactions where the adsorptive properties of the reaction product differ markedly from those of the adsorbed reactant layer.

The present investigation was undertaken because of the importance to the theory of photo-

graphic sensitizing of the reaction of thioureas with silver bromide. Sheppard,[1] who discovered the sensitizing action of these compounds, showed that it was not the thioureas themselves but reaction products, presumably silver sulfide, which were responsible for the increase in sensitivity of the photographic emulsion. Carroll and Hubbard[2] studied the kinetics of the reaction of silver bromide with allylthiourea, and Collins and Dickinson[3] the reaction with thiourea. Both reactions are catalyzed by silver sulfide. In both investigations, the rate of reaction was followed by potentiometric determination of the bromide ion liberated in the reaction, and in both the amount of thiourea or allylthiourea used exceeded by 100- to 1000-fold the amounts reported in the literature as optimum for photographic sensitizing.[4] The amounts used in the present investigation correspond to an adsorbed monolayer of the thiourea, and are of the same order of magnitude as those reported for photographic sensitizing.

Experimental Procedure

The following experimental procedure was adopted as standard for the kinetic experiments: The silver bromide sample (about 4.2–4.6 g.) was placed in a stoppered flask containing 50 cc. of water which was made acid to *p*H 3.5 with acetic acid; 1 cc. of 0.01 *M* allylthiourea was added, and the flask and contents were shaken vigorously for 5 minutes. The contents of the flask were allowed to settle for 2 minutes, the supernatant liquid was poured off, and the precipitate washed by decantation with two 50-cc. portions of water containing 0.5 cc. of 0.1 *M* acetic acid. The precipitate was then transferred to the reaction vessel, together with 190 cc. of dye solution. The dye solution was prepared by adding 12 cc. of 0.0001 *M* 3,3′-diethyloxacarbocyanine *p*-toluenesulfonate and 1 cc. of a mixture of 0.1 *M* acetic acid and 0.1 *M* sodium acetate to 177 cc. of water. This solution had a *p*H of 4.75. Solution and precipitate were brought to the temperature of the thermostat before mixing. To start the reaction, 10 cc. of a phosphate buffer (*X* cc. of 0.2 *M* Na_2HPO_4 + *Y* cc. of 0.2 *M* NaH_2PO_4), also at the temperature of the thermostat, was added at time zero. The final *p*H of the solution was measured on a Beckman meter.

The reaction vessel consisted of a three-necked, 500-cc. round-bottom flask. Agitation by a motor-driven stirrer kept the silver bromide well suspended in the solution. Samples of the reaction mixture were removed from time to time with the aid of a 5-cc. pipet which had had its tip cut off to permit faster flow. Each sample was added rapidly to a centrifuge tube containing 2 cc. of 0.1 *M* acetic acid and 0.1 *M* sodium acetate mixture at *p*H 4.75 to stop the reaction. The tubes were then centrifuged to settle the silver bromide, and the supernatant liquid was pipetted off for colorimetric analysis. The dye concentration was determined by reading the density at the maximum of the absorption band (480 mμ) in the Beckman Model DU spectrophotometer. Preliminary experiments showed that the rate of reaction is not influenced by the presence of the dye. In these experiments, the silver bromide was introduced into the buffer solution without dye. Samples of silver bromide were removed from time to time; reaction was stopped by lowering the *p*H, and dye added. The amounts of dye adsorbed by the partially reacted surface agreed within 5% with the amounts adsorbed when dye was present during the reaction.

Materials Used.—The allylthiourea was Eastman Kodak Company White Label grade.

Two samples of silver bromide were used in the present investigation. Sample I was prepared by adding a solution of 170 g. of silver nitrate in 1000 cc. of water to a solution of 120 g. of potassium bromide in 1000 cc. of water at room temperature over a period of 2 minutes, with vigorous mechanical agitation. Stirring was continued for 15 minutes. The silver bromide was washed by decantation five times, using 3 l. of water each time, and was permitted to age several months under water at room temperature so that the surface area could reach a stable value before use. Sample II was prepared by adding 2000 cc. of 1.00 *M* silver nitrate and 2000 cc. of 1.02 *M* hydrogen bromide solutions simultaneously at the rate of 10 cc. each per minute to 1000 cc. of 0.0001 *M* hydrogen bromide solution, with vigorous mechanical stirring. All solutions were at 55°. The precipitate was then washed and aged as before. In the subsequent experiments, sample II was used except when otherwise stated, since the particles of this sample were of more uniform size and shape than those of sample I.

Sulfide determinations on the silver bromide samples after reaction were made by R. S. Miller, of these Laboratories, as follows: The silver bromide was washed, then dissolved in approximately 75 cc. of 50% potassium iodide solution, which was adjusted to the oxidation–reduction equivalence point before use by the appropriate addition of 0.0001 *N* iodine or arsenite solution. The solution was diluted to exactly 100 cc. with 50% potassium iodide solution, and a suitable aliquot transferred to a beaker containing 50 cc. of 50% potassium iodide solution and 0.05 g. of potassium bicarbonate. By use of a blanket of nitrogen and a magnetic stirrer, standard 0.0001 *N* iodine solution was added until an excess of 1 to 5 cc. was present. The solution was stirred for 3 minutes to ensure complete reaction with the silver sulfide and 5 cc. of standard 0.0001 *N* arsenite solution was added. The excess arsenite was back titrated with standard iodine solution.

Experimental Results

To determine the dependence of adsorbed allylthiourea on the amount present in solution, a series of tests was made in which the silver bromide samples were treated in the standard way except that the amount of allylthiourea added was varied from sample to sample. The washed samples were allowed to react completely with the allylthiourea remaining adsorbed after washing and the sulfide was determined as described. The concentration of allylthiourea remaining in solution was calculated as the difference between the amount added and the amount adsorbed. The results are given in Table I.

TABLE I

DEPENDENCE OF ADSORBED ALLYLTHIOUREA (ATU) ON THE AMOUNT IN SOLUTION

Residual concn. in soln., $M \times 10^6$	μmole ATU adsorbed per gram AgBr	Residual concn. in soln., $M \times 10^6$	μmole ATU adsorbed per gram AgBr
0.0	0.19	261	0.53
6.2	.36	284	.53
85	.53	1233	.70
240	.53	1355	.49

The specific surface of the silver bromide was determined from the adsorption of two dyes, 3,3′-diethyl-9-methylthiacarbocyanine chloride (Dye II) and 1,1′-diethyl-2,2′-cyanine chloride (Dye VI). The amounts of Dye II adsorbed by two samples of silver bromide were 0.320 and 0.323 micromole per gram; of Dye VI, 0.305 and 0.300. Assuming areas of 74 and 79 sq. Å.,[5] respectively, for these dyes, we obtain the values of 1430, 1440, 1450 and 1430 cm.^{2} per gram for the specific surface of the silver bromide.

The percentage of dye adsorbed during the reaction calculated in terms of the total dye adsorbed when reaction has gone to completion is indicated in Fig. 1 for *p*H 6.8 and 20.25°. Each curve, or set of points, represents a sample to which the designated amount of allylthiourea was initially added. Essentially the same reaction curve was obtained whether 0.5, 1.0 or 4.0 cc. of 0.01 *M* allylthiourea was added in the preparation of the sample. When only 0.1 or 0.2 cc. was added, some adsorption of dye occurred before addition of buffer to start the reaction, and this

(1) S. E. Sheppard, *Phot. J.*, **65**, 380 (1925); *Colloid Symposium Monograph*, **3**, 75 (1925).

(2) B. H. Carroll and D. Hubbard, *Bur. Standards J. Research*, **12**, 329 (1934).

(3) R. B. Collins and H. O. Dickinson, *Science et inds. phot.*, [2] **22**, 92 (1952).

(4) S. E. Sheppard, *Phot. J.*, **66**, 399 (1926).

(5) W. West, B. H. Carroll and D. H. Whitcomb, THIS JOURNAL, **56**, 1054 (1952).

must correspond to silver bromide surface not adequately protected by adsorbed allylthiourea. In all subsequent experiments, the amount of allylthiourea added was sufficient to saturate the surface. Reaction rates are determined in terms of the maximum slopes of the curves. These slopes represent about the first 10% of the reaction course in general, where the curves are nearly linear. Rates determined at some other fixed point on the curve lead to consistent relative values, except when that point is near completion of the reaction, where the experimental error is relatively high and the curves tend to become erratic.

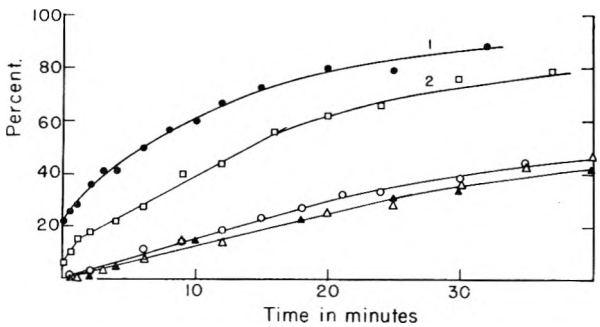

Fig. 1.—Dependence per cent. of dye adsorbed on amount of allylthiourea used in preparation of sample: ●●, 1.0 cc. of 0.001 *M*, *p*H 6.83; □□, 2.0 cc. of 0.001 *M*, *p*H 6.81; ○○, 5.0 cc. of 0.001 *M*, *p*H 6.79; ΔΔ, 1.0 cc. of 0.01 *M*, *p*H 6.83; ▲▲, 4.0 cc. of 0.01 *M*, *p*H 6.82.

Bromide ion in the solution decreases the rate of reaction of the adsorbed allylthiourea This effect is illustrated by the reaction curves shown in Fig. 2. No dye was adsorbed at any bromide ion concentration before the reaction was started by addition of the buffer, indicating that no significant displacement of allylthiourea by bromide occurred. The initial reaction rates vary approximately as the logarithm of the reciprocal of the bromide ion concentration.

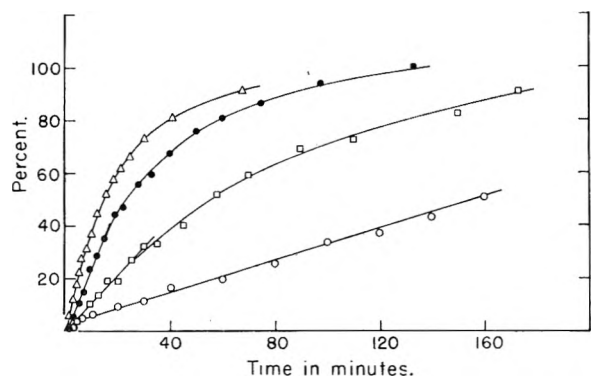

Fig. 2.—Effect of bromide ion at *p*H 7.22, 20.2°, per cent. of reaction completed is plotted against time: ΔΔ, no added KBr, $[Br^-] = 10^{-6}$, rate 4.6; ●●, 10^{-5} *M* KBr, rate 2.5; □□, 3×10^{-5} *M* KBr, rate 1.15; ○○, 10^{-4} *M* KBr, rate 0.3.

If a sample of silver bromide which has already reacted with an adsorbed layer of allylthiourea in the absence of dye is washed and then recoated with allylthiourea, by the standard procedure, the reaction of the second layer is faster than that of the first. This is illustrated by the curves in Fig. 3, which represent reaction in the presence of 0.0001 *M* excess bromide ion. Curves 1 and 2 represent reaction of the first and second layers, respectively. Curves 3, 4 and 7 represent the reaction of layers adsorbed after two, three and six previous layers had reacted. In the sample used to obtain the data for curve 45, layers 1 and 2 were allowed to react in succession, then 130 micromoles of allylthiourea was added at *p*H 8.2. After 30 minutes had elapsed, the supernatant liquid was decanted, the sample washed as before, and another layer of adsorbed allylthiourea added for the kinetic determination. Analysis of the sample at the end of the kinetic experiment showed that it contained a total of 110.5 micromoles of sulfide in a total weight of 3.05 g. of silver bromide. The data for the amounts of sulfide

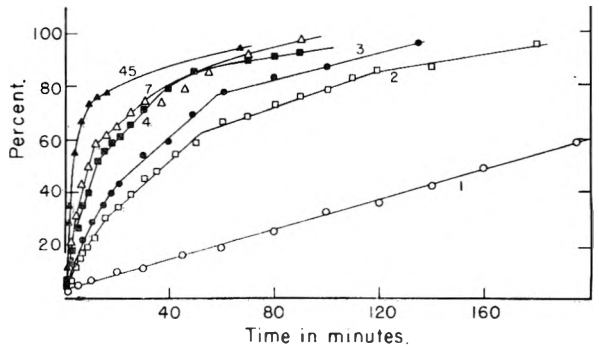

Fig. 3.—Sulfide catalysis in presence of 0.0001 *M* KBr at *p*H 7.22, 20.2°, per cent. of reaction completed is plotted against time: curve 1, ○○, untreated AgBr; curve 2, □□, after 1 reaction cycle; curve 3, ●●, after 2 reaction cycles; curve 4, ■■, after 3 reaction cycles; curve 7, ΔΔ, after 6 reaction cycles; curve 45, ▲▲, after 2 reaction cycles + 130 μ moles of allylthiourea.

found at the end of 1, 2, 3, 4 and 7 reaction cycles (Table II) show that no increase in adsorption of allylthiourea occurs from layer to layer over this range.

TABLE II

SULFIDE FOUND IN SAMPLES AFTER SUCCESSIVE REACTION CYCLES

Reaction cycles prior to kinetic run	Total AgBr at end of expt.	Ag_2S/AgBr, μmole/gram
0	3.91	0.53
1	3.68	1.19
2	3.90	1.39
3	3.76	2.46
6	2.56	2.83
2 + 130 μmole ATU (110.5 reacted)	3.05	20.87

Similar results were obtained in a series of experiments with no excess bromide ion present during the kinetic runs. Similar results also were obtained when the original sulfide was derived from sodium sulfide (added in very dilute solution to a vigorously stirred silver bromide sample) rather than from previous allylthiourea reaction.

The sulfide formed by the reaction of one adsorbed allylthiourea layer may not be uniformly distributed over the silver bromide surface. This is suggested by a comparison of the form of the reaction curve for the second adsorbed layer with that for the first. To make comparison easier, the curve for the second layer reaction may be compared with one for the first layer reaction at a *p*H sufficiently higher so that the initial portions of the two curves coincide. Such curves are shown in Fig. 4. Beyond about 30% reaction, the curve representing the second layer falls below that of the first.

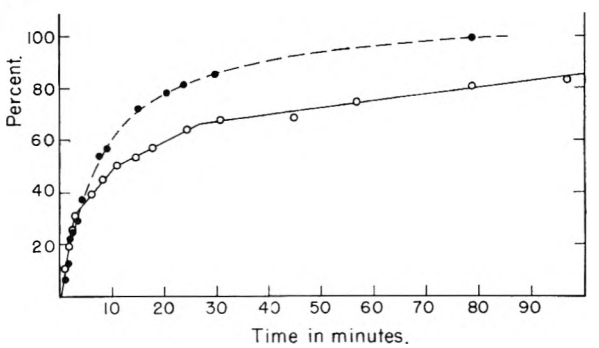

Fig. 4.—Comparison of shapes of reaction curves for first and second layers: ●●, first layer (no prior reaction), *p*H 7.49; ○○, second layer, *p*H 7.09, 20.2°.

The surface formed by reaction of the first adsorbed layer of allylthiourea resembles that of silver bromide more closely than that of silver sulfide, insofar as chromatographic

properties are concerned. This was shown in a series of experiments carried out in chromatographic columns packed with silver bromide, using the technique previously described.[6] Each column contained approximately 6 g. of silver bromide. Ten cubic centimeters of 0.001 *M* allylthiourea was passed through a column, followed by a water wash, then 20 cc. of 0.01 *M* borax to instigate reaction, and finally 50 cc. of water. The rate of passage of the borax was adjusted to permit reaction of the allylthiourea to go to completion. A dye was then added (4 cc. of 0.0001 *M* solution) and chromatographic development was carried out with water as developer A silver bromide column had been washed with borax and then water, but without allylthiourea addition, was used as a control. The silver sulfide columns used for comparison were treated similarly, and contained an amount of silver sulfide to give a specific surface for dye adsorption equal to that of the silver bromide.

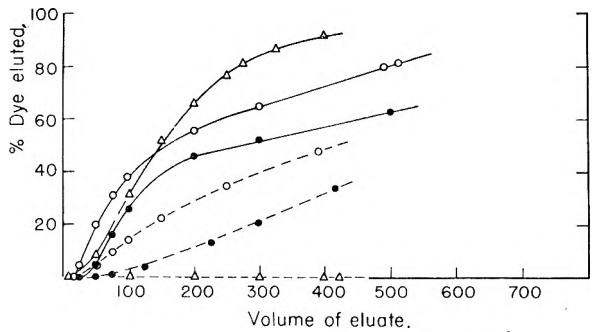

Fig. 5.—Chromatographic displacement of dyes by water developer from: ○○, AgBr control; ●●, AgBr after allylthiourea reaction; ΔΔ, Ag_2S; ——, phenosafranin; - - - -, merocyanine.

Figure 5 shows the results obtained with two dyes, one the positively charged phenosafranin and the other the negatively charged solubilized merocyanine, 4-[(3-ethyl-2-(3H)-benzothiazolylidene)-ethylidene]-3-methyl-1-(*p*-sulfophenyl)-5-pyrazolone. The amount of dye eluted (in terms of percentage of the total dye present) is plotted against the volume of required developer (eluate). The curves show that the surface formed by the allylthiourea reaction differs somewhat in adsorptive properties from that of the original silver bromide, but the modified surface still resembles the original silver bromide more closely than it does the silver sulfide.

The rate of reaction of allylthiourea with silver bromide is very dependent on *p*H, as noted by Carroll and Hubbard in their kinetic studies. Data obtained in the present work are given in Tables III, IV and V. A straight line is obtained by plotting log rate against *p*H for any particular silver bromide sample at constant temperature. Rates which were determined for silver bromide samples I and II, fall on the same straight line of slope 1.5. When 0.0001 *M* excess bromide ion is present in the solution surrounding the sample, the reaction is even more dependent on *p*H, and the straight line has a slope of about 2. The reaction of a second adsorbed layer of allylthiourea on a silver bromide sample which has already reacted with the first layer is less dependent on *p*H. Data were obtained in two sets of experiments. In the first, an adsorbed layer was allowed to react at *p*H 8, and the second layer was added to the washed sample. In the second set, the first adsorbed layer was allowed to react, then 20 micromoles of allylthiourea was added to the sample without removing the alkaline solution surrounding it. After this had reacted, the sample was washed in 0.001 *M* acetic acid and an adsorbed layer of allylthiourea was formed in the usual way for the kinetic determinations. Within each set of data, the rates are roughly proportional to the first power of the hydroxyl ion concentration.

The variation of rate with temperature was determined over a range of 20–40° under various conditions. The reaction rates obtained are given in Tables IV and V. Satisfactorily straight lines are obtained in an Arrhenius plot of these data. The apparent energy of activation of the reaction in the adsorbed layer is approximately 32 kcal./mole in the absence of added bromide ion, and 40 kcal./mole in the presence of 0.0001 *M* excess bromide ion. In the presence of sulfide formed by previous reaction of adsorbed allylthiourea, the apparent activation energy is only 22 kcal./mole, *i.e.*, 10 kcal. lower than that for the reaction of the first adsorbed layer. The sulfide catalysis, therefore, lowers the activation energy of the reaction.

(6) T. H. James and W. Vanselow, *J. Am. Chem. Soc.*, **73**, 5617 (1951).

TABLE III

DEPENDENCE OF REACTION RATE UPON *p*H AT 20.25°

Added KBr	AgBr sample	*p*H	Rate
None	II	6.59	0.65
		6.70	0.92
		7.01	2.40
		7.22	5.1
		7.39	8.6
	I	7.11	3.3
		7.34	8.1
		7.56	16.6
0.0001 *M*	II	6.93	0.065
		7.22	0.30
		7.58	1.46
		7.90	5.4

TABLE IV

DEPENDENCE OF REACTION RATE ON TEMPERATURE

Added KBr	*p*H	Abs. Temp.	Rate
None	6.40	293.25	0.36
	6.71		0.98
None	6.40	302.65	2.1
	6.70		5.7
None	5.95	312.4	2.4
	6.40		9.6
0.0001 *M*	6.93	293.25	0.063
.0001 *M*	6.93	302.65	0.57
.0001 *M*	6.93	312.4	4.4

TABLE V

DEPENDENCE OF RATE OF CATALYZED REACTION ON TEMPERATURE AND *p*H

Catalyst derived from	*p*H	Abs. temp.	Rate
1 Reaction cycle	5.95	293.25	1.1
	6.40		2.6
	7.09		12.0
	5.95	302.65	3.6
	6.40		8.5
	5.95	312.4	11.6
1 Reaction cycle + 20	4.74	293.25	0.04
μmoles allylthiourea	5.60		1.5
	5.96		2.7
	6.40		6.9

The reaction rates of thiourea itself and several of its derivatives were determined at *p*H approximately 7.2. The results are listed in Table VI in the order of increasing reaction rate.

TABLE VI

RELATIVE RATES OF REACTION OF SUBSTITUTED THIOUREAS AT CONSTANT *p*H

Substituent	*p*H	Max. rate, %/min.	Substituent	*p*H	Max. rate, %/min
1,1,3,3-Tetramethyl	7.20	0.00	None (thiourea)	7.17	3.7
1,3-Diethyl	7.18	0.27	Allyl	7.19	4.8
1,1-Dimethyl	7.18	0.33	Phenyl	7.18	18.2
Methyl	7.18	2.4	Acetyl	7.18	46

Discussion

Allylthiourea is strongly adsorbed by silver bromide. As the concentration of allylthiourea in

solution is increased, a well-defined adsorbed layer of material which is not removed by washing forms on the silver bromide surface. This layer contains 0.53 micromole per 1440 cm.^{2}, and probably represents a monolayer. The allylthiourea molecule covers about 46 sq. Å. The areas estimated from a molecular model of allylthiourea are about 39 sq. Å. for the molecule adsorbed on its side, and 57 sq. Å. for the molecule lying flat.

The adsorbed allylthiourea reacts with the silver bromide at a rate which is dependent on the *p*H, bromide ion concentration and temperature of the solution. The presence of excess bromide ion decreases the rate of reaction. The rate varies inversely as the logarithm of the bromide ion concentration, and hence directly as the logarithm of the equilibrium concentration of silver ions in the solution. This relation is consistent with the assumption that the rate varies as the concentration of adsorbed silver ions, since the latter should vary as the logarithm of the concentration of the ions in solution.[7]

The rate of the reaction between the allylthiourea and pure silver bromide varies as about the 1.5 power of the hydroxyl ion concentration in the absence of excess bromide, and as about the 2.0 power in the presence of 0.0001 *M* KBr. If the reaction involves the thiol ion, a part of this *p*H dependence is accounted for, since the rate of formation of the ion should vary as the first power of the hydroxyl ion concentration. The assumption that the thiol ion is the active form is strengthened by other considerations. Tetramethylthiourea, which cannot exist in the thiol ion form, is essentially inert. Electron acceptor groups, such as acetyl, phenyl and allyl, should increase the tendency to form the thiol ion, and these groups increase the rate of reaction of thiourea. Electron donor groups, such as methyl and ethyl, should decrease the tendency to form thiol ion and do decrease the rate of reaction.

The following reaction scheme is suggested: Two silver ions are involved in the formation of the silver sulfide. The adsorption of the thiourea involves a strong bond between the sulfur of the thiourea molecule and a silver ion of the silver bromide surface. This silver ion, accordingly, is not a variable in the reaction. The second silver ion involved is one adsorbed by the silver bromide surface, and is dependent on bromide ion concentration. We may represent the adsorption bond between the sulfur and silver ion schematically

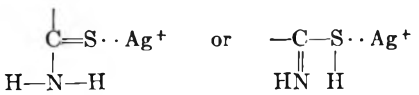

depending on whether the thiourea is adsorbed in the thione or thiol form. The former seems more probable, since the thiourea exists in solution primarily in the thione form, and adsorption shows little or no dependence on *p*H. In the presence of hydroxyl ion, ionization occurs with the formation of an ionic bond between the thiol ion and silver ion.

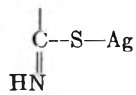

This silver thiourea compound reacts with the adsorbed silver ion.

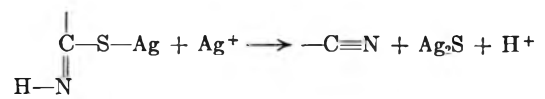

Possibly this stage is catalyzed both by silver sulfide and by hydroxyl ions. In the presence of sulfide catalysis, hydroxyl ion catalysis is insignificant. In the absence of sulfide catalysis, hydroxyl ion catalysis becomes important and increases the dependence of the over-all reaction on the hydroxyl ion concentration.

The curves representing the reaction of the adsorbed allylthiourea with silver bromide which has had no previous sulfiding treatment show no evidence of autocatalysis in spite of the fact that silver sulfide is formed. This, however, is not surprising. If the allylthiourea molecules react at the points at which they are adsorbed, only about one sulfide ion will be formed for every three to four surface lattice positions. A silver sulfide molecule formed at one point is unlikely to exert any catalytic influence on the reaction of a neighboring allylthiourea molecule when the zone of reaction of the latter is this far removed. Some pairs of molecules, because of the random distribution of positions, may be close enough together that sulfide formed by reaction of one could catalyze reaction of the other, but such an event would not be detected because the dye molecule requires a larger area for adsorption than the allylthiourea molecule. When a second layer of allylthiourea is adsorbed, many of the molecules should be adsorbed by silver ions adjacent to the silver sulfide molecules formed in the reaction of the first layer, and thus react at a greater rate. The shape of the reaction curve of the second layer (see Fig. 4) suggests, however, that the catalysis is not exerted uniformly over the entire surface, and it is probable that some of the molecules of the second layer react without the aid of catalyst. This, again, would be anticipated from purely space considerations.

The rate of reaction of adsorbed allylthiourea continues to increase with increasing amount of sulfide initially present, even when that amount exceeds by several-fold that necessary to form a uniform monolayer of silver sulfide over the silver bromide surface. This suggests that the silver sulfide is not present as a uniform layer, but rather as islands on the silver bromide surface. Such islands could form by a migration of sulfide ions along the surface to form aggregates of silver sulfide molecules, which could then crystallize. The catalytic activity of sulfide formed by the reaction of a single adsorbed layer of allylthiourea decreases on aging of the sample, and this supports the suggestion that some rearrangement of the sulfide on the surface does occur. It is possible that nuclei of silver sulfide may form in this way, even when the amount of thiourea reacting is less than that required to form a monolayer.

(7) I. M. Kolthoff, THIS JOURNAL, **40**, 1027 (1936); I. M. Kolthoff and J. J. Lingane, *J. Am. Chem. Soc.*, **58**, 1528 (1936).

ELECTRON AND X-RAY DIFFRACTION STUDIES OF IRON FISCHER–TROPSCH CATALYSTS

By James T. McCartney, L. J. E. Hofer, Bernard Seligman, James A. Lecky, W. C. Peebles and Robert B. Anderson

Contribution from the Synthetic Fuels Research Branch, Bureau of Mines, Region VIII, Bruceton, Pennsylvania

Received February 28, 1953

Pretreated and used iron Fischer–Tropsch catalysts were studied by electron and X-ray diffraction using powder techniques. For precipitated catalysts that had been carbided or nitrided the same phases were identified by both electron and X-ray diffraction. Nitrided fused or sintered catalysts showed diffraction patterns of iron nitrides, but carburized samples produced only the electron diffraction patterns of magnetite or structural promoters although X-ray lines for the carbides were obtained. Before extraction with toluene used catalysts gave electron diffraction patterns only of wax. Except for some samples of extracted, used, nitrided catalysts for which electron diffraction patterns of ϵ-iron carbonitride were obtained, most extracted, used catalysts showed only the electron diffraction lines of magnetite or of the structural promoters. For all catalysts the electron diffraction patterns of the interstitial phases were less complete than the corresponding X-ray diffraction patterns. The implications of the diffraction data with respect to the mechanism of the synthesis are considered.

Electron diffraction has been frequently mentioned as an excellent method for studying solid catalysts. The electrons usually penetrate less than 0.1 μ, and hence the diffraction pattern results from the crystal structure of the solid within about 1000 Å. of the surface. However, almost all of the published work on electron diffraction by catalysts has been on those of the evaporated-film type[1] and not on the granular or powdered types used in commercial processes.

X-Ray analysis yields diffraction patterns resulting from both surface and bulk phases, since X-rays penetrate solids. However, the phases near the surface of a heterogeneous solid may comprise only a small fraction of the solid and may therefore not be detectable by X-ray diffraction analysis. X-Ray analysis and electron diffraction are thus complementary. Both types of diffraction patterns result from diffraction by crystallites larger than about 30 Å. in diameter. In both cases the degree of order within the crystallite and its size are important in determining the completeness and sharpness of the resulting diffraction pattern.[2] The present diffraction study was made with granular iron Fischer–Tropsch catalysts after various pretreatments and use in the synthesis.

Experimental

Materials.—The type and composition of the catalysts employed in these experiments are given in Table I. The methods of preparing fused, sintered, cemented and precipitated catalysts have been described previously.[3–5]

Table I

Type and Composition of Catalysts

Catalyst type and no.	Fe	K_2O	MgO	Al_2O_3	SiO_2	Cu
Fused						
A2102	100	0.5	...	..	...	...
D3001	100	.85	6.8	..	1.05[a]	...
D3008	100	1.39	...	2.83	.29	...
Sintered						
A2101	100	.61	...	..	...	...
A2106.11	100	.94	...	..	...	...
A2106.03						
Cemented						
A3213.24	100	.52	...	5.9	...	...
A3215	100	.85	...	3.6	...	...
A3218.20	100	1.75	...	3.5	...	...
Precipitated						
L2002	100	.06	...	..	...	0.0
LH3001	100	.5	...	..	...	10.
P3002.1	100	.12	...	..	...	.56
P3003						
P3003.1						
P3003.05	100	.5	...	..	...	10.
P3003.24						

[a] Also contains 1% Cr_2O_3.

Catalyst Pretreatment and Testing.—The fused, sintered and cemented iron catalysts were reduced in electrolytic hydrogen at hourly space velocities of 1,000 to 2,500 and temperatures of 400 to 550° for 20 to 60 hours, the conditions of reduction varying with the type and composition of the catalyst.[4,5] The reduced catalysts were used directly in the synthesis or carbided with carbon monoxide or nitrided with ammonia prior to use. Hägg carbide was prepared by carbon monoxide treatment of the catalyst at a constant temperature between 225 and 275°. However, a more rapid method of carburization with carbon monoxide entails progressively increasing the temperature from 180 to 350° at such a rate that the carbon dioxide content of the exit gas remains about 25%. Cementite was prepared by heating a mixture of iron and Hägg carbide (carbon–iron atom ratio about 0.33) in helium at 500° for 6 hours.[6] Hexagonal iron nitride was prepared by treating the reduced catalyst with ammonia at hourly space velocities of 1,000 to 5,000 for 6 hours at 300 to 400°.[5]

Most of the precipitated catalysts were pretreated with $1H_2$:1CO synthesis gas at a space velocity of 100 and atmospheric pressure for 24 hours at 235 to 270°.[7] In this pre-

(1) O. Beeck, *Rev. Modern Phys.*, **17**, 61 (1945).

(2) An incorrect but widely held view is that the electron diffraction patterns of finely divided, nearly amorphous material will give sharp, easily identifiable patterns, while X-ray diffraction patterns of the same sample may be diffuse to the point of unrecognizability. This "effect" is attributed to the relatively short wave length of the commonly used 50 kv. ($\lambda \leqq 5 \times 10^{-10}$ cm.) electrons. Although electron diffraction has many advantages over X-ray diffraction in the study of colloidal materials, the above is not one of them. The angle of deviation, 2θ, of a difracted beam is given by Bragg's law, $2\theta \leqq 2 \arcsin \theta = \lambda/d$. The line broadening, B, due to small crystallite size is given by the equation of Laue $B = 0.9\lambda/t \cos\theta$, where t is the particle size. If θ is less than ~22°, $\cos\theta$ is approximately constant, and $\arcsin\theta \leqq \theta$. This is the region of θ most generally used for identification. Both B and θ vary directly with λ; thus, the resolution is not improved with change in wave length.

(3) W. K. Hall, W. H. Tarn and R. B. Anderson, *J. Am. Chem. Soc.*, **72**, 5426 (1950).

(4) R. B. Anderson, B. Seligman, J. F. Shultz, R. Kelly and M. A. Elliott, *Ind. Eng. Chem.*, **44**, 391 (1952).

(5) R. B. Anderson, J. F. Shultz, B. Seligman, W. K. Hall and H. H. Storch, *J. Am. Chem. Soc.*, **72**, 3502 (1950).

(6) L. J. E. Hofer and E. M. Cohn, *J. Chem. Phys.*, **18**, 766 (1950).

(7) J. F. Shultz, B. Seligman, L. Shaw and R. B. Anderson, *Ind. Eng. Chem.*, **44**, 397 (1952).

treatment the ferric oxide was reduced to magnetite and small to moderate amounts of higher-iron carbides. Fairly complete carburization of precipitated catalysts to iron carbides may be accomplished by treatment of either the raw or reduced catalyst with carbon monoxide at atmospheric pressure. The formation of hexagonal carbide free of Hägg carbide requires a relatively low carburization temperature, perhaps below 200°, whereas Hägg carbide free of cementite can be prepared at temperatures from 225 to 300°. Precipitated iron catalysts can be reduced in hydrogen at relatively low temperatures, such as in 17 hours at 300° with a space velocity of hydrogen of 1,000.[3] The reduced catalysts may be converted to ϵ-nitride by ammonia treatment at space velocities of 1,000 for 6 hours at 300 to 400°.

The pretreated catalysts were started in the synthesis at 200 or 220° (depending upon the expected activity), and at absolute pressures of 7.8 or 21.4 atmospheres of $1H_2:1CO$ gas. Space velocities of about 100 and 300 were used for tests at 7.8 and 21.4 atmospheres, respectively, and the temperature of operation was increased 7° per hour until the apparent (carbon dioxide-free) contraction increased to 63–65%. Thereafter, this conversion was maintained by varying the temperatures. In detailed studies of the changes in catalyst composition during the synthesis, the temperature of operation was maintained constant and the space velocity was varied to maintain constant conversion. The testing apparatus has been described previously.[5,8]

X-Ray Diffraction Methods.—The X-ray diffraction methods were essentially the same as those previously described.[9] In the case of used catalysts, the samples, wet with hydrocarbons, were ground to about 120 mesh in either a simple mortar or a Plattner diamond mortar, depending on hardness and malleability. The wet samples were mixed with collodion, packed in 19-gage stainless-steel tubes of 0.7 mm. i.d., and extruded. These procedures avoided oxidation detectable by X-ray diffraction.

Electron Diffraction Methods.—To obtain satisfactory transmission electron diffraction patterns of solids, the particles must be very fine, since electrons can penetrate only a very thin layer of material before they are inelastically scattered and incapable of contributing to the diffraction rings. For 60 kv. electrons the greater part of the diffraction pattern is formed by electrons that have penetrated not more than 0.1 μ of materials as dense as metals.[10] The particles need not be as small as this, because diffraction can occur through protrusions on and around the periphery of larger particles. However, the smaller the average size of the particles, the greater will be the amount of material that is sufficiently thin to contribute to the diffraction pattern.

The precipitated catalysts were easily ground to very fine particles, but the fused catalysts were much harder, often necessitating rigorous and prolonged grinding in a synthetic sapphire mortar. The catalysts were covered by liquid toluene or heptane during this operation to prevent oxidation. Several drops of concentrated slurry were then placed on a microscope slide, about 4 drops of a 2% solution of Parlodion in amyl acetate were added, and the slurry was mulled with a glass rod to disperse the particles. More amyl acetate was added until the material appeared well dispersed. A little of the slurry adhering to the rod was then quickly drawn out on a clean slide, leaving upon drying a dispersion of particles embedded in a Parlodion film. This was scored into $^1/_4$-inch squares and floated off on a water surface. Two superimposed $^1/_8$-inch discs of 200-mesh screen were brought up under one of the squares which appeared of suitable density, and the screens and film were lifted out and blotted on cloth. The top screen was then lifted off, and the sample was ready for examination.

The diffraction patterns were obtained with the diffraction adapter of an RCA Model B electron microscope, using 60 kv. electrons. They were photographed on lantern-slide medium plates, with exposures of about one minute. The instrument was calibrated by measurement of the diffraction rings of magnesium oxide smoke. The d-values of these were taken from the tables of Hanawalt, Rinn and Frevel.[11] The formula $d/n = K'/D$, derived from the Bragg diffraction equation, for fixed accelerating voltage (λ of electrons) and fixed specimen-to-plate distance was used to calculate the interplanar spacing, d, from the diameter of the rings, D, after determining K' with the calibrating material.[12]

The first electron diffraction patterns of used iron catalysts showed only adsorbed wax, the patterns being identical with those obtained from the Fischer–Tropsch wax alone. Extraction of the catalysts with toluene for 48 hours in a modified Soxhlet apparatus was found to be sufficient to greatly reduce or eliminate the diffraction lines corresponding to wax, and based on these preliminary experiments the following method was established for extracting used catalysts: The catalyst was dropped from the reactor (in synthesis gas and at operating temperature) directly into heptane. A representative sample of the catalyst was crushed in a mortar containing heptane, and the wet material was transferred to a small bottle. The bottle was put into a conventional extraction apparatus, and a small funnel was placed in the bottle as shown in Fig. 1. The condensed toluene flowed into the funnel (which extended to the bottom of the bottle) over the catalyst, and out of the top of the bottle. The catalyst was thus always maintained under liquid toluene to prevent oxidation. To ensure rather complete removal of the adsorbed hydrocarbons, the samples were extracted for about 72 hours, after which the bottle was removed and stoppered.

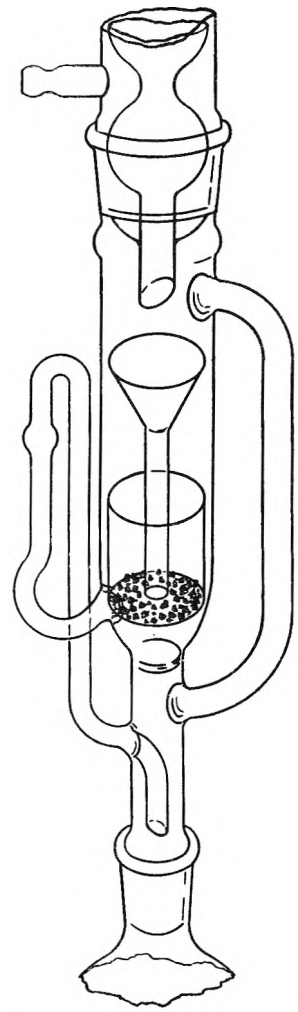

Fig. 1.—Extraction apparatus.

To make sure that no oxidation occurred during this procedure, a sample of a precipitated catalyst (P3002.1) was reduced in hydrogen at 350°, transferred to a bottle without contact with air, and stored in heptane. One portion of the reduced catalyst was used directly for electron diffraction, while a second sample was extracted with toluene (as described above) before analysis. Both samples produced patterns of metallic iron only.

Results

Figure 2 presents a schematic comparison of the X-ray and electron diffraction patterns of α-iron, magnetite, Hägg carbide, hexagonal close-packed iron carbide, cementite, ϵ-iron nitride, ϵ-iron carbonitride and magnesium oxide. The data from which these diagrams were prepared are given in Table II. Some of the X-ray patterns were taken from previous work in this Laboratory, while others were taken from the tables of Hanawalt, Rinn and Frevel. In general, there is good agreement between the X-ray and electron diffraction patterns.

(8) R. B. Anderson, A. Krieg, B. Seligman and W. E. O'Neill, *ibid.*, **39**, 1548 (1947).

(9) L. J. E. Hofer, E. M. Cohn and W. C. Peebles, *J. Am. Chem. Soc.*, **71**, 189 (1949).

(10) G. P. Thomson and W. Cochrane, "Theory and Practice of Electron Diffraction," The Macmillan Co., London, 1939

(11) J. D. Hanawalt, H. W. Rinn and L. K. Frevel, *Ind. Eng. Chem., Anal. Ed.*, **10**, 457 (1938).

(12) R. B. Picard, *App. Phys.*, **15**, 678 (1944).

Table II

Comparison of X-Ray and Electron Diffraction Patterns of Phases in Iron Fischer-Tropsch Catalysts[a]

Diffraction: Electron d/n	Electron I/I₁	X-Ray d/n	X-Ray I/I₁
α-Fe[b]			
2.03	S	2.01	1.00
1.43	W	1.428	0.15
1.17	S	1.166	.38
1.02	VW	1.010	.10
0.903	M	0.904	.08
.829	VW	.825	.03
.767	M	.764	.10
.674	W	.676	.03
Fe_3O_4[b]			
2.97	W	2.97	0.28
2.52	S	2.53	1.00
		2.42	0.11
2.10	W	2.10	.32
1.71	W	1.71	.16
1.61	M	1.61	.64
1.48	M	1.483	.80
		1.326	.06
1.28	W	1.279	.20
		1.210	.05
1.12	VW	1.121	.10
1.09	M	1.092	.32
		1.049	.10
.971	W	0.970	.16
		.940	.06
.877	VW	.880	.10
.857	W	.859	.20
		.853	.08
.809	W	.814	.10

Diffraction: Electron d/n	Electron I/I₁	X-Ray d/n	X-Ray I/I₁
Fe_2C (Hägg)[c]			
		2.62	VW
2.45	W	2.48	W
		2.39	W
		2.26	M
2.19	W	2.18	M
		2.06	VS
2.04	S	2.03	VS
		1.98	W(br)
		1.91	M
1.79	W	1.80	S
		1.76	VW
		1.72	VW
1.68	VW	1.67	VW
		1.62	VW
1.59	VW	1.57	S
1.50	VW	1.50	VW
		1.37	VW
		1.34	VW
		1.32	VW
		1.27	W
1.24	VW	1.25	W
1.21	M	1.21	M
		1.17	W
1.16	W	1.16	W
		1.14	W
1.11	M	1.13	M
		1.11	W(br)
		1.09	W(br)

Diffraction: Electron d/n	Electron I/I₁	X-Ray d/n	X-Ray I/I₁
Fe_2C (hex.)[c]			
		2.38	W
		2.16	M
2.10	S	2.08	VS
1.61	M	1.60	M
1.39	W	1.37	M
1.24	M	1.24	M
1.16	M	1.16	M
Fe_3C[c]			
2.45	VW	2.37	M
		2.25	W
		2.18	W
		2.10	W
2.06	S	2.06	M
		2.01	VS
		1.97	M
		1.87	M
		1.85	M
		1.68	W
		1.58	W
1.51	VW	1.51	W
		1.403	VW
1.28	W	1.322	M
		1.222	M
1.21	M	1.214	M
		1.189	M
		1.159	S
		1.149	M
		1.124	S
1.09	M	1.104	S
		1.096	VW
		1.087	VW
		1.052	W
		1.002	VW
		.986	M(br)

Diffraction: Electron d/n	Electron I/I₁	X-Ray d/n	X-Ray I/I₁
ε-Fe_2N[d,e]			
		2.37	M
		2.19	M
2.08	S	2.08	VS
1.60	M	1.61	M
1.37	W	1.375	M
1.24	M	1.25	S
		1.17	S
1.16	M	1.15	S
		1.10	VW
		1.05	W
		1.00	W
ε-Fe_2X[d,e,f] (carbonitride)			
		2.37	M
		2.19	M
2.09	S	2.08	VS
1.60	M	1.615	M
1.36	W	1.37	S
1.24	W	1.25	S
		1.17	S
1.14		1.15	S
		1.10	VW
		1.05	W
		1.00	W
MgO[b]			
2.45	W	2.42	0.06
2.10	S	2.10	1.00
1.49	S	1.485	.75
		1.266	.06
1.21	W	1.213	.15
		1.050	.04
.936	W	.94	.10
.857	W	.86	.04

[a] d/n = interplanar spacing in ångströms; I/I_1 = estimated relative intensity; S = strong; M = medium; W = weak; V = very; br = broad. [b] X-Ray data from Hanawalt, Rinn and Frevel, *Ind. Eng. Chem., Anal. Ed.*, 10, 457 (1938). [c] X-Ray data from Hofer, Cohn and Peebles, *J. Am. Chem. Soc.*, 71, 189 (1949). [d] X-Ray data from unpublished Bureau of Mines work. [e] Contains a trace of magnetite. [f] C/Fe atom ratio = 0.16; N/Fe atom ratio = 0.37.

Complete agreement would not be expected, since there are fundamental differences between electron waves and X-rays. The discrepancies found in the present study between the results of X-ray diffraction and electron diffraction seem to be beyond the scope of Thomson and Cochrane's[10] findings.

In the electron diffraction patterns of the interstitial compounds, iron carbides, nitrides and carbonitrides, many reflections are missing. On the whole, the electron diffraction patterns of the other phases are quite complete. Recently, Trillat and Oketani[13] have published essentially complete electron diffraction patterns of cementite and Hägg carbide. Their metal specimens were made by subliming iron on single crystals of rock salt and then dissolving the salt from the film. Metal prepared in this way is almost entirely strain-free, since completely reversible electrodes can be made from it.[14] Metals prepared by the reduction of catalysts at temperatures so far below the melting point and in the presence of promoters are probably highly disordered and stressed. The interstitial phases derived from such metals will also be highly stressed. Furthermore the structures of interstitial compounds of iron are much more susceptible to stress and the results of stress will be much more dramatic than in the case of the original metal. This conclusion derives from the Hägg classification[15] of interstitial compounds into the stable and unstable forms depending on whether the ratio of the carbon atom radius to the metal atom radius is less than or greater than about 0.58. The iron interstitial compounds belong to the unstable group and reflect this instability by the relatively low temperatures at which they either decompose or rearrange to form new phases, the large number of structures which they can assume, and the rela-

(13) J. J. Trillat and S. Oketani, *Compt. rend.*, **230**, 2203 (1950); **232**, 1116 (1951); **233**, 51 (1951).

(14) B. C. Bradshaw, *J. Chem. Phys.*, **19**, 1026 (1951)

(15) G. Hägg, *Z. Physik. Chem.*, **B12**, 33 (1931).

tive complexity of some of these structures. Apparently surface disorder can be observed only by electron diffraction.

In Tables III to V, the phases are reported in the order of decreasing intensity of the diffraction patterns. When the diffraction pattern was very weak or many lines were missing, the phases reported in the tables are indicated as questionable.

TABLE III

X-RAY AND ELECTRON DIFFRACTION DATA OF PRETREATED IRON CATALYSTS

Experiment	Catalyst Number	Type[a]	Pretreatment[b]	Phases indicated by[c] X-Ray diffraction	Electron diffraction
29-1	D3001	F	R, C	χ	MgO
30-1	D3001	F	R	α	MgO
2			R, C	χ	MgO
3			R, C, R	α	MgO
4			R, C	α, χ	MgO
32-1	P3003.1	P	R, C, R	α, Cu	α, M
2			R, C	ϵ-C	ϵ-C, M
3			R	α, Cu	α, ?
4			R, C	ϵ-C, α	ϵ-C
36-1	P3003.1	P	R	α, Cu	α, M
2			R, C	....	ϵ-C
3			R, C	α, ϵ-C	ϵ-C
4			R, C	ϵ-C, Cu	ϵ-C
4II			R, C, T	C	C
43-3	P3002	P	R, C	ϵ-C, α	M, ϵ-C
4			R, C	ϵ-C, α	ϵ-C
45-1	P3002.1	P	C	M, χ	M
4			C	M, χ	M
46-1	P3002.1	P	C	χ, M	χ
4			C	M, ϵ-C	M
47-1	P3002.1	P	R, C	χ, M?	χ
2			R, C	χ, M	χ
3			R, C	χ, M	χ
4			R, C	M, χ	M
48-1	P3002.1	P	R, C, R	α, χ	α
2			R, C, R, C, R	α, χ	α
3			R, C, R	α, χ	α
...	A2106.052	S	R, C	χ	M
N-32	A2106.05	S	R, N	ϵ-N	ϵ-N
N-40	D3001	F	R, N	ϵ-N	ϵ-N, MgO

[a] F = fused, P = precipitated and S = sintered. [b] R = reduced in H_2, C = carburized in CO, T = heat treatment in helium or vacuum at 450°, and N = nitrided in NH_3. [c] α = α-iron, M = magnetite, χ = Hägg carbide, C = cementite, ϵ-C = hexagonal iron carbide, ϵ-N = hexagonal iron nitride, MgO = magnesia and Cu = copper. Phases are listed in order of decreasing intensities of diffraction patterns; questionable patterns are marked "?".

TABLE IV

X-RAY AND ELECTRON DIFFRACTION DATA OF SAMPLES OF A FUSED CATALYST (D3001) TAKEN DURING THE SYNTHESIS. ($1H_2$ + 1CO GAS AT 7.8 ATM.)

Testing, days	Av. temp., °C.	Phases identified by[a] X-Ray diffraction	Phases identified by[a] Electron diffraction
	Test X194, Catalyst reduced		
0	...	α	MgO, α
2	234	α, M	MgO, M
8	258	α, M, χ	MgO, M
22	258	.....	MgO, M
50	257	α, M, χ	MgO, M
64	257	M, χ, α	M, MgO
79	256	M, χ, α	M, MgO
90	272	M, χ, α	M, MgO
97	300	M, χ, α	M, MgO
	Test X294, Catalyst reduced and carburized to Hägg carbide		
0	...	χ, α	MgO
2	210	χ, α	MgO
12	230	χ, α, M?	MgO
54	228	χ, M	MgO, ?
61	229	χ, M	MgO, ?
68	228	χ, M	MgO, ?
89	229	χ, M	MgO
	Test X317, Catalyst reduced, partially carburized to Hägg carbide, and then heated to produce cementite		
0	...	C	MgO
4	220	C	MgO
10	230	C	MgO
24	231	C	MgO
42	234	C, M	MgO
56	236	C, M	MgO, M ?
70	237	C, M	MgO, M
84	237	C, M	MgO, M ?

[a] α = α-Fe, M = magnetite, χ = Hägg carbide, C = cementite, and MgO = magnesia. Phases listed in order of decreasing intensities of diffraction patterns; questionable patterns are marked "?".

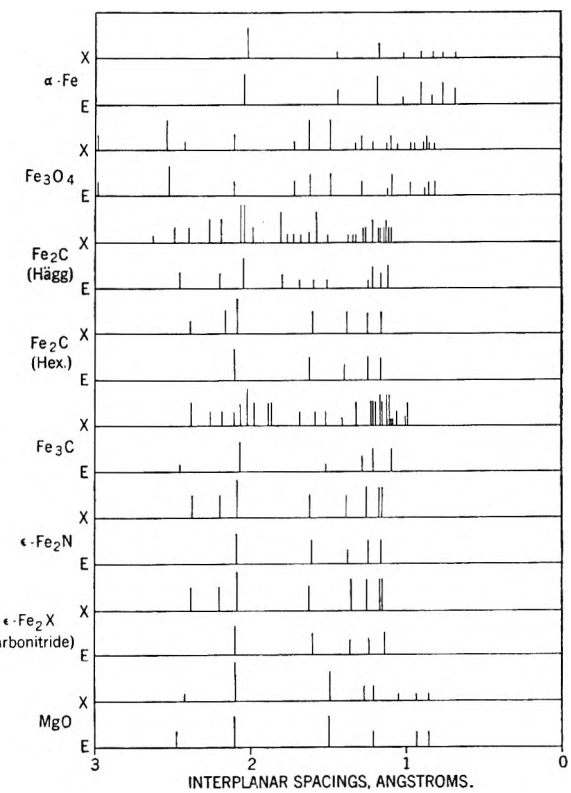

Fig. 2.—Comparison of X-ray (X) and electron (E) diffraction patterns of phases in iron Fischer-Tropsch catalysts.

The data of Table III (obtained with specimens that were not used for synthesis) indicate that iron and the iron carbides in precipitated catalysts were usually identified by both electron and X-ray diffraction. Hägg carbide in these catalysts was obtained by both methods, regardless of whether the

Table V

Phases Indicated by X-Ray and Electron Diffraction of Used Fischer–Tropsch Catalysts. (All Tests with $1H_2 + 1CO$ Gas Unless Otherwise Noted)

Catalyst type and no.	Test no.	Pre-treatment[a]	Synthesis conditions: Pressure, atm.	Synthesis conditions: Av. temp., °C.	Synthesis conditions: Testing, wk.	Phases indicated by[b]: X-Ray diffraction	Phases indicated by[b]: Electron diffraction
Fused							
D3001	X-100	R	7.8	267	6	M, α	M, MgO ?
	152	R	7.8	270	7	M, α, χ	M, MgO ?
	162	R	7.8	250	5	M, χ, α	M, MgO ?
	225	R, N	21.4	236	15	ϵ-CN[c]	ϵ-CN[c]?, ?, M?
	236	R, N	7.8[c]	230	7	ϵ-CN[c]	MgO, M
	275	R, N	1.0	265	3	.....	.....
			7.8	228	6	ϵ-CN[c]	MgO, M
	286	R, N, C	7.8	219	6	ϵ-CN[c]	MgO, M
	289	R, C	7.8	229	28	χ, M ?	MgO, ?
	327	R, N	21.4[c]	212	9	ϵ-CN[c], M?	?
D3008	253	R, N	7.8	230	7	ϵ-CN[c]	M?, ϵ-CN?[c]
A2102	164	R	7.8	286	4	M, α, χ	M
Sintered							
A2101	166	R	7.8	234	7	χ, M	M
A2106.11	266	R, N	7.8	216	6	ϵ-CN[c]	ϵ-CN[c], M
A2106.052	389	R, C	7.8	210	5	χ, M, S	?
Cemented							
A3213.24	131	R	7.8	232	4	α, χ, M	?[d]
A3215	138	R	7.8	242	6	α, M, χ	?[d]
A3218.20	186	R	7.8	264	1	χ	?[d]
Precipitated							
L2002	119	I	7.8	244	5	M, χ	M
LH3001	81	I	7.8	233	9	.....	M
P3003.05	86	I	7.8	236	10	.....	M
P3003	87	I	7.8	250	11	.....	M
P3003.24	143	X	7.8	236	5	M, ϵ-C[e], Cu	M
	245	R	7.8	229	7	ϵ-C[e], M, Cu, χ	?
	273	R, N	7.8	229	6	ϵ-CN[c], Cu	ϵ-CN[c]
	324	R, C	7.8	229	8	χ, S	M, ?

[a] R = reduced in H_2, N = nitrided in NH_3, C = carburized in CO, I = inducted in synthesis gas, and X = no pretreatment. [b] α = α-iron, M = magnetite, χ = Hägg carbide, ϵ-C = hexagonal carbide, ϵ-CN = ϵ-carbonitride, S = siderite, and MgO = magnesia. Phases listed in order of decreasing intensities of diffraction patterns; questionable patterns are marked "?." [c] $1H_2 + 1.5CO$ gas used. [d] Possibly an alumina phase or phases. [e] The diffraction patterns of hexagonal carbide and ϵ-carbonitride are essentially indistinguishable. The one or the other phase is indicated depending on which phase is the more probable in the light of its previous history.

oxides were first reduced and then carburized or whether they were carburized directly. In a few cases the less-intense pattern was not found by one or the other method. However, the electron diffraction patterns of iron carbides were not obtained with reduced and carburized catalysts which originally contained massive, non-porous magnetite. Thus a carburized sintered catalyst (A2106.052) produced the electron diffraction pattern of magnetite, whereas X-ray diffraction indicated the presence of Hägg carbide only. Although X-ray diffraction patterns of many samples of a reduced and carburized fused catalyst (D3001) indicated the presence of iron and Hägg carbide, electron diffraction patterns usually contained only the lines of the structural promoter, magnesium oxide. Only in the first sample of test X194 with a fused catalyst (Table IV) were electron diffraction lines of iron observed in addition to those of magnesium oxide. However, lines of ϵ-nitride were found in the electron diffraction patterns of sintered and fused catalysts that had been nitrided.

Similarly, the examination by electron diffraction of samples of a fused catalyst (D3001), removed from the reactor at various intervals during the synthesis, showed the pattern of magnesia most prominently; however, the magnetite pattern was also observed (Table IV). In test X194, X-ray and magnetic analyses[16] indicated the relatively rapid formation of at least about 20% of Hägg carbide and a slower rate of formation of magnetite. However, the Hägg carbide content reached its maximum and decreased slowly after about 8 days, whereas the magnetite content increased throughout the period of testing. The electron diffraction data indicate the presence of magnetite, even in the reduced catalyst. The magnetite pattern increased in intensity and became more intense than that of magnesia after 9 weeks of synthesis.

In test X294 (Table IV) the same catalyst (D-3001) was converted to Hägg carbide before use in the synthesis. Magnetite lines were observed by X-rays after 12 days of testing, but these remained secondary to the Hägg carbide lines throughout the test. With the exception of several unidentified lines found in three of the samples, only magnesia lines were found by electron diffraction. Thus, both X-ray and electron diffrac-

(16) R. B. Anderson, L. J. E. Hofer, E. M. Cohn and B. Seligman, *J. Am. Chem. Soc.*, **73**, 944 (1951).

tion indicate that this carbided catalyst was oxidized at a slower rate than the reduced catalyst.

Similar results were obtained in test X317, in which this catalyst was converted to cementite prior to the synthesis. Here again, both X-ray and electron diffraction indicate a slower rate of oxidation than for the reduced catalyst. The electron diffraction pattern contained only lines of magnesia for the first 42 days of the test; after this period, weak lines of magnetite appeared in addition. The precarbided samples of this fused catalyst were considerably more active than the reduced one.

Data from other tests of catalyst D3001 (Table V) are similar to those in Table IV. After several weeks of use in synthesis, samples that were reduced initially (tests X100, X152, and X162) produced the electron patterns of magnetite and possibly magnesia, while X-ray analysis indicated the presence of Hägg carbide and iron in addition to magnetite. A sample that was initially converted to Hägg carbide (X289) produced the electron diffraction pattern of magnesia plus some unidentified lines. Fused catalysts D3001 and D3008 were reduced and nitrided before use in tests X225 and X253. In the synthesis the ϵ-iron nitride was converted to ϵ-iron carbonitride, and no magnetite was found by X-ray diffraction. The electron diffraction lines were difficult to interpret but appeared to be those of ϵ-iron carbonitride and magnetite. In tests X236, X275 and X327, catalyst D3001 was reduced and nitrided; however, after synthesis lines corresponding to the ϵ-iron nitride or carbonitride phases were not found in the electron diffraction pattern. In test X286 this catalyst was reduced, partly nitrided, and carburized to form an ϵ-carbonitride, but the electron diffraction pattern of the ϵ-phase was not obtained from the used catalyst.

The results with sintered catalysts were similar to those obtained with fused catalysts. After synthesis a sample that had been reduced initially (X166) produced the electron diffraction pattern of magnetite only, whereas X-ray analysis indicated Hägg carbide as the major phase. A used, initially carburized sintered catalyst produced an electron diffraction pattern that could not be identified (X389). A used, sintered catalyst that had been nitrided (X266) produced patterns of ϵ-carbonitride and magnetite by both electron and X-ray diffraction.

A used cemented catalyst (X186) showed an exceptionally sharp and well-defined X-ray pattern of Hägg carbide. Its electron diffraction pattern contained only unidentified lines. Catalysts of this type were made by cementing a magnetite powder into coherent granules with alumina from aluminum nitrate. Hence, each particle of iron oxide was surrounded by a coating of alumina, and thus it is not unreasonable to attribute the observed lines to an alumina phase.

Precipitated catalysts that were inducted in synthesis gas produced the electron diffraction pattern of magnetite only, although in test X143 the X-ray diffraction patterns of hexagonal iron carbide and copper were also observed. The electron diffraction pattern of a reduced precipitated catalyst (X245) could not be identified, and the pattern of the reduced-and-carbided precipitated catalyst (X324) was also difficult to identify but appeared to contain the lines of magnetite. The reduced-and-nitrided catalyst used in test X273 produced electron and X-ray diffraction patterns of ϵ-carbonitride.

The experimental results may be summarized as follows: (a) For reduced, carbided, or nitrided precipitated iron catalysts electron and X-ray diffraction indicated the presence of the same phases. The electron and X-ray diffraction patterns of interstitial compounds are similar but have some characteristic differences.

(b) After use in the synthesis and extraction, precipitated iron catalysts usually produced electron diffraction patterns of magnetite only, even though the X-ray diffraction patterns contained lines of Hägg carbide and/or hexagonal iron carbide. Only a used reduced-and-nitrided precipitated catalyst showed an interstitial phase, ϵ-carbonitride by both electron and X-ray diffraction.

(c) After suitable pretreatment or use in the synthesis, fused catalysts containing magnesia usually produced electron diffraction patterns of magnesia or magnetite, although X-ray diffraction indicated the presence of metallic iron, Hägg carbide, and/or cementite. Nitrides and carbonitrides were the only interstitial phase identified by electron diffraction.

(d) Nitrides and carbonitrides were the only interstitial phases detectable by electron diffraction of sintered and cemented catalysts.

(e) Catalysts converted to cementite, Hägg carbide, or ϵ-iron nitride resisted oxidation during the synthesis; nitrides were more resistant than carbides.

Discussion

An interesting result of these studies is the apparent absence of iron carbides in the surface layers of used Fischer–Tropsch catalysts. However, interpretation of the data is complicated by the following factors: (a) If the carbide consists of small and/or highly disordered crystallites, it may produce either indistinct electron diffraction patterns or patterns that differ considerably from those of the bulk phases.

(b) Unidentified lines found in some of the electron diffraction patterns may correspond to an unknown iron carbide or a related phase. However, no lines corresponding to the carbide reported by Ekstrom and Adcock[17] were found by either electron or X-ray diffraction.

(c) With sintered or fused catalysts, electron diffraction patterns of carbides were not obtained, although X-ray and magnetic analyses indicated that Hägg carbide or cementite was the principal phase in a given sample. However, since the electron pattern due to magnetite either appeared or became more intense during synthesis, it must be inferred that iron or some of its compounds in some amorphous form is present in the surface. In

(17) H. C. Ekstrom and W. A. Adcock, *J. Am. Chem. Soc.*, **72**, 1042 (1950).

some cases, catalysts converted to ϵ-iron nitride produced the electron diffraction pattern of the ϵ-phase both after pretreatment and after use in the synthesis. Hence the ϵ-phase must be present near the surface.

By electron diffraction, magnetite is usually found in iron catalysts that have been used in the synthesis, whereas metallic iron and carbide phases may be indicated by X-ray diffraction. These facts suggest that the catalysts are oxidized from the surface. Although mixtures of hydrogen and carbon monoxide are reducing and carburizing agents for iron and iron oxide, the gas becomes an oxidizing agent as the concentrations of water and carbon dioxide increase due to synthesis reactions.

Considerable attention has been given to the role of carbide in the synthesis.[18] Although this paper presents no direct evidence concerning "surface" carbide, the presence of magnetite and apparent absence of carbides near the surface of active used iron catalysts does not add support to the already questionable carbide theory. In most tests, catalytic activity and selectivity remained essentially constant over periods in which the surface layers, as well as the bulk of the catalyst, were converted to magnetite, so that magnetite may be a principal surface phase in the synthesis. This is not so with nitrided catalysts, and the activity and selectivity of such catalysts show marked differences from those of inducted, reduced, or carbided catalysts.

The prominence of the electron diffraction pattern of magnesia in fused catalysts containing magnesia indicates the presence of the structural promoter at the surface of the catalysts. Since the diameters of crystallites required to produce a satisfactory electron-diffraction pattern must exceed 30 Å., magnesia does not appear to be dispersed molecularly in reduced catalysts, but must be present in moderately large crystallites. Although the crystallites of magnesia are larger than expected, these results are not necessarily contradictory to the present concept of the role of structural promoters in fused-magnetite catalysts.[3]

(18) S. R. Craxford and E. K. Rideal, *J. Chem. Soc.*, 1604 (1939); S. Weller, L. J. E. Hofer and R. B. Anderson, *J. Am. Chem. Soc.*, **70**, 799 (1948); J. T. Kummer, T. W. DeWitt and P. H. Emmett, *ibid.*, **70**, 3632 (1948); H. H. Storch, N. Golumbic and R. B. Anderson, "The Fischer-Tropsch and Related Syntheses," John Wiley and Sons, Inc., New York, N. Y., 1951, p. 571.

PROCEDURES in EXPERIMENTAL METALLURGY

By A. U. SEYBOLT *and* J. E. BURKE, *both with the General Electric Company*. The material presented here—never before collected in one work—outlines in detail the major unit operations carried out in doing experimental work with metals. This is the first book to deal directly and comprehensively with the techniques of preparing metal samples up to the point of observation. It will not only be of great value to the metallurgy student, but will materially assist those in peripheral fields in gaining a better application and appreciation of the methodology of the research metallurgist.

Featured in this book are: a summary of the methods of growing single crystals; an examination of the techniques of vacuum metallurgy; the application of refractories to metal research; an outline of the major unit operations carried out in doing experimental work with metals; and a list of the pure metals and their sources of supply.

1953. Approx. 340 pages. Probably $6.00

MICROWAVE SPECTROSCOPY

Written at Duke University by WALTER GORDY, WILLIAM V. SMITH, *and* RALPH TRAMBARULO. Here is the first book in its field, providing up-to-date theory, experimental techniques and applications of this rapidly expanding research method. It has already caused comments such as this one from Professor James H. Burkhalter, The University of Georgia, "I use it constantly. I think it has an easy to read style, is as up-to-date as a book in this field could be, and is very clear. Among the significant advantages of this book are the appendices and the thousands of references . . . . It is a combination textbook, reference book and handbook . . . . I feel that 'if it isn't in this book or referred to in this book, it hasn't been done.'"

1953. 446 pages. $8.00.

INTRODUCTION to SOLID STATE PHYSICS

By CHARLES KITTEL, *University of California*. Basic, yet comprehensive, this is the only book on an introductory level to cover a large part of the field of solid state physics. It gives a concise treatment of representative areas of the physics of solids. Mr. W. V. Houston, President of The Rice Institute, writes, "In particular, I was impressed by the fact that not only does it give an elementary outline of a variety of subjects, but it contains indications and references to fuller treatments. I could imagine that it would not only be a useful text in junior and senior courses, but that it would be an excellent outline for a more advanced course based on the original publications."

"Altogether, I feel this is a most outstanding and valuable contribution," adds Professor Harvey Brooks of Harvard University.

1953. 396 pages. $7.00.

Send for on-approval copies

JOHN WILEY & SONS, Inc.

440 Fourth Avenue, New York 16, N. Y.